Multisensory navigation in tethered walking insects

Hannah J. M. Haberkern

UNIVERSITY OF CAMBRIDGE

University of Cambridge

Multisensory navigation in tethered walking insects

by

Hannah J. M. Haberkern

Murray Edwards College

Department of Zoology

A dissertation submitted for the degree of

Doctor of Philosophy

September 2016

Declaration

I hereby declare that my dissertation entitled 'Multisensory navigation in tethered walking insects' is not substantially the same as any that I have submitted for a degree or diploma or other qualification at any other University.

I further state that no part of my dissertation has already been or is being concurrently submitted for any such degree or diploma or other qualification.

Except where explicit reference is made to the work of others, this dissertation is the result of my own work and includes nothing, which is the outcome of work done in collaboration.

Contents of chapter 2 of this thesis have been accepted for publication:

Haberkern H and Hedwig B. Behavioural integration of auditory and antennal stimulation during phonotaxis in the field cricket *Gryllus bimaculatus* (DeGeer). *J. Exp. Biol.* (Accepted, August 2016)

Some sections of the introduction chapter are based on a review that I wrote together with my advisor, Vivek Jayaraman:

Haberkern H and Jayaraman V. (2016). Studying small brains to understand the building blocks of cognition. *Curr. Opin. Neurobiol.* 37, 59–65.

This thesis does not exceed the limit of length (60,000 words) specified by the Degree Committee for the Faculty of Biology.

Date: ..... Signed: ……..

Hannah J. M. Haberkern
Murray Edwards College
Cambridge
September 2016

Abstract

Animals navigate complex natural environments to find food, mates or shelter. Depending on the animal's goal and the environmental context, animals may employ a range of different navigational strategies. Studies of navigational behaviours in tethered walking animals navigating tightly controlled, simplified sensory environments combined with neurophysiological techniques have generated some understanding of the neuronal processing underlying navigation. However, in its natural habitat an animal will likely face complex sensory environments, which it can actively sample and interact with. Such environments pose complex navigational challenges and support sophisticated navigational strategies. We know little about the neural mechanisms underlying coordination and control of different behaviours under such conditions. The goal of this thesis is to extend existing spherical treadmill systems for crickets and flies, which permit the study of navigation in tethered walking animals, to capture some of the complexity of natural environments. I developed new virtual reality (VR) paradigms for studying different aspects of multisensory navigation in the context of phonotaxis in crickets and visually guided navigation in fruit flies.

First I explored how female crickets tracking a male's calling song during phonotaxis respond to antennal mechanosensory stimuli, which occur during navigation in a natural terrain. I found that in the presence of antennal stimulation, which is achieved by presenting an object within antennal reach, phonotactic steering manoeuvres were suppressed while crickets slowed down and oriented toward the object to explore it with their antennae. This suggests that responses to antennal stimuli, at least transiently, are given higher priority than phonotactic steering. Consequently, mechanosensory antennal stimulation can explain differences in phonotactic behaviour in field and laboratory studies.

In my second project I worked on landmark-guided navigation in walking fruit flies. Studies in tethered walking flies in a simple, one-dimensional environment showed that flies have an internal compass, which they update using visual and self-motion cues. My goal was to develop a paradigm to study how the fly uses its internal compass in a naturalistic navigational behaviour. As a first step toward this goal I developed a VR setup for studying landmark-guided navigation in two-dimensional virtual visual environments. Using this VR system I investigated how flies use visual landmarks in a variety of contexts. First, I validated that naïve head-fixed flies track prominent visual landmarks and interact with them in my VR system in much the

same way that freely walking flies interact with real objects. I then paired sensory stimuli of other modalities with the visual environment to imbue specific objects with negative valence. By coupling, for example, the spatially restricted optogenetic activation of heat sensing neurons to the visual environment, I found that flies avoid virtually hot areas in the VR. Furthermore, flies are able to exploit visual landmark cues to more effectively avoid aversive areas in the VR. In the future this system can be used to examine, both behaviourally and neurophysiologically, whether and how flies use visual landmarks for navigation and how experience can shape the control and coordination of different behaviours into navigational strategies.

Acknowledgements

First and foremost, I would like to thank my supervisors Berthold Hedwig and Vivek Jayaraman for their gentle guidance, dependable support, encouragement and all they have taught me over the last four years.

I had a wonderful time at Cambridge in the Hedwig lab and I would like to thank all current and former lab members, Hannah ter Hofstede, Stefan Schöneich, Tim Bayley, Pedro Jacob and Konstantin Wolf, for frequent and lively discussions and the traditional joint lab lunch with mocha.

At Janelia I was lucky to be in the diverse and stimulating Jayaraman lab and my thanks goes to all past and present members for patiently responding to all my questions and for engaging discussions about flies, navigation, learning and the central complex: Johannes Seelig, Romain Franconvillie, Sung Soo Kim, Chuntao Dan, Dan Turner-Evans, Stephanie Wegener, Saba Ali and Yi Sun. I would also like to thank Sharon Rowell and Emily Nielson for their quick and friendly administrative support. Throughout my time at Janelia I had many insightful discussions with TJ Florence, Claire Eschbach, Yoshi Aso and Tilman Triphan. I would also like to thank two Janelia Undergraduate Scholars who I supervised, Dimitra Varderlaki and especially Mélanie Basnak, for their help and enthusiasm. Some of the data that Mélanie collected contributed to Figures in chapter 3.

Building new setups for behavioural studies is challenging and it would not have been possible without the help of others. For excellent support providing essential mechanical devices of the cricket antennal stimulation apparatus and the electronic control circuits I thank Steve Ellis and Glen Harrison. I am also indebted to a number of people at Janelia for help with the development of the virtual reality setup for head-fixed walking flies presented in this thesis. The software for the fly virtual reality was derived from ‘MouseoVeR’, a virtual reality system for mice developed by Jeremy Cohen and Albert Lee at Janelia. ‘FlyOver’, the fly version of ‘MouseoVeR’ was developed over several years in an interactive collaboration between two programmers in Janelia’s Scientific Computing facility and me: the program was originally written by Mark Bolstad and then adjusted and extended by Christopher Bruns. Various hardware components of the virtual reality rig were developed together with Brian Coop from Janelia’s Instrument Design & Fabrication group. Furthermore, I thank Biafra Ahanohu, a Janelia

Undergraduate Scholar, for building a prototype version of the projector-based virtual reality for tethered walking flies and thereby pioneering the project.

I am thankful for advice I received at various stages of my PhD from Matthias Landgraf, Simon Laughlin, Michael Reiser and Joshua Dudman. I would also like to thank Eugenia Chiappe for urging me to try experiments with freely walking flies, which proved to be a valuable addition to my tethered walking experiments.

Throughout my PhD I was supported by the Janelia Graduate Scholars program, and I would like to thank especially Susan Jones and Maryrose Franko.

I would also like to thank the gardeners at Murray Edwards College for keeping the view out of my room ever changing and delightful and the person responsible for bringing flowers to the Janelia Research Campus, especially the ones that attracted humming birds.

Finally, I am most grateful to my family, Susanne, Bernd, Wulf, Daut und Karl: Vielen Dank dafür, dass ihr immer ein offens Ohr für mich und meine Sorgen hattet und es immer intuitiv verstanden habt mir Zuversicht und mehr Gelassenheit zugeben. And of course, I thank my boyfriend, Davis Bennett, for his creativity and optimism that was essential for making the best of our time at Janelia, for always believing in me and for balancing out my worries.

Table of contents

List of figures

List of abbreviations

WTB – wild-type Berlin, *Drosophila melanogaster* strain

HC – Hot cell

DL – Dickinson lab wild-type *Drosophila melanogaster* strain

HD – head direction

CX – Central complex

IQR – Interquartile range

VR – Virtual reality

1D – One-dimensional

2D – Two-dimensional

FOV – Field of view

IR – Infrared

LED – Light emitting diode

CX – Central complex

EB – Ellipsoid body

Chapter 1

Introduction

1. Introduction

1.1. Navigation poses complex computational challenges

Animals across phyla move through space to find food, mates and shelter. The specific strategies they use vary depending on their motivations and sensory environments. Foraging trips, for example, can be exploratory, e.g. when desert ants search for scarcely distributed individual food items (Buehlmann et al., 2014), or highly targeted when ants collect food from a familiar feeder or bats exploit a known fruit tree rich with ripe fruits (Graham and Cheng, 2009; Tsoar et al., 2011). Furthermore, an animal's movements can cover vastly different spatial scales, ranging from movements that span only a few dozen centimetres, such as homing in field crickets (Beugnon and Campan, 1989), to the seasonal long-distance migration of birds and many insects (Chapman et al., 2015; Guerra and Reppert, 2015; Shaffer et al., 2006; Weimerskirch et al., 2015).

While there is a long tradition of studying animal movements, relatively little is known about the neural computations that give rise to them (Huston and Jayaraman, 2011; Webb, 2004a; Wehner, 2003). We do, however, know a lot about the diversity of distinct behavioural strategies that different animals employ for navigation, which provides us with important clues towards identifying the computations that brains must carry out for successful navigation (Trullier et al., 1997). I will begin by providing a few important definitions. Then I will describe how identifying the strategy that an animal uses to solve a certain navigational problem can guide research on the underlying neural computations with path integration as an example. Finally, I will review a few behavioural strategies and highlight examples of complex navigation in animals that have neither a large brain nor a cortex —namely, insects. I will then justify this focus on smaller-brained animals by discussing why studying neural circuits controlling navigational behaviours is challenging, especially in organisms with large, complex brains, but may be more tractable in insects.

1.1.1. Which movements qualify as navigation?

Ordered movement of an animal through space is often referred to as **navigation**. According to the Oxford English Dictionary, navigation is "the process or activity of accurately ascertaining one's position and planning and following a route". Specifically in the context of describing

animal behaviour, Gallistel (1990) provides the following definition of navigation: “Navigation is the process of determining and maintaining a course or trajectory from one place to another. Processes for estimating one’s position with respect to the known world are fundamental to it. The known world is composed of the surfaces whose locations relative to one another are represented on a map.” Thus, strictly speaking navigation only covers directed movements from one place to another. Furthermore, these definitions assert that for a movement to qualify as navigation, the animal needs to have explicit knowledge of its location and heading in the world and needs to plan its route based on knowledge about its environment. However, it appears that many animals do not necessarily form and use ‘mental maps’ and we will therefore use the term ‘navigation’ in a more general sense to refer to goal-directed movement of an animal in general.

An other term that often comes up when describing goal-directed movements of animals is guidance. In the context of navigation, ‘guidance’ refers to the process of “directing the motion or position of something” (Oxford English Dictionary). In other words, guidance mechanisms are what an animal might use for estimating its position in space and to direct movement along a planed or spontaneously chosen trajectory. Gallistel (1990) refers to these processes (guidance mechanisms) as essential for navigation in his definition. Hence, navigation refers to solving the general problem of getting from one point in space to an other, the ‘goal’, while guidance refers to the mechanism by which information from the environment is turned into directions on where to move next.

Often for a given navigation problem there are multiple strategies for finding or moving along a path to the goal. In the literature— and in this thesis — the terms ‘navigational strategy’ and ‘guidance strategy’ are used interchangeably to describe the different mechanisms animals use to solve a given navigational problem (Geva-Sagiv et al., 2015; Trullier et al., 1997). A certain strategy is based on a specific set of computations. Therefore, establishing the use of a certain navigational strategy during a navigational behaviour of interest can help to identify the underlying neural circuitry that needs to implement the necessary computations.

1.1.2. Linking a behaviour to a navigational strategy and to underlying neural processing

I would like to illustrate with an example how determining the navigational strategy behind a certain navigational behaviour can be helpful for identifying the underlying neural circuitry. Animals with a fixed home or nest often encounter the following navigational problem: Suppose the animal left its home and explored its environment, leading it away from its home to an arbitrary position in space. Now the animal faces the navigational problem of finding its way back home. Foraging desert ants face this problem when they need to return to their nest after having found food. Since these tiny organisms are at risk of dehydrating in the hot dry desert climate, it is essential for them to return back to the nest on the shortest path. Indeed, behavioural studies of desert ants have shown that, upon finding food, rather than backtracking their outbound route these ants take a straight path back to their nest (Müller and Wehner, 1988). This suggests that a foraging ant is able to keep track of where its nest is located relative to its own position. While desert ants exemplify this behaviour, which they perform with remarkable precision, similar homing behaviours have been described in mammals, too (Geva-Sagiv et al., 2015; McNaughton et al., 2006).

A navigational strategy that would allow an ant to perform this behaviour is path integration (also called 'dead reckoning'). This strategy allows an animal to keep track of where it came from by integrating its own movements. By integrating changes in movement direction and the distance moved along a given direction, the animal could construct and maintain directions toward its nest. This abstract internal representation which directs path-integrating animals back to their nest is often referred to as the 'homing vector' (Wehner, 2003). A number of elegant behavioural experiments have provided overwhelming evidence that foraging desert ants indeed perform path integration (Wehner, 2003). Path integration has the advantage of being independent of guidance cues, but it quickly accumulates errors (Etienne et al., 1998; Müller and Wehner, 1988) and is therefore often only used on a small spatial scale or in combination with other external guidance cues. I will discuss this topic further in chapter 3.
So how could an animal execute this strategy? In other words, which information does the animal need to collect from its environment and what does it need to compute from this information? Path integration requires measurement and integration of heading angle changes as well as distance moved in a given direction. This suggests that an animal capable of path integration possesses some form of compass. Indeed, behavioural studies have demonstrated that desert ants can see the polarisation pattern that sunlight creates across the sky and can use this visual cue as a compass signal, providing the animal with an absolute sense of angular

orientation (Wehner, 2003). Many other insects are also able to see polarised light and appear to use the sky's polarisation pattern as a guidance cue (Heinze and Homberg, 2007; Labhart et al., 2001; Mappes and Homberg, 2004b; Philipsborn and Labhart, 1990). Especially work in locusts, crickets and monarch butterflies has since contributed to our understanding of how the sky's polarisation pattern is transferred into an 'internal compass' (Labhart and Meyer, 2002; Sakura et al., 2008). To perform full path integration in addition to a compass the ant would also need to have a mechanism for measuring how much distance it moved, a so-called odometer. Again, behavioural studies show that ants can count their steps and somehow transform this into a distance measurement (Wittlinger et al., 2007). Other animals may use other mechanisms for measuring distance. Studies in bees, for example, suggested that these insects use the optic flow they experience during flight (Esch et al., 2001). Ants also appear to be capable of optic flow-based odometry (Pfeffer and Wittlinger, 2016). To date little is known about the neural the neural correlate of extracting and integrating distance measurements from step counts or optic flow.

Summing up, connecting the foraging behaviour of desert ants to a navigational strategy, path integration, was helpful in directing further research on identifying sensory inputs and abstract computations required for this behaviour, which are likely to apply to many other animals as well.

1.1.3. Classifying behaviours according to the use of a certain navigational strategies

Different frameworks for classifying orientation and guidance strategies have been proposed. This has lead to ambiguous nomenclature, which can be confusing. In the following I will review two proposed frameworks, a classic one by Kühn (1919) and a more recent one by Trullier and colleagues (1997), which has a strong focus on the computational complexity of the different strategies. I will try to merge the latter framework with less systematic classification schemes (Collett and Collett, 2002; Collett and Graham, 2004; Geva-Sagiv et al., 2015).

An early classification of different forms of orientation behaviours was proposed by Kühn (1919). Kühn's classification is based on analysing an animal's orientation and movement relative to a guiding stimulus. He distinguishes between four forms of taxis:

- Tropotaxis: Orientation responses based on positioning relevant sensors symmetrically with respect to a guiding stimulus. The example Kühn provides is negative phototaxis of a

planarian moving in a straight line away from a light source by adjusting its body orientation such that it senses the same light intensity with both eyespots (Kühn, 1919).

- Menotaxis: Keeping a fixed, but arbitrary (not necessarily symmetric) relative position to a guiding stimulus. As an example for menotaxis Kühn cites a study of a caterpillar moving in fixed angle relative to a single light source. Here, when the light source is moved the caterpillar changes its direction of movement in such a way that it resumes the same angular position as before the manipulation of the light. Also fixation behaviours in fruit flies, which I will investigate in detail in chapter 3 of this thesis, shows characteristics of menotaxis.
- Telotaxis: Orientation toward a goal, which is specified by a sensory stimulus. The reorientation movements during telotaxis often result in positioning the relevant stimulus at specific point on a sensory organ. A dragonfly, for example, fixates a potential prey in its fovea by making precisely directed head movements (Mischiati et al., 2014).
- Mnemotaxis: Orientation based on experience, i.e. following a memory. During mnemotaxis an animal takes a previously performed trajectory. Here Kühn refers to flight trajectories of homing bumble bees and bees, i.e. animals finding their way back to their next after a foraging trip.

More recently a hierarchical categorisation of navigational strategies according to the computational complexity of the strategy that is executed has been proposed (Franz and Mallot, 2000; Trullier et al., 1997). For this classification scheme three criteria are considered: (a) the necessary spatial information and how it needs to be structured, (b) the movement selection procedure and (c) the behavioural repertoire that this strategy supports. More complex navigational strategies require increasingly more complex computational skills but also provide the animal with more and more navigational competence (***Table 1.1***). In this framework a basic distinction is made between *local navigation* and *way finding* based on the sufficiency of guidance cues from the immediate sensory environment (Prescott, 1994). A detailed description of each of these strategies goes beyond the scope of this thesis, but can be found in (Franz and Mallot, 2000; Trullier et al., 1997). Here I can only give a brief overview.

Local navigation strategies rely only on information from within the animal's range of perception. Four types of local navigation strategies, in order of increasing complexity, are search, direction-following, aiming and guidance (***Table 1.1***):

- During search an animal does not show any active orientation toward the goal. The animal only needs to be able to recognise the goal once it has arrived.

- During direction-following an animal uses locally available directional cue, could be from odour trail or following sky compass or homing vector generated during path integration (see ***section 1.1.2***. and Franz and Mallot, 2000). Keeping a fixed heading based on distant visual cues is the navigational strategy used during compass orientation. Monarch butterflies use a sun and magnetic compass to guide their long-distance migration to distant but valued food sources (Guerra and Reppert, 2015). Compass navigation is a navigational strategy that is often used by animals to move in a straight path, even in the absence of a precisely defined goal. Dung beetles, for instance, use the sun or the moon as guidance cues to roll their dung balls in a straight path away from potential competitors who might hijack their cargo (el Jundi et al., 2015). Many insects use the polarisation pattern on the sky as a compass cue (Mappes and Homberg, 2004a; Philipsborn and Labhart, 1990; Wehner, 2003), the underlying neural circuitry has been extensively studied in the locusts (Bech et al., 2014; Heinze and Homberg, 2007).
- Aiming requires a salient cue at the location of the goal, which can be sensed from a far distance. To approach the goal the animal fixates this cue in its frontal field of view and moves forward (Franz and Mallot, 2000). The sensory cue, which can be visual landmark, the source of an odour or an acoustic signal, is also referred to as beacon and the navigational strategy as taxis or beaconing. The advantage of aiming over direction-following is that the goal can be approached from any direction. Female crickets in search of a mating partner, for example, follow the calling song of a conspecific male, a behaviour known as phonotaxis (Regen, 1913). I will explore course control during cricket phonotaxis in more detail in chapter 2 of this thesis. Interestingly, foraging geckos and parasitic flies take advantage of such broadcasted calling songs to localise their prey (Cade, 1975; Sakaluk and Belwood, 1984). Auditory beaconing has also been reported in foraging mammals, for example in bats (Buchler and Childs, 1981).
- Guidance allows an animal to navigate toward a goal that is not marked by any salient cue. Rather, the animal memorises the spatial configuration of other sensory landmarks and their relation to the goal. It then uses this information to guide its path by making movements that minimise the mismatch between the currently perceived landmark configuration and the memorised configuration that marks the goal location (Trullier et al., 1997). In the insect navigation literature on landmark guidance the memory of the landmark configuration is also often referred to as snapshot memory. The existence of snapshot memories has been postulated based on behavioural experiments in bees and ants (Cartwright and Collett, 1987; Judd and Collett, 1998; Wystrach et al., 2013), but so far no neural correlate has been found.

Note that local navigation is not necessarily limited to small spatial scales: monarch butterflies, for instance, use a local navigation strategy based on a sun compass (locally available information) to migrate hundreds of kilometres (Guerra and Reppert, 2015).

Way finding strategies are necessary for navigation when some relevant guidance cues, especially the final goal, are out of an animals sensory range.

- The simplest form of way finding is a recognition-triggered response strategy, where an animal moves sequentially from one familiar place to the next (Trullier et al., 1997). It is also sometimes referred to as route following, as the sequence of navigational decisions is aided by environmental cues positioned along a familiar route. It has been suggested that this strategy is used by ants and bees when they navigate on idiosyncratic routes (Cartwright and Collett, 1987; Judd and Collett, 1998; Narendra, 2007; Zhang et al., 1999). The idea is that a sequence of snapshots is stored during learning of the route and the animal later follows the guidance of one snapshot to the next to find their way to a known food source or their nest. Similarly, flying pigeons follow the patterns of highways during homing (Lipp et al., 2004), a strategy that bats may also employ during some of their foraging runs (Tsoar et al., 2011).
- Topological and metric navigation is possible if an animal is able to build up internal representations of its environment, i.e. some sort of map (Trullier et al., 1997). Such an internal representation of space stores information about known places in the environment as well as information on their relative spatial relationship. The map used during topological navigation is essentially a graph composed of a set of known routes along which the animal can move using the route following strategy. In contrast, metric navigation requires a full map of the environment, which allows the animal to plan and navigate new trajectories to the goal. These internal representations of space have also been termed 'cognitive maps' (Tolman, 1948). Since cognitive maps are not strictly task-bound they can form a substrate that can be flexibly used for course control, planning, spatial learning and memory (Menzel et al., 2005; Moser et al., 2008). The idea of cognitive maps has become increasingly popular with the discovery of potential neural correlates thereof, which I will briefly discuss later (Moser et al., 2008).

Thus, to support more flexible forms of navigation, i.e. way finding strategies, the animal needs to build up some sort of internal representation of space or routes, which form a substrate for route planning through known or even novel terrain. If an animal has no knowledge about its environment it may use search strategies to explore the space (Wehner and Srinivasan, 1981).

Once a navigating animal has acquired knowledge about its environment, it may use more complex and versatile strategies (Trullier et al., 1997).

Table 1.1: Navigation hierarchy proposed by Trullier and colleagues (1997) and extended by Franz and Mallot (2000). Table modified from Franz and Mallot (2000). LM, landmark.

	Strategy	Stored spatial information	Procedure	Navigation competence
Local navigation	Search	None	Taxis, goal-recognition	Finding the goal without active goal orientation
	Direction-following / compass navigation	None	Align course with locally available global direction cue; approach	Finding the goal from one direction
	Aiming/ beaconing	None	Identify and fixate goal in front, approach	Finding a salient goal from a catchment area
	Guidance	Identity of LM configuration, raw state of sensory inputs at goal	Attain spatial relation to the surrounding objects	Finding a goal defined by its relation to the surroundings
Way finding	Recognition-triggered response / route following	LM configurations defining places each with local directional reference frame; direction of movement that leads to the recognition-triggered response	Self-localise through place recognition; orient relative to known place; move in goal-associated direction	Following fixed routes
	Topological navigation	Set of LM configurations linked by topological relationships	Plan route as sequence of places linked to previously experienced places	Flexible concatenation of route segments
	Metric navigation	Set of LM configurations linked by metric relationships	Plan trajectory, which will be followed by lower level strategies (can be new path)	Finding path over novel terrain

Of course, extrapolating directly from complex behaviour to complex internal representations can be misleading (Braitenberg, 1986) and in some cases it is difficult to distinguish between different navigational strategies and related computations based on behavioural studies alone. Foraging desert ants, for example, display impressive navigational skills, including memorising long, stereotypic foraging routes, path integration and the ability to flexibly combine route-guiding cues across different sensory modalities (Bregy et al., 2008; Collett, 2012; Collett et al., 2002; Wehner, 2003). However, this complex behaviour may rely on simpler internal representations of spatial information than those employed by many mammals. Navigating

desert ants may not form an explicit representation of their environment in the form of a cognitive map, but may instead rely on implicit knowledge. This could be in the form of directions, such as a homing vector (Müller and Wehner, 1988), or in form of templates of visual scenes along the path that can be used to compute and maximise familiarity metrics (Baddeley et al., 2012; Judd and Collett, 1998). Generally, proving that an animal uses a complex search strategy or even a cognitive map, rather than relying on a combination of the other strategies has proved challenging (Bennett, 1996; Capaldi and Dyer, 1999). The strongest evidence for abstract internal representations in insects come from studies in honey bees. Honey bees can learn the location of their nest and foraging sites (Menzel et al., 2005) and are able to communicate this knowledge to conspecifics (Esch et al., 2001; von Frisch, 1967). Bees can also be trained in a delayed-match-to-sample task to learn abstract association rules such as 'sameness' or 'difference' of the cue and sample pattern to predict the location of food (Avarguès-Weber and Giurfa, 2013; Giurfa et al., 2001). This capacity for flexibility, abstraction and generalisation in learning honey bees suggests the use of sophisticated internal representations rather than just the modification of reflexes or generation of new reflex pairs (Webb, 2004b; Webb, 2012).

To solve a given navigational task, many of the strategies described above are used in combination, with animals flexibly switching between different guidance mechanisms depending on their suitability in a given context. This has been extensively studied on a behavioural level in foraging ants (Bregy et al., 2008; Graham and Cheng, 2009; Narendra, 2007; Wystrach et al., 2013). Besides being able to switch between different navigational strategies, an animal that is engaged in a given navigational strategy needs to remain responsive to sudden changes in its environment. For example, an animal following a sun-compass or an auditory beacon still needs to avoid predators or collision with objects in its path. Recent studies in the locust have demonstrated a neural mechanism by which insects may be able to switch between compass-guided navigation and escape from approaching predators (Bockhorst and Homberg, 2017). Neurons in the locust sky-compass network not only respond to polarised light, but also to certain visual cues: novel small visual objects moving through their field of view and expanding disks creating so-called looming stimuli characteristic of an approaching predator (Bockhorst and Homberg, 2015; Rosner and Homberg, 2013). Responses of these neurons to polarised light adapted over time when the polarisation direction remained constant. When the locust was simultaneously presented with small moving objects and stationary polarised light, some of the bimodal neurons showed dis-adaptation to the stationary polarised light (Bockhorst and Homberg, 2017). The authors suggest that this may

represent a mechanism for how a locust can realign itself with its previous direction of travel after an escape manoeuvre. In chapter 2 of this thesis we will discuss a similar problem, namely obstacle negotiation during cricket phonotaxis behaviour.

Executing any one of the behavioural strategies detailed above requires that an animal's brain performs an associated set of underlying cellular and circuit-level computations. Typically, several kinds of computations need to be carried out to support any one of the above-mentioned navigational strategies. In case of path integration, for example, the animal needs to be able to extract a compass signal, integrate a measure of how far it moved, and it needs to store and combine this information. In practice each of these abstract computations can be implemented in multiple ways. For example, from behavioural experiments we know that ants can use both optic flow and step count to measure how far they moved (Pfeffer and Wittlinger, 2016; Wittlinger et al., 2007). Similarly, the compass signal can be updated based on external cues such as the polarisation pattern of the sky or by precisely integrating ones own movements (Collett and Collett, 2000). Recent work in the fruit fly has shed light on the neural correlate of such a flexible angular path integrator, which receives multimodal information and is able to update an internal representation of the animals heading based on both visual and self-motion cues (Seelig and Jayaraman, 2015).

1.1.4. Navigational behaviours studied in this thesis

This thesis will focus on navigational behaviours in two species, auditory beaconing in female field crickets during phonotaxis, and landmark-guided navigation in walking flies. I will now briefly introduce the navigational challenges associated with these two behaviours.

Chapter 2 of this thesis describes how crickets integrate course corrections in response to mechanosensory antennal signals with phonotactic steering. During phonotaxis a female cricket selectively responds to the song of a conspecific male, which requires the animal to perform auditory pattern recognition (Kostarakos and Hedwig, 2012). At the same time the animal has to extract directional information from the stimulus, i.e. localise the direction of the call (von Helversen and von Helversen, 1995). Finally, the cricket has to convert this directional information from the guidance cue into adequate course adjustments, a sensorimotor integration problem, which female crickets have solved by integrating minute steering responses directly into their regular walking pattern (Hedwig and Poulet, 2005; Witney and Hedwig, 2011). In a natural environment, crickets engaged in phonotaxis still need to be ready

to respond to other stimuli of importance to avoid, say, obstacles and predators. This issue will be discussed in more detail in chapter 2.

Chapters 3 and 4 of the thesis focus on landmark-guided navigation in walking fruit flies. As described earlier, visual landmarks are used as guidance cues in a number of navigational strategies — beaconing, compass-guided navigation and route-following — where they can either directly mark the location of a goal or serve as a more general orientation aid (Trullier et al., 1997), Visual landmarks are often used in conjunction with other sensory guidance systems (Collett et al., 2002; Taube, 2007; von Helversen and Wendler, 2000). Beaconing and compass-guided navigation require the animal to keep a fixed heading angle relative to a visual landmark, a behaviour known as tracking or fixation. I will investigate landmark fixation in naïve walking flies and discuss the use of visual landmarks as a calibration tool during path integration-based navigation in chapter 3. In chapter 4 I will test whether flies are able to exploit visual landmark cues to more effectively avoid spatially localised aversive stimuli, a behaviour which I will refer to as landmark-assisted avoidance.

1.1.5. Challenges when studying the neural circuitry underlying navigational behaviours

A number of characteristics of animal navigation render the study of neural processing underlying navigational behaviours challenging. One such characteristic is the tight interaction between navigation and sensory experience. An animal's sensory experience strongly depends on its own actions, as they govern how it moves around in space and samples its environment. Those experiences, in turn, can shape an animals future perception, responses and actions. To gain a complete understanding of neural mechanisms underlying navigational behaviours we therefore likely need to study neural circuitry in moving animals. Indeed, early electrophysiological studies in freely moving rats led to the discovery of internal representations of space in mammals such as place and head-direction cells (O'Keefe and Dostrovsky, 1971; Taube et al., 1990), which had a lasting effect on navigation research. Where recordings in freely moving animals are not feasible, virtual reality (VR) techniques, allowing a restrained and head-fixed animal to interact with a virtual sensory environment, are an alternative. I will discuss this approach in more detail in ***section 1.2***. Besides being technically challenging, the partial loss of control over the stimulation protocol when allowing an animal to interact with its sensory environment often entails challenges when it comes to data analysis.

Furthermore, neural processing during navigational behaviours frequently involves recurrent computations with multiple internal feedback loops, which pose challenges when trying to dissect the function of the underlying neural circuitry (Knierim and Zhang, 2012; Moser et al., 2008). Often, targeted perturbations of specific circuit components are necessary to test hypotheses about the neural circuit architecture. Finding suitable targets for perturbations and interpreting the effect of a perturbation often requires detailed knowledge of the circuit connectivity.

Some parameter of interest of the external environment or of an animals relation to the environment, such as head direction, are encoded by a population of cells (Taube, 2007). Detecting such population codes can be challenging, when activity is only recorded from a subset of the respective population or when a mixed population of cells is monitored. Calcium imaging permits the recording of a large number of neurons, but selectively recording from a defined population of cells requires targeting of the calcium sensor. A specific type of cell may be targeted by localised injections, by using genetic techniques or a combination of both.
The above mentioned head-direction cells generate an internal representation of the animals heading based on both visual and self-motion cues (Taube, 2007; Taube et al., 1990). Integration of information from several sensory modalities — and thus typically from various brain regions — is common to many navigational tasks. In addition to integration of external stimuli, animals must often take into account their internal metabolic state and the physical constraints of their bodies (Bisch-Knaden and Wehner, 2003; Dus et al., 2013; Mischiati et al., 2014). Understanding such distributed computations without knowing the activity of all involved neural populations is difficult.

Internal representations underlying mammalian navigation have been amongst the most evocative phenomena described in neuroscience (Moser et al., 2008; Moser et al., 2014; Taube, 2007). However, the challenges outlined above have limited the progress that has been made toward dissecting the mechanisms involved in generating such representations and understanding how they are used during navigational tasks.

1.1.6. Studying the neural basis of complex computations is tractable in insects

Gaining a mechanistic understanding of dynamic, recurrent neural computations distributed across populations of neurons in multiple brain regions far from the periphery requires not only monitoring and manipulating specific neural populations during behaviour, but also knowing the connectivity of the underlying circuitry. This is still experimentally challenging in mammals, but is feasible in numerically simpler and smaller insect brains. Their physically small brains render electron microscopy-based reconstruction of circuits more tractable and allow simultaneous imaging of multiple brain regions (Cardona et al., 2010; Lemon et al., 2015; Takemura et al., 2015). The calcium activity of single neurons or of large populations of cells can be imaged either by injecting dyes or expressing genetically encoded fluorescent sensors (Sobel and Tank, 1994; Tian et al., 2009). In the fruit fly *Drosophila melanogaster*, genetic tools enable targeted physiology and optogenetic perturbation of neural activity in actively behaving animals with high temporal and spatial control (Bath et al., 2014; Chiappe et al., 2010; Claridge-Chang et al., 2009).

It is plausible that some neural computations carried out during navigational behaviours are shared between insects and mammals. Many insects use behavioural strategies that share similarities with those employed by vertebrates, and recent work on the underlying neural computations suggests that insects may rely on similar neural processing and internal representations. I would like to illustrate this point with two examples: Computations underlying efference copy mechanisms and the use of an internal compass in fruit flies.

Internal models underlying efference copy mechanisms that allow the animal to predict effects of its own actions and distinguish self-generated from externally generated sensory signals have been studied in the context of eye saccades and head movements in primates (Duhamel et al., 1992; Wurtz and Goldberg, 1971). Flies carry out similar computations when suppressing flight stabilisation reflexes during voluntary turns (von Holst and Mittelstaedt, 1950). A recent study investigated the cellular basis of this suppression and found that optic-flow processing neurons in the fly visual system receive turn-direction-specific feedback with the appropriate sign and latency to suppress self-generated sensory input (Kim et al., 2015). The amplitude of the feedback signal scales with the visual drive, which depends not only on the turn speed but also on the structure of the visual environment. Investigations into how the flexible scaling of the motor-related feedback signal is achieved should clarify the level of sophistication of the underlying internal model.

Mammals possess abstract neural representations of space that support a variety of navigational strategies (Etienne and Jeffery, 2004; Moser et al., 2014). Behavioural studies in dragonflies, ants and bees, amongst others, suggest that also insects use internal representations to encode the direction and distance of a goal, let it be prey, the nest or food (Esch et al., 2001; Mischiati et al., 2014; Müller and Wehner, 1988; von Frisch, 1967). Direct evidence for neural circuitry implementing such an abstract representation comes from flies (Seelig and Jayaraman, 2015). Calcium imaging in walking fruit flies revealed the existence of a neural compass, which can be flexibly updated based on visual or self-motion cues, depending on availability of sensory information. I will discuss this finding in more detail in the context of landmark guidance and path integration in chapter 3.

Thus, there is mounting evidence that mammalian and insect brains carry out similar computations and that essential features of the implementation of specific neural computations can generalise well beyond a single system (Seelig and Jayaraman, 2015; Taube, 2007). Studies in the olfactory and visual systems have already highlighted similarities between insect and mammalian sensory circuit function (Borst and Helmstaedter, 2015; Wilson, 2013). Although studies of cognitive computations in insect brains are still in their early stages, these simpler systems may provide a more navigable path toward understanding some of the fundamental synaptic, cellular and circuit mechanisms underlying cognition (Chittka et al., 2012).

1.2. Approaches to studying neural computations involved in navigation

While there is increasing evidence that insect brains rely on similar computations and internal representations that are thought to underlie navigation in mammals (Knierim and Zhang, 2012; Seelig and Jayaraman, 2015), challenges remain in causally linking physiological data to behaviour.

Physiological recordings in immobilised, i.e. non-behaving animals, have provided many examples of high-level sensory representations in insects (Heinze and Homberg, 2007; Hige et al., 2015a; Perez-Orive et al., 2002) and revealed the existence of synaptic plasticity that is likely used to associate these sensory representations with appetitive or aversive experiences (Cassenaer and Laurent, 2012; Hige et al., 2015a; Hige et al., 2015b; Owald et al., 2015). However, a comprehensive assessment of the nature of internal representations and their potential role in goal-directed navigation requires that such recordings be performed in actively behaving animals. Understanding the neural basis of the remarkable navigational behaviour of bees and ants, for example, may require monitoring the activity of specific neural circuits in foraging animals.
Two closely related obstacles have limited progress so far: Recording neural activity during navigation behaviour and designing suitable behavioural paradigms that can be used under such conditions. I will begin with addressing the first issue before discussing solutions for overcoming the latter.

1.2.1. Techniques for recording neural activity in behaving animals

Owing to the development of a miniaturised two-photon microscope, which can be mounted on an animal's head, neural activity of large neuron populations can be monitored in freely moving rats with subcellular resolution (Helmchen et al., 2001). Due to their smaller size and more fragile exoskeleton, this approach, however, is hard to transfer to insects. An alternative method for recording neural activity in freely moving animals is implanted electrodes (Taube et al., 1990). Further development of extracellular recording techniques in freely behaving large insects (Chan and Gabbiani, 2013; Duer et al., 2015; Martin et al., 2015; Thomas et al., 2012) may eventually enable study of neural dynamics in navigating insects, although identifying and targeting the relevant neurons with these techniques remains a challenge. A different physiological strategy, which has been the mainstay of primate research for decades, is to record neural activity during head-fixed behaviour. Head-fixation constrains behavioural output,

but allows for the sensory environment to be carefully controlled and enables high quality neural recordings. This strategy has been employed in bees to study how olfactory representations are affected by learning (Carcaud et al., 2009) and how visual stimulus-evoked local field potentials are modulated by behavioural choices (Paulk et al., 2014). It has also been applied in many other insects to examine sensory representations and sensorimotor integration in the context of orienting (Bender et al., 2016; Mason et al., 2001; Poulet and Hedwig, 2005).

In adult *Drosophila*, the development of head-fixed behavioural paradigms has allowed the combination of powerful genetic tools with whole-cell patch clamp recordings and two-photon imaging of genetically encoded calcium indicators (Maimon et al., 2010; Seelig et al., 2010). The fly's small brain size allows physiological access to the entire central brain with a minimally invasive preparation. Comprehensive anatomical and behavioural genetics studies (Aso et al., 2014; Wolff et al., 2015) help to guide the search for cellular correlates of specific internal representations. Repeatable access to these genetically identified cell types permits precisely targeted monitoring and perturbation of neural activity during behaviour. Overall, the ability to reliably access the same sets of identified neurons across trials and animals enables rigorous and mechanistic circuit analysis. In *Drosophila* it may also be possible to exploit genetic targeting of small populations of neurons for low-resolution fluorescence imaging in free walking flies with 'chronically' implanted windows (Grover et al., 2016).

1.2.2. Development of paradigms to study navigational behaviours in head-fixed animals

A challenge when studying navigational behaviours in head-fixed animals has been the development of behavioural paradigms that capture the complexity of a navigational task while being compatible with the restrained preparation. Mammals are usually trained for several weeks before they perform cognitively demanding tasks in physiological settings. Insects have shorter memories, a shorter lifespan, and only a few species can be chronically implanted with recording devices. Thus, insect physiologists seldom have the opportunity of using training protocols that last more than a few hours. Instead, they typically rely on tasks that exploit or extend an animal's natural behaviour.

Simple course control mechanisms have been studied in the context of stabilisation reflexes such as optomotor responses and stripe fixation (Bahl et al., 2013; Götz, 1975; Maimon et al., 2008). Foraging and courtship behaviours have been a fruitful source of more complex naïve

behaviours. Examples of navigational courtship-related behaviours are cricket phonotaxis (see chapter 2, Hedwig, 2000; Zorović and Hedwig, 2011) and pheromone tracking in moth (Gray et al., 2002). Despite numerous descriptions of sophisticated navigation in the context of foraging in freely moving animals (Collett and Collett, 2002), to my knowledge no foraging assays have been developed for head-fixed insects yet.

An alternative to studying innate navigation behaviours is to extend an animal's behavioural repertoire through operant conditioning. Conditioned behaviours can be targeted to answer a specific research question. This has been used extensively in vertebrate neuroscience, for example in odour or visual discrimination tasks (Abraham et al., 2004; Fetsch et al., 2012). In insects, conditioning of navigational behaviours has been most successful with paradigms building on natural predispositions to learn certain associations. For example visual sucrose-reward learning in honey bees (Giurfa et al., 2001) and heat-avoidance in a visual place learning assay for walking fruit flies (Ofstad et al., 2011). However, none of the available operant conditioning paradigms for head-fixed insects captures the complex navigational behaviours observed in the wild. Instead, the animals behavioural output is typically restricted to left/right turn decisions such as in a commonly used visual operant conditioning task for tethered flying flies (Brembs and Heisenberg, 2000; Liu et al., 2006).

Some of the previously described complex navigation behaviours may be elicited in head-fixed animals by providing the relevant sensory environment and a broad interface for the animal to interact with it. In the next section I will present approaches of how such a sensory environment can be built with a focus on using virtual reality (VR) techniques.

1.2.3. Studying navigational behaviours using virtual reality techniques

There are two basic approaches to building a sensory environment for behavioural studies in head-fixed animals. One is to provide sensory stimuli in a so-called 'open-loop' manner, where the animal's actions do not serve as an input to the sensory stimulus provided by the experimenter. An advantage of this approach is the high degree of control over the stimulus, which allows experimenters to average the animal's responses over the course of many short trials. This approach has been used successfully to study early sensory processing but also to dissect basic course-control mechanisms based on stereotyped steering responses, for example to visual stimuli in flies (Götz, 1964; Tuthill et al., 2014) and auditory stimuli in crickets (Hedwig and Poulet, 2005; Kostarakos and Hedwig, 2012). However, the unnatural temporal pattern of

the sensory stimulus and the lack of interactions between the animal and its environment render this approach ill-suited to study more complex navigational behaviours.
An alternative approach is the use of a VR environment based on 'closed-loop' feedback of the animal's behaviour onto the presented stimulus, which allows the animal to interact with its sensory environment. This approach has a number of advantages. Firstly, it makes high-quality neurophysiological recordings compatible with the study of complex navigational behaviours (***section 1.2.1***). Secondly, the experimenter has full control over the environmental stimuli and is not limited to recreating a faithful virtual replica of the real world. This means that the virtual environment and behavioural tasks therein can be shaped to test specific hypothesis about the computations underlying a navigational behaviour. For example, one can limit the sensory environment to a small set of stimuli and investigate how this defined set of stimuli affects a behaviour of interest (Schuster et al., 2002). Furthermore, the experimenter can provide reduced versions of rich natural stimuli to probe which stimulus features are used by the animal during navigation. This is much harder or even impossible to do in field studies (Legge et al., 2014). Thirdly, the experimenter can change the rules that govern the interaction between an animal's actions and the virtual environment (Schuster et al., 2002). By introducing short delays or temporarily switching to open-loop conditions, for instance, it is possible to disentangle sensory from motor-related neural processing (Minderer et al., 2016). Finally, behavioural experiments can relatively easily be combined with closed-loop perturbations of neural activity. Amongst others, this can be used to flexibly add new virtual sensory stimuli to the virtual environment by optogenetically activating sensory neurons, as we will see in chapter 4. Alternatively, closed-loop optogenetic activation or inhibition of neurons, which are thought to be involved in the execution of a navigational behaviour, offers a sensitive method for testing hypotheses regarding underlying neural computations. Tools are available that allow perturbations triggered on behavioural events in free walking flies (Bath et al., 2014), but to understand complex, recurrent neural circuits, one might occasionally need to perform perturbations triggered on neural events and simultaneously observe behaviour, which is only possible in VR-based paradigms. Overall, experimental paradigms in VR may be able to bridge the gap between naturalistic studies during free movement and reductionist approaches in restrained animals.

1.3. Aims of this thesis

As described in previous sections, a major obstacle in understanding neural processing underlying navigational behaviours has been to find ways to combine behavioural with neurophysiological studies. Currently available neural recording techniques require the animal to be tethered or head-fixed, which constrains the animals behavioural output and interaction with its sensory environment. The aim of this thesis was to develop new behavioural assays for studying navigation in tethered insects. I extended existing spherical treadmill systems for tethered walking crickets (Hedwig and Poulet, 2004) and flies (Seelig et al., 2010) by providing the animals with a more complex sensory environment. Specifically I developed assays for studying multisensory integration in field crickets and visually guided navigation in fruit flies.

In chapter 2 of this thesis I present a paradigm for studying bimodal integration in tethered walking crickets and I investigate how responses to antennal mechanosensory stimuli are integrated with phonotactic steering manoeuvres. To do this I characterise walking responses to antennal stimulation during spontaneous walking and compare them to responses during goal-directed phonotaxis.
In the following chapter I transition to work with *Drosophila*, where I first present a novel two-dimensional VR system for studying landmark-guided navigation in head-fixed walking flies. This new system was carefully validated to ensure its technical functionality. Then I show that tethered walking flies in this VR behave similar to free walking flies. Furthermore, I characterise sex- and genotype specific differences in innate landmark interaction behaviour in free and tethered walking flies. In chapter 4 I extend this visual VR environment by adding aversive optogenetically delivered virtual sensory stimuli. This allows me to I investigate whether flies exploring a bimodal VR are able to use visual landmark cues to more effectively avoid aversive areas.
While the scope of this thesis is limited to behavioural studies, it opens up new possibilities for studying neural processing in tethered insects during navigation in complex, multimodal and virtual environments.

Chapter 2

Behavioural integration of auditory and antennal stimulation during phonotaxis in the field cricket *Gryllus bimaculatus* (DeGeer)

2. Behavioural integration of auditory and antennal stimulation during phonotaxis in the field cricket *Gryllus bimaculatus* (DeGeer)

2.1. Introduction

Mating success reflects an animal's fitness (Rodríguez-Muñoz et al., 2010; Simmons, 1988). This renders mating behaviour a convenient system for behavioural studies as it combines behavioural robustness and low variability with a range of interesting computational problems such as multi-modal sensory integration, the control of complex behavioural sequences and action selection. We present a novel behavioural paradigm that allows studying bimodal integration in the context of cricket mating behaviour.
The mating behaviour of female field crickets consists of several stages: acoustically guided approach of a mate, close-range courtship, and finally copulation (Adamo and Hoy, 1994). We focus on the first stage, during which female crickets orient and walk toward a male's calling song while searching for a mating partner, a well-studied behaviour known as phonotaxis (Adamo and Hoy, 1994; Murphey and Zaretsky, 1972; Regen, 1913).

Most studies of phonotaxis have been performed under tightly controlled laboratory conditions as a purely auditory orientation task (Gerhardt and Huber, 2002; Schmitz et al., 1982; Weber and Thorson, 1989). However, in its natural habitat a female cricket has to navigate through potentially dense grassland while tracking the male's calling song. Under these conditions its phonotactic behaviour will be affected by other environmental stimuli, which could influence course control. Indeed, tracking speed and tracking accuracy of female crickets performing phonotaxis are lower when measured in the field compared to results obtained under controlled laboratory conditions (Hirtenlehner and Römer, 2014; Hirtenlehner et al., 2014).

Besides auditory cues, mechanosensory stimuli perceived via the antennae may play an important role in course control. Antennal detection and exploration of objects during navigation has been described in cockroaches (Harley et al., 2009; Okada and Toh, 2006; Ritzmann et al., 2012). Walking crickets also constantly move their long antennae, sampling the near space ahead (Horseman et al., 1997).
We characterise responses to mechanosensory antennal stimulation in walking crickets and investigate how they affect phonotaxis and whether they are modulated during phonotaxis. To

do this, we have developed a behavioural paradigm in tethered crickets that combines a well-established experimental approach for studying steering manoeuvres during phonotaxis (Hedwig and Poulet, 2005) with antennal mechanosensory stimulation. While previous studies of antennal sensing in walking insects have used solid objects such as a plate or a rod (Okada and Toh, 2006; Ritzmann et al., 2012; Schütz and Dürr, 2011), we chose a sound-transparent metal wire mesh, which allowed us to deliver antennal and acoustic stimulation independently. We stimulated the antennae by moving the wire mesh into antennal reach of tethered female crickets walking in darkness on a trackball. To investigate how potentially conflicting steering manoeuvres are integrated during phonotaxis, we measured responses to antennal stimulation both in the absence and in the presence of acoustic stimulation.

2.2. Materials and Methods

2.2.1. Experimental protocol

Animals

All experiments were performed with virgin female crickets (*Gryllus bimaculatus* DeGeer). Animals were isolated before their final moult, and tested at least ten days after, to ensure phonotactic responsiveness. At least one day before the first behavioural experiments an insect pin, which served as a tether, was waxed onto the first abdominal tergite.

Experimental setup

Females were positioned in normal walking posture and tethered above a freely rotating trackball. The trackball system (details in Hedwig and Poulet, 2005) was used to record each cricket's forward walking and steering velocity. Briefly, a 2D optical mouse sensor positioned underneath the trackball records any ball rotations along the forward-backwards (pitch) and left-right (roll) axis. Ball movement increments of 127 µm along these two axes are encoded as a single 150 µs long analogue voltage pulse in two electrical channels. For the pitch axis channel positive pulses encode forward movement increments and negative pulses backwards movement. Similarly, positive and negative pulses in the roll axis channel encode left and right movements. The trackball system was placed in a chamber lined with sound damping foam, which was closed during experiments to exclude environmental light and noise. Two speakers were installed at a distance of 57 cm from the trackball at 45 degrees off the longitudinal axis of the cricket, to provide acoustic stimuli from the left and right side (***Figure 2.1 A***). An acoustically transparent metal mesh (60 x 65 mm, 0.7 mm wire thickness, 5.0 x 3.0 mm openings) was used

to generate a mechanosensory stimulus. It was attached to a linear motor (LM1247-060-01 Quickshaft Linear Motor, Faulhaber GmbH, Schoeneich, Germany) allowing controlled movement toward and away from the cricket's right antenna along the radial axis at 45 degrees (***Figure 2.1 A***). Video recordings (Common Vision Blox, Stemmer Imaging, Puchheim, Germany) were conducted at 60 Hz frame rate with a camera (DALSA Genie-HM640, Stemmer Imaging Ltd., Surrey, United Kingdom) placed above the cricket under illumination with red light (690 nm, LED, ELJ-690-629, Roithner Lasertechnik, Vienna, Austria), to which cricket eyes are insensitive (Labhart et al., 1984). The two pulse trains recorded by the trackball system, the envelope of the sound signals sent to the left and right speakers, and a copy of the signal that was sent to the linear motor to control the mesh position were all recorded at 10 kHz using an A/D board (PCI-Mio 16-E-4; National Instruments, Newbury, UK) controlled by software programmed in LabView (National Instruments, 5.01). In trials with simultaneous video recordings an additional channel with a pulse indicating the start of each video frame was saved with the data.

Behavioural paradigm

To elicit phonotactic walking, the calling song of *G. bimaculatus* was played alternatingly from the left and the right speaker in 40-second blocks. The parameters of the artificial calling song were chosen based on previous studies to elicit maximal phonotactic steering (Hedwig and Poulet, 2005).

To achieve antennal stimulation, the metal mesh was presented at a *'far'* position where the mesh could only be touched by the very tip (2-5 mm) of the antenna or at a '*close'* position, which was 1 cm nearer. Because body size and antennal length vary across animals, we determined for each animal individually the *far* and *close* distance. Presentation of the metal mesh will be referred to as *far* and *close* antennal stimulation, respectively (***Figure 2.1 A***). Whenever no antennal stimulation was intended, the object was moved into a resting position out of antennal reach. The movement of the mesh between the resting position and the presentation position took 1.25 s and 2.5 s for the *far* and *close* position, respectively. The beginning of the antennal stimulation period is referred to as time 0; it is defined as the moment at which the object reached its trial-specific, i.e. *far* or *close*, position.

The cricket's response to 10 s long presentation of the object was tested under three stimulus configurations: (a) antennal stimulus presented alone, (b) simultaneously with acoustic stimulation from the same side, i.e. ipsilateral, or (c) from the opposite side, i.e. contralateral (***Figure 2.1 B***). Within one trial the object was presented once at the *far* and once at the *close* position. Each experimental condition was tested twice, presenting the mesh at the two

distances in both possible orders. This resulted in a total of 6 trials per animal, which were tested in random order. Responses to 30 s long antennal stimulation were not measured in spontaneously walking crickets, but only in crickets engaging in phonotaxis, and only one trial per animal was recorded measuring first responses to *far*, then to *close* antennal stimulation.

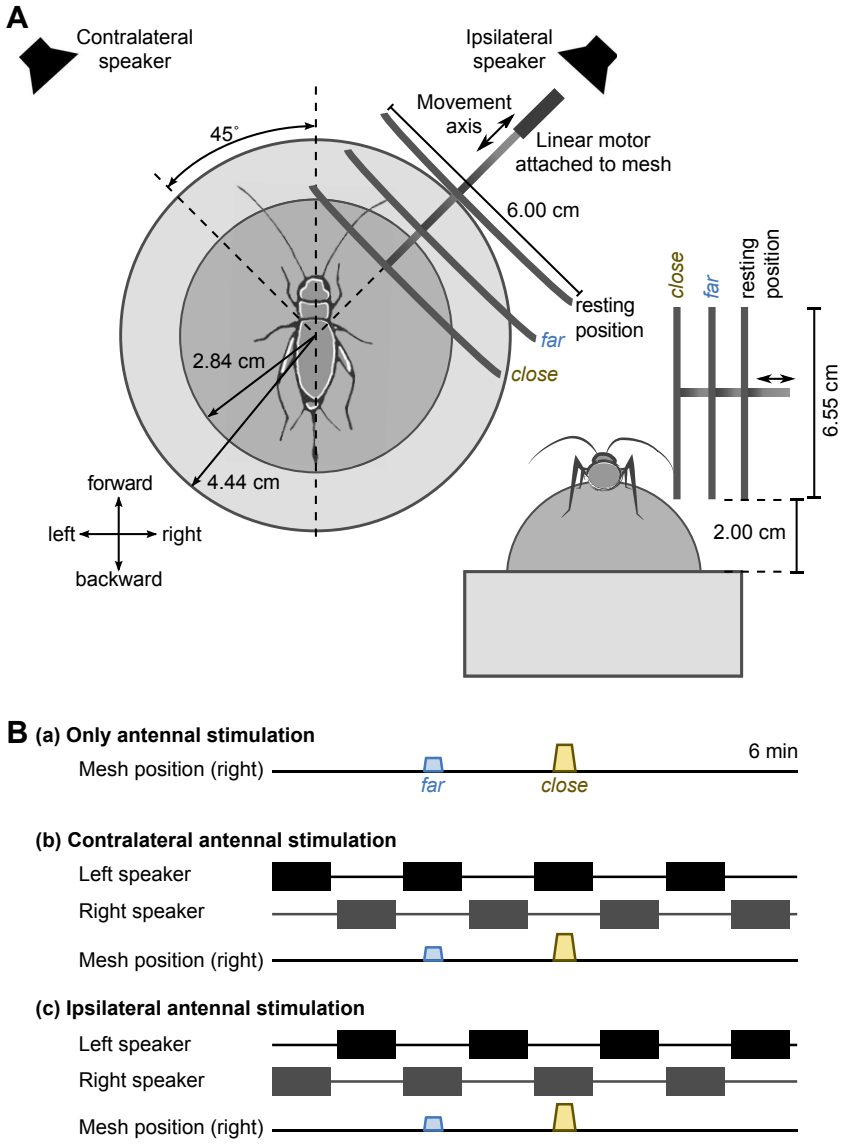

Figure 2.1: Setup and experimental protocol.
A: Arrangement of the antennal stimulation setup. The cricket is placed on a trackball. A metal mesh can be moved into and out of reach of the cricket's right antenna. Two loudspeakers are placed 57 cm away from the animal at 45 degree to the left and right.
B: Building blocks of the experimental protocols. Three protocols for acoustic stimulation are combined with two presentation orders of the antennal stimulus resulting in a total of six test conditions.

2.2.2. Data analysis

Analysis of walking velocities

The trackball, sound and mesh movement data were all recorded simultaneously (***section 2.2.1***), stored to file using custom LabView software (National Instruments 5.01) and subsequently processed with Matlab (MathWorks, Inc., Natick, MA, USA). All five data channels (pitch and roll axis channels from the trackball, the sound signals for the left and right speaker and the mesh position) were downsampled to 100 Hz. Forward and lateral walking velocities were computed from the downsampled pitch and roll trackball recordings by scaling each pulse event by the known displacement length (127 µm, see description of experimental setup in ***section 2.2.1***) and dividing by the length of the time bin (0.01 s). The recorded sound and mesh movement signals were parsed to identify the time periods of specific stimulation blocks within a trial. Trials were excluded from analysis if a cricket did not walk for most of the trial or did not show clear phonotactic steering. This selection procedure led to different sample sizes among experimental groups ranging from 14-19 out of the 31 tested animals (see ***Table 2.1*** for details). All statistical analysis was performed using R (version 3.0.0) on data that was binned into 5 s time intervals. In trials with 10 s long antennal stimulation we focused the statistical analysis on three time intervals, 'pre', 'stim' and 'post', chosen to cover the time before, during and directly after antennal stimulation. For the 'pre' interval we chose seconds [-10, -5), i.e. all data points between -10 s and -5s, including -10 s but excluding -5 s. The first half of the antennal stimulation period with seconds [0, 5) was chosen for the 'stim' interval, and seconds [10, 15) for the 'post' interval. Thus, the 'post' interval covers a time period during which crickets might still interact with the retracting mesh. In trials with 30 s of antennal stimulation we performed statistical tests on a 'pre' time interval and a 'stim' interval defined as above. In a Kruskal-Wallis test we further compared all six 5 s intervals covering the full antennal stimulation period. The placement of the time intervals is also indicated above the time axis in ***Figures 2.2 C, 2.3 B, 2.4 B*** and ***2.8 B***. Generally, the data were not normally distributed during and, in some cases, after antennal stimulation (Shaipiro tests on per fly averages computed over 5 s long time intervals) and are therefore described using median and interquartile range (IQR). For comparisons between two groups we used the Wilcoxon signed rank test for matched samples and for comparisons between more than two groups we used the Kruskal-Wallis test. The exact conditions, such as whether a one- or two-sided test was performed, are listed in the results section. We found that the order of the 10 s long mesh presentation at the two mesh distances had no significant effect on the response during the 'stim' interval, neither for lateral velocity (Wilcoxon text, $p = 0.201$) nor forward velocity (Wilcoxon test, $p = 0.471$). Therefore data were pooled over the presentation order for subsequent analysis.

Table 2.1: Sample sizes. Number of animals that have contributed to the different experimental groups before (in brackets) and after filtering out trials that did not fulfil the criteria listed in the materials and methods section. Overall 31 animals were tested, of which different subsets have contributed to the different experimental groups. For the 10 s long antennal stimulation 23 animals were tested in total, all but one under all 6 conditions. We measured responses to 30 s long contralateral or ipsilateral antennal stimulation in a subset of these 23 and 8 additional animals.

	Mesh alone (10 s)	Ipsilateral (10 s)	Contralateral (10s)	Ipsilateral (30 s)	Contralateral (30 s)
Ascending (*far*, then *close*)	18 (23)	14 (22)	17 (22)	19 (26)	19 (26)
Descending (*close*, then *far*)	19 (22)	14 (22)	18 (22)	–	–

Video analysis of antennal contacts

Video frames and trackball recordings were temporally aligned using a TTL frame indicator pulse, generated by the camera. Video frames during which an antennal contact occurred were identified manually using a custom-written Python (2.7) script. Subsequently the data were imported into Microsoft Excel and Matlab for further processing.

2.3. Results

2.3.1. Antennal stimulation evokes steering responses in spontaneously walking crickets

A comprehensive description of the walking and steering responses to antennal stimulation in walking crickets is required to understand how these responses are integrated with phonotaxis.

Walking crickets scan the space ahead by swinging their 2.0 – 2.75 cm long antennae in circulating movements. We simulated an obstacle in the cricket's walking path by positioning a metal mesh within reach of the right antenna at either a *far* or a *close* position. The cricket itself generated the mechanosensory stimulus during active exploration of the mesh. Because the mesh approached the animal in a linear movement, it came within antennal reach before it reached its final position. Video recordings showed that once the mesh came within antennal

reach, the cricket repeatedly made contact, gliding over the mesh's surface with the tip of its right antenna. Upon initial antennal contact, crickets typically turned their head toward the detected object and explored it with one or both antennae (***Figure 2.2 A*** b, c, h).

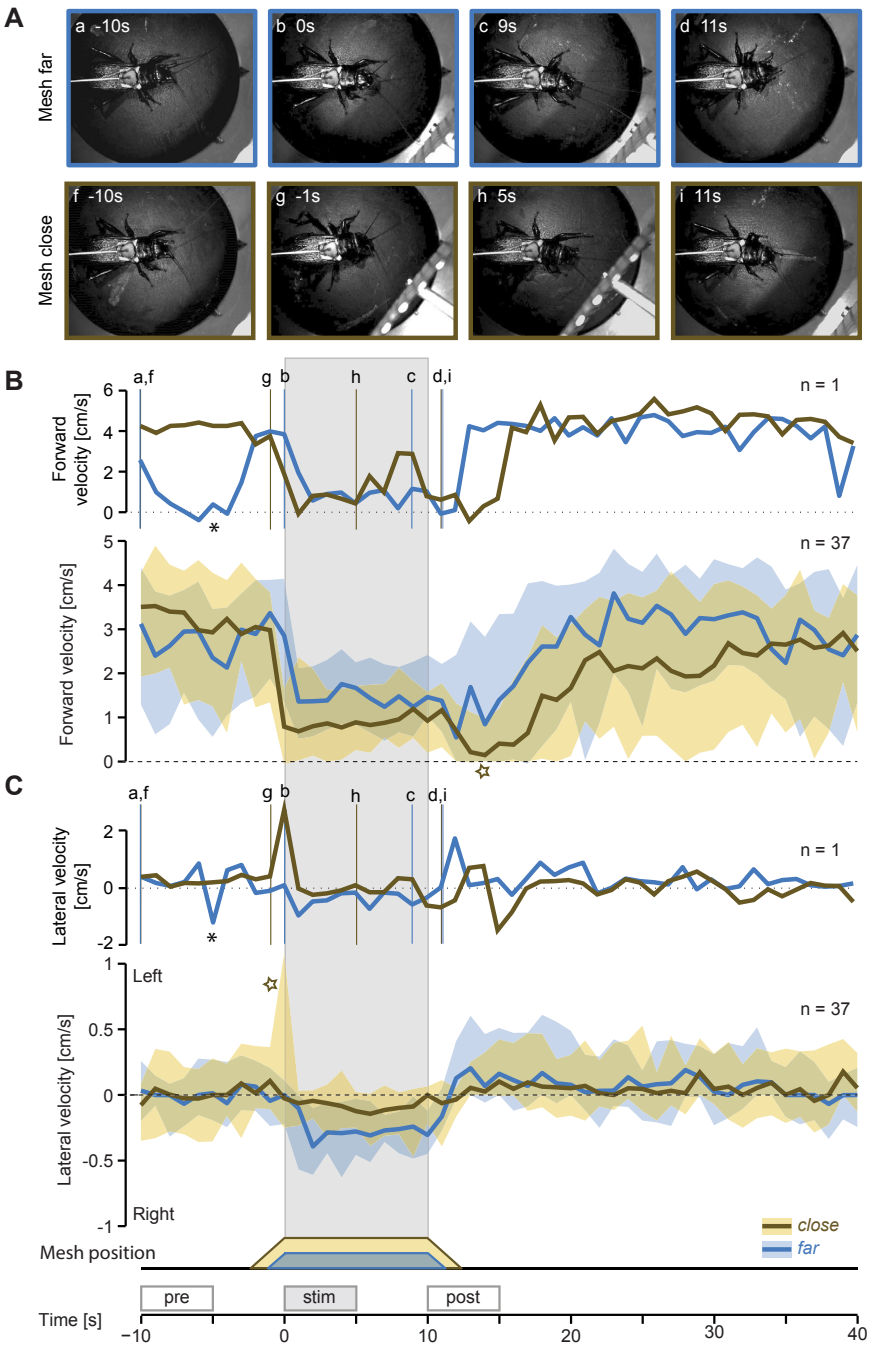

Figure 2.2: Responses to antennal stimulation in spontaneously walking crickets.
A: Video stills recorded during a *far* (top, blue frame) and a *close* (bottom, ochre frame) antennal stimulation trial. The corresponding forward and lateral walking velocities, which were recorded from the trackball, are shown in the upper panel of B and C. Positive and negative forward velocities indicate forward and backward movement.

Lateral walking velocities of 0 cm/s indicate straight walking; positive and negative lateral velocities indicate steering toward the left and right side, respectively. B: Time-course of the forward velocity over a 50 s time window averaged over one-second time intervals. Responses to *far* (blue line) and *close* (ochre line) antennal stimulation are superimposed. We show a 10 s interval before the object presentation as a reference, then 10 s of antennal stimulation (highlighted by grey shading) beginning at time 0, followed by 30 s succeeding the antennal stimulation. The upper panel shows a single trial and the lower panel the median and IQR of n = 37 trials from 20 animals with 1-2 trials per animal. Vertical lines mark the time points of the video stills shown in A. C: The time-course of the lateral steering velocity over the same 50 s time window as the forward velocity. The plot layout is analogous to B. The 5 s time intervals used in the statistical analysis ('pre', 'stim' and 'post') are marked above the time axis.

To quantify the response to antennal stimulation, we measured the cricket's forward walking (***Figure 2.2 B***) and lateral steering velocity (***Figure 2.2 C***). For both velocity measurements we present single trials (top) and the median over all measurements (bottom). Walking velocities are illustrated over a 50 s period covering the 10 s of antennal stimulation. The walking velocities of spontaneously walking crickets showed transient fluctuations (***Figure 2.2 B*** top, ***C*** top). The low-amplitude forward velocity and the simultaneously occurring short right turn before *far* antennal stimulation (see asterisks in ***Figure 2.2 B, C***) are examples of these animal-specific fluctuations. Averaging across trials and individuals, revealed systematic walking velocity changes in response to antennal stimulation (***Figure 2.2 B***, ***C*** bottom).

Preceding antennal stimulation the median forward velocity was 2.89 cm/s with an IQR of 2.44 cm/s (*close* and *far* trials pooled, 'pre' interval). In response to antennal stimulation we observed an abrupt reduction in forward speed. The deceleration occurred within the first second of *far* antennal stimulation, whereas crickets slowed down already before the start of *close* antennal stimulation, likely due to early antennal contacts with the approaching mesh. With a median walking speed of 0.91 cm/s during *close* and 1.68 cm/s during *far* antennal stimulation, crickets slowed down more in *close* trials ($p < 0.05$, paired two-sided Wilcoxon test, 'stim' interval). The cricket's forward velocity remained low throughout the antennal stimulation period independent of presentation distance. In *close* trials, crickets reduced their walking speed further after the mesh moved out of reach (see ochre star in ***Figure 2.2 B***, bottom).

The median steering velocity of spontaneously walking crickets was close to zero (i.e. -0.05 cm/s) indicating that there was no systematic turning bias before the antennal stimulation (IQR was 0.43 cm/s, centred on the median, 'pre' interval in ***Figure 2.2 C*** bottom). Within 2 s of antennal stimulation crickets on average turned toward the mesh. Steering towards the mesh was more

pronounced during *far* presentation as compared to *close* presentation; steering velocity changed significantly in *far* but not in *close* trials (*far*: $p < 0.001$, *close*: $p = 0.370$, paired two-sided paired Wilcoxon test comparing 'pre' and 'stim' interval). Crickets kept turning toward the static mesh with a constant median velocity, i.e. the response was plateau-shaped for the duration of the stimulus presentation. After *far* antennal stimulation, turning toward the mesh abated within 2 s and was followed by a weak turn toward the contralateral side during the 'post' interval (***Figure 2.2 C*** bottom).

In some antennal stimulation trials, for example in the *close* trial presented in ***Figure 2.2 C*** top, crickets initially made a fast turn away from the approaching mesh before orienting towards the stationary mesh (compare ***Figure 2.2 A*** g, h). We observed those sharp initial turns away from the mesh in 6 *close* trials and one *far* trial (***Figure 2.3***). In the median response this observation manifested itself as a peak in the IQR of the steering velocity but not in the median (see ochre star in ***Figure 2.2 C***).

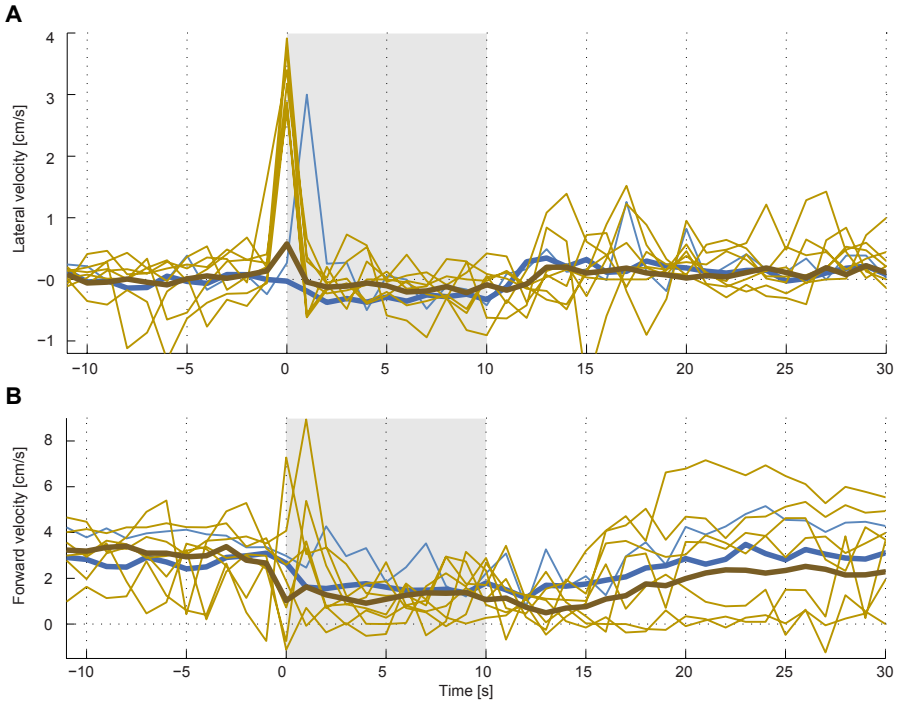

Figure 2.3: Fast 'escape-like' turns away from the approaching objects.
Lateral velocity (A) and forward velocity (B) traces of the six *close* (ochre) and one *far* (blue) pure antennal stimulation trials where animals initially performed sharp turns away from the approaching object are shown as thin lines. As a reference, the median walking velocities computed from all *close* and *far* trials is plotted with thick lines. After the initial avoidance response, animals turned towards the object and explored it with their antenna. Grey shading marks the antennal stimulation period.

These data demonstrate that in walking female crickets tactile antennal stimulation evoked a robust deceleration and a turning response directed toward the mesh in 68% of the *close* and 97% of the *far* trials. At the beginning of antennal stimulation, we observed initial rapid turns away from the approaching mesh in 16% of *close* trials and in one *far* trial (***Figure 2.3***).

Next we investigated whether female crickets performing phonotaxis are responsive to antennal stimulation and if so, how antennal-evoked and auditory-evoked responses presented from the same or different sides are integrated at the level of behaviour.

2.3.2. Crickets respond to antennal stimulation during phonotaxis with a pronounced reduction of walking speed

Phonotactic steering can be elicited in female crickets walking on a trackball by playing an acoustic model of a conspecific male's calling song (Hedwig and Poulet, 2005). We paired 10 s of antennal stimulation with an ongoing presentation of the calling song. The antennal stimulus was always presented from the right side, while the acoustic stimulus was presented from either the right, corresponding to ipsilateral stimulation (***Figure 2.4 A***), or the left, resulting in contralateral stimulation (***Figure 2.4 B***).

Crickets showed generally higher forward velocity and lower variance during phonotaxis compared to spontaneous walking: the median forward velocity was 4.05 cm/s in ipsilateral trials and 3.24 cm/s in contralateral trials (***Figure 2.4 A***, ***B***, 'pre' interval, *close* and *far* trials pooled), which was considerably faster than the median spontaneous walking velocity, 2.89 cm/s (see ***Figure 2.2 B***). Like spontaneously walking crickets, animals engaging in phonotaxis abruptly slowed down at the onset of antennal stimulation (***Figure 2.4 A, B***) and significantly reduced their forward speed compared to pre-stimulation levels in ipsilateral as well as contralateral trials (one-sided paired Wilcoxon test comparing 'pre' and 'stim' intervals: $p < 0.001$ for both ipsilateral and contralateral stimulation trials). This reduction in forward walking velocity was dependent on the presentation distance of the mesh: crickets slowed down more during *close* as opposed to *far* presentation (***Figure 2.4 C***).
Phonotaxis did not substantially alter the responsiveness to the antennal stimulus. The time-course of the responses to antennal stimulation differed between contra- and ipsilateral trials. During ipsilateral stimulation crickets maintained a low constant forward speed (grey-shaded box in ***Figure 2.4 A***) resembling the plateau-shaped response of spontaneously walking crickets (grey-shaded box in ***Figure 2.2 B***). Curiously, following *close* ipsilateral antennal stimulation,

crickets reduced their forward speed further (star in ***Figure 2.4 A***) similar to *close* antennal stimulation in spontaneously walking crickets (star in ***Figure 2.2 B***) before slowly accelerating to pre-stimulus conditions. In contralateral trials the deceleration was more transient and the forward speed significantly increased already during ongoing antennal stimulation ($p < 0.001$, two-sided paired Wilcoxon test comparing the 'stim' and 'late stim' intervals, i.e. the first and second half of the antennal stimulation period, *close* and *far* trials pooled).

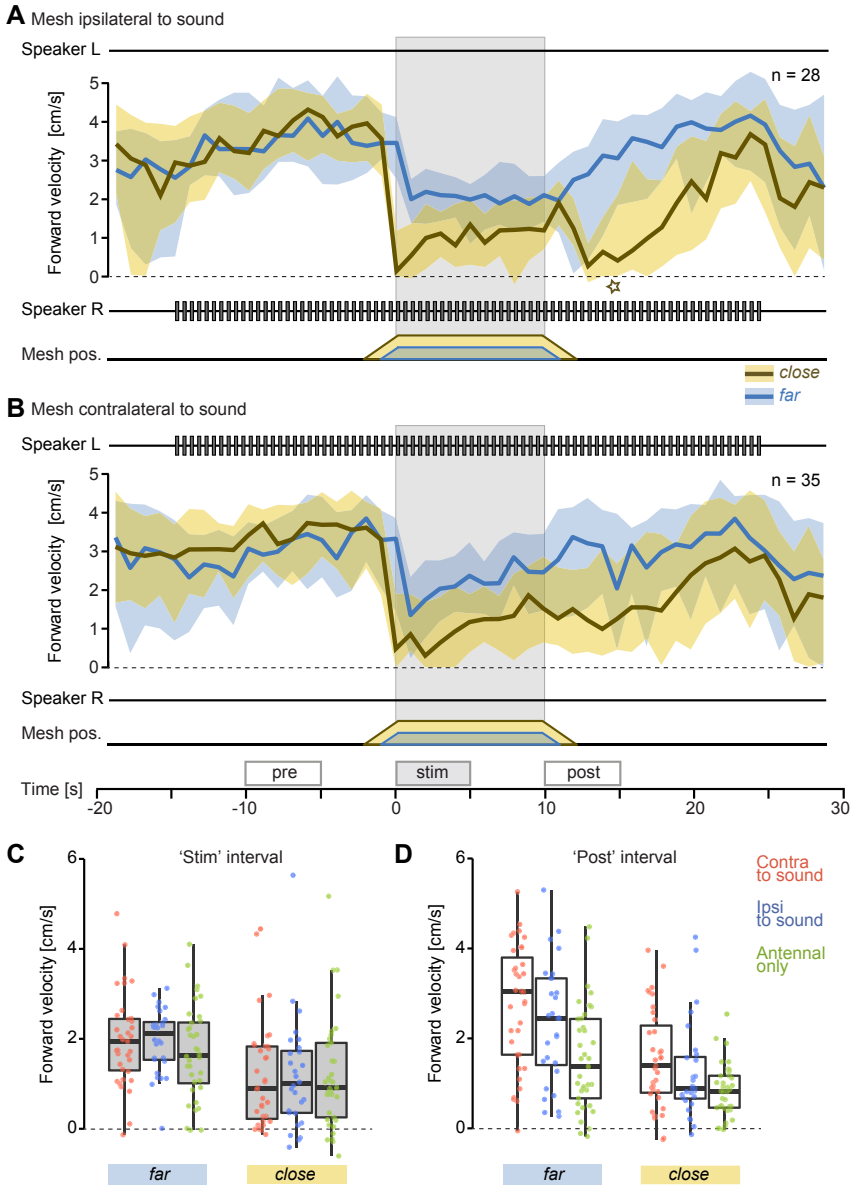

Figure 2.4: Deceleration response to antennal stimulation.
A, B: Temporal dynamics of the median forward walking velocity during a 50 s time window centred around a 40 s long presentation of a male's calling song with antennal stimulation from either the right/ipsilateral side (A) or left/contralateral side (B). The acoustic stimulus is represented by the speaker traces above and below each plot. Antennal stimulation, indicated by the mesh position trace and grey shading, occurred

during seconds 0 to 10. Responses to *close* and *far* antennal stimulation trials are colour-coded in ochre and blue, respectively. *A:* Median and IQR of forward velocity calculated from 28 ipsilateral antennal stimulation trials (15 animals). *B:* Median and IQR of forward velocity calculated from 35 contralateral antennal stimulation trials (20 animals). The boxes on the time axis in B mark the 'pre', 'stim' and 'post' intervals used in the statistical analysis. In ipsilateral trials crickets reduced their forward speed by 3.09 cm/s in *close* and 1.34 cm/s in *far* trials, while in contralateral trials they slowed down by 2.51 cm/s in *close* and 1.08 cm/s in *far* trials (comparing 'pre' and 'stim' interval). **C, D:** Boxplots of forward velocity during the 'stim' (**C**) and 'post' (**D**) interval. Grey filling marks data from the antennal stimulation period. For each period data from *far* antennal stimulation trials is shown on the left, data from *close* trials on the right. The average velocities of individual trials are overlaid on the corresponding boxplot to visualise the spread of the individual data points. Data from contralateral antennal stimulation trials are plotted in red (n = 35, 20 animals), ipsilateral antennal stimulation trials in blue (n = 28, 15 animals) and trials without acoustic stimulation in green (n = 37, 20 animals).

While the forward speed during antennal stimulation with a given presentation distance did not differ between the three experimental conditions (contralateral, ipsilateral and antennal only, ***Figure 2.4 C***), systematic differences were observed during the 'post' interval following antennal stimulation (***Figure 2.4 D***). During and after retraction of the mesh, forward velocities generally remained lower than before antennal stimulation. This after-effect was significantly stronger after *close* antennal stimulation and seemed more pronounced in ipsilateral compared to contralateral stimulation (***Figure 2.4 D***, Wilcoxon test comparing forward velocity during 'pre' and 'post' intervals: *far* contralateral trial: $p = 0.452$; *far* ipsilateral trial: $p < 0.05$, *close* contralateral and ipsilateral trials both: $p < 0.001$).

2.3.3. Phonotaxis is impaired during antennal stimulation

Following the observation that antennal stimuli had a strong effect on the crickets forward velocity even during phonotaxis, we investigated how antennal-evoked and auditory-evoked steering is integrated at the level of behaviour.

During unperturbed acoustic stimulation preceding *far* or *close* antennal stimulation, crickets responded with phonotactic steering toward the sound with similar turn amplitude: crickets turned right with 0.39 cm/s in contralateral trials, while they turned left with 0.56 cm/s in ipsilateral trials (***Figure 2.5 A, B***, 'pre' interval, *close* and *far* trials pooled). When presented with the mesh to their right side, walking crickets engaged in phonotaxis slowed down and orientated toward the antennal stimulus, similar to spontaneously walking crickets. During ipsilateral acoustic stimulation, crickets were already steering toward the side of the object and

weakly reduced their steering velocity by 0.25 cm/s in *close* and 0.13 cm/s in *far* trials ($p < 0.001$, two-sided Wilcoxon test comparing 'pre' and 'stim' intervals). In contralateral trials, antennal stimulation induced a strong shift in steering velocity away from the sound and toward the object (*close*: 0.35 cm/s, *far*: 0.41 cm/s; $p < 0.001$ two-sided Wilcoxon test comparing 'pre' and 'stim' intervals). As a consequence, phonotactic steering was abolished during contralateral antennal stimulation (***Figure 2.5 B***, 'stim' interval).

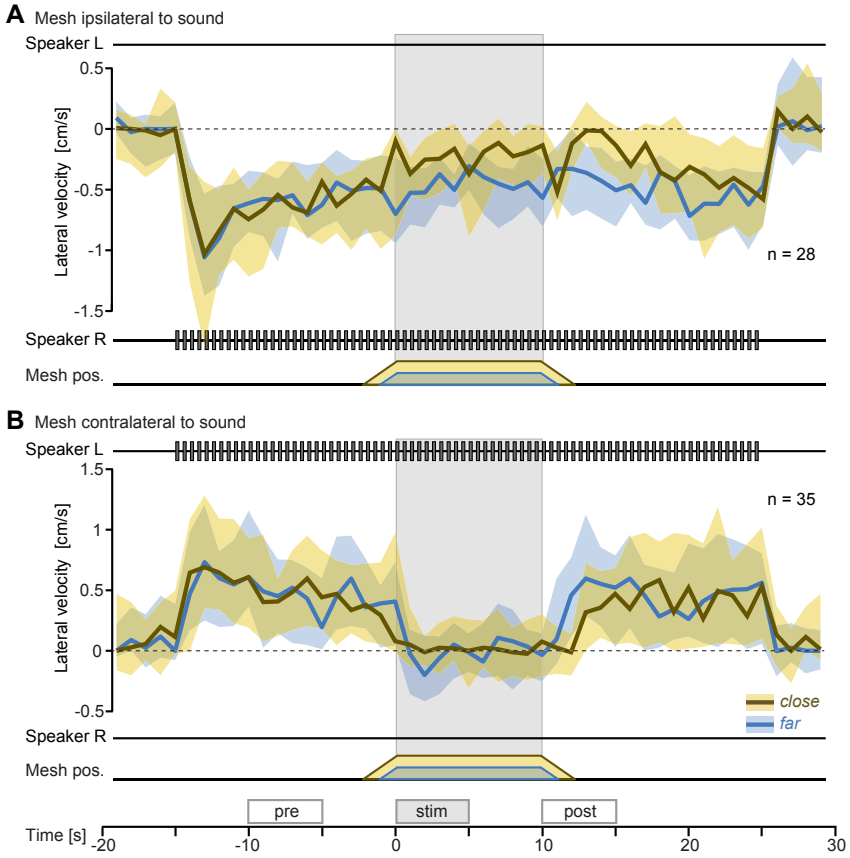

Figure 2.5: Turning responses to antennal stimulation during phonotaxis.
A, B: Median lateral steering velocity during phonotaxis combined with antennal stimulation. The data is based on the same set of trials as in *Figure 2.4* and is presented analogously. The median and IQR of 35 ipsilateral trials from 15 animals (A) and 28 contralateral trials from 20 animals (B) are shown. The boxes above the time axis in B mark the 'pre', 'stim' and 'post' intervals used in the statistical analysis.

We found that in ipsilateral trials crickets turned slightly more to the side of antennal and acoustic stimulation when the mesh was presented further away with a response of 0.41 cm/s in *far* trials and 0.31 cm/s in *close* ($p < 0.1$, paired two-sided Wilcoxon test, comparing the 'stim' interval of *close* and *far* antennal stimulation). Thus, the orientation response was distance-dependent as observed in pure antennal stimulation trials. No distance-dependence was observed in contralateral trials ($p = 0.226$, paired two-sided Wilcoxon test comparing *close* and

far trials during 'stim' interval). During *close* stimulation, some animals i.e. 21 % in ipsilateral and 3 % in contralateral trials initially displayed fast turns away from the approaching mesh — similar to what we had observed in spontaneously walking crickets — before they started exploring the object.

During the 5 s following antennal stimulation, phonotactic steering remained reduced compared to pre-antennal stimulation levels possibly due to continuing antennal contacts with the retracting mesh (***Figure 2.5***, 'post' interval). In crickets exposed to ipsilateral acoustic stimulation the steering velocity after antennal stimulation was significantly reduced compared to pre-stimulation levels (single-sided paired Wilcoxon test comparing 'pre' and 'post' intervals, $p < 0.001$). This reduction of phonotactic steering after antennal stimulation was more pronounced after *close* antennal stimulation (single-sided paired Wilcoxon test comparing *far* and *close* trials in 'pre': $p = 0.455$; in 'post': $p < 0.001$), i.e. it was distance-dependent consistent with the hypothesis that it results from interactions with the retracting mesh. Also after contralateral stimulation there is a distance-dependent after-effect (single-sided paired Wilcoxon test comparing *far* and *close* trials in 'post': $p < 0.001$).

This data demonstrate that the amplitude of the phonotactic steering velocity is generally smaller during antennal stimulation. The response to antennal stimulation depends on the presentation side and distance and results in transiently reduced phonotaxis.

2.3.4. Phonotactic steering manoeuvres are reduced during antennal stimulation

Reduced phonotactic steering could be the effect of linear superposition of conflicting steering manoeuvres and does not necessarily imply that during antennal stimulation the cricket is unresponsive to the male's calling song. Goal-directed phonotaxis is accomplished by reactive steering manoeuvres in response to single chirps (Hedwig and Poulet, 2004). Hence, chirp-triggered lateral steering bouts indicate the cricket's engagement in phonotaxis and a reduction of those steering bouts may suggest that it no longer responds to the acoustic stimulus. To estimate the magnitude of auditory steering over time, we averaged the chirp-triggered steering velocity to 10 consecutive chirps over 5 s long intervals covering the time before, during and after antennal stimulation (***Figure 2.6***). In addition to the previously introduced 'pre', 'stim' and 'post' intervals, we analysed a 'late stim' interval covering the second half of antennal stimulation and a 'late post' interval covering the 5 s following the 'post' interval.

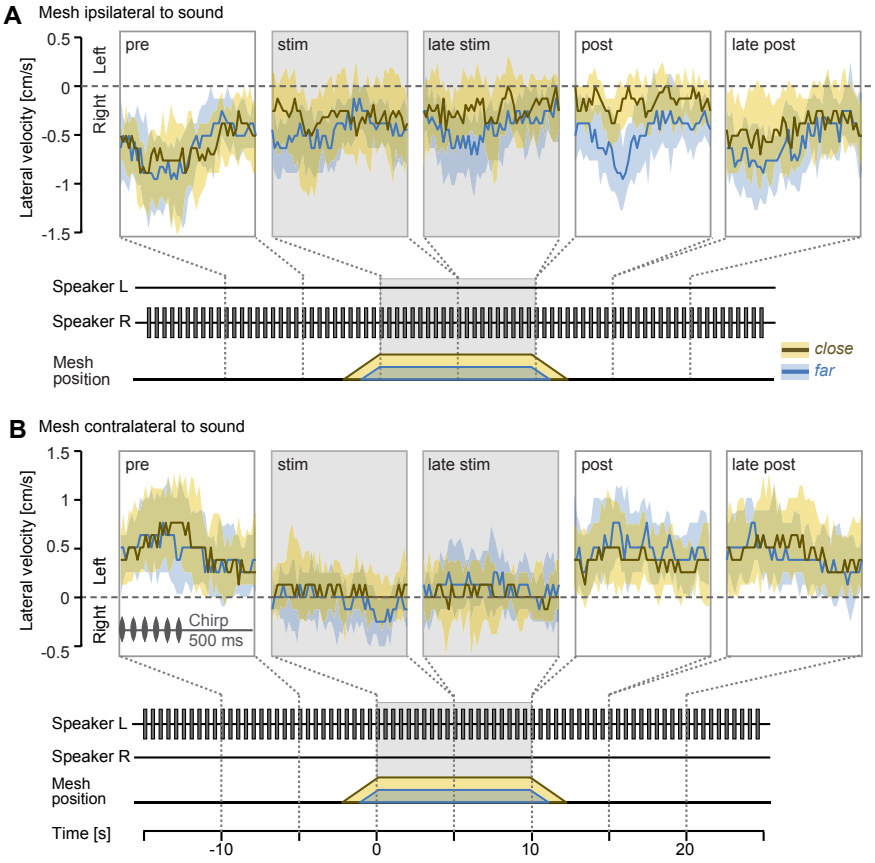

Figure 2.6: Reduction of chirp-triggered acoustic steering bouts during antennal stimulation.

A, B: Median and IQR of the lateral steering velocity per chirp period averaged over 10 consecutive chirps within 5 s long time intervals spanning the trial period. Five time intervals were chosen to cover the acoustic stimulation before, during and after antennal stimulation. These five intervals include the previously introduced 'pre', 'stim' and 'post' intervals. Two additional intervals, 'late stim' with seconds [5 s, 10 s) and 'late post' with seconds [15 s, 20 s), were introduced. Steering bouts to *close* and *far* stimulation are overlaid for ipsilateral trials (A, n = 28, 15 animals) and contralateral trials (B, n = 35, 20 animals). Acoustic and antennal stimulation during the analysed time period are schematised by speaker traces and mesh position. Grey shading highlights intervals during which the crickets were exposed to antennal stimulation.

During unperturbed phonotaxis, crickets showed characteristic lateral steering bouts toward the sound source that were coupled to individual chirps. We quantified the modulation amplitude of chirp-coupled steering bouts as the difference between the minimum and the maximum steering amplitude within one chirp period. During unperturbed phonotaxis the median modulation amplitude of the steering bouts was 0.57 cm/s in contralateral and 0.67 cm/s in ipsilateral trials (***Figure 2.6** A, B*, 'pre' interval, mean of *close* and *far* trials). In all experimental conditions, the sound induced steering bouts were reduced during antennal stimulation compared to unperturbed phonotaxis (***Figure 2.6***, grey-shaded 'stim' and 'late stim' intervals). The decrease between the 'pre' and 'stim' interval was more pronounced in *close*

(reduction by 0.51 cm/s in contralateral and 0.25 cm/s in ipsilateral trials) as compared to *far* trials (decrease by 0.25 cm/s in contralateral and 0.19 cm/s in ipsilateral trials) and stronger during ipsilateral compared to contralateral stimulation. Acoustic steering bouts continued to be reduced in the 5 s following *close* ipsilateral antennal stimulation, possibly due to continuing contacts with the retracting mesh (***Figure 2.6 A***, 'post' interval). Impairment of phonotactic steering bouts during antennal stimulation suggests that motor responses triggered by antennal stimulation at least partly override phonotactic steering.

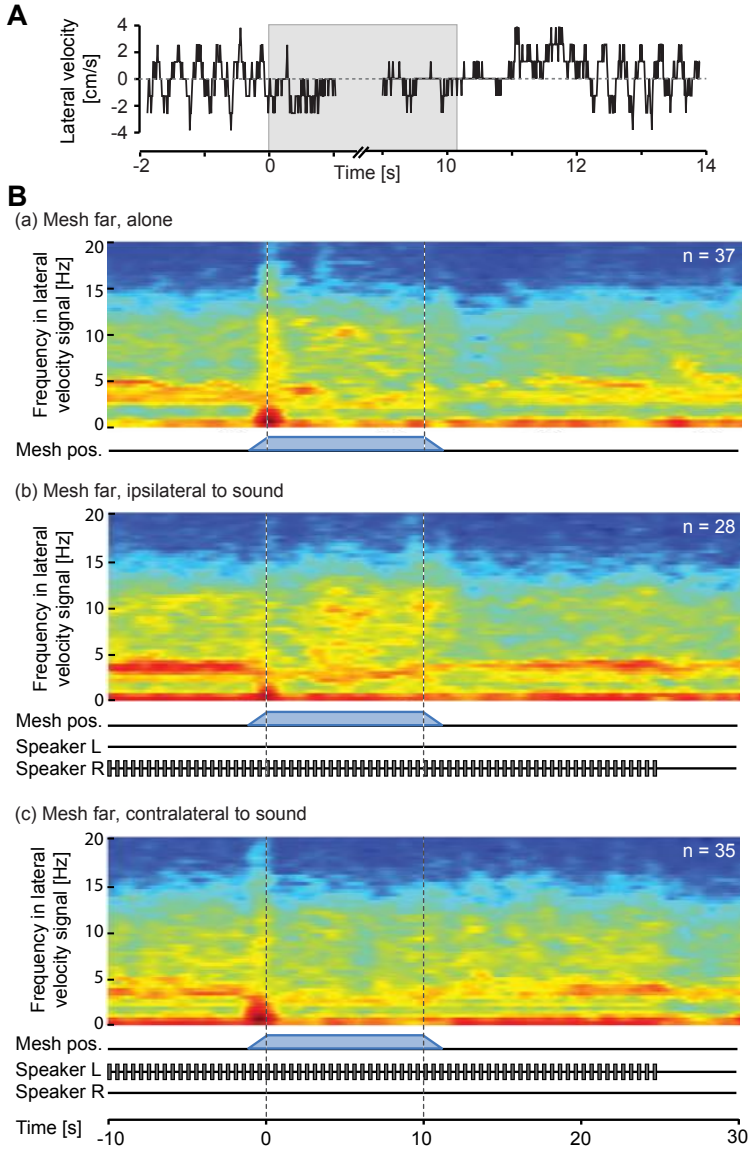

Figure 2.7: Disruption of the cricket's regular walking pattern during antennal stimulation.

A*:* Regular oscillations in the raw steering velocity signal of a spontaneously walking cricket during a *far* antennal stimulation trial (same measurement as shown in *Figure 2.2 C,* top). Grey shading marks the antennal stimulation period. Similar oscillations were observed in the steering velocity signal during phonotaxis (not shown). B**:** Power

spectrograms of the lateral velocity during *far* antennal stimulation trials. The velocity signal can be understood as a linear combination of oscillations and the contribution of oscillations of different frequencies to a measured signal can be visualised in a frequency power spectrogram. We computed spectrograms of the lateral velocity signal during pure antennal stimulation (a, n = 37, 20 animals) and during antennal stimulation with ipsilateral (b, n = 28, 15 animals) or contralateral (c, n = 35, 20 animals) acoustic stimulation. Spectrograms were computed for each trial and then averaged. During spontaneous walking and unperturbed phonotaxis, there is high power in a frequency band around 3-5 Hz. In all three experimental groups the power of this 3-5 Hz frequency band is reduced during, and to varying degrees after, antennal stimulation. Dashed lines mark the beginning and end of the antennal stimulation period and speaker traces indicate acoustic stimulation. Only spectrograms from *far* trials are shown, as they closely resemble those from *close* trials.

2.3.5. No reduction of the response to extended antennal stimulation

The persistent impairment of phonotaxis during antennal stimulation raised the question if crickets might adapt to a long-lasting antennal stimulus, for example by reducing antennal exploration of the mesh, and if they eventually return to phonotaxis. We therefore measured behavioural responses to ipsilateral and contralateral presentation of antennal and acoustic stimuli over a 30 s time period. The acoustic stimulus was presented alone for 10 s before the object was moved into antennal reach and kept there for the remaining 30 s.
Prior to antennal stimulation crickets turned to the direction of the phonotactic stimulus with a similar median steering velocity across experimental conditions (contralateral: 0.52 cm/s, ipsilateral: -0.78 cm/s, *close* and *far* trials pooled, ***Figure 2.8 A***, ***B***, 'pre' interval). With the onset of antennal stimulation, crickets reduced their steering velocity toward the sound significantly by 0.63 cm/s in contralateral trials and by 0.54 cm/s in ipsilateral trials (both: $p < 0.001$, paired two-sided Wilcoxon test comparing the 'pre' and 'stim' interval, *close* and *far* trials pooled). The orientation response was accompanied by a significant reduction in median forward speed by 1.16 cm/s in contralateral and by 1.35 cm/s in ipsilateral trials (both: $p < 0.001$, two-sided Wilcoxon test, comparing the 'pre' and 'stim' interval, *close* and *far* trials pooled).

Phonotactic steering remained impaired throughout the 30 s antennal stimulation period (***Figure 2.8 A***, ***B***, grey shaded box). To determine whether the steering or forward velocity varied with the presentation time we performed a Kruskal-Wallis test over the entire stimulation period (six 5 s intervals marked above time axis in ***Figure 2.8 D***).

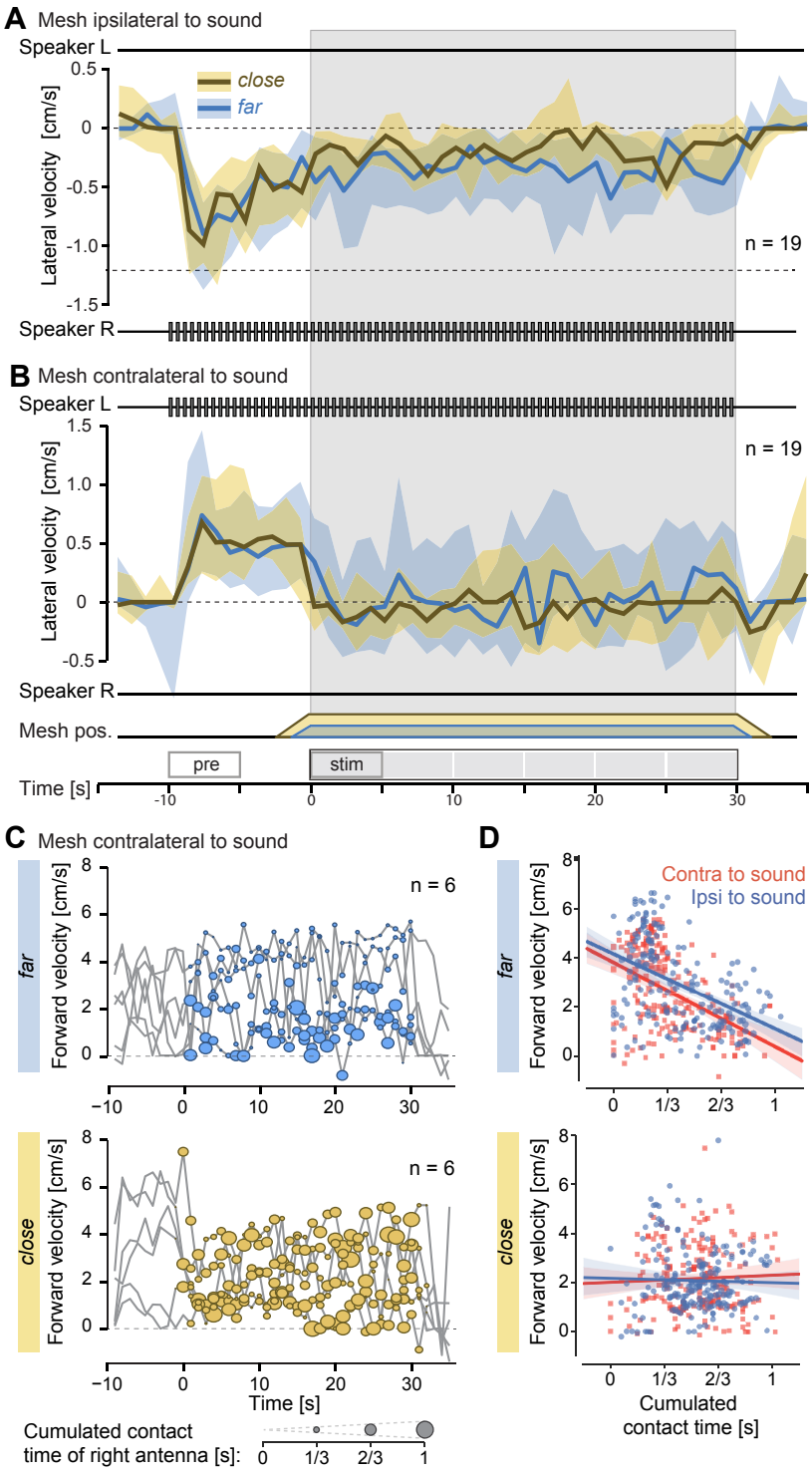

Figure 2.8: Impairment of phonotaxis during long lasting antennal stimulation.
A, B: Temporal dynamics of the lateral velocity during phonotaxis combined with a 30 s long antennal stimulation period. Layout of A and B is analogous to *Figure 2.5 A, B.* Median and IQR of lateral steering velocity calculated from 19 ipsilateral trials (A) and 19 contralateral trials (B) are shown. Data from *far* and *close* trials is shown in blue and ochre, respectively. In both experimental groups the same 19 animals were tested, each contributing one trial. The boxes on the time axis in B mark the 'pre' and 'stim' intervals used in the statistical comparisons as well as the intervals that were compared

in the Kruskal-Wallis test. **C:** Antennal contacts extracted from video data overlaid onto the corresponding forward velocity trace of 6 crickets during contralateral antennal stimulation (seconds 0 to 30). The forward velocity and the cumulated antennal contact time were computed over 1 s time intervals. Data from *far* and *close* trials are shown in the top and bottom plot, respectively. Cumulated antennal contact time is visualised as disks, whose size encodes the fraction of each second during which the respective cricket held antennal contact with the mesh. **D:** Correlations between the forward velocity and the cumulated antennal contact time. The Pearson correlation coefficients are -0.44 ($p < 0.001$) for *far* contralateral and -0.46 ($p < 0.001$) for *far* ipsilateral stimulation. For *close* contralateral and ipsilateral stimulation the correlation coefficients are 0.05 and -0.03, respectively (both n. s.).

The orientation responses did not vary significantly with presentation time in neither contralateral ($p = 0.760$) nor ipsilateral trials ($p = 0.868$). Also the forward speed did not change significantly over the 30 s stimulation period (contralateral: $p = 0.500$, ipsilateral: $p = 0.433$). Crickets generally slowed down more in response to *close* compared to *far* antennal stimulation (paired, one-sided Wilcoxon test, contralateral and ipsilateral: $p < 0.001$). Also the presentation distance affected the orientation response, where females made larger turns toward the mesh when presented at the *far* position (paired, two-sided Wilcoxon test, contralateral: $p < 0.01$; ipsilateral: $p < 0.001$).

We evaluated video recordings of 6 animals to quantify when crickets made contacts with the mesh and plotted the contact times combined with the forward velocity. This revealed that crickets made repeated antennal contact with the mesh throughout the 30 s simulation period (***Figure 2.8 C***). The first antennal contact occurred on average 1.25 s (+/- 0.25 s) earlier in *close* compared to *far* antennal stimulation trials, as the approaching mesh came within antennal reach before moving to its final position. For the same reason, antennal contact could be maintained for up to 2 s after *close* antennal stimulation. In *far* trials, contacts were primarily made with the right antenna, while additional contacts with the left antenna occurred in *close* trials. We found a negative correlation between the amount of antennal contacts a cricket made with the mesh and its forward velocity during *far*, but not during *close* presentation (***Figure 2.8 D***). Thus, in *far* trials the cricket slowed down more the longer antennal contacts were (***Figure 2.8 C***).

Under our experimental conditions phonotactic steering was impaired and forward walking reduced for the entire 30 s of antennal stimulation. Responses to antennal stimulation did not vary significantly over the stimulation period and crickets persistently made antennal contact with the mesh indicating no behavioural adaptation to antennal stimulation.

2.4. Discussion

The natural habitat of *G. bimaculatus* is grassland (Van Wyk and Ferguson, 1995). Female crickets performing phonotaxis when approaching a singing male thus have to navigate a cluttered terrain, where they encounter obstacles and predators. Walking crickets use their antennae to scan the space ahead, allowing them to detect objects along their path (Horseman et al., 1997). Further, antennal sensing plays an important role in the initiation of courtship following phonotaxis in two cricket species, *G. bimaculatus* and *Teleogryllus oceanicus* (Adamo and Hoy, 1994; Balakrishnan and Pollack, 1997). Therefore, sensory signals generated by antennal contact with objects in the cricket's path are likely of interest for a female cricket during phonotaxis. We provide a quantitative description of the responses to mechanosensory antennal stimulation generated by presenting an object to tethered walking female crickets. During antennal stimulation crickets reduced their forward speed and turned toward the side of the object. Crickets engaged in phonotaxis responded to antennal stimulation in a similar manner with phonotactic steering manoeuvres being impaired for up to 30 s with no evidence for behavioural adaptation to the antennal stimulus. We found a negative correlation between the time crickets spent making contacts with the presented object and their forward walking speed. In short, crickets show immediate and persistent responses to antennal mechanosensory stimuli, which affect course control and impair phonotaxis.

Methods considerations

Before discussing the implications of our findings, we would like to draw attention to a few potential concerns regarding the experimental methods used in this study. Firstly, in our setup the crickets walking behaviour does not affect the presentation of the acoustic nor the antennal stimulus, i.e. both stimuli are presented in open loop. Open-loop stimulation offers a high level of experimental control and is commonly used in studies of phonotaxis (Hedwig and Poulet, 2005; Schildberger and Hörner, 1988) and antennal sensing (Nishiyama et al., 2007; Okada and Toh, 2006). However, in a natural setting the animal's behaviour affects its sensory experience. For example, when a cricket turns away from an obstacle in its path, the antennal stimulus ceases. It would be relatively easy to add partial closed-loop control for the antennal stimulus by coupling the angular mesh position to the cricket's lateral steering velocity. It would be interesting to see how adding such partial feedback of the cricket's behaviour onto the sensory stimulus presentation would change the animal's response to antennal stimulation, both when presented alone and during phonotaxis. A second concern was the surface structure of the mesh. Previous studies of antennal sensing in walking insects have used solid objects such as a

plate or a rod (Okada and Toh, 2006; Ritzmann et al., 2012; Schütz and Dürr, 2011). Here we chose a sound transparent metal mesh, which allowed us to deliver antennal and acoustic stimulation independently. As a side effect the object had a rough surface texture, which might have prevented fast adaptation of the antennal mechanosensors as the antennae were touching the mesh's corrugated surface. It is also possible that this kind of surface had a high saliency for the crickets used in our experiments, potentially because they rarely encounter such rough surfaces, and the animals therefore examined the mesh for extended periods of time. Thirdly, we did not control for any possible effects by pheromones, for example by cleaning the mesh and trackball between trials. However, in this study only female crickets were used and to our knowledge crickets do not actively deposit pheromones on surfaces. Finally, we did not quantify head and antennal movements. Crickets posses a joint between the head and the pronotum, which was not fixed during the tethering procedure. Video recordings showed that crickets turned their heads to the object and adjusted their antennal movements as part of their orientation response (Witney and Hedwig, 2011).

Antennal stimulation can elicit both exploratory and avoidance behaviour

Mechanosensory antennal sensing is involved in a variety of behaviours, ranging from flight-control over wall-following behaviour to escape responses (Comer et al., 1994; Hinterwirth and Daniel, 2010; Okada and Toh, 2006). Within those behaviours it often leads to turning responses toward or away from the stimulus source.

Female *G. bimaculatus* in the field walk less straight and take longer to reach the sound source than crickets walking on a treadmill under laboratory conditions, a discrepancy that may result from rough terrain and obstacle negotiation during phonotaxis in the field (Hirtenlehner et al., 2014); similar observations were made in bushcrickets (von Helversen et al., 2001). Based on these findings we expected that crickets perform transient turns away from an object in an attempt to bypass the obstacle. Surprisingly, in our paradigm crickets primarily slowed down and turned toward the object. These changes in walking behaviour, which could last for tens of seconds, were accompanied by an orientation of the cricket's head toward the object and antennal palpation. These observations suggest that the mechanosensory stimulus induced exploratory behaviour. However, some crickets responded to the approaching mesh with avoidance behaviour. It was more frequently observed in spontaneously walking females and in ipsilateral trials, where females already turned toward the approaching mesh. We hypothesise that these animals detected the movement of the approaching object and that this stimulus elicited avoidance behaviour. In *G. bimaculatus* weak antennal contact with spider legs elicits

primarily antennal search, whereas strong contact elicits avoidance behaviour (Okada and Akamine, 2012). These findings together with observations of antennal use in cockroaches (Comer et al., 1994; Okada, 2004; Okada and Toh, 2006; Stierle et al., 1994) indicate that behavioural responses to antennal stimulation depend on fine characteristics of the perceived stimulus. Both exploratory and avoidance behaviour in response to mechanosensory antennal stimulation may be mediated by identified descending neurons, some of which have been shown to elicit turning upon current injection (Schöneich et al., 2011; Zorović and Hedwig, 2013).

Interaction of phonotaxis and antennal stimulation

The deceleration and orientation response to antennal stimulation impaired calling song tracking, temporarily overriding a robust behaviour such as phonotaxis. Behavioural studies in tethered crickets have shown that phonotaxis emerges from small reactive steering manoeuvres in response to single pulses and chirps (Hedwig and Poulet, 2004, 2005). Thus, a characteristic feature of phonotactic steering is that the temporal pattern of the acoustic stimulus is preserved in the motor output. We found that during antennal stimulation, phonotactic steering bouts were abolished and that the regular stepping pattern was disrupted. This suggests that turns towards the antennal stimulus, in contrast to phonotactic steering, are not integrated into the regular walking pattern but rather initiate a different motor program: the animal stops and explores the object. In accordance with this, we found that when the mesh was presented alone, crickets slowed down and turned towards the mesh. Characteristic features of the response, such as the persistent reduction in forward speed and an additional deceleration after the retraction of the mesh, are preserved during ipsilateral acoustic stimulation. In contrast, during contralateral acoustic stimulation the forward speed recovers already during antennal stimulation. This suggests that the behaviour during antennal stimulation is primarily governed by the sequence of antennal contacts, which in turn may be influenced by the recent mechanosensory experience of the animal but also by simultaneous acoustic stimulation. In trials with contralateral acoustic stimulation, crickets occasionally may be ‘pulled’ away from the antennal stimulus, make fewer antennal contacts with the object and as a consequence the temporal dynamics of the forward velocity differ from those in spontaneously walking crickets and in trials with ipsilateral acoustic stimulation. By comparison, integration of phonotaxis with responses to visual stimuli shows different characteristics. In *G. bimaculatus*, orientation responses to a male’s calling song and to a simultaneously presented black vertical stripe, an attractive visual stimulus, are additive (Böhm et al., 1991; Payne et al., 2010) and in bush crickets phonotactic tracking improves in the presence of stationary visual

cues (von Helversen and Wendler, 2000). The apparently different mechanism of integration of phonotaxis with responses to antennal stimulation may be explained by the qualitatively different requirements of responses to mechanosensory and visual stimuli. Visual, like acoustic signals, act on a long-range and do not necessarily require immediate action. In contrast, antennae are contact-sensors, providing information about the animal's close-range environment. Consequently, antennal stimuli may often require an immediate response, for example during obstacle negotiation, mate recognition or predator avoidance. Our data shows that mechanosensory antennal stimuli are important to female crickets during phonotaxis. This has implications for the design of phonotaxis experiments and may lead to differences in phonotactic behaviour across laboratory paradigms.

In future studies the behavioural paradigm presented in here could also be used to further probe the rules governing integration of antennal mechanosensory stimuli with phonotaxis. One could, for example, investigate whether crickets integrate the two stimuli approximately linearly (Frye and Dickinson, 2004) by systematically varying the saliency of one of the two stimuli. Given the limited knowledge we have about antennal stimulation, it may not be straightforward to systematically vary the saliency of the mechanosensory stimulus, however, more is known about how varying the calling song pattern affects phonotaxis (Hedwig, 2006). Here we used a highly attractive artificial calling song pattern, which induces in robust phonotaxis in mature female crickets. We could reduce the attractiveness of the calling song by either increasing or decreasing the syllable period. If mechanosensory and acoustic stimuli were integrated linearly, we would expect to see that responses to antennal stimulation during acoustic stimulation with a less attractive song resemble more closely the responses to antennal stimulation in the absence of acoustic stimulation.

Why do we not see adaptation to the antennal stimulus?

We were surprised to find sustained impairment of phonotaxis even over a 30 s long antennal stimulation period. Okada & Toh (2004a) demonstrated in free walking, blinded cockroaches that antennal contact marks the beginning of a motor sequence, where detection of an object induces changes in antennal movement, followed by head turning, approach and climbing attempts. Under natural conditions, walking manoeuvres, head movements and antennal movements jointly control the distance and orientation of the antennae relative to an object. Changes in any of these movement patterns have an impact on antennal sensing. When feedback of the animal's behaviour onto its own sensory experience is largely removed, as is the case in our quasi open-loop antennal stimulation paradigm, we may only see the beginning

of this behavioural sequence. Instead of a transient turn initiated by antennal contact, after which the animal reaches the object and terminates the approach manoeuvre, the behavioural sequence stalls as the animal persistently aims to reach the object. Under open-loop conditions also cockroaches walking on a trackball turn toward a rod brought into reach of one antennae for up to 30 s (Okada and Toh, 2006). Interpreting the antennal stimulation-evoked orientation toward the object as an attempt to approach the object would also explain why turn responses were more pronounced when the object was far away from the cricket: the animal might attempt to approach the more distant object in order to further explore it. Consistent with the hypothesis that turns toward the mesh were aimed at exploring the object, we observed repeated contacts with both antennae during *close* antennal stimulation.

Where do antennal and phonotactic pathways converge?

Female crickets sense the male's calling song via ears on their front legs, from where auditory afferents project to the thoracic ganglion (Eibl and Huber, 1979; Esch et al., 1980). Ascending interneurons convey the signal to the brain, where the pattern is processed by a series of interneurons in a frontal auditory neuropil of the protocerebrum and in the lateral accessory lobe (Kostarakos and Hedwig, 2012; Schöneich et al., 2015; Zorović and Hedwig, 2011). From the lateral accessory lobe descending interneurons, whose activity weakly reflects the calling song's pattern as well as walking velocities, project to thoracic ganglia (Zorović and Hedwig, 2013).

The pathway for mechanical information is very different. Mechanosensory afferents coming from the cricket's antennae enter the brain via the antennal nerve and project to the deutocerebrum and the subesophageal ganglion (Rospars, 1988; Staudacher and Schildberger, 1999; Yoritsune and Aonuma, 2012). From the deutocerebrum giant descending interneurons convey information to the ventral nerve cord (Gebhardt and Honegger, 2001; Schöneich et al., 2011). Three of these interneurons respond to both visual and mechanosensory stimuli and one has been shown to elicit walking bouts and contralateral steering upon current injection (Zorović and Hedwig, 2013). These findings are consistent with a fast descending escape circuit that receives, amongst others, mechanosensory input from the antennae. Antennal contact with an approaching, but not a stationary, object might activate this circuit to elicit the stereotypic avoidance manoeuvre observed in a subset of animals. A descending neuron, which responds to antenno-mechanosensory and visual stimuli, may participate in the detection of objects in the cricket's walking path (Gebhardt and Honegger, 2001), suggesting involvement in exploration or obstacle negotiation. Notably, antennal interneurons so far described, do not

receive strong auditory inputs (Zorović and Hedwig, 2013). Therefore, antennal mechanosensory and auditory stimuli are processed in different brain areas, suggesting that early sensorimotor processing of these signals is performed by separate pathways and convergence might only occur in the thoracic ganglia. Alternatively, acoustic stimulation may influence antennal sensing by changing the antennal search patterns. In cockroaches attractive and aversive odours have been shown to have differential effects on both locomotion and antennal search patterns (Nishiyama et al., 2007). To further probe the neural computations underlying the processing of antennal stimuli and how responses to antennal and acoustic stimuli are integrated, our behavioural paradigm may be combined with neurophysiological techniques as well as video tracking of antennal movements.

Impairment of phonotaxis by antennal stimulation as a model system for studying action selection and active sensing

Studies on multimodal integration have focused on understanding the mechanisms underlying integration of cross-modal stimuli (Stein and Stanford, 2008). Integrating cross-modal stimuli increases reliability of the extracted information about the object or event. We looked at bimodal integration in a different context: an animal is confronted with two independent stimuli that affect the same behaviour, i.e. course control. In this case, processing of two sensory inputs needs to select the appropriate behavioural response and to ensure a coordinated motor output.

We found that antennal mechanosensory stimuli strongly reduce phonotactic steering. Suppression or interruption of an ongoing behaviour by a novel stimulus is a common phenomenon. For example, stimulation of the cerci, another mechanosensory organ, interrupts singing in male crickets (Hedwig, 2000; Jacob and Hedwig, 2015). In feeding crayfish the escape response is suppressed by a mechanism called ‘tonic inhibition’, which has been suggested as a mechanism for action selection (Krasne and Lee, 1988; Vu and Krasne, 1992; Vu et al., 1993). Hierarchical suppression has also been proposed as a mechanism for generating behavioural sequences (Seeds et al., 2014).

While crickets responded to a conspecific male’s calling song reliably with phonotaxis, both exploration or avoidance behaviour was observed during antennal stimulation. This was likely a consequence of letting the animal generate the mechanosensory stimulus rather than imposing controlled antennal movements and contacts. A situation like this, in which an animal controls stimulus intensity and frequency, has been classified as active sensing (Prescott et al., 2011;

Staudacher et al., 2005). Examples of active touch sensing in mammals are whisking in rodents (Grant et al., 2009) and palpation with the hand in capuchin monkeys (Visalberghi et al., 2009). Active touch sensing is also found in many insects (Comer and Baba, 2011), especially in the context of navigation (Harley et al., 2009; Okada and Toh, 2004; Okada and Toh, 2006; Schütz and Dürr, 2011). The interaction of the crickets' active antennal movements and the experimentally controlled positioning of the mesh resulted in slightly different tactile stimuli possibly activating different motor programs. This variability observed in our paradigm could be exploited to study selection and coordination of different motor programs in the context of active sensing.

Data presented in this chapter has been accepted for publication:

Haberkern, H., and Hedwig, B. Behavioural integration of auditory and antennal stimulation during phonotaxis in the field cricket *Gryllus bimaculatus* (DeGeer). *J. Exp. Biol.* (Accepted, August 2016)

Chapter 3

A 2D visual virtual reality system for studying landmark-guided navigation in tethered walking flies

3. A 2D visual virtual reality system for studying landmark-guided navigation in tethered walking flies

3.1. Introduction

Many navigational behaviours rely on salient visual features, so-called landmarks, as orientation aid. How landmarks are used during visually guided navigation depends on the navigational strategy that the animal employs. Directional information extracted from visual landmarks can either directly serve as a guidance cue in form of a beacon, or it can be integrated with other guidance systems.

Landmark cues and the 'internal compass'

Having a sense of direction or orientation is critical for many navigational tasks. While moving around in space it is theoretically possible to maintain an absolute sense of direction, an 'internal compass' so to say, by precisely integrating all changes in body orientation, a process known as angular path integration. Many animals rely on path integration to orient themselves in the absence of external guidance cues (Etienne and Jeffery, 2004). Female rodents searching for their displaced pup in darkness, for example, return to their nest on a straight path after finding the pup (McNaughton et al., 2006). A very similar navigational pattern has been observed in foraging desert ants, which leave the nest on a meandering search path but take the shortest path back once they find food (Müller and Wehner, 1988; Wehner, 2003). As in these two examples, animals often perform path integration on an outbound route to update a stored direction toward their home and use this information on the homebound route. However, during path-integration errors accumulate (Müller and Wehner, 1988) and it is therefore desirable to occasionally recalibrate this internally maintained sense of direction, using salient visual features, so called landmarks. Indeed, many animals appear to use landmarks as a guidance cue jointly with self-motion derived information. Foraging desert ants flexibly use a combination of path integration and landmark cues (Bregy et al., 2008; Legge et al., 2014; Wehner et al., 1996). Even when navigational behaviours are primarily driven by external cues, internal representations that outlast the sensory cues and that can be updated based on idiothetic, i.e. self-motion cues, allow animals to orient towards landmarks when they are temporarily obscured. Such short-term orientation memory can be seen in walking flies tracking visual landmarks: flies appear to store the angular position of a targeted landmark after extended exposure to it and retrieve this information when the landmark disappears (Neuser et

al., 2008). While the use of landmarks during navigation has been extensively studied on a behavioural level in a variety of animals, we still know very little about the neural processing underlying visually guided goal-directed navigation.

What is known about the cellular basis of landmark-guided orientation?

Monitoring neural activity in behaving animals has shed some light on the cellular basis of internal representations of direction. Recordings of cells in the hippocampus of freely moving rats, for instance, led to the discovery of head direction (HD) cells (Taube et al., 1990a; Taube et al., 1990b). HD cells are tuned to a specific, preferred heading direction and are thought to encode heading information as a population: as the animal moves around, the firing pattern across the HD cell population shifts, leading to an update of the encoded heading direction. Interestingly, the preferred directions of HD cells can be updated — for example by visual landmark cues (Goodridge and Taube, 1995; Yoder et al., 2015; Zugaro et al., 2003). When idiothetic information and heading direction information based on visual cues are in conflict, HD cells often follow the visual landmark cue suggesting a vision-based recalibration of this 'internal compass' (Taube, 2007).

Compelling evidence for an HD-like system in insects comes from a recent study in walking flies investigating the computational role of neurons in a conserved midline brain neuropil, the central complex (CX), during spatial orientation behaviour. Imaging of a population of genetically defined CX neurons in flies walking in either darkness or in a simple visual virtual reality (VR) environment revealed that flies also possess an internal representation of their angular orientation (Seelig and Jayaraman, 2015). The CX has been previously implicated in motor control, orientation and navigation behaviour in various insect species (el Jundi et al., 2015; Heinze and Homberg, 2007; Martin et al., 2015; Strauss, 2002) and recently cells with similar properties to HD cells in rodents were also found in the cockroach CX (Varga and Ritzmann, 2016). In flies, the central complex is also required for short-term orientation memory (Neuser et al., 2008) and visual learning (Liu et al., 2006; Ofstad et al., 2011).
In the CX angular orientation is encoded as a single 'bump' of increased activity that rotates around a ring-shaped CX subunit, called the ellipsoid body, as the animal changes it's heading direction (Seelig and Jayaraman, 2015). This 'internal compass' can be updated based on self-motion signals, but preferentially follows visual cues. Interestingly, the representation of the fly's orientation persists even when the fly is standing in place in darkness, that is, in the absence of visual or motor information. The mapping between a location in the ring-shaped ellipsoid body and the fly's heading direction is not fixed and the activity 'bump' occasionally

jumps to a new location within the neuropil. The significance of the changes in mapping between activity in individual cells and the fly's heading is still unclear.

The neural computations involved in generation and use of the HD cell system and the fly's 'internal compass' likely involve multiple brain regions and are probably highly recurrent. Studying such complex, distributed circuits is challenging, especially in large mammal brains. The task might be more tractable, though, in the comparatively smaller insect brain. Further studies of the circuit components are required to establish whether the HD system found in the insect CX implements computational mechanisms similar to the theoretical models that have been proposed in the context of vertebrate HD cells (Knierim and Zhang, 2012). The work presented here, however, aims to provide tools and behavioural paradigms that allow us to address questions regarding a different aspect of the observed HD-like system in flies: how it is used during navigational behaviours.

Open questions we would like to address in walking flies

Ultimately, we would like to understand how the internal representation of heading found in walking flies is used during visually guided navigation. Many open questions arise around this general theme. How are visual landmarks utilised for course-control? What happens if multiple visual landmarks are present? How are visual features in an environment selected as navigational guidance? We would also like to gain a better understanding of what is encoded by the fly's internal heading signal. Is the heading signal tethered to points of interest for the animal? Or does it just represent a general reference? By monitoring neural activity in behaving animals engaging in visually guided goal-directed navigation we can approach these questions and we believe that they can be effectively addressed in fruit flies, where we can profit from a numerically simple brain and powerful genetic tools. However, existing paradigms for head-fixed walking flies need to be extended to support more complex navigational behaviours. Furthermore, some questions require a goal-directed navigational task that head-fixed flies could perform during calcium imaging. As a first step toward addressing the above and related questions, we decided to build an experimental setup that would allow head-fixed flies to explore a two-dimensional (2D) VR environment and interact with visual landmarks.

Using virtual reality systems to study neural dynamics during navigation behaviour

In neuroscience VR systems have been successfully used to study spatial orientation behaviour in a range of head-fixed animals. The neural correlates of internal representations of space have been studied in navigating head-fixed mice using a spherical treadmill and a visual VR (Dombeck

et al., 2010; Harvey et al., 2012; Hölscher et al., 2005). Very similar setups have been developed for a range of insect species (cockroach: Takalo et al., 2012, moth: Gray et al., 2002,fly: Seelig et al., 2010; Stowers et al., 2014). Besides enabling neurophysiological studies in navigating animals, there are a number of other advantages of studying visually guided navigation in VR. VR systems permit highly flexible yet controlled visual environments, and the visual environment as well as the rules that govern the interactions between the animal and the VR can be adjusted to ask specific questions about visual processing during navigation. VR systems have therefore also been used in freely walking (Schuster et al., 2002; Strauss et al., 1997) and flying (Stowers et al., 2014) flies. Finally, giving the animal partial control over the sensory stimulation it receives helps to generate stimulation patterns with temporal profiles that match statistics of natural stimuli, which is what the nervous system evolved to process. It also preserves certain relationships between the animal's movements and changes in the sensory environment, which — if violated — can cause error signals that can interfere with the behaviour.

Motivations and guiding design principles behind the 2D virtual reality for walking flies

While VR systems have been used extensively to study visual behaviours in tethered fruit flies (Borst, 2014; Götz, 1994), the existing VR systems and behavioural paradigms have a number of shortcomings that rendered them unsuitable for addressing the questions outlined above.
For decades, studies of visual orientation behaviour of fruit flies used tethered flight (Götz, 1987; Maimon et al., 2008). One limitation of this approach is that it is difficult to accurately deduce a flight path in 3D space from the wing stroke pattern. Freely flying flies flap their wings with 200-300 Hz and minute changes in their wingbeat amplitude and wing angle result in quick changes in flight direction, saccades, during which the fly simultaneously rotates around multiple axes (Fry et al., 2003). In addition the reduced or artificial mechanosensory feedback of flight manoeuvres in tethered flight may cause observed differences in the wing stroke pattern of tethered compared to freely flying flies (Fry et al., 2005). As a consequence, studies of visual behaviours in tethered flying flies have been limited to relatively simple, one-dimensional (1D) environments consisting of a circular visual panorama. In this setting the fly can only control its angular orientation relative to the panorama by initiating turns, which are typically deduced from a difference in wingbeat amplitude.

A visual VR system for head-fixed walking flies has been developed more recently (Seelig et al., 2010). Here the fly walks on a spherical treadmill, a small air-supported ball. The ball movement induced by the walking fly is recorded, processed online and used to update a visual LED

display. While this setup permits accurate readout of the full rotational and translational walking manoeuvres, to date this system too has only been used together with 1D visual environments (Bahl et al., 2013; Seelig and Jayaraman, 2015).

Thus, existing behavioural paradigms for head-fixed flies use a highly reduced sensory environment, in which only a small subset of the fly's navigational manoeuvres feed back onto the sensory stimulus. Since it is not well known which aspects of the sensory environment affect the fly's internal representation of orientation and visual guidance in general, we thought that it was better to study its functionality and use in a more realistic virtual environment. We therefore decided to extend the existing VR for walking flies to allow flies to navigate a 2D space. This increase of dimension brings about a number of changes in how the animal can interact with its visual surroundings: in addition to rotational, now also translational movements affect the relative orientation of the fly to visual landmarks. Additionally, translational movements introduce expansion and contraction motion stimuli. In a 2D environment it is also possible to disambiguate to which landmark the fly's internal heading representation is tethered when there are multiple visual landmarks. Finally, increasing the complexity of the virtual environment and the number of ways in which the animal can interact with it ultimately extends the types of behaviours we can study in head-fixed animals.

Experimental approach

In this chapter we present a new visual VR system for tethered walking flies based on the existing spherical treadmill setup (Seelig et al., 2010). We use a projector-based visual display rather than an LED arena to gain spatial resolution and more flexibility in the presentation of visual stimuli. We will begin by describing in detail the hardware composition of the newly developed VR system before explaining the custom-written program that generates the visual stimulus for the VR. In a first set of behavioural experiments, using a simple stripe tracking paradigm, we test whether the quality of visual stimulation and the feedback loop are sufficient for flies to interact with the visual stimulus. We then conducted a series of experiments aimed at characterising how walking flies interact with visual landmarks in the 2D VR. When analysing walking behaviour in the VR, we were concerned about potential artefacts induced by the tethering procedure. Moreover, the more complex virtual environment and the larger number of degrees of freedom in the interaction of the fly with its environment made it difficult to define and detect landmark interaction behaviour. We addressed these issues by generating ground-truth datasets in freely walking flies. We characterised how naïve freely walking flies exploring a 2D plane interact with a landmark and how this behaviour is affected by genotype

and sex in a free walking assay. We then compared the landmark interaction behaviour of freely walking and tethered walking flies to get a sense of how behaviours were affected by the head-fixed preparation. Finally, we evaluated how walking and landmark interaction behaviour in tethered flies changed with extended exposure to the VR environment.

3.2. Material and Methods

3.2.1. Preparation of flies for tethered and free walking experiments

Flies were reared at 23 ˚C in 60 % relative humidity with a 16:8 light:dark cycle on fly food that was prepared according to a recipe from the University of Würzburg, Germany. To prepare 10 l of standard Würzburg food, 180 g yeast (inactive dry yeast, Genesee Scientific, San Diego, CA, USA), 1600 g corn meal (Quaker Yellow Corn Meal, Quaker Oats Company, Chicago, IL, USA), 100 g soy flour (Genesee Scientific, San Diego, CA, USA) and 400 g malt extract (Genesee Scientific, San Diego, CA, USA) were mixed in 10 l of water. The 75 g agar (fly agar, Tic Gums Inc, Belcamp, MD, USA) is dissolved in 1 l of water before being added to the mixture. Finally, 400 g corn syrup and an antifungal agent, Tegosept (20%, 125 ml, Genesee Scientific, San Diego, CA, USA), are added. For all experiments, 3-5 day old flies were cold anesthetised, sorted by sex and the distal two thirds of their wings were clipped. After wing clipping, male and female flies were transferred into fresh food vials and kept separately. A small piece of filter paper was stuck into the food to provide flies with an additional, dry surface to walk or groom on. Wing-clipped flies were given 2-3 days to recover before experiments. All experiments were performed with 5-10 day old wing-clipped flies, unless noted otherwise.

The decision to use wing-clipped flies was motivated by two observations. Firstly, clipping the wings 1-2 days prior to experiments strongly reduced the rate of attempted take-offs or jumps of tethered flies on the ball. Secondly, many previous studies on visual navigation in flies used wing-clipped flies, thus comparing our data to published results would be more direct if we also used wing-clipped flies. In some experiments we used an alternative technique to render flies flightless: gluing the wings together in a relaxed position with a small drop of glue right behind the thorax. Wing-glued flies were given at least a day of recovery before using them in experiments.

Tethering of flies for VR experiments

For experiments in the VR, wing cut flies were cold-anesthetised and glued to a thin tungsten wire pin with UV-curable glue (KOA 300, KEMXERT, York, PA, USA). With an additional small droplet of glue, deposited above the neck connective close to the ocelli, the head was fixed to the thorax keeping it in relaxed natural position. We decided to fix the head in tethered experiments to keep conditions similar to those in imaging experiments and to minimise movements of the fly that would break the closed-look visual stimulation. After being tethered to the pin, flies were transferred to VR rig, positioned on the ball and tested within 3-6 h. Thus, flies were effectively dry-starved for up to 6 h prior to experiments. After positioning a fly on the ball it was given 15-30 min to adjust before starting an experiment.

Genetic backgrounds used behavioural experiments

To assess the effect of different genetic backgrounds on landmark interaction, we tested the behaviour of three fly strains: Wild type Berlin (WTB), Dickinson lab (DL) and WTB x pBDP-GAL4 hybrid flies. Hybrid flies were generated by crossing WTB virgins with males from a so-called 'empty GAL4' line. As 'empty GAL4' we used pBDPGAL4U in attP2, an enhancerless GAL4 construct (Pfeiffer et al., 2010). WTB x pBDP hybrid flies were included to more closely match the genetic background of flies used in optogenetic activation experiments presented in chapter 4. The WTB stain is an isogenic wild type strain and the DL strain was founded in M. Dickinson's laboratory by 200 wild-caught females.

3.2.2. Spherical treadmill system

For the spherical treadmill we used a hand-milled ball made from polyurethane foam (Last-A-Foam, General Plastics Manufacturing Company, Tacoma, WA, USA) with a diameter of 9.93 mm and a weight of 37.4 mg. The ball was freely floating on an aircushion in a custom-made holder. The airflow to the ball was maintained at 0.45 l/min using a mass flow controller (Alicat Scientific, Tucson, AZ, USA) and humidified by passing it through a bottle humidifier (Salter Labs, Lake Forest, IL, USA). The ball motion was captured by a previously described ball tracker system (Seelig et al., 2010). Briefly, two optic flow tracking cameras positioned at the equator of the ball at 135˚ azimuth to the left and the right side (***Figure 3.1 E)*** were used to capture the ball rotation around all three axes of movement — pitch, roll and yaw — at 20 kHz. The optic flow measurements from the two tracking cameras were sent to a custom-programmed microcontroller (MCU, ***Figure 3.1 E***) via a serial interface. The microcontroller downsampled and converted this input to a digital data stream at 4 kHz, which was sent to a computer

running the VR software via a serial port interface. In this output stream the ball rotation is captured by four values, x_1, y_1, x_2 and y_2, corresponding to the measured movement of the ball along the x and y axis in the field of view of the two tracking cameras. The ball surface was illuminated from below and the side with a set of four IR LEDs emphasising the texture of the ball surface for high tracking performance (***Figure 3.1 A, B)***.

The treadmill readout has arbitrary spatial units per time (a.u./s). To obtain a ball rotation velocity measurement in mm/s the treadmill output was calibrated using a third (calibration) camera positioned at the ball equator at 180˚ behind the ball. With this camera a video of the balls movement sampled at 500 Hz could be obtained simultaneously to measuring the ball's rotation with the tracking cameras. This video was analysed offline to generate an independent measurement of the ball movement in pixel/s. By comparing the measurement of ball rotation from the calibration camera to the one from the two tracking cameras, we obtained a scaling factor to convert the treadmill velocity measurements from a.u./s to pixel/s (see details in Seelig et al., 2010). A second scaling factor, to convert the measurement from pixel/s to mm/s, was obtained by taking an image on a calibration cube of known physical dimensions with the calibration camera. The two calibration factors as well as the ball radius are provided to the VR software. The VR software used these scaling factors to compute the fly's walking velocities from the treadmill's ball rotation measurements as described in (Seelig et al., 2010). Briefly, the forward, lateral and rotational velocities are computed from the four treadmill measurements (x_1, y_1, x_2 and y_2) as

$$\nu_{fwd} = -(y_1 + y_2)\cos(\gamma)$$
$$\nu_{lat} = -(y_1 - y_2)\sin(\gamma)$$
$$\nu_{rot} = -\tfrac{1}{2}(x_1 + x_2)$$

with γ = 45˚, corresponding to the azimuthal angle between the tracking camera and the pitch axis. The negative sign accounts for the conversion from ball rotation to the corresponding movement of the fly in virtual space.

3.2.3. Projector-based visual display

The visual display consisted of a triangular screen onto which a panoramic image was back-projected by two DLP (Digital Light Processing) projectors (DepthQ WXGA 360 HD 3D Projector, developed by Anthony Leonardo, Janelia, and Lightspeed Design, Bellevue, WA, USA). DLP projectors are also sometimes referred to as DMD because they utilise a so-called digital mirror device (DMD) to generate a grey-scale image. Each microscopically small mirror in the DMD

corresponds to a pixel in the projected image. An image is generated by controlling the light intensity of each pixel, which depends on the amount of input light and the percentage of light that each oscillating mirror lets pass to the screen. The two projectors each generated an image with 720 x 1280 pixel resolution. The two projections were aligned to generate a continuous image (1440 x 1280 pixel). At the closest point (90 ˚ to either side), where the screen is only 21.9 mm away from the fly, a pixel subtended a visual angle of about 0.743˚. The furthest pixels on the screen, located in the upper back corners of the screen, had a distance of 106.5 mm from the fly and subtended an angle of 0.153˚. The maximum angular pixel size in our setup is well below 5˚, the approximate interommatidial angle of *Drosophila melanogaster* (Land, 1997), ensuring that the movement of images across the screen appears smooth to the fly.

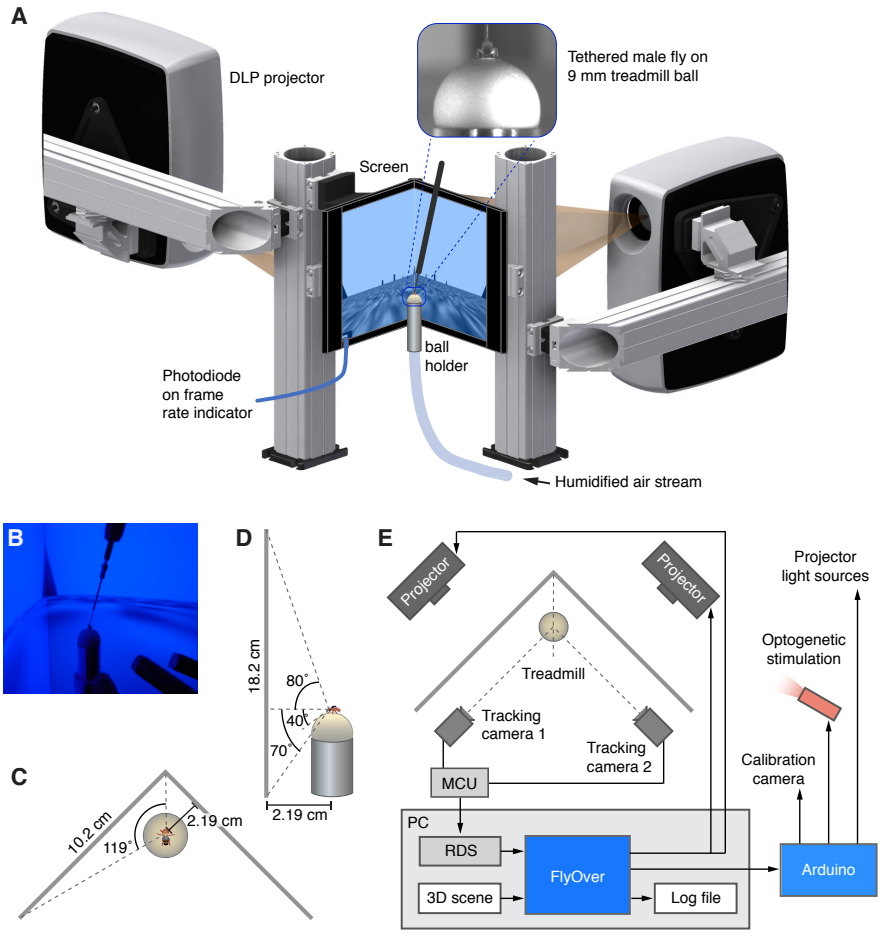

Figure 3.1: A 2D virtual reality system for head-fixed walking fruit flies.
A: Schematic of the primary hardware components of the VR set-up. The inset shows a still from a video of a tethered fly on the ball taken with the IR camera used for calibration and fly positioning. Bright areas on the ball surface show where the IR illumination of the trackball is targeted. B: Photograph of a fly on the ball viewed from the side taken with a regular camera. The IR LEDs are visible in the lower right image

corner. C, D*:* Schematic of the screen geometry and relative positioning of the fly, for top view (C) and side view (D). The range of the horizontal field of view indicated in (D) corresponds to the closest screen distance relative to the fly, which occurs at 90 degrees on both sides. E: Diagram of the hardware control loops. DLP, digital light processing; RDS, remote data server; MCU, microcontroller unit.

We measured the irradiance of the projected image on the panoramic screen with a power meter (PM100D with S130C Sensor, Thorlabs Inc, Newton, NJ, USA, sensor facing toward the projector) for a wavelength of 459 nm (peak wavelength in previously measured spectrogram). When a bright scene with one dark landmark (similar to Figure 3.4 D) was projected onto the screen, we measured a light intensity of 0.52 mW/cm^2 in the centre of the right screen and 0.54 mW/cm^2 on the left screen. The light intensity within the dark area of an image of a black landmark projected onto the centre of the right screen was 0.02 mW/cm^2. Thus, the projected image has a Michelson contrast of about 0.926 with a minimum and maximum intensity of 0.02 mW/cm^2 and 0.54 mW/cm^2, respectively.

3.2.4. Free-walking arena design

The design of our free-walking arena (***Figure 3.2 A, B***) was inspired by (Robie et al., 2010). The arena consisted of a large circular walking platform (radius 11.4 cm) made from textured matt acrylic (TAP Plastics Inc, San Leandro, CA, USA) surrounded by an acrylic cylinder (inner diameter 22.8 cm, height 17.8 cm) mounted on a laser cut acrylic base. The walking platform could be taken out for cleaning. Wing-clipped flies were maintained within the arena by coating the arena wall with a siliconising fluid (Sigmacote from Sigma-Aldrich, St. Louis, MO, USA), which makes it hard for flies to walk up the arena wall. The arena wall was mantled with a white diffusor sheet (V-HHDE-PM06-S01-D01 sample, BrightView Technologies, Durham, NC, USA) and backlit with blue LEDs (470 nm, Super Bright LEDs Inc. St. Louis, MO, USA) mounted on a wire mesh-based scaffold that was fixed onto the arena base. Blue-coloured backlight was chosen to match conditions in the VR setup as well as conditions in the two-photon calcium imaging rigs used in our lab. We measured the light intensity inside the free walking arena with a power meter (PM100D with S130C Sensor, Thorlabs Inc, Newton, NJ, USA) for an expected wavelength of 461 nm (peak wavelength in previously measured spectrogram) by placing the sensor either at the border of the arena or in the arena centre, facing toward the arena wall. At the border we measured a light intensity of 0.115 mW/cm^2 and in the centre 0.105 mW/cm^2. These measured light intensities are slightly lower than the intensities measured at the screen in the VR, but differ less than an order of magnitude. Furthermore, it is not straightforward to compute quantitatively from the measured light intensities presented above (given how they

were obtained), in how far the perceived luminance that a fly experiences in the VR rig and the free walking arena are different.

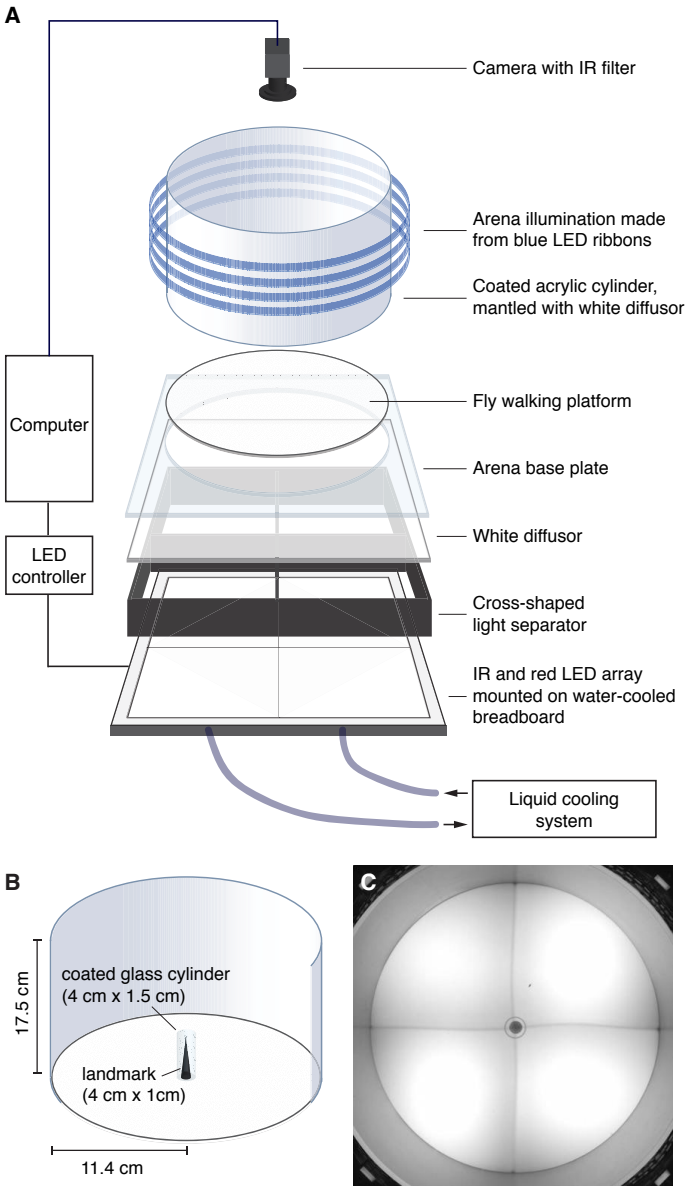

Figure 3.2: Arena for studying landmark interaction in freely walking flies.
A: Schematic of the complete free walking rig. B: Schematic of the free walking arena with a landmark. C: Single video frame from a trial with a male fly exploring the arena with a single landmark. The fly is visible above the cone. The image was taken with an IR camera and does not reflect the lighting conditions visible to the fly.

The fly's walking behaviour was recorded with BIAS (Basic Image Acquisition Software, version v0p49, IO Rodeo, Pasadena, CA, USA) using a video camera (Flea3 1.3 MP Mono USB3 Vision, Point Grey, Richmond, Canada) placed 120 cm above the walking platform. A lens with 16 mm

focal length, low distortion (Edmund Optics Inc, Barrington, NJ, USA, stock #63245) and a 760 nm infrared filter (52 mm, Neewer Technology Ltd., Guangdong, China) were mounted to the camera. High-contrast illumination of the flies for video recording was achieved by using an infrared backlight mounted on a water-cooled breadboard (breadboard from Thorlabs Inc, Newton, NJ, USA, liquid cooling system from Koolance, Auburn, WA, USA) below the arena floor. The entire rig was placed inside a light-tight black enclosure. Videos were recorded at 12.3 Hz with 1008 x 1008 pixel large images covering an area slightly larger than the diameter of the arena. This resulted in a spatial resolution of about 40 pixel/cm with the image of a fly being roughly 8-10 pixels long and 3-4 pixels wide. Temperature and relative humidity within the arena were passively kept at approximately 28-30 ˚C and 28-32 % by controlling the temperature and humidity in the room.

3.3. Results

We will begin by presenting the newly developed VR system, first the hardware components and then the software, before presenting data on the validation of our system. Finally we will present results from behavioural experiments aimed at characterising landmark interaction of flies exploring virtual 2D worlds.

3.3.1. A 2D visual virtual reality system for tethered walking flies

Virtual reality rig

The layout of the VR rig is illustrated in ***Figure 3.1 A***. A fly glued to a thin wire tether was fixated above a spherical treadmill (see ***section 3.2.2*** for details, Seelig et al., 2010) and its position manually adjusted with a set of micromanipulators. The fly positioned on the ball was surrounded by a triangular screen formed by two 18.2 cm high and 10.2 cm wide display faces (***Figure 3.1 B-D***). The fly was located symmetrically between the two faces, 3.1 cm behind the tip of the triangle and at one third of the screen height. The distance between the fly and the screen varied along the azimuthal direction and was smallest at 90˚ to either side with 2.19 cm. The screen spanned 119˚ of the fly's azimuthal field of view (FOV) on both sides. The coverage along the vertical FOV was limited by the ball at the lower edge to 40˚ below the horizon line. The vertical coverage above the horizon line varied with the distance of the fly from the screen being highest where the fly was closest to the screen with 80˚ and lowest at the two tips of the screen with 57˚. The screen was made from a single white diffuser sheet (V-HHDE-PM06-S01-

D01 sample, BrightView Technologies, Durham, NC, USA) that was enforced around the edges, folded along the middle and mounted onto a custom-made metal frame. The visual stimulus was back-projected onto the screen by two DLP (Digital Light Processing) projectors (DepthQ WXGA 360 HD 3D Projector, details in ***section 3.2.3***), each covering one face of the triangular screen. The full projected image had a size of 1440 x 1280 pixel with a maximum angular pixel size of about 0.7˚. A number of modifications were made to the projectors to optimise the visual stimulus delivery for the fly (all developed by A. Leonardo and ID&F Janelia). The colour-wheel was removed allowing the display of 8-bit grey-scale images at 360 Hz frame rate instead of coloured images at 120 Hz. This ensured that subsequent frames of the visual stimulus could be projected at a rate above the animal's flicker fusion frequency, making the projected movements look continuous to a fly. Furthermore, the optics were optimised for close-range projection. We also replaced the lamp by a light guide to a blue LED light source (458 nm wavelength, SugarCUBE LED Illuminator, Edmund Optics Inc, Barrington, NJ, USA). While blue light may not be the ideal choice for behavioural assays, dim blue light is compatible with calcium imaging and we wanted to develop a behavioural paradigm that would be transferable to an imaging rig. The projectors were connected to a computer via two display ports on a graphics card (GeForce GTX 770, Nvidia, Santa Clara, CA, USA) with three independent outputs. We used a custom programmable microcontroller to allow communication between the VR software and various hardware components (Arduino Mega 2000, ***Figure 3.1 E***). The humidity and temperature in the VR rig were controlled by adjusting the room temperature and humidity. We aimed at a room temperature of around 28-30 ˚C and a relative humidity of 28-32 %, which in our experience promoted flies to walk on the ball.

Software for closed-loop visual virtual reality

An overview of the software architecture and how it ties in with the hardware components of the VR rig is given in ***Figure 3.1 E***. The central component of the VR system was a feedback loop formed by the spherical treadmill that captured a fly's walking movements and a custom-written program, FlyOver, which used those measurements to simulate the fly's position in a virtual world and generated a corresponding visual stimulus, which was presented to the fly, closing the loop. The treadmill system tracked the fly's movements at 4 kHz and sent this data to the rig computer via serial communication. A custom-written C++ program (Remote Data Server, RDS) read the ball tracking data, downsampled it to 400 Hz and passed it on to a second custom-written C++ program, 'FlyOver'. FlyOver formed the core software of our VR system. The program was developed in collaboration with Scientific computing (C. Bruns, M. Bolstad) based on the OpenSceneGraph framework and can be downloaded from Github (https://

github.com/JaneliaSciComp/FlyOverJovian). The user could load a custom 3D scene into FlyOver (see also ***section 3.3.3***). The scene file specified the virtual world, its geometry as well as the position and appearance of arbitrarily placed and shaped objects inside it. It also specified the initial placement of the fly inside the virtual world. After loading the scene file, the FlyOver graphical user interface (GUI) could be used to set a few other parameters affecting the final display of the virtual world to the fly. FlyOver could, for example, correct for distortions of the visual panorama introduced by the screen geometry using the rig-specific dimensions of the screen and parameters describing the placement of the fly relative to the screen. This means that FlyOver can be flexibly adjusted for the use with different screen geometries. In addition, the GUI was used to introduce virtual 'fog' to hide distant objects.

During a trial, FlyOver continuously updated the fly's virtual position based on the treadmill tracking data and rendered the virtual scene from the fly's point of view. Sets of three frames were generated at a time and sent as one package to the graphics card at 120 Hz. Those packages were passed on to the projectors, which projected a new frame onto the screen at 360 Hz. To monitor the actual frame rate, each rendered frame included a frame rate indicator in the form of a small square at the edge of the image, whose colour was toggled between white and black with each newly drawn frame (lower left corner in ***Figure 3.2 A-D***). The changes in light intensity of this frame rate indicator were measured with a photodiode.

For each frame, i.e. at 360 Hz, the following parameter were logged to file:

- Time that had passed since start of trial [s]
- Position of the fly in the virtual world in x [mm], y [mm] and z [mm]
- Translational velocity [mm/s]
- Global heading in the virtual world [degrees]
- Treadmill readout integrated over the time period of the current frame [arbitrary units]
- Collision distance [mm] indicating the distance to the closest virtual object

In addition, each log file contained a header with information about the loaded scene file, various user-defined FlyOver settings such as the parameter specifying the virtual fog, the FlyOver version as well as the time and date of the measurement. For each trial FlyOver also generated a *.coord file, which contained the locations of the centres of all objects within the scene in virtual world coordinates.

FlyOver also sent a second, reduced output stream (at 60 Hz) via a serial port to a microprocessor (Arduino Mega 2000). This second output stream only contained the trial time

[s] and the fly's virtual position in x [mm] and y [mm], and was read and parsed by a custom script running on the microprocessor. The microprocessor controlled for example the light source of the projectors and could be used to trigger video recordings of the fly or initiate e.g. optogenetic stimulation (***Figure 3.1 E***, right side).

Building 3D scenes for our virtual reality system

We used Blender (version 2.73), an open source software tool, to create virtual 3D scenes for our experiments. Each object within the 3D scene had a unique name and a set of properties. Properties such as the colour and texture were specified in Blender as 'materials' that were then assigned to the respective object. Three other properties were communicated to FlyOver as part of the object's name string:

- *Visibility:* An object could be marked as invisible by placing underscores at the beginning and end of an object name, e.g. '_Cone_'.
- *Penetrability:* An underscore followed by 'p' as in 'Cone01_p' marked an object as 'physical', i.e. not penetrable by the fly.
- *Concavity:* An underscore followed by 'c' as in 'Cone01_c' marked an object as 'concave'. This property was only relevant for objects that were hollow and impenetrable, as it defined whether the fly was excluded from the inside or the outside. For example, the fly should not be able to enter a small hollow cylinder used as a virtual landmark, while it should not be able to exit a large hollow cylinder that marked the arena wall. Consequently, the landmark model had to be marked as 'convex', while the arena model had to be marked as 'concave'.

The flags for visibility, penetrability and concavity could be combined in the name of a single object. By default objects were 'visible', 'penetrable' and 'convex'. The 3D scenes were exported from Blender to the Collada format, a standardised XML format used to describe 3D graphics.

When loading a new scene file, FlyOver parsed the names of each object and assigned corresponding properties to the objects composing the virtual scene. Invisible objects could be used to mark special areas within the scene, such as the starting point of each trial, and control the delivery of other stimuli based on the fly's position inside the VR.

3.3.2. Validation of the visual closed-loop system using stripe fixation

As a first step toward validating our VR system, we wanted to confirm that it could support known visual behaviours, specifically that the closed-loop feedback was sufficiently fast and reliable to let flies engage with the visual stimulus.

To do this, we tested whether in our setup tethered flies reliably performed a well-studied naïve behaviour: 'stripe tracking'. In the stripe tracking paradigm, a circular panorama with a single vertical 20˚ wide bar was presented to a tethered fly walking on the ball. The angular orientation of the panorama was coupled to the fly's steering manoeuvres on the ball allowing the fly to actively control the angular position of the stripe relative to its own heading direction. Only rotations around the yaw axis, i.e. on the spot rotations to the left or right were coupled to the visual panorama. The fly's position relative to the panorama was fixed, i.e. the fly cannot change its distance to the stripe. It has been reported that under these conditions, tethered walking flies actively keep the stripe in their frontal field of view (Bahl et al., 2013). Thus, the stripe tracking paradigm forms a simple 1D test case for the quality of the visual closed loop system.

When we tested flies under these conditions in our VR system, some flies indeed showed robust stripe fixation over a 10 min trial, indicating that both the stimulus presentation as well as the speed of the feedback loop were sufficient to sustain active interaction with the visual stimulus (see ***Figure 3.3 A*** for a representative example of good fixation). We tested stripe fixation in male and female flies of two wild type strains: Dickinson lab (DL) and wild-type Berlin (WTB). Since stripe tracking can only be evaluated if the fly is walking, we increased the probability of walking by performing the stripe tracking experiments at high room temperature (30˚ C, see also Bahl et al., 2013). To prevent flies from flying we glued their wings behind the thorax one day prior to experiments on the ball following instructions in (Bahl et al., 2013). Under these conditions most flies walk well on the ball. However, we found that the extent to which flies track the stipe varied extensively both between sex and genotype (***Figure 3.3 B, C***). Female DL flies showed pronounced and reliable stripe fixation in their frontal FOV (peaks around 0 in ***Figure 3.3 B***, left), whereas female WTB flies only had a mild preference for relative heading angles in the front (***Figure 3.3 C***). In male flies only a subset showed clear fixation and the differences between genotypes were less pronounced (right panels in ***Figure 3.3 B, C***).
We conclude from the clear and reliable fixation behaviour in female DL flies that the visual stimulation in our VR system is able support visual behaviours. Robust fixation of a black stripe in the frontal FOV may be observed in other genotypes too, for example with Canton S flies as reported in (Bahl et al., 2013).

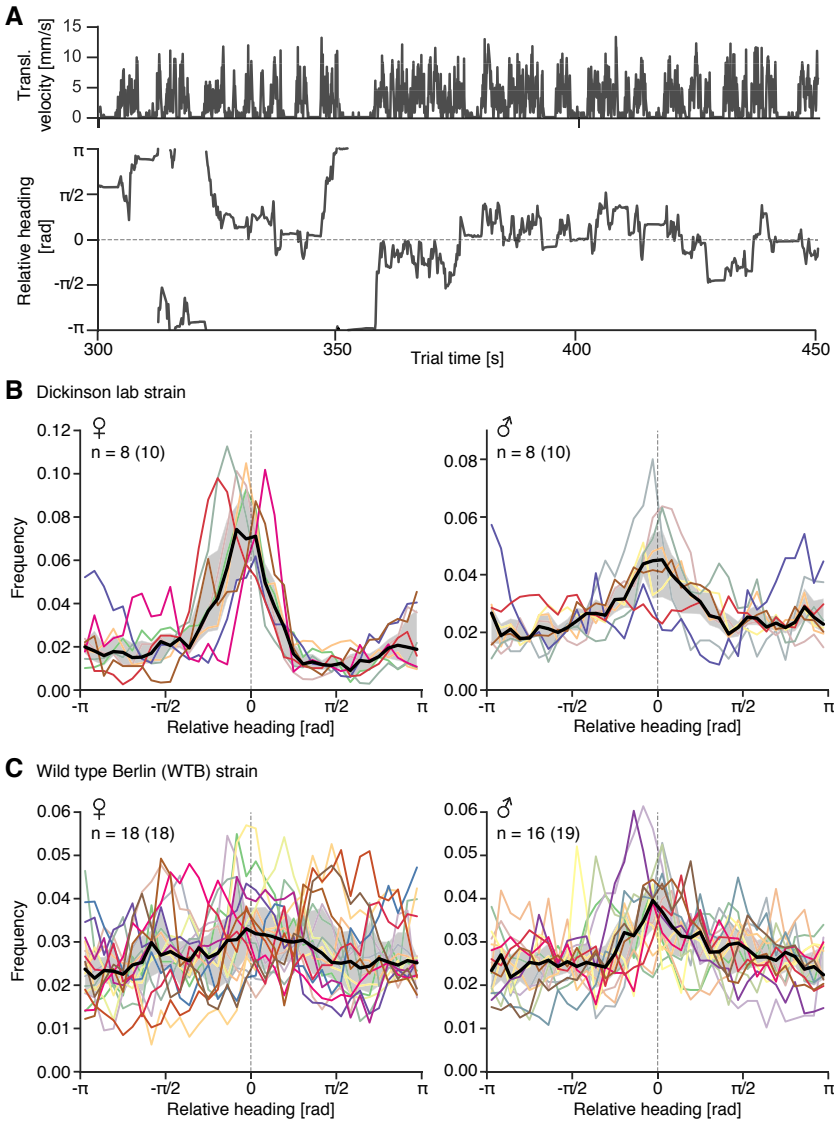

Figure 3.3: Stripe fixation ('dark on bright', 20 ˚ wide stripe) in female and male flies of two genotypes.

A: Example traces of translational velocity (top) and relative heading angle (bottom) of a male wing-cut WTB fly measured at high temperature. A relative heading angle around 0 rad corresponds to the frontal field of view (grey dashed line). The time series was recorded at 360 Hz and downsampled to 20 Hz. B, C: Relative heading distributions measured in wing-glued flies at high (30 ˚C) room temperature. Heading distributions of single flies are shown as coloured lines and the median response as black line. The grey shaded region indicates the interquartile range (IQR). A relative heading angle of 0 corresponds to a position of the stripe or landmark in front of the fly, +/-π to positioning behind the fly. Note the different scales on the y-axis. Flies that walked for less than 20 % of the time were excluded from the analysis. B: Female (left, n=8 (10)) and male (right, n=8 (10)) flies from the Dickinson lab strain. C: Female (left, n=18 (18)) and male (right, n=16 (19)) flies from the Wild type Berlin (WTB) strain. Sample sizes after exclusion, initial sample sizes are given in brackets.

3.3.3. Design of 2D virtual worlds for studying landmark interaction in tethered flies

We developed this VR system to study navigation in 2D rather than 1D. Thus, the next step, after validating the basic functionality of our VR system, was the design of a suitable virtual visual environment in which flies could explore space and interact with landmarks. The design of 3D scenes used in our experiments was guided by the following principles:

- Minimise the potential for the fly to collide with impenetrable virtual objects, as the VR cannot provide adequate feedback in these situations and flies sometimes 'get stuck' at virtual walls as they keep running into them.
- Keep the visual panorama simple, with just a few salient landmarks to simplify the analysis of trajectories of flies exploring the virtual world.

The second principle was also motivated by the specific question we wanted to address with our behavioural paradigm. We were primarily interested in understanding how flies use visual landmarks for goal-directed navigation. Specifically, we wanted to connect the visual stimulus to the fly's walking manoeuvres and ultimately also dynamics of neural circuits involved in controlling the behaviour. Simplifying the visual panorama not only eases the analysis of behavioural data but might also simplify the task of connecting the behaviour to imaging. Following these two principles led us to design large periodic worlds, in which a freely exploring fly would repeatedly encounter equivalent conditions. The virtual worlds consisted of a textured ground plane with black landmarks sparsely placed on the nodes of a hexagonal grid (***Figure 3.4 E, F***). We used virtual fog to visually separate the landmarks by hiding far objects to reduce visual clutter: objects that were far from the fly's current location in the virtual world appeared at increasingly lower contrast and eventually blended into the background (***Figure 3.4 A-D***). The fog started at a user-defined distance and increased linearly in density to reach full coverage at a second, larger user-defined distance. Both distances were specified though the FlyOver GUI.

As landmarks we used 1 cm wide, 4 cm high cones. The dimensions of the virtual landmarks were chosen to match landmarks that induced frequent object interactions in flies exploring a real-world free walking arena (data from a pilot study with freely walking flies not presented here). The angular width and height of a cone with these dimensions, viewed from the fly's virtual position close to the ground plane, varied with the fly's distance from the landmark as visualised in ***Figure 3.4. G***. At a distance of about 28 mm from the landmark centre, the base of the cone has an angular width of 20˚, which corresponds to the width of the stripe used in the fixation experiments presented in ***Figure 3.3***. The image of the cone on the panoramic screen is only clipped at distances smaller than 10 mm.

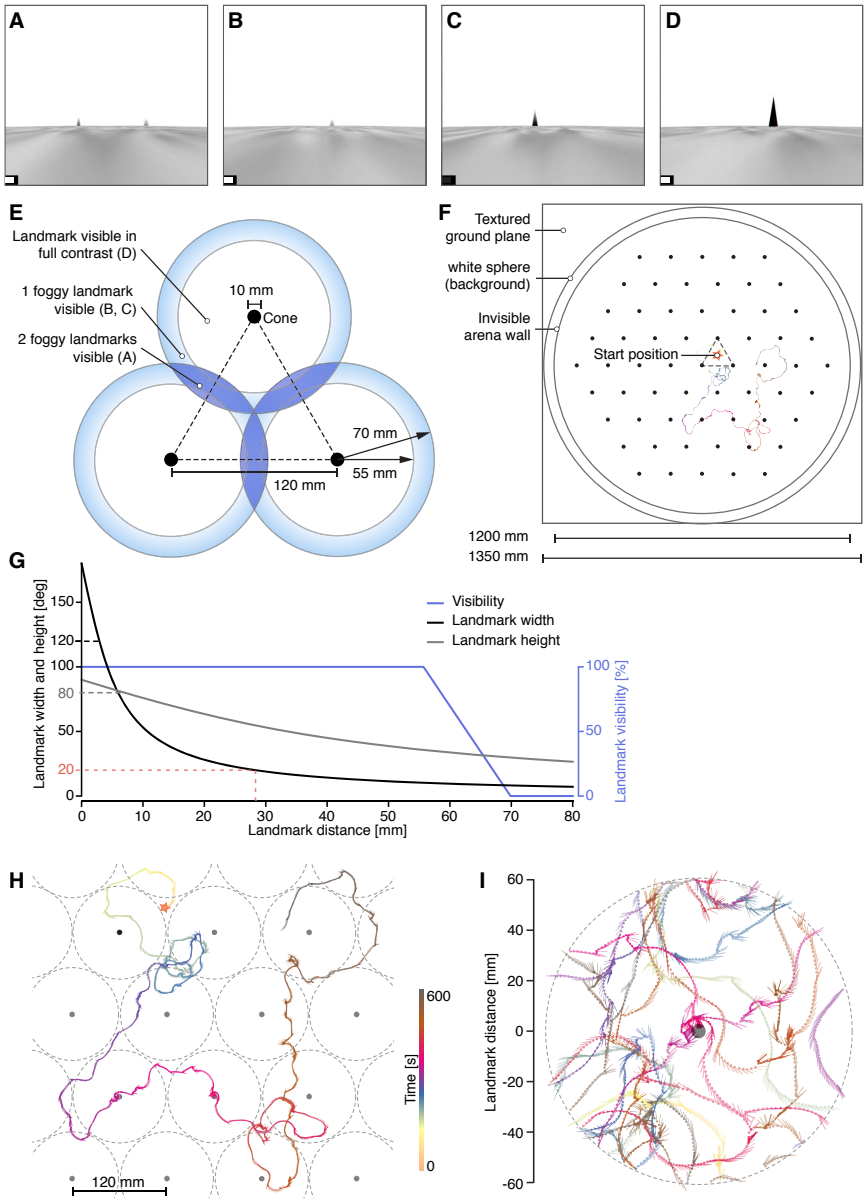

Figure 3.4: Design of virtual worlds for studying landmark-guided navigation.
A-D: Frames from different time points during the approach of a landmark. Two landmarks are visible in A, both partially hidden in the virtual fog. B-D show the view on one landmark from decreasing distances. Over the course of the approach, the landmark increases in size and comes into full contrast. E: Three landmarks arranged on the nodes of an equilateral triangle form the unit cell of the hexagonal grid (F). Based on pilot experiments the distance between landmarks was chosen to be 120 mm. Blue shading around each landmark indicates where the respective objects begins to be visible (outer circle, 70 mm away from object) and where it starts to appear in full contrast (inner circle, 55 mm away from object). F: The complete virtual world consisted of a lightly textured ground plane, a spherical while backdrop, an invisible cylindrical arena wall and the 2D array of landmarks. The orange star marks the starting position of each fly at the beginning of a trial. An example trajectory from one 10 min trial (see H) is overlaid for reference. G: Schematic illustrating the angular width (black line) and height (grey line) of a 1 cm wide and 4 cm high cone as seen from a point of view close to the ground plane as a function of distance from the centre of the cone.

The blue line indicates visibility of the cone through virtual fog with 100 % corresponding to full visibility and 0 % corresponding to no visibility. The dashed salmon line indicates the distance at which the cone has an angular width of 20˚ **H:** Example trajectory in a world with landmarks (dark grey circles) placed on the nodes of a hexagonal grid. An orange star marks the fly's starting position. The colour of the trajectory indicates the progression of time over the course of a 10 min trial. The grey dashed circles mark the circular area around each landmark, which were included in the analysis. **I:** Trajectory shown in **H** after 'collapsing' the trajectory fragments within a 60 mm radius circle around any landmark onto the 120 mm wide circular arena around the landmark positioned on the origin.

The virtual fog was set to fully hide any landmarks that were further than 70 mm away from the fly's point of view. Landmarks gradually emerged from the virtual fog at distances of less than 70 mm and came into full contrast at distances smaller than 55 mm, at which point the cones had an angular width of 10.39˚ at the base and an angular height of 36.03˚ (***Figure 3.4. G***). Thus landmarks emerging from the fog should be detectable by the fly, as the angular width and height of a landmark are well above the interommatidial angle of *Drosophila melanogaster*, which is about 5˚ (Land, 1997).

Free walking experiments also informed the spacing of the virtual landmarks relative to each other (see ***Figure 3.4 E*** for details). The overall size of the virtual world was chosen based on pilot experiments in the VR to ensure that most flies did not reach the arena border within a 10 min trial (***Figure 3.4 F***). For most of our experiments we chose black landmarks on a bright background and a light grey, textured ground plane, matching conditions used in our free walking arena experiments. For the ground plane texture, we chose white noise grey scale pattern with pixels varying between 0 % and 50 % black level (low contrast condition) or between 0 % and 100 % (high contrast condition). The images in ***Figure 3.4 A-D*** show a virtual world with the low contrast ground plane.

For the analysis of walking trajectories we exploited the periodic nature of the virtual worlds we used in the experiments. We largely restricted the analysis of trajectories to the trajectory fragments that were within 60 mm radial distance from any landmark (area within grey dashed circles in ***Figure 3.4 H***). As the virtual world within each of these 'mini arenas' was identical, we then collapsed these trajectory fragments onto the 'mini arena' centred around the landmark placed on the origin. We will refer to this as the 'collapsed' trajectory (***Figure 3.4 I***). For the projection, the trajectory fragments were only shifted and thus only the fly's position but not its absolute heading angle was changed.

3.3.4. Dimensionality increase: From stripe tracking in a 1D world to tracking visual landmarks in 2D

We showed that flies readily track stripes in our VR system. By comparing tracking performance of a stripe in a 1D panorama to tracking of a landmark in a 2D plane, we would like to illustrate how adding degrees of freedom influences visual orientation behaviour in walking flies. The primary effect of increasing the number of spatial dimensions is the addition of translational movements. During translational movements visual landmarks expand or contract depending on their position relative to the fly. In our high-contrast worlds, expansion of the dark landmarks brings about an overall change in luminance. This connection between landmark fixation and brightness change does not occur in 1D worlds. This means that object fixation, but not necessarily stripe fixation, could be influenced by a fly's photopreference. It is easy to change specific parameters of the visual environment in VR and we therefore decided to test the effect of contrast polarity on fixation behaviour. We tested both stripe tracking and object tracking under two contrast conditions, 'dark on bright' and 'bright on dark'. For the 'dark on bright' condition, we used a black stripe (20˚ wide) on a bright background or a black landmark (1 cm wide and 4 cm tall cone) in front of a bright background on a lightly textured plane (***Figure 3.5 A***). The 'bright on dark' condition was generated by inverting the brightness in the 'dark on bright' worlds (***Figure 3.5 B***).

By measuring walking behaviour of individual tethered flies in all four virtual worlds, we were able to compare how stripe fixation in 1D relates to object tracking in 2D under varying contrast polarity conditions. We computed the relative heading distribution over the course of a 10 min trial as a measure of the fly's heading preference. In case of perfect stripe fixation the relative heading distribution should have a single peak at the angle at which the fly fixated the stripe. We defined the heading angle such that 0 corresponds to fixation in the front and +/-π to fixation behind the fly. For trials in the plane, we computed the heading relative to the closest landmark but otherwise disregarded the distance to the landmark. An example for stripe and landmark fixation in the same fly in a 'dark on bright' world is shown in ***Figure 3.5 C*** and an example for fixation in the inverted case is shown in ***Figure 3.5 D***.

We would like to point out a few important differences between fixation in 1D and 2D. As mentioned before, in the stripe fixation task in a 1D world only the fly's rotational movements affect the stripe's position. This means that if a fly moved the stripe to its side and then kept walking perfectly straight, the stripe would remain at the fly's side. In contrast, if a fly was positioned next to a landmark in a 2D plane and started walking straight, the landmark would

slowly move behind the fly due to the translational movement. A second difference between 1D and 2D worlds is, that if a fly fixates a stripe in its frontal FOV in a 1D world and runs toward it, the stripe does not change its size. This is not the case for fixation of a landmark in the frontal FOV in a 2D world, where the landmark expands as the fly approaches it, resulting in a looming stimulus.

We can improve our intuition for how fixation relates to course control by comparing the relative heading distributions with the trajectory of a fly through the 2D plane. Firstly, fixation of a landmark in the frontal FOV (around 0 rad) leads to approach as long as the fly is moving forward. Thus, a fly would eventually reach the landmark in which case it can either stop there or move on (***Figure 3.5 E***). This means that fixation in the front will necessarily lead to sampling of other relative heading angles when the fly moves on from the previously fixated landmark. This necessary alternation between fixation and antifixation has previously been discussed in the context efficient search in freely walking flies (Bülthoff et al., 1982; Götz, 1994). Secondly, actively fixating a landmark in 2D at one side, i.e. at a relative angle around -π/2 or +π/2, leads to circling around that landmark as illustrated in ***Figure 3.5 F***.

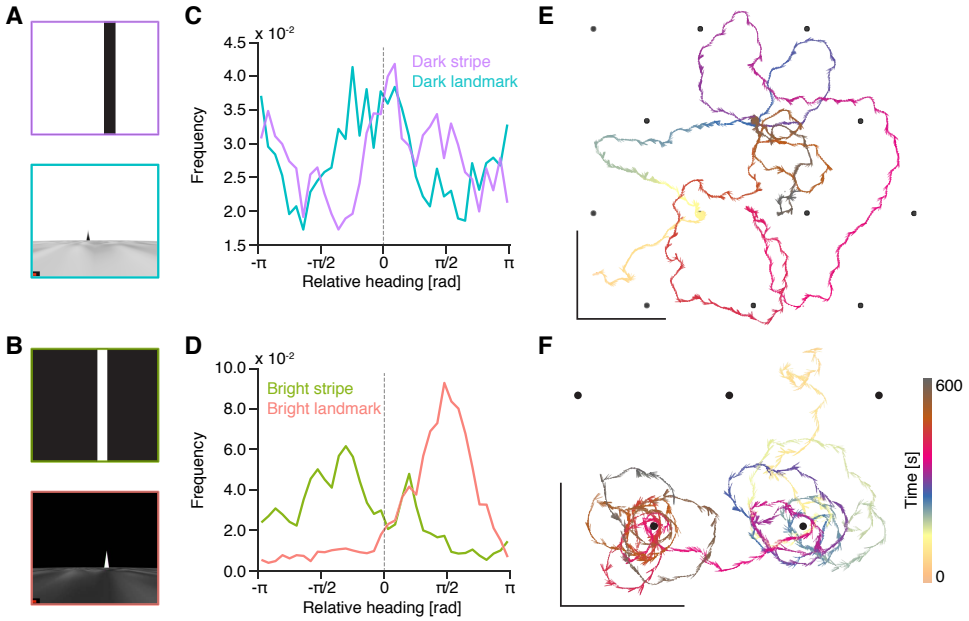

Figure 3.5: Fixation behaviour in one and two dimensions.
A, B: The four tested trial types. Two contrast conditions were tested: 'Dark on bright' (A) with a black stripe on a bright background and black landmarks in a bright plane as well as 'bright on dark' with a bright stripe on black background and bright landmarks in a dark plane (B). C, D: Examples for relative heading distributions during stripe fixation and exploration of a 2D plane. A relative heading of zero means that the fly kept the stripe or the landmark straight in front, π and -π/2 correspond to the object

being the side of the fly and +/-π corresponds to the object being behind the fly. **C:** Heading distribution in 'dark on bright' scenes of a male, wing-glued fly measured at high room temperature. **D:** Heading distribution in 'bright on dark' scenes of a male, wing-cut fly measured at high room temperature. **E, F:** Traces of two flies exploring the 2D plane with landmarks (black circles). The position and the heading of the fly are indicated with a dot and a small bar pointing into the direction that the fly was looking at. The traces are colour-coded to mark the temporal progression of the 10 min trial. The black size marker indicates 10 cm distance in x and y direction. **E:** Same fly as in D, exploring a bright plane with black landmarks. **F:** Same fly as in E, exploring a dark plane with bright landmarks.

To systematically validate our setup and to analyse the relationship between stripe and landmark fixation more quantitatively, we measured fixation behaviour of 60 male and 59 female wild type (WTB) flies in the four virtual worlds conditions introduced ***Figure 3.5***. Within this group of flies we tested the effect of different wing-preparation techniques, i.e. cut or glued wings, and of the room temperature (low with 25˚ C and high with 30˚ C). This data is summarised in ***Figure 3.6*** and ***Figure 3.7***. We will begin with a coarse population-level description of preferred relative heading angles under the four different conditions before taking a closer look at the fixation behaviour across individual flies. In our analysis we only included trials, in which flies were walking for more than 20 % of the time. This led to exclusion of up to 17 % of trials in high temperature condition and up to 42 % of trials in the low temperature condition. In the low temperature conditions, flies generally walked less in the 'bright on dark' trials resulting in a larger number of exclusions (***Figure 3.7 J***, see also legend of *Figure 3.6*).

Scene contrast polarity and dimensionality have systematic effects on relative heading preferences

As a fist step toward assessing the effect of scene contrast polarity and dimensionality on fixation behaviour, we compared the frequency distributions of relative heading angles across the four conditions. Despite large inter-fly variability we found several trial-specific features in the heading distribution that were consistent across individual flies within a single experimental group, for example male wing-cut flies measured at high temperature (***Figure 3.6 B-E***). These characteristics of fixation behaviour seemed to be primarily related to the contrast condition. In 'bright on dark' trials, the heading distribution of many flies shows a pronounced peak. This fixation peak was often at angles around -π/2 or π/2, corresponding to fixation at the side (***Figure 3.6 D, E***). This trend in heading preference was consistent enough across flies to show up in the median response. In contrast, only few flies had a clearly preferred fixation direction in 'dark on bright' trials (***Figure 3.6 B, C)*** and correspondingly the median response showed only a

very small modulation. These subtle but systematic variations in preferred relative heading were consistent across sexes and preparations (***Figure 3.6 F-I***). Curiously, flies on average showed a bias toward fixating the bright stripe on one side (toward -π), whereas no such asymmetries were detected in the other three conditions. At this point we do not have a definite explanation for this asymmetry in the heading distributions. It is possible that there are asymmetries in the stimulus delivery such as minor brightness differences of the two projected images or systematic asymmetries in the tethering and positioning of flies on the ball. Potentially a fly's fixation behaviour is more easily biased by these asymmetries during 'bright on dark' stripe fixation compared to the other three conditions.

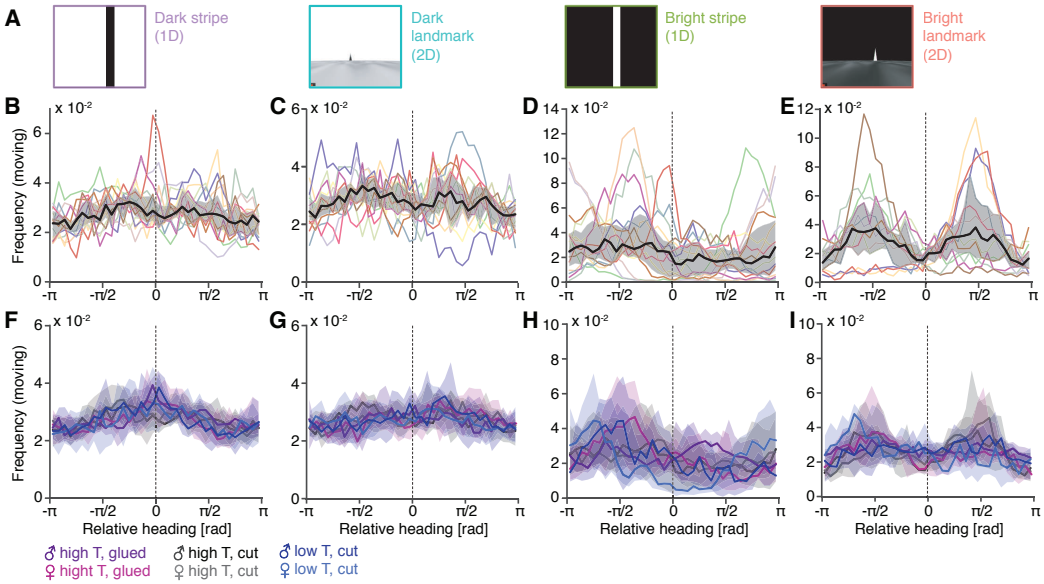

Figure 3.6: **Preferred relative heading directions in stripe and landmark fixation trials under two different contrast conditions.**
A: Schematics of the four trial types. Each fly was tested in all four conditions. **B-E:** Relative heading distributions measured in male wing-cut flies at high (30 ˚C) room temperature. Heading distributions of single flies are shown as coloured lines and the median response as black line. The grey shaded region indicates the interquartile range (IQR). A relative heading angle of 0 corresponds to position of the stripe or landmark in front of the fly, +/-π to positioning behind the fly. Note the different scales on the y-axis. In total 15 flies were measured, but some flies were excluded from the analysis, if they walked for less than 20 % of the trial time. This lead to varying sample sizes in the four conditions: n=15 (dark stripe (DS), **B**), n=14 (dark landmark (DL), **C**), n=15 (bright stripe (BS), **D**) and n=13 (bright landmark (BL), **E**). **F-I:** Average response of flies in the six tested conditions. Median is shown as a think line and the IQR as coloured shading. Again, the sample size varied between groups due to the selection of trials where flies walked for at least 20 % of time. 18 male wing-glued flies tested at high temperature (dark violet): n=15 (DS), n=17 (DL), n=15 (BS) and n=15 (BL). 18 female wing-glued flies tested at high temperature (pink): n=17 (DS), n=16 (DL), n=16 (BS) and n=16 (BL). 15 male wing-cut flies tested at high temperature (dark, see exact sample sizes listed above). 15 female wing-cut flies tested at high temperature (grey): n=15 (DS), n=15

(DL), n=15 (BS) and n=14 (BL). 27 male, wing-cut flies tested at low temperature (dark blue): n=17 (DS), n=17 (DL), n=10 (BS) and n=12 (BL). 26 female wing-cut flies tested at low temperature (light blue): n=18 (DS), n=18 (DL), n=11 (BS) and n=11 (BL).

How much flies fixate is influenced by scene contrast, while dimensionality affects where flies fixate

Next, we sought to quantify in more detail differences in the relative heading distributions of individual flies across the four conditions. Specifically, we wanted to classify whether a fly was fixating the stripe or landmark in a given trial and if it did, how pronounced this fixation was and at which azimuthal angle the fly kept the stripe or landmark. To do this, we settled on the following strategy: We first tried to fit a von Mises distribution, a continuous circular distribution approximating the circular analogue of the normal distribution. The von Mises distribution can be mathematically described as

$$f(x|\mu,\kappa) = \frac{e^{\kappa cos(x-\mu)}}{2\pi I_0(\kappa)}$$

It is a unimodal distribution, i.e. it has a single peak whose location is set by the location parameter μ, which can take any value between -π and π. The height of the peak is a function of κ, the so-called shape parameter. The larger κ, the more mass is centred on the peak at μ. If κ = 0, the von Mises becomes a uniform circular distribution. ***Figure 3.7 A*** shows the relative heading trace (left) and the frequency distribution (right) of a representative trial in grey. The fitted von Mises with location parameter μ = -1.28 and shape parameter κ = 0.53 is overlaid in black. We classified a fly's behaviour as 'unimodal fixation', if a good fit with a von Mises distribution could be achieved ($p > 0.1$ with a Kolmogorov-Smirnov test for the null hypothesis that the measured and the fitted frequency distributions are the same) and the fit had a shape parameter $\kappa > 0.5$. Thus, the example trial in ***Figure 3.7 A*** would be classified as 'unimodal fixation'. In some cases flies showed a very narrow fixation peak on top of a baseline, which generally could not be well fitted by a von Mises. We therefore allowed trials to be classified as 'unimodal fixation' even if not got fit was achieved, if the length of the mean angular vector, i.e. the inverse of the circular variance, was larger than 0.5. We noticed that amongst the heading distributions that did not match the criteria for 'unimodal fixation' were several that showed two defined peaks. We therefore added a second step in which we tried to fit heading distributions that failed to meet the criteria for 'unimodal fixation' with a bimodal distribution generated by adding two von Mises that share the same shape parameter:

$$f(x|\mu_1,\mu_2,\kappa) = \frac{1}{2}\left(\frac{e^{\kappa\cos(x-\mu_1)}}{2\pi I_0(\kappa)} + \frac{e^{\kappa\cos(x-\mu_2)}}{2\pi I_0(\kappa)}\right)$$

If a good fit with a shape parameter $\kappa > 0.5$ could be achieved with this bimodal distribution, the respective trial was classified as 'bimodal fixation'. Any trials that met neither the conditions for 'unimodal fixation' nor 'bimodal fixation' were classified as 'unclassified'.

We then used the fitted parameter location and shape parameter to generate a relatively compact yet comprehensive visual summary of the observed fixation behaviour across conditions and experimental groups (***Figure 3.7 C-J***). The unimodal fit of the heading distribution of a single fly in a given trial corresponds to a point in a polar coordinate system defined by the shape parameter κ (radial coordinate) and the location parameter μ (angular coordinate, see also ***Figure 3.7 B***). The results from the unimodal and bimodal fits for the four conditions and three experimental groups are shown in ***Figure 3.7 C-J*** with males on the left and females on the right. The proportion of walking flies that fixate in one or in two angular locations varies drastically between the four trials, however, it relatively conserved across sexes and the three tested experimental conditions. In 'bright on dark' conditions flies did not only show more pronounced unimodal fixation peaks (larger shape parameter κ, ***Figure 3.7 G, I***), but 'unimodal fixation' was also much more frequent compared to 'dark on bright' conditions (***Figure 3.7 L***). In the trials with a bright stripe fixation 'unimodal fixation' was the most commonly observed behaviour (>= 50 % of walking flies in all groups). Also the frequency with which flies fixate in two angular locations varies between the four trials, but the pattern appears to be less consistent across experimental groups. Generally, fixation in two locations is relatively rare and was observed more frequently in 2D worlds (***Figure 3.7 F, J***) compared to 1D worlds (***Figure 3.7 D, H***). In males, throughout experimental groups, two fixation peaks were most commonly observed in the bright 2D scene, but only in males with glued wings measured at high room temperature 'bimodal fixation' was also somewhat frequent in the dark 2D scene (***Figure 3.7 M***). In contrast, in female flies 'bimodal fixation' was observed with similar frequency in the bright 1D and 2D scene as well as in the dark 2D scene (***Figure 3.7 L***).

We also found some consistent patterns in the distribution of angular fixation locations. Male, but not necessarily female, flies that showed 'unimodal fixation' preferentially fixated the dark stripe in 1D trials in the frontal FOV (***Figure 3.7 C***). In contrast, flies did not preferentially fixate the bright stripe in any particular angular location (***Figure 3.7 G***). Interestingly, flies tended to fixate landmarks in 2D trials to either side, rather than fixating it in the frontal or rear FOV (***Figure 3.7 E, I***). This was particularly pronounced in 'bright on dark' trials, where many flies showed pronounced fixation at +/- $\pi/2$ (***Figure 3.7 I***). Fixation at the side results in virtual walking trajectories that circle around the landmark (see ***Figure 3.5 D, F***). In case of 'bimodal

fixation', we found that the two peaks of the fitted bimodal distribution (location parameter μ_1 and μ_2) were frequently separated by an angle of π, i.e. they lay on opposite points within the fly's FOV (***Figure 3.7 D, F, H, J***, μ_1 and μ_2 from the same fly are connected by a line). Notably, the fitting procedure did not enforce an angle of π between the two peak locations. Beyond that, the angular locations of the fixation peaks in 'bimodal fixation' trials did not show any clear patterns across experimental groups and trial conditions — with one exception. Male flies across experimental groups fixated the dark landmark either in the front and back or to the two sides.

Summing up, we found that 'contrast polarity' of the scene can affect walking frequency (***Figure 3.7 K***) as well as the frequency of fixation (***Figure 3.7 L-N***). While fixation frequency does not vary much between trials in 1D and 2D worlds, flies show characteristic differences in the frequency of different fixation locations, with a preference for fixation at the sides for landmark tracking in 2D trials.

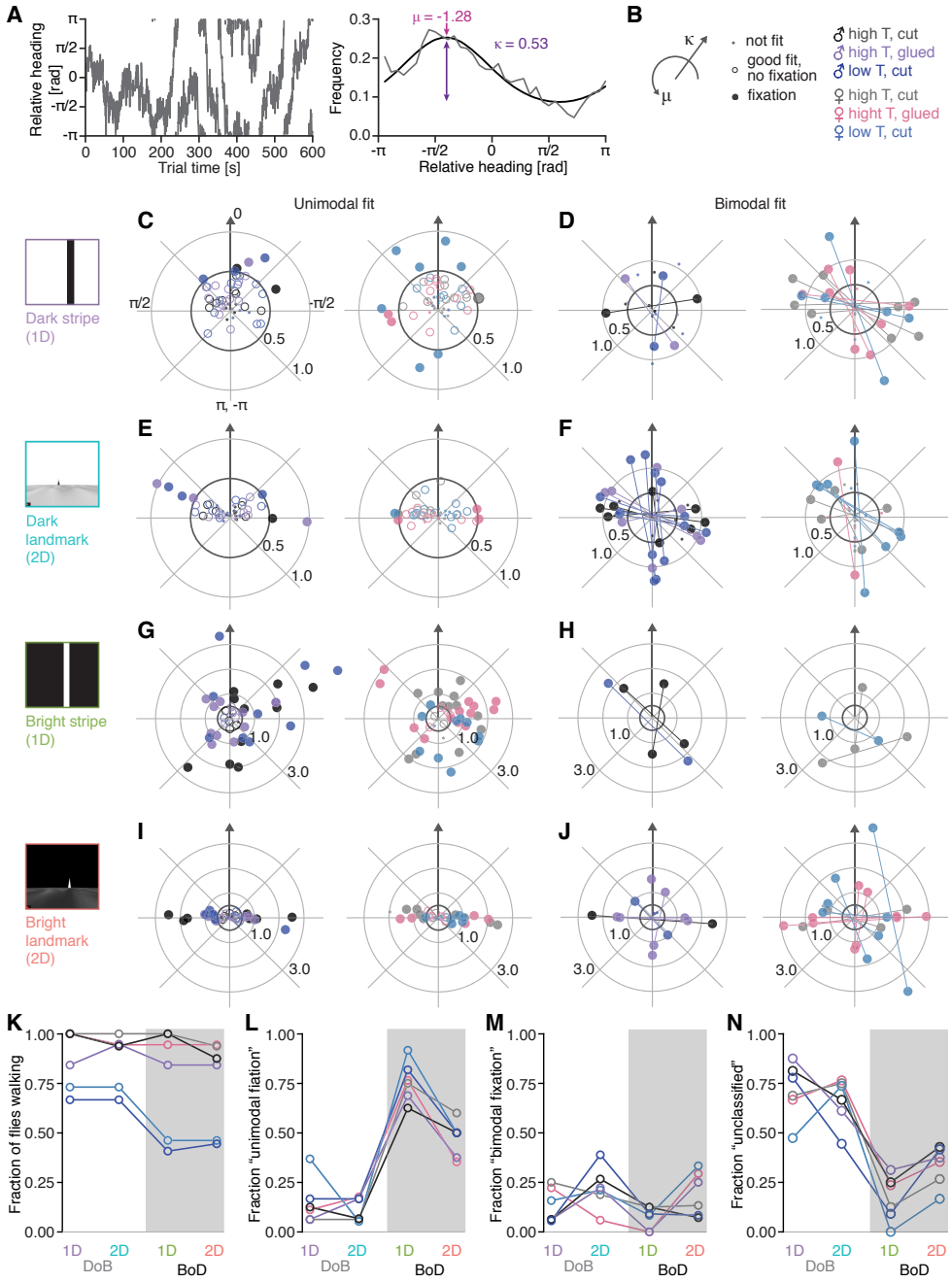

Figure 3.7: Classification of fixation behaviour on single trial level.

A: Time series (left) and frequency distribution (right) of the relative heading angle from a single fly in a 'dark on bright' stripe fixation trial (grey line). A von Mises fit is overlaid onto the frequency distribution (black). B: Left: illustration of the polar plot of the parameter from the von Mises fit. Centre and right: Legend for the plots in C-J. Data points from trials for which the unimodal or bimodal von Mises was not a good fit are plotted with a small dots, data from well-fitted distributions that did not qualify as fixation with an empty circle and fixation trials with a solid large dot. C, E, G, I: Location and shape parameter from fits to a unimodal von Mises distribution for male (left) and female (right) flies across four trial conditions. Data from the three experimental groups are colour-coded according to the legend in B. D, F, H, J: Location and shape parameter from fits to a bimodal von Mises distribution. A thin line connects the two points that

indicate the location parameters from each fit. **K-N***:* Frequency of trials classified as walking (**K**), 'unimodal fixation' (**L**), 'bimodal fixation' (**M**) and 'unclassified' (**N**). Note that only 'unimodal fixation', 'bimodal fixation' and 'unclassified' trials sum up to one.

Within a fly fixation strength and angular location in 1D and 2D appear to be uncorrelated

Finally, for 'unimodal fixation' we looked for a correlation of fixation strength, as measured by the shape parameter **κ** (***Figure 3.8 A***), or peak position quantified by the location parameter μ (***Figure 3.8 B, C***) between stripe fixation in 1D and landmark fixation in 2D. For this analysis we only took into account trials where a good fit with a unimodal von Mises was achieved in both the 1D and 2D trial of a given contrast polarity condition. We found no evidence for a correlation of fixation strength in 1D and 2D trials (***Figure 3.8 A***), neither for 'dark on bright' nor 'bright on dark' trials. Also the angular location of fixation in 1D and 2D appears to be uncorrelated (***Figure 3.8 B***). When we loot at the absolute angular location, i.e. pooling fixation locations across the left and right FOV, we found a weak positive correlation in 'dark on bright' trials (***Figure 3.8 C***, Pearson correlation coefficient r = 0.176).

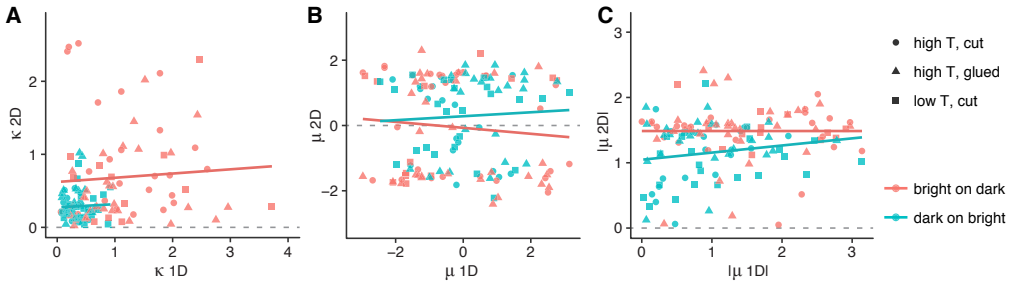

Figure 3.8: **Correlation of fixation strength and location between 1D and 2D trials.**
A: Correlation of fixation strength and fixation location in 1D stripe and 2D landmark tracking trials. Scatter plot of the shape parameter in 1D and 2D trials, obtained by fitting a unimodal von Mises distribution. Each point corresponds to a measurement in a single fly. Only trials for which the von Mises was a good fit in both the 1D and 2D trial were considered. Measurements from 'bright on dark' trials are displayed in orange, measurements from 'dark on bright' in turquoise. Data points from the 3 experimental groups are shown with different shapes, but data has been pooled across sexes. A linear regression for both contrast conditions suggested that there is no correlation between the peak size in stripe and landmark fixation trials. 'Dark on bright': Pearson correlation coefficient r=0.040. 'Bright on dark': r=0.078. **B:** Correlation of fixation peak position in stripe and landmark tracking trials. Scatter plot of the fitted location parameter, analogous to panel A. Linear regression showed no correlation between the peak position in stripe and landmark fixation trials for both contrast conditions. 'Dark on bright': Adjusted r=0.061. 'Bright on dark': Adjusted r=-0.099. **C:** Correlation of absolute fixation position. We found a weak correlation in 'dark on bright' trials (r=0.176) and no correlation in 'bright on dark' trials (r=0.000).

Summing up, we found that some flies do show strong stripe fixation behaviour in our visual VR system, validating its basic functionality. Flies tended to walk less but showed clearer fixation with bright objects on dark background than with dark objects on bright background. In 1D 'dark on bright' trials flies showed a weak tendency for fixation in the frontal field of view, whereas flies did show any preferred fixation angles in 'bright on dark' 1D trials. Further, flies preferentially kept landmarks in 2D trials at the sides, but no such trend was found in 1D stripe tracking trials. Finally, we did not find a clear relationship between fixation strength and preferred angular fixation location for a given fly in 1D and 2D trials. These observations were consistent across sex, the two tested room temperatures and wing modification techniques. It is possible, however, that observations regarding stripe and landmark fixation in the two tested contrast conditions are specific to the tested genotype, WTB.

3.3.5. Comparison of landmark interaction in tethered and freely walking flies

These first experiments of our VR suggested that interactions with the more naturalistic dark landmarks were more variable than stripe fixation and behavioural correlates of landmark interaction therefore harder to detect. Additionally, we suspected that the landmark interaction behaviour could be affected by the tethering procedure and the lack of mechanosensory feedback from virtual objects. To judge the degree to which these limitations of our VR system distorted the behaviour and to get a better idea of what would be quantifiable behavioural correlates of landmark interaction, we decided to compare the behaviour of flies navigating in VR to that of freely walking flies. Walking trajectories obtained from freely walking flies could be used as a 'ground truth' for what to expect and we could deduce which aspects of walking behaviour in VR may be confounded by tethering or imperfect sensory feedback. A requirement for this approach is to closely match the tethered and the free walking group and the experimental conditions across the two assays.

To achieve this, we built a free walking arena according to the following guiding principles:

- Give flies a large open space to walk without interacting much with walls, as walls are largely absent in the virtual worlds we used.
- Match the lighting conditions in the free walking arena to those in the VR setup.
- Introduce small objects into the arena to investigate interaction with visual landmarks.
- Make landmarks 'non-climbable', as flies are not able to walk on landmarks in the VR.

A full description of the free walking arena can be found in ***section 3.2.4***. We will now briefly describe the behavioural paradigm before comparing landmark interaction in tethered and freely walking flies.

Landmark interaction assay with freely walking flies

We used the free walking arena to characterise how walking flies interact with a single salient dark landmark, which could be approached from any direction. Small 3D-printed black objects served as landmarks. The surface of the object was polished to reduce surface texture. A variety of object shapes were produced, but all experiments shown in this chapter were performed with a 4 cm high cone that was 1 cm wide at the base, matching the size of landmarks used in VR experiments. The cone was placed in the centre of the arena (***Figure 3.2 B***). To prevent flies from climbing and resting on the cone, a coated (SurfaSil, Fisher Scientific, Thermo Fisher Scientific, Waltham, MA, USA) glass cylinder (ø = 1.5 cm) was placed around the cone. Flies were unable to walk on the coated horizontal glass surface. Before experiments, flies were dry starved for 4-6 h. A single wing-clipped fly was introduced to the arena and it was given 1-2 min to explore the space before starting the video recording for a 10 min trial (***Figure 3.2 C***). After each measurement the fly was removed from the arena and the arena floor was wiped with humidified tissue paper.

Differences in landmark fixation behaviour in freely walking flies across genotypes and sexes

As we have seen, stripe fixation behaviour can vary with genotype and sex. We therefore decided to also investigate landmark interaction behaviour in both male and female freely walking flies of two genotypes: Wild-type Berlin (WTB) and WTB x pBDP-GAL4 hybrid flies. The pBDP-GAL4 line is a frequently used 'empty-GAL4' control line. We chose WTB flies, because this genotype has been used in many previous publications on various walking behaviours. The second tested genotype, WTB x pBDP-GAL4 hybrid flies, was chosen to approximate the genotypes used in many activation experiments presented in chapter 4, where an effector line with WTB background is crossed to GAL4 driver lines with variable genetic backgrounds. Also, there was anecdotal evidence that hybrid flies showed better fixation behaviour.

For each of the four groups, we tested 20 flies and analysed their general locomotion and landmark fixation behaviour (***Figure 3.9***). We restricted our analysis to trajectories within the central area of the arena (less than 60 mm distance from landmark) excluding also the area immediately around the landmark (more than 15 mm distance) to reduce edge effects (***Figure 3.9 A***). Furthermore, we only included time periods during which a fly was moving, using a simple empirical threshold criterion (translational velocity larger than 5 mm/s). Due to this filtering procedure a variable number of time points contributed to the estimates for locomotion parameters and heading in each fly (***Figure 3.9 B***). The median translational velocity varied widely both within and across groups (***Figure 3.9 C***) with the largest variance in male

WTB flies. The median absolute rotational velocity seemed to be higher in WTB compared to WTB x pBDP-GAL4 hybrid flies (***Figure 3.9 D***), and female flies tended to walk with lower translational and rotational velocities than male flies of the respective genotype.

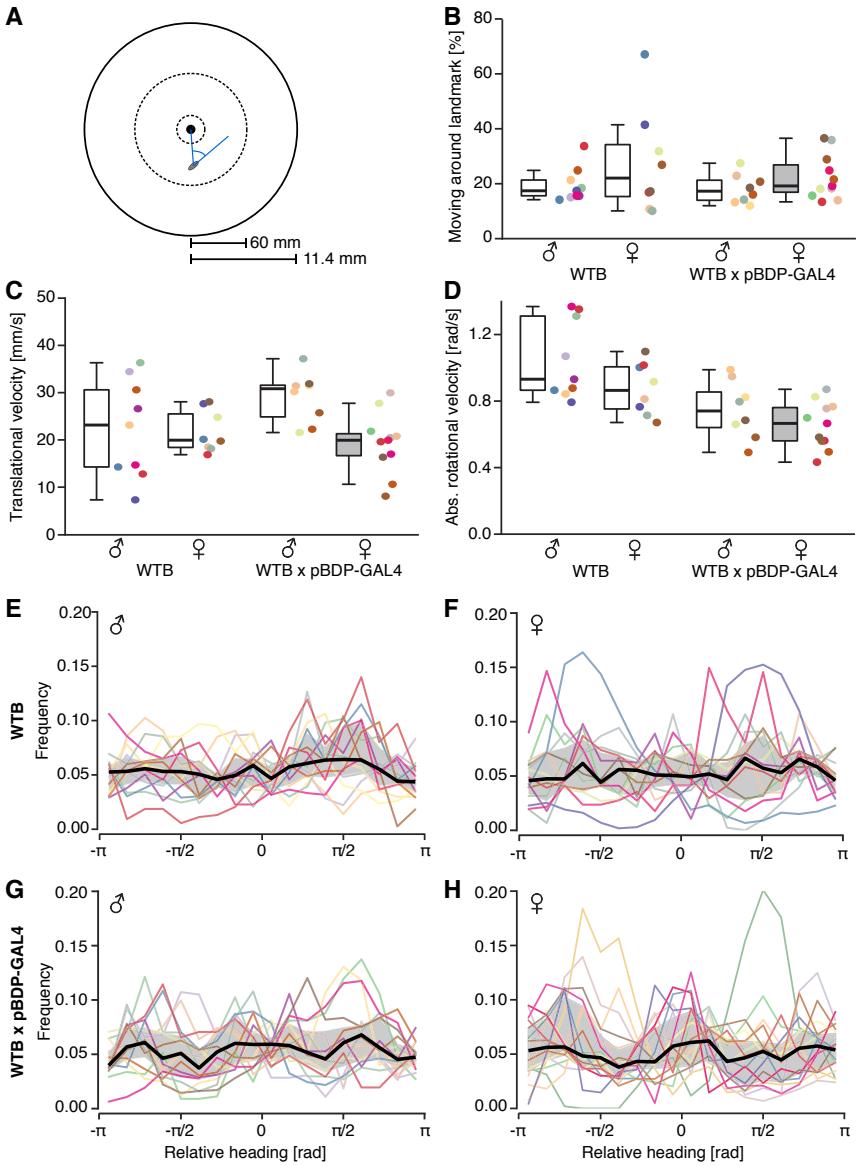

Figure 3.9: Landmark fixation in freely walking flies.
Comparison of locomotion and landmark fixation behaviour in freely walking male and female homozygous wild-type Berlin (WTB) and WTB x pBDP-GAL4 hybrid flies. **A:** Schematic of the spatial dimensions of the free walking arena. All data presented in this figure is based on walking trajectories within the area between the two dashed circles, corresponding to landmark distances between 15 mm and 60 mm. The black dot indicates the approximate landmark position and the grey oval symbolises a fly in the arena (fly not to scale). The relative heading, defined as the angle between the fly's heading direction and the direction of the landmark relative to the fly's position, is indicated in blue. **B-D:** Per-fly quantification of different locomotion parameters. Data from four experimental groups is shown: male and female WTB flies as well as male and

female WTB x pBDP-GAL4 hybrid flies. For each of the four groups a boxplot as well as the individual data points are presented. The individual data points, shown as coloured dots, correspond to different flies and the colour-code is maintained throughout the three panels. **B:** Percentage of the 10 min trial that a fly spent moving (movement criterion: translational velocity above 5 mm/s) within the area around the landmark described by the dashed circles in A. This gives an indication of the number of time points that contributed to the per-fly averages presented in C and D and to the relative heading distributions presented in E-H. **C, D:** Median translational velocity (**C**) and rotational velocity (**D**) of a moving fly. **E-H:** Relative heading distribution based on trajectories within arena area between the two dashed circles marked in A. The frequency distributions were computed as the density of heading angles normalised to an area of 1. The relative heading distribution of individual flies and the median and interquartile range are shown for the four experimental groups: male (**E**) and female (**F**) WTB flies as well as male (**G**) and female (**H**) WTB x pBDP-GAL4 hybrid flies

As a behavioural read-out of interaction with the landmark, we computed for each fly the distribution of relative heading angles, which we defined as the angle between the fly's heading direction and the direction of the landmark seen from the fly's current position. As in our stripe fixation experiments, we expected a non-uniform distribution of relative heading angles in cases where a fly would interact with the landmark. For example, we would expect a peak around zero relative heading in flies that repeatedly approached the landmark. To ensure a reasonable sampling, heading distributions were only computed for flies that moved within the analysed arena area for more than 20 % of the 10 min trial. While the relative heading distributions varied widely across flies, we found some genotype-specific tendencies. The average heading-distribution of male and female WTB flies showed no clear peaks (thick black lines in ***Figure 3.9 E, F***), whereas the heading distribution in female, and to a lesser degree in male, WTB x pBDP-GAL4 hybrid flies on average showed a small fixation peak around zero relative heading (***Figure 3.9 G, H***). The average absolute rotational velocity seemed to be inversely correlated with the magnitude of the modulation in the average relative heading distribution. The fixation peak was most pronounced in female WTB x pBDP-GAL4 hybrid flies (***Figure 3.9 H***), suggesting that out of the four tested groups, these flies showed the clearest landmark interaction behaviour. We therefore decided to use female WTB x pBDP-GAL4 hybrid flies for the comparison of landmark interaction in freely and tethered walking flies.

Flies in VR walk and explore landmarks in much the same way as freely walking flies

To compare landmark tracking behaviour in freely walking and tethered walking flies, we tested flies taken from the same vials and measured them in parallel on the two setups, which were located in the same room. In free walking experiments each fly's behaviour was only recorded for one 10 min trial, while we performed several 10 min long trials with tethered flies in the VR.

For the comparison of tethered with free walking behaviour, we restricted our analysis of trajectories in VR to the first trial with a visual landmark.

When we compared the walking velocities of 20 freely and 20 tethered walking female WTB x pBDP-GAL4 hybrid flies, we found generally higher translational and rotational velocities in free walking compared to tethered walking (compare ***Figure 3.10 A, B*** to ***G, H***). The lower walking velocities in VR might have been an artefact due to a too small gain factor used to translate ball rotations to movement in the VR or it could have been a bias induced by how flies were positioned on the ball. In addition to this shift in mean translational velocity, the variability in translational velocity distributions was higher in VR compared to free walking (***Figure 3.10 A, G***).

Next, we investigated how, on the level of individual flies, the observed relative heading distribution and the walking velocities related to walking trajectories. For convenience, the relative heading distributions of freely walking female hybrid flies from ***Figure 3.9 H*** are reproduced here (***Figure 3.10 C***). To illustrate extreme cases of landmark interaction behaviour, we picked out trajectories from three example flies. Their trajectories in the full free walking arena are shown in ***Figure 3.10 D-F*** and the corresponding walking velocity and relative heading distributions are highlighted with thicker lines in ***Figure 3.10 A, B***. Two of the three flies were circling around the object resulting in a single peak in the relative heading distribution. One fly showed counter-clockwise rotations around the landmark (***Figure 3.10 D***) with a fixation peak around -π/2 and the other clockwise rotations (***Figure 3.10 F***) with a fixation peak around π/2. A third fly made repeated straight, head-on approaches to the landmark followed by similarly straight departures (***Figure 3.10 E***) resulting in a heading distribution with two fixation peaks, one around zero and one around +/- π. The trace in ***Figure 3.10 E*** also exemplifies that some flies repeatedly approached the landmark even though it was not possible to climb it. The two circling flies had a small bias in their rotational velocity distribution and were walking on average with a higher translational velocity than the landmark-approaching fly.
Tethered walking flies of the same genotype on average showed less pronounced modulation of their relative heading distributions (***Figure 3.10 I***). Especially flies moving at high translational velocity could visit the landmark many times over the course of the 10 min trial without showing a clear peak around zero in the relative heading distribution (***Figure 3.10 J***). In contrast, clear peaks around zero and +/- π were visible in slower moving flies that repeatedly approached to the landmark (***Figure 3.10 K***). Trajectories of those slower moving, landmark-tracking tethered walking flies resembled those from landmark-tracking freely walking flies. Occasionally we also saw circling around the landmark in VR (clockwise rotations and a

corresponding relative heading distribution peak around π/2 ***Figure 3.10 I, L***). Thus, several characteristics of locomotion and landmark-interaction behaviour observed in freely walking flies were preserved in tethered walking flies exploring a visual VR.

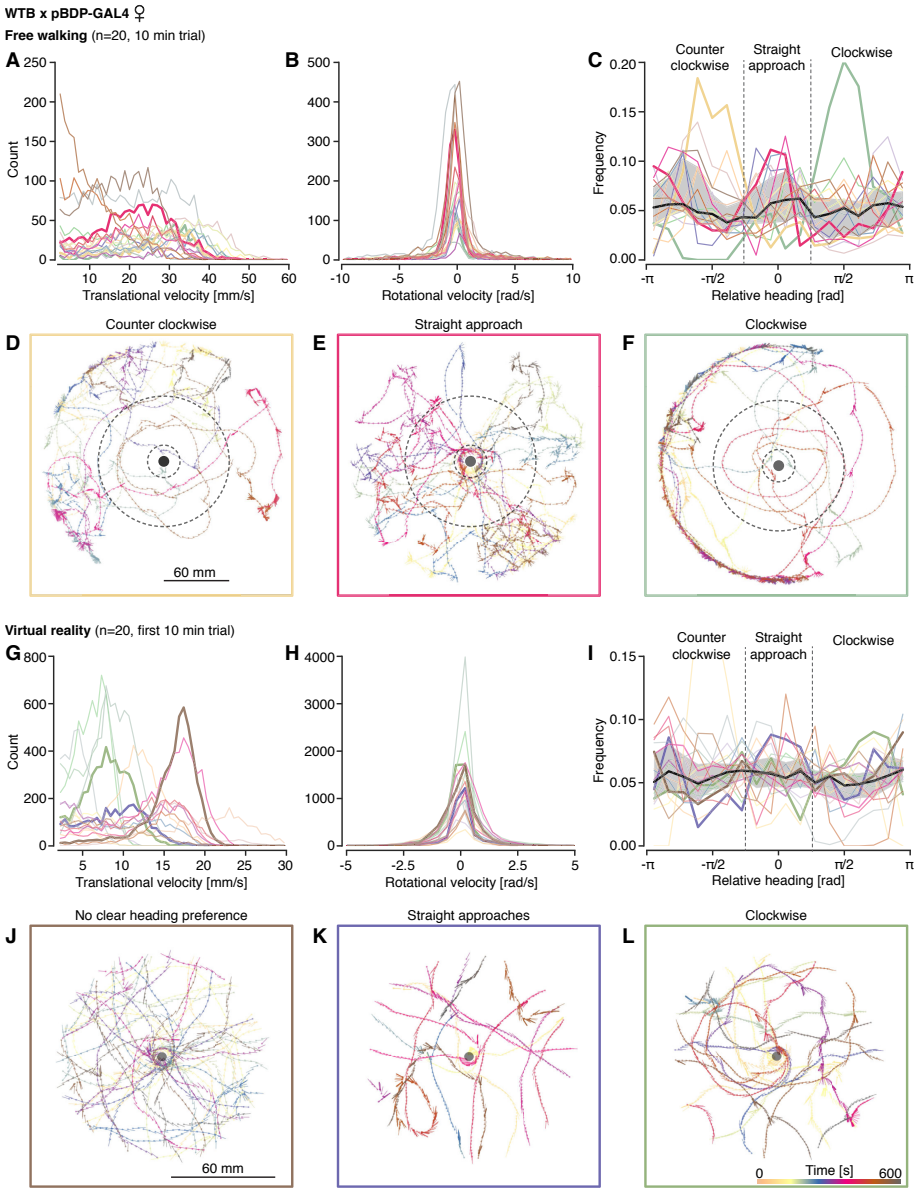

Figure 3.10: Walking velocities and landmark interaction in freely and tethered walking flies.
Data from female WTB x pBDP-GAL4 hybrid flies is shown. Panels **A-F** show data from free walking and panels **G-L** from tethered walking in VR (only first out of three VR trials with visible landmarks included). In both groups n=20 flies were measured and each trial lasted 10 min. The free walking data was sampled at 12.27 Hz, the VR data at 360 Hz and subsequently downsampled to 20 Hz. To compute the histograms of translational and rotational velocity as well as the relative heading distributions we only included time points within 60 mm radial distance from a landmark, at which a fly was moving (movement threshold of 5 mm/s in free walking and 2 mm/s in tethered walking). We also excluded time points very close to the landmark (closer than 15 mm

in free walking and 10 mm in VR). Panels A-C and G-I show data from all 20 flies with different colours indicating flies of different identity. Panels D-F and J-L each show example trajectories from single flies. A, G: Histogram of the translational velocity of freely walking (A) and tethered walking (G) flies. B, H: Histogram of the rotational velocity of freely walking (B) and tethered walking (H) flies. C, I: Relative heading distributions of freely walking (C) and tethered walking (I) flies. Visualisation is analogous to Figure 3.9 E-H. C shows the same data as Figure 3.9 H. D-F: Example trajectories of individual flies in the full free walking arena. The fly's position and heading are visualised with a dot and a line pointing in the fly's heading direction. The trajectories are colour-coded according to trial time (see colour bar in the bottom right). Only the area of the arena between the two dashed circles was considered in the above analysis. The translational and rotational velocity histograms and the relative heading distributions corresponding to the depicted traces are marked with thicker lines and lines of the corresponding colour frame the panels with the traces. J-L: 'Collapsed' example trajectories of individual flies in VR. Trajectories are visualised as in D-F.

Freely and tethered walking flies preferentially reside close to the landmark

We next investigated whether the observed landmark-fixation behaviour affects residency within the arena and whether there is spatial structure to location and heading preferences. We again compared freely walking and tethered walking female WTB x pBDP-GAL4 hybrid flies to see whether any observed residency preferences would be conserved across the two assays. We took differences in residency as an estimate for preferences between different spatial locations. This type of analysis requires a good coverage of samples across the investigated space and was therefore conducted on pooled data from all 20 measured flies rather than on single fly level. The analysis of freely walking flies included data from one 10 min trial per fly, whereas we pooled data from three 10 min trials for the analysis of tethered walking data.

We compared the residency of freely and tethered walking flies within a 60 mm radius around the landmark (***Figure 3.11 A, B***). Under both conditions we found that flies preferentially reside close to the landmark. Residency was only increased within a small radius around landmark, in particular in the tethered walking trials. Thus, we did not find any indication for long-range interaction with the visual stimulus for example in form of a gradual increase in residency with decreasing landmark distance. The visualisation in ***Figure 3.11 A, B*** only takes into account the position of the fly. To test for spatial modulation of the fly's relative heading angle, we visualised preferred residency in landmark-centric polar coordinates instead of Cartesian coordinates by parameterising the fly's position inside the arena with the distance to the (closest) landmark and the relative heading angle to that landmark (***Figure 3.11 C, D***). In freely walking flies, the polar 2D residency showed three peaks along the relative heading angle dimension at small radial distances from the landmark: One around zero and two around + ¾ π and - ¾ π (***Figure***

3.11 C). Thus, when flies were close to the landmark, they either kept it in their frontal or in their lateral rear FOV. The fixation peak in the frontal FOV corresponded to landmark approaches, while the peaks toward the back corresponded to departures from the landmark (corresponding analysis not shown here). With increasing distance the lateral peaks quickly flattened and seemed to shift further toward the back of the fly, indicating that departure trajectories on average had a curved shape and were not stereotyped at larger landmark distances. In contrast, the peak around zero relative heading was visible at distances up to 40 or 50 mm, although this peak too flattened with increasing distance from the landmark. This suggests that the approaches were relatively stereotyped across flies and that flies preferentially approached the object by fixating the landmark in their frontal FOV.

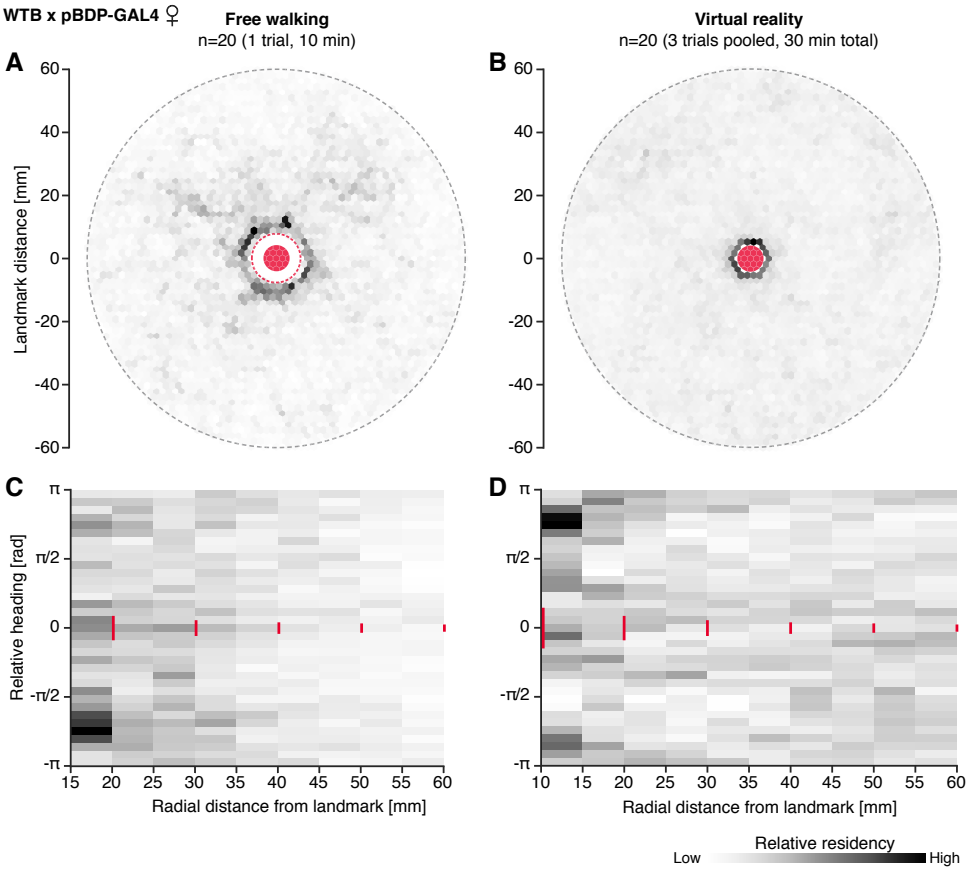

Figure 3.11: Residency around the landmark in freely and tethered walking flies.
Pooled data from n=20 freely walking and n=20 tethered walking female WTB x pBDP-GAL4 hybrid flies is shown. Preferred residency is visualised using 2D histograms with grey shades encoding the count. Bright shades indicate low and dark shades high count. The scale of the colour-code was adjusted within each plot to match the respective range of counts. For the analysis in freely walking flies we evaluated one trial à 10 min and for the analysis of tethered walking in VR we pooled data from 3 trials à 10 min. The free walking data was sampled at 12.27 Hz, the VR data at 360 Hz and subsequently downsampled to 20 Hz. We only included data points from moving flies

using a movement threshold of 5 mm/s in free and 2 mm/s in tethered walking. The different threshold levels reflect the difference in translational velocity observed in freely and tethered walking flies. We chose 2 mm/s in tethered walking as movement corresponding to approximately one fly body length. In free walking experiments the threshold was scaled according to the relative difference in translational velocity. **A, B:** 2D residency histograms in Cartesian coordinates showing the area within a 60 mm radius around the landmark. The location of the landmark is marked with a red dot. The dashed red circle in A marks the diameter of the glass cylinder surrounding the landmark. **C, D:** 2D residency histograms in landmark-centric polar coordinates: radial distance from the landmark and relative heading angle. For a subset of distances the approximate angular width of the landmark is indicated with a red bar.

The pattern of residency preferences in tethered walking flies was less pronounced, but overall resembled the one observed in freely walking flies (***Figure 3.11 D***). At distances very close to the landmark, tethered walking flies fixated the landmark either in their frontal FOV or kept it in their rear, similar to freely walking flies. However, at larger distances, two fixation peaks emerged in the frontal FOV, suggesting that tethered walking flies did not approach the landmark on a straight, head-on trajectory. This observation is consistent with the bimodal relative heading frequency distribution, which we measured in WTB flies (***Figure 3.6 C, G, Figure 3.7 E, F, M***). These two fixation peaks also flattened with increasing radial distance from the landmark. We do not have a good explanation for the occurrence of two rather than just one fixation peak in the frontal FOV. It might be an artefact from the display geometry of the projection of the visual stimulus. However, we also found that under certain conditions flies readily fixated a stripe in the frontal FOV (***Figure 3.3***).
Taken together, the spatial structure in the object-centric 2D-residency histogram suggests that both freely and tethered walking flies show somewhat stereotyped interactions with the visual landmarks even at landmark distances up to 40 mm (***Figure 3.11 C, D***).

3.3.6. A closer look at landmark interaction in virtual reality

Generally two aspects of a landmark can influence a fly's walking trajectory: The visual signal, which can act on a long range, and its physical dimensions, which block the fly's path through a small area of the plane. We were wondering how much of the residency preference for the landmark could be explained by non-visual properties of the landmark, e.g. flies 'getting stuck' at the landmark upon random collisions. Establishing long-range effects of the visual landmark on a fly's walking trajectory would implicate active steering manoeuvres in response to the visual cue, whereas the mechanically-induced 'preference' due to getting stuck would not necessarily require any long-range, active (visual) interaction with the landmark. As there are

many ways in which the visible cue could influence a fly's walking trajectory, it can be difficult to distinguish landmark-induced steering manoeuvres from spontaneous course adjustments.
We can exploit VR to generate a control condition for the non-visual influence of a landmark on a fly's trajectory. To do so, we generated a virtual scene just like the one used for probing landmark interaction behaviour, but with invisible landmarks. Invisible landmarks were placed and shaped like their visible counterparts and equally (virtually) impenetrable. To investigate to which degree the visual landmark cue induces changes in the trajectories, we tested 20 flies (female WTB x pBDP-GAL4) in three trials with visible and one trial with invisible landmarks.

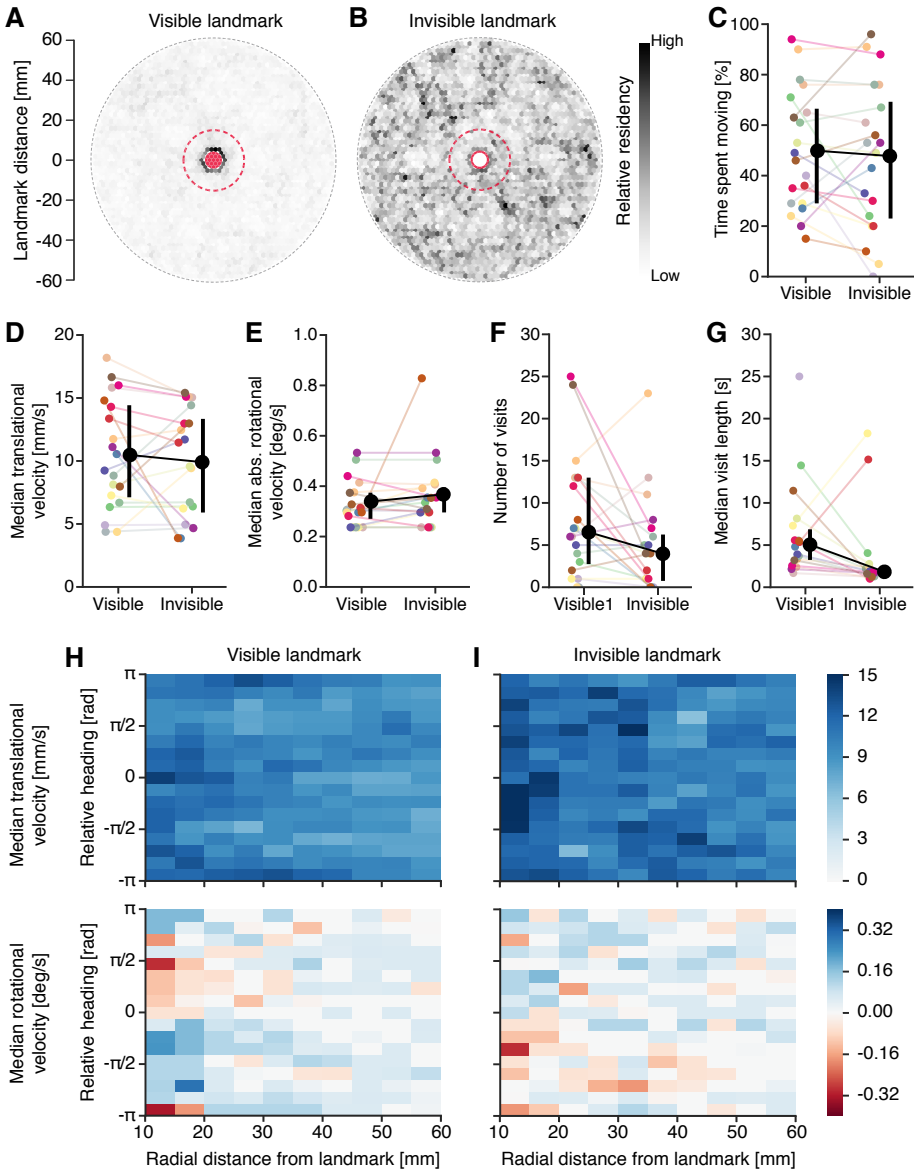

Figure 3.12: The presence of a visual landmark has long-range effects on walking behaviour.
Comparison of behaviour in a VR with visible and invisible impenetrable landmarks. Data from n=20 tethered walking female WTB x pBDP-GAL4 hybrid flies is shown. Each

fly was tested in three trials with visible and one trial with invisible landmarks. **A, B:** 2D residency histograms from the first trial with a visible landmarks (**A**) and a trial with invisible but equally impenetrable landmarks (**B**). Residency of collapsed traces within a 60 mm radius around the landmark is shown. Residency is visualised as in Figure 3.11 B. The solid red dot marks the location of a visible landmark (**A**), the empty dot that of an invisible landmark (**B**). The red dashed circle marks the area around each landmark used for quantifying visits (**F, G**). **C-E:** Comparison of the locomotor behaviour in trials with visible and invisible landmarks on a per-fly basis. For this analysis data from three trials with visible landmarks was pooled. The coloured dots represent average values computed per fly and a thin line connects the corresponding values in the visible and invisible landmark condition. For each group the median and the interquartile range between the 25th and 75th quartile are shown in black and the medians of corresponding groups are connected with a black line. **C:** The percentage of trial time that the fly moved with a translational velocity > 2 mm/s. **D:** The median translational velocity. **E:** The median absolute rotational velocity. **F, G:** Per-fly comparison of number of landmark visits (**F**) and median visit length (**G**) in the first visible landmark trial and the invisible landmark trial. A visit was defined as the event of a fly approaching a landmark within a 15 mm radius (red dashed circles in *A, B*). The visit duration was defined as the time period between entering and exiting this 15 mm zone around a landmark. **H, I:** Maps in landmark-centric polar coordinates, radial distance from the landmark and relative heading angle, of two trajectory-deprived locomotor parameter: a map of the median translational velocity (top) and rotational velocity (bottom). Each one was computed based on pooled data from the first trial with a visible landmark (**H**) or with data from the trial with an invisible landmark (**I**).

Comparison of trials with visible and invisible virtual landmarks shows long-range effects of the visual cue on walking trajectories

We first compared residency within a 60 mm radius around the landmarks (***Figure 3.12 A, B***). The previously described increase in residency directly around the landmark was only observed in trials with visible, but not with invisible virtual landmarks, even though flies spent a similar amount of time moving and sampling the virtual plane (***Figure 3.12 C***). This suggests that collisions with the impenetrable objects upon random encounters are not sufficient to explain the increased residency in trials with visible landmarks, but that flies actively steer toward them. We therefore compared a number of trajectory derived behavioural parameters in trials with visible and invisible landmarks. Surprisingly, flies moved with comparable translational and rotational walking velocities in both conditions (***Figure 3.12 D, E***). However, when we analysed 'visits' to a landmark, defined as a landmark approach of 15 mm radial distance or less, we found that flies systematically made more and longer visits to the visible compared to the invisible landmark (***Figure 3.12 F, G***) resulting in the observed increased residency. This made us wonder about the range at which the visible landmark was affecting the flies' walking behaviour. Was it possible that flies only actively responded to the visible landmark when they were already very close to it? Or could flies use the landmark at further distances as a visual cue for orientation?

To assess at what distance flies responded to a visual landmark, we computed 2D maps of the median translational and rotational velocity in landmark-centric polar coordinates (***Figure 3.12 H, I***). We decided to compute 2D maps rather than separating values solely by landmark distance, because we expected the trajectory to be modulated in different ways dependent on the angular position of the landmark relative to the fly. The median translational velocity measured at a given combination of landmark distance and angular position is colour-coded with darker values indicating higher velocities. In the presence of visible landmarks flies walked faster when they face the landmark in their frontal FOV or when the landmark was directly behind the fly (***Figure 3.12 H,*** *top*). The modulation of translational velocity was a function of landmark distance and absolute heading angle, but did not depend on whether the landmark was to the left or the right of the fly. This spatial modulation pattern of translational velocity, reflecting the residency pattern described earlier (***Figure 3.11 D***) was absent in trials with invisible landmarks (***Figure 3.12 I,*** *top*). Also the relative rotational velocity showed spatial modulation in the presence of visual landmarks. Close to the landmark flies on average turned right, when the landmark was located on their right (relative heading angles < 0) and left, when it was in the left FOV (***Figure 3.12 H,*** *top*). This turn bias shrank with increasing distance from the landmark and completely subsided at distance larger than 40 mm. In trials with invisible landmarks we also observed a turn bias depending on the location of the object, but with the opposite polarity (***Figure 3.12 I,*** *top*). This pattern was likely the effect of transforming walking trajectories from Cartesian to landmark-centric coordinates: A fly exploring the virtual plane on a random trajectory would more likely pass on the right side of the invisible landmark (relative heading angles < 0) if it was turning toward the left and vice versa. Together these results suggest that flies actively steer toward the visible landmarks resulting in an increased frequency of visits and that these steering manoeuvre are initialised at distances of up to 40 mm.

Landmark interaction behaviour in VR can change over time

When flies exploring our visual VR encounter landmarks they neither get the mechanosensory feedback they might expect nor can they climb the object. We were therefore wondering, if flies adapt to the presence of a landmark, for example by reducing the visit frequency. Additionally, flies might adapt more and more to walking on the ball, which could affect walking velocities. Many potential future experiments require comparison of landmark-interaction behaviour over multiple trials to tease out effects of a given experimental manipulation on the virtual environment. For such comparisons to be sensitive, the behaviour should ideally not change over the course of multiple trials within the same virtual environment.

We compared the three trials with visible landmarks to see whether and how landmark interaction behaviour in VR changed over time. In female WTB x pBDP-GAL4 hybrid flies the initially strong preference for residing close around the landmark receded over the course of three 10 min trials (***Figure 3.13 A***). This reduction in preference was correlated with a gradual reduction of activity as the percentage of time spent moving decreased (***Figure 3.13 D***) over time. However, when moving, flies did so with comparable walking speeds across trials (***Figure 3.13 B, C***). As flies moved less and less, they also made fewer visits to the landmarks (***Figure 3.13 H***), resulting in the observed decrease of landmark preference.

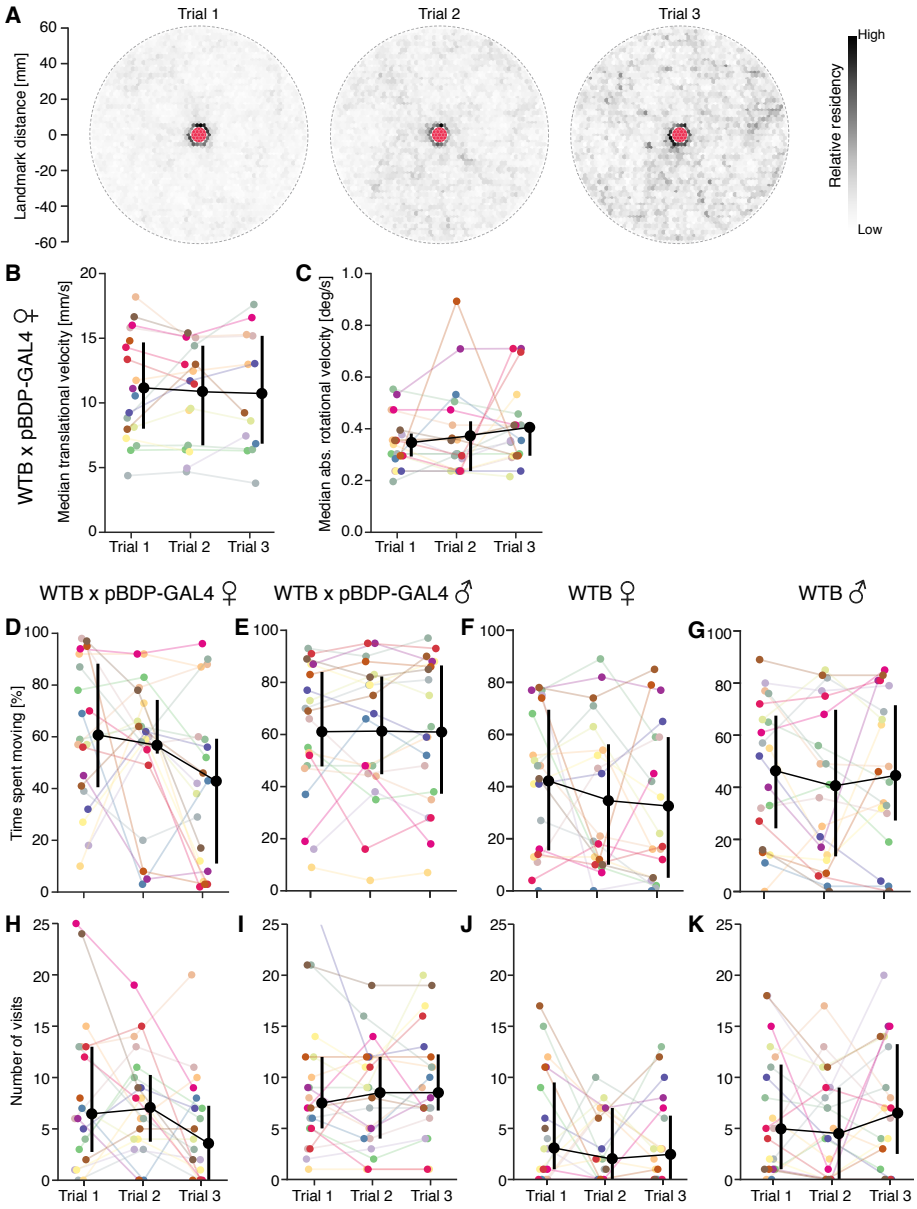

Figure 3.13: In virtual reality landmark interaction behaviour can change over time. A-C: Data from n=20 female WTB x pBDP-GAL4 flies in three consecutive trials with visible landmarks. A: Residency histograms of collapsed traces. Residency is visualised

as in Figure 3.11 B. The landmark location is marked with a red dot. **B, C:** Per-fly comparison of the median walking velocities over the three trials. Median translational velocity (**B**) and median absolute rotational velocity (**C**) were computed for each fly over all time points during which the fly was moving with > 2 mm/s. Visualisation is analogous to Figure 3.12 F, E. **D-K:** Comparison of four experimental groups: female WTB x pBDP-GAL4 flies (**D, H**), male WTB x pBDP-GAL4 flies (**E, I**), female WTB flies (**F, J**) and male WTB flies (**G, K**). In each experimental group n=20 flies were tested. Visualisation is analogous to Figure 3.12 C, F. **D-G:** The percentage of time flies spent moving in each of the three trials computed per fly. **H-K:** Number of times a fly visited a landmark. A visit is defined an approach to the landmark within 15 mm distance.

Landmark interaction behaviour in VR varied with sex and genotype

Comparison of stationarity of activity over the three trials varied with sex and genotype (***Figure 3.13 D-G***) and was generally correlated with the number of landmark visits (***Figure 3.13 H-K***). While the most drastic reduction in activity was observed in female WTB x pBDP-GAL4 hybrid flies (with only a few exceptions), male hybrid flies showed consistent behaviour across the three trials. WTB flies were generally less active and made fewer visits to the landmarks than hybrid flies. Furthermore, sex-differences were less pronounced in WTB compared to hybrid flies. Thus, landmark interaction behaviour was overall more pronounced in WTB x pBDP-GAL4 hybrid flies than in homozygous WTB flies. Due to the large changes in landmark interaction behaviour across trials observed in female hybrid flies, however, comparisons across trials with different experimental conditions may be insensitive as condition-induced differences in behaviour could be masked by the changes in behaviour over time.

3.4. Discussion

Here we present a new VR system that enables the study of visually guided navigation in head-fixed walking flies in a 2D virtual environment. We carefully validated this new setup. The basic functionality of the visual display and the feedback system was tested using a simple stripe-fixation paradigm. We compared fixation behaviour of tethered walking flies in 1D and 2D virtual environments and showed that tethered walking flies interact with virtual landmarks in our 2D VR in much the same way as freely walking flies behaviour with real landmarks.
In the process of validating our system, we discovered striking behavioural differences between male and female flies and between wild-type flies of different genotypes, both in general locomotor and tracking behaviour. These differences as well as the non-stationarity of the landmark-interaction behaviour over time needs to be taken into account when designing experiments in the VR.

3.4.1. Limitations and applications of our virtual reality system

How real is virtual reality?

A prominent criticism of VR-based approaches to studying neural computations has been the possible distortion of behaviour and neural activity in an artificial and reduced sensory environment (Minderer et al., 2016). However, due to limitations of neural recordings in freely moving animals there are many questions that can only be addressed in head-fixed preparations. Careful design of the virtual environment and the behavioural paradigm targeted at the specific research question can make VR techniques a useful tool complementing studies in freely walking animals. In addition, thorough validation can create the necessary awareness of artifactual behaviour or neural activity in VR environments.

We did not expect flies in our VR to behave identically to freely walking flies, for instance, due to the lack of mechanosensory feedback during collisions and experimental biases introduced by tethering. To get a sense of how these and other issues influenced a fly's landmark interaction behaviour in our VR, we compared the behaviour of freely and tethered walking flies under closely matched experimental conditions. We found that many characteristics of landmark interaction behaviour were conserved between the two groups, suggesting that visual landmark-guided navigation may well be studied in VR. The extend of artefacts due to reduced and contradictory sensory feedback in VR systems for studying neural representations of space in rodents has been addressed by comparing those neural representations such as hippocampal place fields in freely moving and head-fixed animals (Acharya et al., 2016; Aghajan et al., 2015; Ravassard et al., 2013). These studies have found systematic differences in neural activity between navigation in the real and the virtual world, but the effect on behaviour has not been analysed in detail. How much differences in neural activity and behaviour influence the conclusions we can draw from VR experiments, will depend on the scientific question that is being addressed. Certainly it is possible that if an animal is capable to perform a certain navigational task successfully when it is freely moving, but fails to do so in VR. Thus, we should be careful to conclude from the absence of evidence for a certain navigational skill in VR, that the animal lacks this skill in general. This might also apply to evidence for neural representations of space.

Applications of our system

We extended existing techniques for studying visually guided navigation from one to two spatial dimensions. Allowing more degrees of freedom in the behaviour and the interaction with the sensory environment opens up the possibility to study 'higher-order' motor patterns and navigational strategies and their neurophysiological basis. The system we developed is flexible

and easy to use and could be applied to study a range of navigational behaviours beyond landmark-guided orientation in walking flies. It can also be adopted to study visually guided navigation in other insects by combining it with existing paradigms for tethered walking insects (Hedwig and Poulet, 2004; Lott et al., 2007; Nishiyama et al., 2007).

3.4.2. Fixation of visual landmarks in 1D and 2D

In this chapter we characterised naïve landmark interaction behaviour as a first step toward studying landmark-guided navigation in tethered walking flies in VR. In the following we will first explore the differences between fixation in 1D and 2D worlds, before connecting fixation behaviour to course control during navigational tasks.

What distinguishes fixation in 2D from fixation in 1D?

In 1D stripe fixation paradigm the tethered walking fly can only control its angular orientation relative to a single prominent stripe on an otherwise blank background. The translational movements of the animal are not incorporated in updating the visual stimulus, which means that the fly can never approach and reach the stripe. We translated this paradigm to 2D by presenting the fly with landmarks that were sparsely distributed in a large plane and visually separated by virtual fog. In this paradigm all walking manoeuvres of the fly have an effect on the visual stimulus. Most prominently, the fly can now move towards or away from landmarks. Thus, both in the 1D and 2D fixation paradigm the only ever sees one visual landmark at a time and it can orient itself relative to the landmark such that the latter may be visible at any azimuthal position within the fly's FOV. However, only in the 2D paradigm the appearance of the landmark also changes as a function of the fly's distance from it, which in turn depends on the fly's walking manoeuvres.

In the 1D fixation paradigm many flies showed a tendency to keep the stripe in a specific angular location as they walk, i.e. they fixated the stripe. In the 2D fixation paradigm a fly fixating the landmark in its frontal FOV will eventually reach the landmark, which means that periods of fixation are limited to relatively short intervals. If a fly walked straight at a landmark with an average speed of 15 mm/s in our paradigm it would be less than 4.5 s between the landmark becoming visible (distance of 70 mm) and collision (distance of 5 mm from the centre). During the approach of a landmark in 2D, the landmark continuously increases in size. Importantly, this increase is not linear but rather slow when the landmark is distant and increases as the fly approaches (***Figure 3.4 G***). Hence, the stripe in the 1D fixation paradigm behaves similarly to a very large, distant landmark. By comparison, when seen from a large

distance (> 40 mm) the landmark in our 2D paradigm is relatively small (< 20˚ wide and < 50˚ high) and perhaps not very salient to the fly. Indeed in both free and tethered walking experiments we found no evidence for fixation at distances > 40 mm from the landmark, but flies became more likely to fixate the landmark in the frontal FOV as they came closer (***Figure 3.11***). This observation is consistent with experiments in freely flying flies (van Breugel and Dickinson, 2012). The authors were able to show that if flies approached a stationary pole up to a certain distance, they made directed steering manoeuvres toward the targeted landmark. Curiously, most saccades were made within a radial distance from the post of less than 40 mm, which coincides with the range in which we detected an effect of the visual landmark on the flies' heading distribution. Systematic variations in fixation behaviour with simulated object distance have also been described in tethered flying blow flies (Kimmerle et al., 2000).

For our 2D fixation paradigm we chose cone-shaped landmarks to be able to better compare landmark interaction in VR to an existing study on landmark preferences in freely walking flies (Robie et al., 2010). A virtual plane with very tall, cylindrical landmarks would have been a closer match to the 1D stripe fixation paradigm. Another difference between the visual scenes in the 1D and the 2D fixation paradigms is the presence of a ground plane and correspondingly a horizon line in the 2D scene. In tethered flying flies fixation of a small bar is improved if a textured background is added to the upper half of the FOV (Reichardt and Poggio, 1976). Further experiments are necessary to establish whether this also applies to fixation in walking flies and whether the textured ground plane in our 2D fixation paradigm helped flies to fixate on landmarks.

Visual stimuli generated by approaching objects are called looms. Looms can be either self- or externally generated (Chan and Gabbiani, 2013). Externally generated looming stimuli are for example generated when an animal is targeted by an approaching predator and consequently these stimuli are very effective in eliciting fast escape responses in a variety of insects (Card, 2012; Card and Dickinson, 2008; Chan and Gabbiani, 2013). In contrast, animals show different responses to self-generated looms during active approach of objects. Freely flying flies, for example, decelerate and extend their legs in a coordinated landing response as they approach a pole (van Breugel and Dickinson, 2012). Similarly a walking fly in our paradigm aiming to visit a landmark needs to suppress collision avoidance or escape responses. This suggests that flies are able to distinguish between self- and externally generated looms. To achieve this, flies might employ a similar mechanism to the one used to suppress flight stabilisation reflexes triggered by optic flow stimuli during voluntary turns (Kim et al., 2015). Behavioural state, i.e. whether

the animal is actively moving or quiescent, is known to modulate neural processing in the fly visual system via octopamine signalling (Chiappe et al., 2010; Longden and Krapp, 2009; Maimon et al., 2010; Suver et al., 2012). However, how the modulation of visual processing contributes to the distinct behavioural responses to looming stimuli in quiescent compared to actively moving flies is not well understood. The 2D VR system presented here offers a new approach for studying neural computations underlying the state-dependent behavioural responses to looming stimuli.

Summing up, there are two primary aspects that may result in different behaviours in the 1D and 2D fixation paradigm: (a) the rules that govern interaction between the fly's movements and the visual stimulus, and (b) the types of visual stimuli that are being generated during the experiment. Next, we will attempt to connect the different fixation behaviours described above to course control during navigation.

How does fixation behaviour relate to course control?

We already covered that in a 2D world fixation of a landmark in the frontal FOV leads to approach, which can only take a limited time period, as they are naturally terminated when the landmark is reached. Thus, in a 2D world approaches may alternate with departures corresponding to alternations of landmark fixation in the frontal and rear FOV. Indeed we found evidence for such an alternation between periods of fixation and antifixation (Bülthoff et al., 1982) in some flies, most prominently in male WTB flies exploring 'dark on bright' 2D worlds (***Figure 3.7 F***).

If flies were generally attempting to approach the stripe presented in 1D fixation trials, we would expect to see a strong tendency across flies to fixate the stripe in the frontal FOV. However, this is not what we found. Rather, fixation in WTB flies was heavily modulated by the contrast polarity of the screen. Flies only had a weak tendency to fixate a dark stripe, but did so often in the frontal FOV. In contrast, flies showed no positional preference when fixating a bright stripe but fixation of the bright stripe was frequent and relatively strong (***Figure 3.7 G, L***). One possible reason for the strong fixation of the bright stripe at arbitrary angles in the FOV may be the potential role of landmarks as a guidance cue for maintaining a straight path: Keeping a distant object at fixed angle allows maintenance of straight course. Examples include the sun-compass based navigation of migrating monarch butterflies (Guerra and Reppert, 2015) or orientation of dung beetles according to the milky way or the moon (el Jundi et al., 2015). If object is close, however, fixed angle other than 0 or +/-π will lead to spiralling movement

trajectory. Flies might use a basic heuristic that bright on dark objects are likely bright celestial bodies on the dark night sky and thus 'assume' that they are far away and fixation at any point in their FOV would allow for straight movement.

When we compared fixation in 1D and 2D, we made a second curious observation. In 2D but not 1D trials, landmarks were preferentially fixated at the side at +/- π/2. This fixation angle preference was observed irrespective of the contrast polarity, but it was particularly pronounced in dark scenes. We do not have a definite explanation for this behaviour. A possible reason may be that motion parallax is strongest when an object is located perpendicular to the animal's direction of movement (Schuster et al., 2002). Moving relative to a landmark located to the fly's side would therefore provide the fly with the most information about its distance to the respective landmark. To investigate further what induces fixation to the side and how this relates to initiation of fixation of the respective landmark, we could test flies of a genotype that shows strong naïve fixation behaviour in a virtual world with large landmarks far apart from each other, but where flies can always see a few landmarks at the same time. This would, for example, allow us to test whether flies systematically chose the closes landmark and whether the 'selection' occurs after an episode of fixation to the side.

The observation that flies are able to fixate at any angular position implies that fixation is not simply based on a hard-wired algorithm based on maintaining an 'optomotor balance' (Heisenberg and Wolf, 1979). Fixation at arbitrary angles, or — if viewed from the perspective of the fixated object — active orientation of an animal with a fixed angular relationship to that object, has been termed 'menotaxis' (Kühn, 1919). Kühn (1919) distinguishes between 'real' orientation reactions and various forms of 'tropotaxis', the latter being limited to symmetric orientation of the animal's sensors relative to the source of the guidance stimulus.

Many insects appear to have a naïve tendency to track stripes rotating around the animal and to actively keep a visual landmark in a fixed azimuthal position in their FOV (Bahl et al., 2013; Böhm et al., 1991; Götz, 1975; Kennedy, 1940; Kimmerle et al., 2000; Paulk et al., 2014). Besides helping animals to maintain a straight path, fixation may also aid movement through a complex environment in a repeatable manner. Being able to return to specific points in space can be helpful when navigating visually defined learned routes (Collett and Collett, 2002; Trullier et al., 1997). It could be, that fixating visual landmarks is such an important module in insect navigational behaviour — as a guidance cue during beaconing, during route following

and path integration (Chittka and Kunze, 1995; Collett and Collett, 2002) — that it is frequently observed in exploratory navigation as well.

3.4.3. What causes the large behavioural variability of fixation behaviour?

While flies generally showed a tendency to fixate stripes and to visit landmarks, only some aspects of landmark interaction were stereotyped while other features showed large variability across individual flies. For example, during approaches flies generally fixated the landmark in their frontal FOV, but walking velocities and walking patterns, such as the number of sharp turns, turn biases and curviness of the trajectory, varied. Inter-individual variability within the same genotype has been previously described for handedness and phototactic preferences (Ayroles et al., 2015; Buchanan et al., 2015; Kain et al., 2012). Additionally, we saw clear sex-specific and genotype-specific differences between flies, consistent with previous reports of genotypic and sex-specific differences in locomotion patterns (Ayroles et al., 2015; Martin, 2004; Martin et al., 1999). Differences in approach angles between sexes have been described in the context of inter-fly interactions (Branson et al., 2009). The large degree of genotypic and sex-specific variability may be disconcerting for some experiments and poses a challenge for the design of rigorous controls for genetics studies of these behaviours, but it is also intriguing and emphasises the complexity of the control of movement patterns. One source of the variability may be differences in the animals' motivational state in our experiments. Because it is unclear what factors drive innate stripe tracking and landmark interaction behaviour, we could not guarantee that all animals were motivated to track stripes or landmarks.

Phototactic preferences and absolute light intensities likely affect fixation behaviour

In high-contrast 2D environments landmark tracking and phototaxis are tightly linked, as landmark approaches are coupled to changes in overall luminance. Phototactic preferences do not only vary between individual animals and with genotype (Kain et al., 2012; Strauss and Heisenberg, 1993), but can also be modulated by the environmental temperature (Markow, 1979). The suspicion that phototaxis could at least play a role in landmark interaction behaviour was substantiated by the observation that stripe and landmark tracking was markedly different under opposite contrast polarity conditions, i.e. in 'dark on bright' compared to 'bright on dark' scenes. Fixation was more frequently observed in 'bright on dark' compared to 'dark on bright' scenes. An effect of contrast polarity on fixation behaviour has also been reported in tethered flying flies (Heisenberg and Wolf, 1979; Reiser and Dickinson, 2008). Unfortunately it is challenging to quantitatively compare fixation behaviour across different studies due to

differences in the setup, the behavioural paradigm and the quantification of the behaviour. For example, (Heisenberg and Wolf, 1979) present the visual stimulus in open-loop, slowly rotating a dark or bright stripe around the tethered flying fly. Conditions in the experiments of Reiser and Dickinson (2008) are more similar to those in our experiments, yet there are a few important differences. Reiser and Dickinson (2008) tested stripe fixation with a wider stripe (30˚ compared to 20˚ in our experiments) and only over very short trials (40 s compared to 10 min in our experiments). A wider stripe may be more salient than a thinner one and during shorter trials flies are less likely to fixate at multiple angular locations. Further, for quantifying fixation strength Reiser and Dickinson (2008) chose a metric different from ours, which is insensitive to fixation at more than one angular position. Under natural conditions, landmarks such as grass tufts, bushes and trees form dark features against a bright sky. Many early experiments on visual guidance of walking in flies were performed in a bright arena with dark visual landmarks, while 'bright on dark' conditions are generally preferred when behavioural studies are combined with imaging studies to reduce imaging noise. A more systematic evaluation of the influence of contrast polarity on a given behaviour may help reduce discrepancies across setups and paradigms. Besides contrast polarity, the overall light intensity in an environment may also affect landmark interaction behaviour. In early free walking experiments with bright, white background light following conditions described in (Colomb et al., 2012) as opposed to dim blue background light (0.115 - 0.105 mW/cm^2 at 461 nm), flies generally showed stronger preference for residing close to the dark landmark. This is consistent with the finding that fixation of a black 5˚ wide stripe by tethered flying flies degrades with decreasing background brightness (Reichardt and Poggio, 1976). Also the ambient temperature could affect fixation behaviour, either directly or by altering the fly's phonotactic preference and general locomotion pattern. Most of our experiments were conducted at a room temperature of 28-30˚ C, which is comparable to previous studies (Bahl et al., 2013; Colomb et al., 2012). We did see an increase in walking frequency at higher temperature in WTB flies, but no significant effect on fixation frequency (***Figure 3.7***).

Taken together, this suggests that the primary factor that contributed to the rare occurrence of strong stripe fixation in our VR setup was the relatively low light intensity: 0.52 mW/cm^2 at 459 nm or approximately 213 lux, compared to 7500-8000 lux reported in (Colomb et al., 2012). While higher light levels might be able to elicit more robust behaviour, they are, unfortunately, incompatible with two-photon imaging.

Multiple possible landmark tracking strategies

In our 2D fixation paradigm the fly is exposed to a relatively complex visual environment and has three degrees of freedom of movement. Thus, in addition to the limited control of the flies' motivational state also the increased number of possibilities in which the fly can interact with its environment may have contributed to the observed variability and may reflect the use of different navigational strategies.

A walking fly approaching a static landmark may choose between two basic tracking strategies: Smooth or saccadic pursuit. In smooth pursuit the animal continuously adjusts its relative heading angle to fixate the target in its frontal FOV, whereas the animal keeps a constant relative heading interrupted by discrete course corrections in form of sharp turns, so called saccades. The use of both strategies has been described in wild hover flies tracking flowers and conspecifics in the field (Collett and Land, 1975). Examination of walking trajectories of both freely and tethered walking flies in our landmark-interaction experiments suggests the occurrence of both smooth and saccadic tracking. Saccadic tracking of a single static pole in freely flying fruit flies has been described in the context of landing (van Breugel and Dickinson, 2012). In the future, we hope to use our setup to study of neural computations underlying the choice and execution of both navigational strategies.

In addition to investigating neural computations underlying the execution of different navigational strategies, we could exploit the flexibility in designing the sensory environment to test what influences the selection of a specific strategy. Under some conditions the smooth and saccadic tracking, for example, may be equivalent, while under other conditions one strategy is favourable. Collett and Land (1975) observed variability in how hoverflies tracked static targets — similarly to our observations in walking flies tracking visual landmarks — but they found that systematic patterns emerged during pursuits of other hover flies, i.e. moving targets. Hover flies preferentially used saccadic tracking to follow very fast moving targets, while slower moving targets were followed by smooth pursuit. Saccadic turns reduce the amount of time that visual perception is impaired due to motion blur (Collett and Land, 1975; Tammero and Dickinson, 2002). In accordance, during pursuit of a fast moving target, hoverflies preferentially use saccadic tracking (Collett and Land, 1975). In freely flying flies the frequency of saccades depends on the degree of visual contrast and the corresponding strength of optic flow stimuli perceived during movement manoeuvres: Flies perform more frequently saccades in a high contrast compared to a low contrast visual environment (Tammero and Dickinson, 2002). Varying the visual background in our experiments would allow us to explore whether the visual

environment shapes walking behaviour in similar ways. We could also assess to which degree findings from flight generalise to course control during walking. Another possibility is that in a given visual environment intrinsic differences in walking velocity resulting in different sensory experiences drove animals to prefer certain modes of tracking. This can be addressed by further analysis of the data presented in this thesis, for example by correlating saccade frequency with walking velocity.

3.4.4. Towards goal-directed landmark-guided navigation in a multisensory VR

Because flies tracking landmarks use the same steering manoeuvres as during spontaneous roaming, it is hard to judge when tracking begins and when it is aborted (see also Collett and Land, 1975). The analysis and interpretation of behaviour, but also neurophysiological data is distinctly easier when behavioural motivation is well controlled, for example during goal-directed navigation. Furthermore, we would like to study how internal representations of space, such as the fly's HD cell-like system, are used during landmark-guided, goal-directed navigation.

The naïve landmark interaction paradigm presented here could be extended to elicit goal-directed navigation in head-fixed walking flies in a multimodal virtual environment. Our visual VR system can readily be modified to allow spatially restricted delivery of non-visual stimuli such as heat, using closed-loop stimulation with an IR laser. Alternatively, one could use optogenetic activation of sensory neurons to deliver virtual stimuli (Klapoetke et al., 2014). Visual landmarks could then be paired with aversive or appetitive stimuli and flies might learn to use those visual cues to navigate to the reward or avoid the aversive stimulus.
In the context of conditioning protocols, where landmark interaction would be compared over extended time periods and between trials before and after training, temporal stationarity of the fly's walking behaviour may become more important than robustness of naïve tracking behaviour. We may be able to exploit sex- and genotype-specific differences in landmark interaction behaviour and let our choice be guided by the behavioural characterisation presented in this study.

Chapter 4

Landmark-assisted avoidance of virtual aversive stimuli in a visual virtual reality

4. Landmark-assisted avoidance of optogenetically induced virtual aversive stimuli in a visual virtual reality

4.1. Introduction

Complex navigational behaviours can emerge from connecting behavioural modules such as different generic steering manoeuvres into long behavioural sequences. One example of such a module in flying insects is the sharp turn, or 'saccade', which is commonly observed during cruising flight, but is also an important course-correction manoeuvre during tracking of static and moving targets (Collett and Land, 1975; van Breugel and Dickinson, 2012). Fixation, which we have focused on in chapter 3, is another example. Numerous studies in flies have contributed to an increasing understanding of the control of such behavioural modules, both in terms of sensory triggers and neural mechanisms (Bahl et al., 2013; Götz, 1994; Kim et al., 2015; Maimon et al., 2008; Reichardt and Poggio, 1976; Srinivasan et al., 1993). Yet, we still know very little about how different modules are coordinated to generate more complex navigational strategies and how such strategies are initiated.

Our aim is to understand how individual steering manoeuvres are chained together and coordinated to reach a navigational goal. Because we ultimately want to link behavioural strategies to neural computations, we choose an assay that is compatible with neurophysiological recording techniques: Visually guided navigation in head-fixed walking fruit flies in a 2D virtual reality (VR) environment (see chapter 3 for details). Navigation in visual VR environments has been successfully used in rodents and primates to investigate neural mechanisms underlying orientation behaviours (Aronov and Tank, 2014; Dombeck et al., 2010; Hölscher et al., 2005; Hori et al., 2005). Here we investigate whether and how flies placed in a simple 2D VR environment with sparsely distributed visual landmarks use these cues during a simple navigational task: avoiding spatially restricted aversive areas in the virtual space.

In a behavioural study of visually guided navigation, the experimenter can try to deduce the use of a certain strategy from the task the animal is attempting to solve. However, it can be challenging to detect when an animal is engaged in a navigational task. In the simple case of landmark tracking, for example, periods of successful landmark fixation and visits are easy to detect, but the initiation and potential termination of such epochs are harder to define (Collett and Land, 1975; van Breugel and Dickinson, 2012). Performing quantitative and statistical

analysis on behavioural measurements when studying the mechanisms underlying the control and execution of navigational strategies requires the comparison of multiple occurrences of the respective behaviour. If effects are subtle, the sensitivity of the analysis is critically dependent on accurate categorisation of the behaviour. One way around this obstacle is to increase the frequency with which the behaviour of interest is performed, for example by increasing the animal's motivation to perform it. This can be achieved either by exploiting innate preferences or by operant conditioning.

We decided to exploit the fly's innate aversion to certain stimuli to design a landmark-guided avoidance task. To do this, we paired visual landmarks with an innately aversive stimulus. This allowed us to study not only innate avoidance manoeuvres, but also to probe whether flies are able to use visual cues to more effectively avoid the aversive stimuli. We also wanted to test whether the flies' naïve behaviour would be altered after the landmarks were imbued with negative valence. In this setting, flies could potentially associate a specific visual landmark cue with the aversive stimulus and avoid approaching such landmarks in the future. During both acute and conditioned avoidance, we can make strong assumptions about what the animal is trying to do — escape from the aversive stimulus — which greatly eases the analysis and interpretation of the observed behaviour. Successful visual conditioning of flies may allow the design of behavioural paradigms to study more complex navigational strategies in the genetically tractable fruit fly.

A commonly used paradigm for visual conditioning in flying flies uses a so-called 'flight simulator', in which a fly can control its angular orientation relative to a visual panorama (Götz, 1994; Heisenberg and Wolf, 1979). Visual conditioning in the flight simulator has been used to investigate visual feature discrimination (Liu et al., 2006) and generalisation of learned visual features (Liu et al., 1999) in flies, but this paradigm is not well suited for studying spatial navigation strategies as the sensory environment and the fly's interactions with it are very limited. More recently, a visual place learning paradigm analogous to the Morris water maze (Morris, 1981) has been developed for freely walking flies (Foucaud et al., 2010; Ofstad et al., 2011). In this paradigm, flies learn to use a visual panorama to more effectively find a cool spot in an otherwise aversively hot environment. The visual place learning assay could potentially be used to further investigate navigational strategies underlying conditioned, visually guided heat avoidance. However, it has not yet been successfully adapted to a tethered walking preparation, which limits the tools available for investigation of the underlying neural computations.

Both conditioning paradigms described above use high temperature as an aversive 'teaching' signal. Aversive stimuli have the advantage that the motivation for avoiding them is reliably high, whereas the motivation to seek out a reward in form of an appetitive stimulus may depend on the animal's internal state and vary over time. On the other hand, commonly used aversive stimuli — high temperature or electric shock — can damage the fly, which limits the duration of an experiment and potentially the quality of neurophysiological recordings (personal communication Michael Reiser, Armin Bahl). We therefore decided to attempt eliciting avoidance behaviours with 'virtual aversive' stimuli generated by optogenetically activating neurons that signal the presence of aversive stimuli to the animal.

Our search for suitable neurons that could be used to elicit virtual aversive stimuli was aided by recent advances in the understanding of temperature sensing in fruit flies. The body temperature of small organisms like fruit flies is tightly coupled to the external temperature and flies therefore have exquisite temperature sensing and exhibit strong temperature preferences (Barbagallo and Garrity, 2015). Flies sense innocuous warming with thermal sensors in their antennae through peripheral neurons, Hot cells (HCs), which mediate rapid warmth avoidance in steep temperature gradients (Gallio et al., 2011; Ni et al., 2013). Preferences in shallow temperature gradients unfolding over tens of minutes are mediated by a second class of temperature sensors, the anterior cells (ACs) located in the head capsule (Hamada et al., 2008). AC, but not HC, activation has been associated with aversive olfactory conditioning (Galili et al., 2014). The neural mechanisms for sensing noxious heat, which elicits rapid avoidance and escape jumps, have been characterised in the larval fruit fly (Barbagallo and Garrity, 2015; Tracey et al., 2003), but much less is known in the adult. Responses to noxious heat seem to be mediated by a number of redundant sensory systems involving several nociceptors, and the integration and processing of these signals in the brain is still largely unknown (Barbagallo and Garrity, 2015; Tang et al., 2013).

In our experiments we will exploit aversive responses akin to those observed in flies exposed to moderate and high heat, but we will remain agnostic about the exact nature of virtual, optogenetically induced stimuli as it is not essential for the questions we are asking. That is, whether visual landmark cues can, in general, be integrated with aversive stimuli to generate a directed and thereby more effective avoidance response, and whether flies can learn to associate those aversive stimuli with visual landmarks.

4.2. Methods

4.2.1. Fly rearing, handling and reagents

Reagents and confirmation of expression patterns

Flies used in virtual avoidance experiments were generated by crossing a sparse driver line, targeting neurons that when activated induce avoidance behaviour, to an effector line encoding the red-shifted optogenetic activator CsChrimson (Klapoetke et al., 2014). Specifically, we used Hot cell (HC)-GAL4 (Gallio et al., 2011) and SS01159 as driver lines and 20xUAS-CsChrimson-mVenus inserted in attP18 in a wild-type Berlin (WTB) background as effector line. SS01159 is a split-GAL4 line constructed by the Rubin lab at Janelia from R41C05-p65ADZp in attP40 and VT026019-ZpGAL4DBD in attP2. SS01159 was kindly provided by Yoshinori Aso and TJ Florence shared the HC-GAL4 (Gallio et al., 2011) line with us. The expression pattern of SS01159 was confirmed using the mVenus tag of CsChrimson. To confirm the expression pattern of HC-GAL4, we drove expression of GFP either tagged to mCD8 or myr. Janelia FlyLight and members of the Rubin and Dickinson laboratories at Janelia performed dissections, immunolabelling and imaging as described in (Aso et al., 2014a). Briefly, brains and ventral nerve cords (VNCs) of 3-8 days old female and male flies were immunolabelled using anti-GFP and the nc82 antibody. We looked at the expression pattern of HC-Gal4 in 7 brains and 5 VNCs in female and 5 brains and 4 VNCs in male HC-GAL4; pJFRC2-10XUAS-IVS-mCD8::GFP flies (4-6 days). In addition, we looked at 4 brains and 4 VNCs of female and 5 brains and 4 VNCs of male HC-GAL4; pJFRC12-10XUAS-IVS-myr::GFP flies (6-7 days).

Fly rearing

Flies were reared at 23 ˚C in 60 % relative humidity with a 16:8 light:dark cycle. All flies were kept on fly food prepared according to a recipe from the University of Würzburg, Germany (see chapter 3 for exact recipe). Cornmeal and molasses contain retinol and are thus a potential source for all-*trans*-retinal (Isono et al., 1988; Wang et al., 2012). Due to the use of natural components in the preparation of fly food, the exact retinol content of the fly food may vary, but we expect it to be well below 0.001 mM.

For our experiments we used flies expressing the optogenetic activator CsChrimson (Klapoetke et al., 2014). To produce functional CsChrimson, flies need to have sufficient access to retinal, which was provided through the food. Crosses were set on Würzburg food with all-*trans*-retinal added (0.2 mM concentration) and the offspring was transferred onto food with a higher retinal concentration (0.4 mM concentration). Flies expressing CsChrimson need to be reared in darkness or low-light conditions to prevent (a) activation of CsChrimson-expressing neurons

and (b) degradation of retinal in the food. We decided to rear flies under low-light conditions rather than complete darkness to give flies exposure to visual stimuli prior to behavioural experiments and ensure a normal circadian rhythm. To reduce exposure to red light, which most effectively activates CsChrimson, flies were kept inside a blue acrylic case inside the incubator. The spectrum of light entering the blue case, measured with a spectrometer, showed a transmission peak between 420-500nm. Assuming a wavelength of 450 nm, the light intensity inside the case was approximately 60 µW/cm2. Flies reared under such conditions showed normal levels of optogenetic activation when stimulated during experiments while maintaining a circadian rhythm with two daily activity peaks (personal communication, Stern lab). Control flies for optogenetic activation experiments were also reared inside the blue case, but on standard Würzburg food without the additional retinal.

Preparation of flies for experiments

Prior to experiments flies used in freely walking and in tethered experiments were treated identically. 3-5 day old flies were cold anesthetised, sorted according to sex and the distal two thirds of their wings were clipped. After wing clipping, male and female flies were kept separately and transferred into fresh food vials with a small piece of filter paper, where they were allowed to recover for 2-3 days before experiments. All experiments were performed with 5-10 day old wing-clipped flies. For tethered walking experiments, flies were tethered to a pin as described in the previous chapter in ***section 3.2.1***.

4.2.2. Optogenetic quadrant assay for freely walking flies

Optogenetic free walking arena

We used a free walking quadrant assay inspired by a design presented in (Klapoetke et al., 2014) to screen different sets of neurons and different stimulation paradigms for their capacity to induce avoidance behaviour. We extended the setup described in the previous chapter in ***section 3.2.4*** (Free-walking arena design) with an option to deliver red stimulation light (627 nm) independently in four quadrants of the free walking arena (***Figure 4.1***). The infrared (IR) backlight and the red stimulation light were delivered from below the arena using four LED panels. Each panel contained spatially intercalated IR and red (LXM2-PD01-0050, LUXEON Rebel Color, Philips Lumileds Lighting Company, San Jose, CA, USA) LEDs. The four panels were connected to a microcontroller board built around a Teensy 2.0 processor (PJRC.com, LLC Sherwood, OR, USA). The user could set the light intensities for the IR and the stimulation LEDs from a computer using serial communication with the microcontroller. The LEDs could be

switched on and off with arbitrary temporal profiles and the red LEDs could be targeted to control illumination independently in 16 sectors. For behavioural experiments serial commands to the LED board were sent through a custom-written python (python version 2.7) program, to ensure temporally precise and repeatable delivery of a light stimulation protocol. Four IR LEDs placed at the corners of the arena base plate were coupled to red illumination in the respective quadrant. These four IR LEDs served as indicators for the red light stimulation in videos of the free walking arena recorded with an IR camera from above (***Figure 4.1 C***).
Prior to optogenetic activation experiments we measured the relationship between LED controller input (in %) to the red LEDs and light intensity at 627 nm (***Figure 4.1 E***). These measurements were performed in a dark room with two out of four quadrants, i.e. two out of four LED panels, switched on. The 1 % level resulted in 0.27 mW/cm^2 in the illuminated and 0.01 mW/cm^2 in the non-illuminated quadrants. The 5 % level produces 1.13 mW/cm^2 in the illuminated and 0.05 mW/cm^2 in the non-illuminated quadrants. The 10 % level corresponds to 2.25 mW/cm^2 in the illuminated quadrants and 0.11 mW/cm^2 in the non-illuminated quadrants.

Quadrant assay

To test avoidance in an optogenetic quadrant assay, flies expressing CsChrimson (Klapoetke et al., 2014) under the control of a sparse GAL4 driver line were exposed to a 4 min long stimulation protocol forming one trial. The trial consisted of a 10 s long pre-stimulation period followed by 6 blocks of 30 s of red light stimulation separated by 10 s with no stimulation. During the 30 s stimulation blocks red light illumination was restricted to two opposing quadrants and the illuminated quadrants were alternated in consecutive blocks (***Figure 4.1 D***). In each trial, 12-18 wing-clipped flies were introduced into the arena (***Figure 4.1 C***). Only all-male or all-female groups were tested. The walking behaviour was video recorded at 30 Hz frame rate with a resolution of 40 pixel/mm corresponding to roughly 8-10 pixels long and 3-4 pixels wide images of a fly.

Analysis of walking trajectories

Walking trajectories were extracted from video recordings using Ctrax (Ctrax: The Caltech Multiple Walking Fly Tracker presented in Branson et al., 2009). The video frame corresponding to the beginning of the optogenetic stimulation protocol was determined for each movie using custom macros in Fiji (version 2.0.0-rc-43), by monitoring the brightness of one of the indicator IR LEDs. The tracking data was imported into Python (version 2.7) and further analysed with custom scripts. Some of the statistical analysis on processed data was performed in R (version 3.0.0).

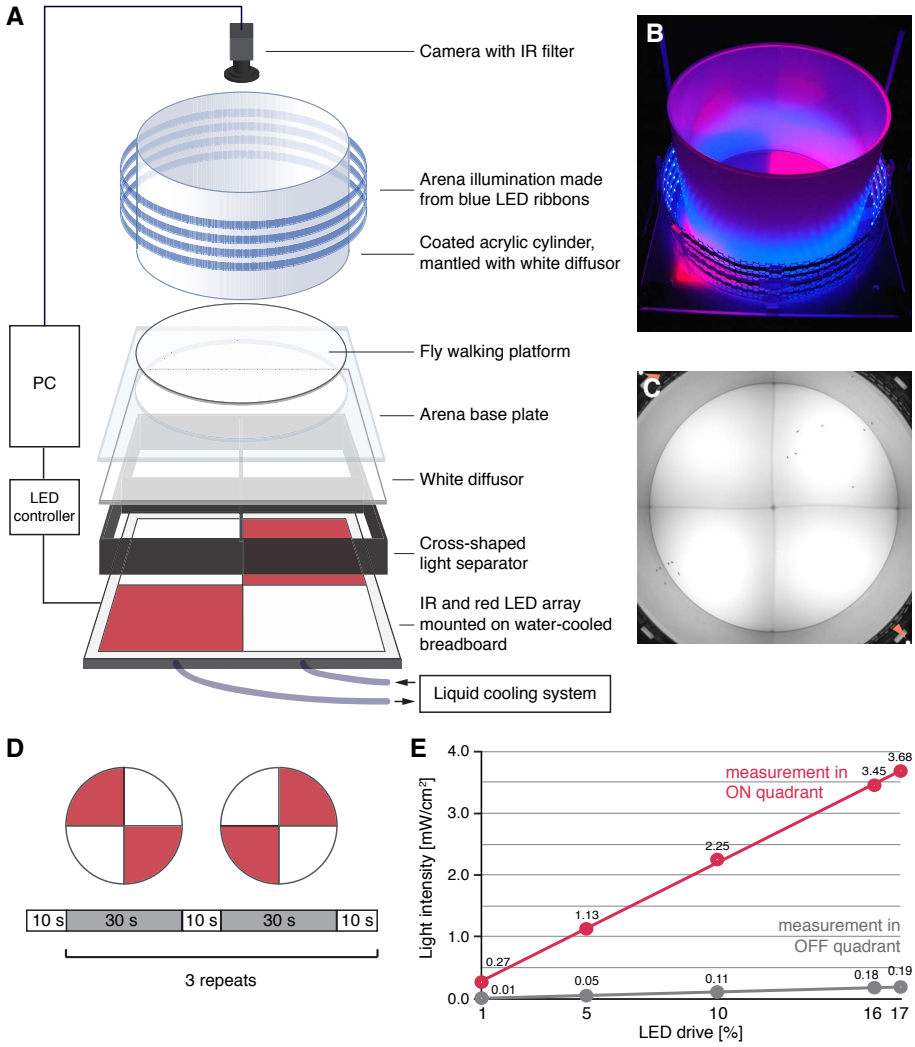

Figure 4.1: Optogenetic quadrant assay for screening fly lines and stimulus conditions for optogenetic virtual aversive stimulus delivery.

A: Schematic of the free walking arena for optogenetic stimulation experiments. IR light and red stimulation light is delivered from an LED array below the walking platform. B: Photograph of the free walking area showing the lighting conditions during experiments. Blue LEDs around the arena wall provide ambient light visible to flies. The red light illuminating two quadrants is invisible to flies. C: One frame from a video recorded during a trial with male HC-GAL4 x 20xUAS-CsChrimson flies. Two IR lights at the corners of the image (orange arrow heads) indicate which quadrants are illuminated. In this frame all flies have moved out of the illuminated quadrants. D: Schematic of the quadrant assay trial structure. E: Measured light intensities as a function of % LED driver current in the illuminated 'ON' (red points) and the not illuminated 'OFF' quadrants (grey points). Measurements were performed during continuous light illumination with a power meter (PM100D with S130C Sensor). The solid lines are the linear regressions for the five measurements. ON quadrants: $y = 0.2125x + 0.074$, $R^2 = 0.9996$. OFF quadrants: $y = 0.0114x - 0.0039$, $R^2 = 0.9993$.

4.2.3. Visual virtual reality with closed-loop optogenetic stimulation

VR system for tethered walking flies

The design of the visual VR system, consisting of a spherical treadmill, a panoramic screen and a custom-written VR software, has been described in detail in chapter 3. For virtual avoidance experiments we extended the basic visual VR by adding closed-loop optogenetic stimulation using a red LED (625 nm, M625F1, Thorlabs Inc, Newton, NJ, USA) focused on the treadmill ball surface (***Figure 4.2 A-C***).

As described in chapter 3, a custom-made scene file defined the dimension and appearance of the visual virtual environment. We used virtual scenes similar to those described in chapter 3 with periodically placed landmarks in a large plane. In some experiments we added spatially restricted optogenetic stimulation. The stimulation zones, in which the fly received optogenetic stimulation, were radially symmetric and defined by (a) the location of their centre, (b) the zone radius r_Z and (c) the optogenetic stimulation intensities at the centre and the outer edge (***Figure 4.2 E***). To mark the centre location of these zones we used invisible objects with a special nametag ('_objectName_r_'). The spatial profile of stimulation intensities within the zone was controlled using FlyOver's graphical user interface. The baseline stimulation intensity at the outer edge of the zone was delivered everywhere else in the virtual plane and was set to 0 in all experiments presented here. Inside each reinforcement zone, the stimulation intensity increased linearly toward the centre of the zone up to the set maximum intensity. The reinforcement zone radius and the maximum stimulation intensity varied between experiments.

The VR software, FlyOver, computed the reinforcement level as a function of the fly's position in the VR, ranging from 0 to 100, and logged it to file together with information on the fly's location and velocity in the VR. During an experiment, the program also sent the current reinforcement level via serial communication to a microprocessor (Arduino Mega 2000) running a custom script. The microprocessor then set the red stimulation LED to the light intensity specified by the reinforcement level variable. We measured the relationship between current input (characterised in % of maximum current) and light intensity for the red stimulation light, which was, with the exception of very low input currents, approximately linear (***Figure 4.2 F***). We used this empirical calibration curve to translate light intensities that we knew worked well for virtual avoidance behaviour in the free walking arena to reinforcement levels to be used in VR.

Virtual avoidance paradigm for tethered walking flies in VR

In virtual avoidance experiments in VR, each fly was tested under three conditions defined by the presence of visual landmarks and optogenetic stimulation (***Figure 4.2 D***). In all trials the fly was placed in the centre of a large virtual plane and was free to explore the space over the course of 10 min. In two of the three conditions, the virtual plane contained visible landmarks arranged in a periodic grid (see chapter 3 for details). We used black cones that were 1 cm wide at the base and 4 cm high as landmarks (same as in chapter 3). The virtual landmarks were impenetrable, thus, when a fly walked into one of them, it slid along the surface rather than passing through the virtual object. In the first condition, the virtual environment consisted only of the plane with sparsely distributed visible landmarks. In a second condition, radially symmetric reinforcement zones in which the fly received optogenetic stimulation were added around each visible landmark. The third condition was identical to the second, but with invisible landmarks. Invisible landmarks were impenetrable and had the same dimensions as the visible landmarks used in the first two conditions. We will refer to these three conditions as

- *'Landmark alone'* for trials with visible landmarks but no optogenetic stimulation
- '*Landmark with optogenetic stimulation*' for trials with optogenetic stimulation surrounding visible landmarks, and
- *'Optogenetic stimulation alone'* for trials with optogenetic stimulation around invisible landmarks.

Each fly was tested twice in the 'Landmark alone' condition and once in the other two conditions. The two 'Landmark alone' trials were always separated by one 'Landmark with optogenetic stimulation' trial and this block of three trials was either followed or preceded by one 'Optogenetic stimulation alone' trial. In all trials, the ground plane was textured with a low contrast white noise grey-scale pattern as described in chapter 3.

Analysis of walking trajectories in VR

Data processing and visualisation was performed in Python (version 2.7) using custom scripts. For each trial the log file was parsed to extract trial-specific information from the header and the time series data. The locations of objects in the 3D scene used in the respective trial were read from the corresponding coordinate file. For analyses on the level of multiple trials the data was downsampled to 20 Hz using linear interpolation. Most of the analysis of walking traces was performed on 'collapsed' trajectories, i.e. after projecting trajectory fragments around each of the periodically placed landmarks onto a circular area ('mini arena', r = 60 mm) around the central landmark (see ***Figure 4.2 D, E*** and chapter 3). Statistical analyses were performed using Python (version 2.7) and R (version 3.0.0).

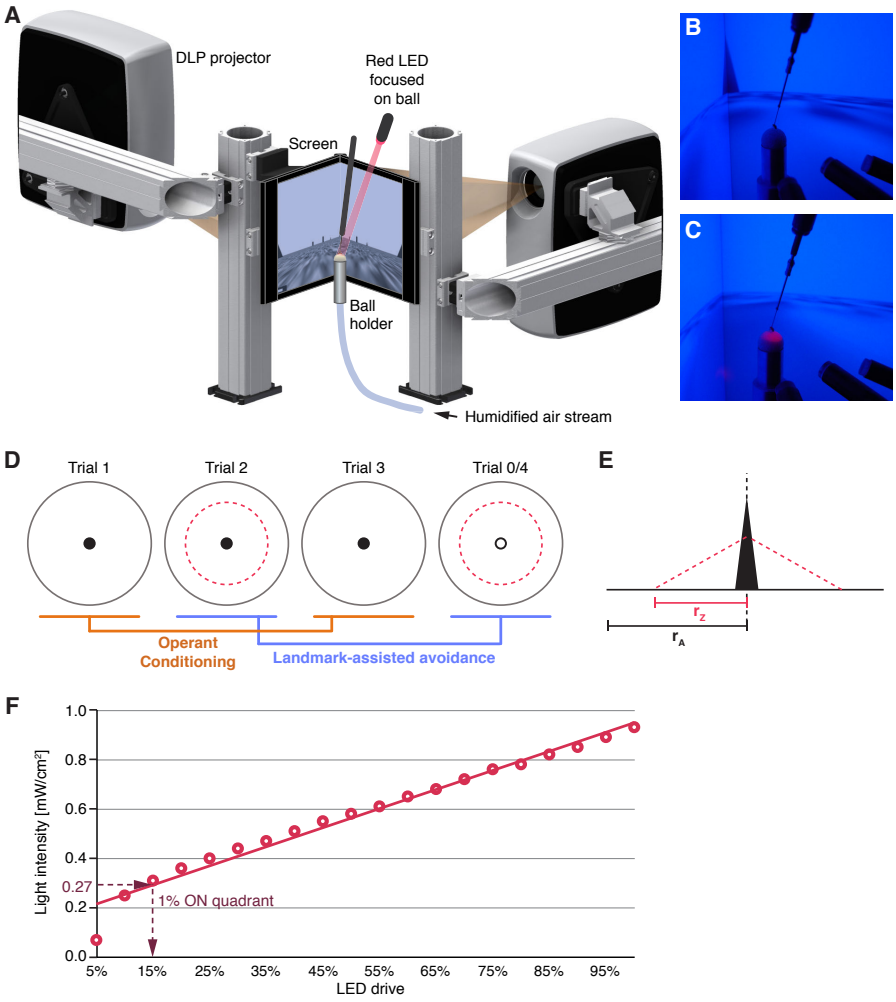

Figure 4.2: Experimental approach for studying avoidance of optogenetically induced virtual aversive stimuli in a 2D visual virtual reality.
A: Schematic of the experimental apparatus. **B, C:** Photographs of a tethered walking fly exploring a 2D virtual world with sparsely placed landmarks (similar viewpoint as in schematic in A). One can see the screen with a back-projected image behind the fly. The IR LEDs used to illuminate the trackball are visible in the lower right corner. **B:** A landmark is displayed on the screen in front of the fly. **C:** The red optogenetic stimulation light is on, illuminating the whole fly from above. **D:** Schematic of trial conditions in our behavioural paradigm. The conditions are illustrated with respect to a circular unit ('mini arena'), which is repeated within a large periodic world. The grey line marks the outer radius of the 'mini arena'. The black circle indicates the position of a visible landmark and the empty circle the position of an invisible landmark. The dashed red line illustrates the outer radius of a circular reinforcement zone. **E:** Profile of the optogenetic stimulation light intensities within 'mini arenas'. r_Z is the radius of the reinforcement zone, r_A the radius of the 'mini arena' in which the behaviour is analysed. **F:** Stimulation light intensity measured on the ball surface at 625 nm with a power meter (PM100D with S130C Sensor) as a function of LED driver current (in %). A linear regression over the data points is superimposed: $y = 0.0386x + 0.1766$, $R^2 = 0.9724$.

4.3. Results

4.3.1. Identification of suitable genetic driver lines for the delivery of optogenetically induced aversive stimuli

As a first step toward investigating whether flies take into account landmark cues when avoiding aversive stimuli in a 2D environment, we set out to identify suitable GAL4 lines to optogenetically deliver virtual aversive stimuli.

Screen for candidate lines for the delivery of optogenetically induced virtual aversive stimuli

We conducted a small behavioural screen using an optogenetic quadrant assay inspired by (Klapoetke et al., 2014) to identify candidate GAL4 lines that, when activated, induced robust avoidance behaviour. Wing-clipped flies expressing CsChrimson under the control of a sparse GAL4 driver line in a small subset of neurons were introduced into a large walking arena, where they could move around freely (***Figure 4.1***). In the arena, flies could choose to reside either in quadrants where they were exposed to red stimulation light, which activates neurons expressing CsChrimson, or in quadrants without red light illumination. We quantified avoidance behaviour as the fraction of flies residing in the red illuminated quadrants compared to the non-illuminated quadrants. Two GAL4 lines showed particularly strong aversion to red light stimulation and were selected for follow-up experiments: Hot cell (HC)-GAL4 and SS01150.

HC-GAL4 labels hot cells (HCs), temperature sensors in the fly's antennae (Gallio et al., 2011). HC activity is tightly coupled to the environmental temperature and changes thereof, and we will refer to the stimulus generated by optogenetically activating these neurons as 'virtual heat'. The second line that caused a strong aversion phenotype when activated was SS01159, a split Gal4 line generated by Yoshinori Aso, targeting a small population of ascending neurons. Optogenetic stimulation of SS01159 can substitute for the unconditioned stimulus in an aversive olfactory conditioning assay (personal communication with Yoshinori Aso). Furthermore, activation in larvae induces roll-responses, a behaviour specific to nociceptive stimuli (data not shown, personal communication with Tihana Jovanic). Based on these observations we hypothesise that neurons labelled by SS01159 carry nociceptive signals from the thorax to the brain, although a more in-depth investigation is necessary to test this hypothesis. For simplicity and in lack of a better term we will refer to the stimulus generated by optogenetically activating these neurons as an ascending aversive stimulus.

Confirmation of expression patterns of lines that induce 'virtual heat' and an ascending aversive stimulus

In our paradigm, specificity of the optogenetic stimulation is primarily controlled by the sparsity of the GAL4 driver line. Before presenting behavioural data from optogenetic activation experiments, we therefore show the expression pattern of the two GAL4 lines we used to deliver virtual aversive stimuli.

We used HC-GAL4 to drive expression of two GFP-based reporters and we examined the brain and the ventral nerve chord (VNC) of several male and female flies. Examples are shown in ***Figure 4.3***. Previous studies have reported that HC-GAL4 only drives expression in HC neurons, whose cell bodies are located in the antennae and which project to the proximal antennal protocerebrum (PAP) in the brain (Gallio et al., 2011). Indeed, we found that arborisations in the PAP were labelled (filled arrow head in ***Figure 4.3 A-D***). However, in addition we found GFP expression in ascending neurons with extensive arborisations in the VNC (asterisk and star in ***Figure 4.3 A-D***) and, in some flies, in a fan-shaped body neuron (empty arrow head in ***Figure 4.3 B-D***). These findings were consistent across sexes and reporters.
The expression pattern of SS01159 contains only ascending neurons (***Figure 4.3 E***). It may label several cell types, as there are about 15-20 cell bodies of labelled neurons distributed across the VNC (filled arrow heads in ***Figure 4.3 E***). Future studies will show whether different subpopulations of these neurons convey different information.

Knowing the exact expression pattern is helpful for the design and interpretation of activation experiments, since the optogenetic stimulation light has to penetrate the tissue to varying degrees to reach neurons arborising at different depths. For example, we expect superficial neurons such as HC to be activated at lower light intensities than central neurons in the brain or VNC.

To explore whether flies can use visual landmark cues to avoid aversive stimuli, we decided to test both HC and SS01159 activation in a virtual avoidance assay. We will begin by presenting behavioural experiments with 'virtual heat' before we move on to experiments with the ascending aversive stimulus. As a first step toward the development of a behavioural paradigm for studying landmark assisted avoidance of 'virtual heat', we analysed virtual avoidance in freely walking flies to identify effective stimulation conditions. These conditions were then transferred to a VR paradigm.

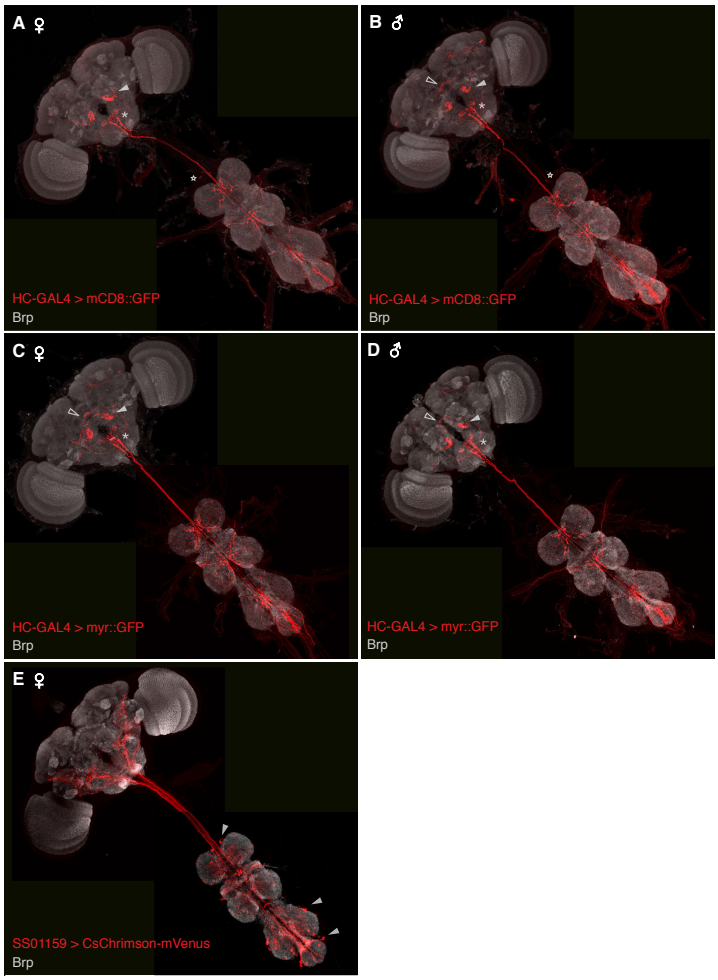

Figure 4.3: Expression patterns of driver lines used to optogenetically generate virtual aversive stimuli.
A-D: Confirmation of the Hot cell (HC)-GAL4 expression pattern. **A, B:** HC-GAL4 drives mCD8::GFP expression in several cell types in the central nervous system (CNS) of a 4-6d old female (**A**) and male (**B**) are shown. The cell bodies of HC neurons are located in the antennae and have been removed during the dissection, but the dendritic arborisations are visible in the proximal antennal protocerebrum (PAP, left cell marked with white filled arrowhead). Additionally HC-GAL4 labels putative ascending neurons in the male and female fly (asterisk, a few cell bodies marked with star). Only in the male fly a brain neuron arborising in the FB is labelled (empty arrow head). The nc82 antibody against Bruchpilot (Brp) is used as background staining. **C, D:** Also in HC-GAL4 > myr::GFP flies HC are labelled (filled arrow) together with ascending neurons (asterisk) and a fan-shaped body neuron (empty arrow). A female (**C**) and a male (**D**) 6-7 day old fly brain are shown. **E:** The split-GAL4 line SS01159 drives CsChrimson-mVenus expression exclusively in a population of ascending neurons (red), which arborise in a number of regions in the brain. A few of the labelled cell bodies are marked with white arrowheads. Background staining of Brp in grey. The brain of a 3-8 day old female is shown. All images shown are overlays generated from the merging the maximum intensity projections of the two colour channels. Each subpanel is a montage of two separate images of the brain and the ventral nerve chord. Dissection, immunolabelling and imaging of brains were performed by Janelia's Fly Light facility (HC line) and members of the Dickson and Rubin labs (SS01159 line).

4.3.2. Avoidance of 'virtual heat'

'Virtual heat' avoidance in freely walking flies in an optogenetic quadrant assay

We used an optogenetic quadrant assay in freely walking flies to find optogenetic stimulation light intensities and a stimulation protocol that could induce robust avoidance behaviour in HC-GAL4 > CsChrimson flies (***Figure 4.4***). Flies were exposed to a 4 min protocol consisting of six 30 s optogenetic stimulation periods during which red light of a fixed intensity was delivered in two opposing quadrants. Two levels of red light intensity were tested: 0.27 mW/cm^2 and 1.13 mW/cm^2 corresponding to an LED input current of 1 % and 5 %. As in our first screen, the avoidance response was measured as the fraction of flies that resided in the red illuminated quadrants. We found that in HC-GAL4 > CsChrimson flies already very low stimulation light intensity levels lead to strong avoidance of illuminated areas (***Figure 4.4 A, B***). There was no adaptation of this response over the 4 min protocol and we saw no difference between groups of male and female flies. Control experiments with flies reared on standard food without addition of retinal, i.e. in flies possessing no or only low levels of functional CsChrimson, confirmed that the avoidance was mediated by activation of CsChrimson, not an innate aversion against the red stimulation light (compare ***Figure 4.4 C*** and ***D***). The average fraction of flies residing in the illuminated quadrants during the last 10 s of optogenetic stimulation was statistically different from an even distribution in all retinal-fed flies, but not in flies without functional CsChrimson (***Figure 4.4 E***).

Somewhat surprisingly, the avoidance response appeared to be less pronounced at higher stimulation light intensities (***Figure 4.4 C, E***). Investigation of trajectories at low light intensity revealed that at low light intensities, avoidance was mediated by directed turns away from the illuminated quadrant upon encounter with the quadrant border (***Figure 4.4 F***). At higher light intensities, however, flies more frequently crossed the border between illuminated and non-illuminated quadrants resulting in less accurate avoidance (***Figure 4.4 G***). Whenever flies did cross the border to illuminated quadrants, they seemed to speed up. The border between quadrants may have been harder to detect at higher light intensities due to bleed-through of light from the illuminated quadrants. Generally, a fly's reaction to high heat might be twofold consisting of an undirected flight response and directed aversion.

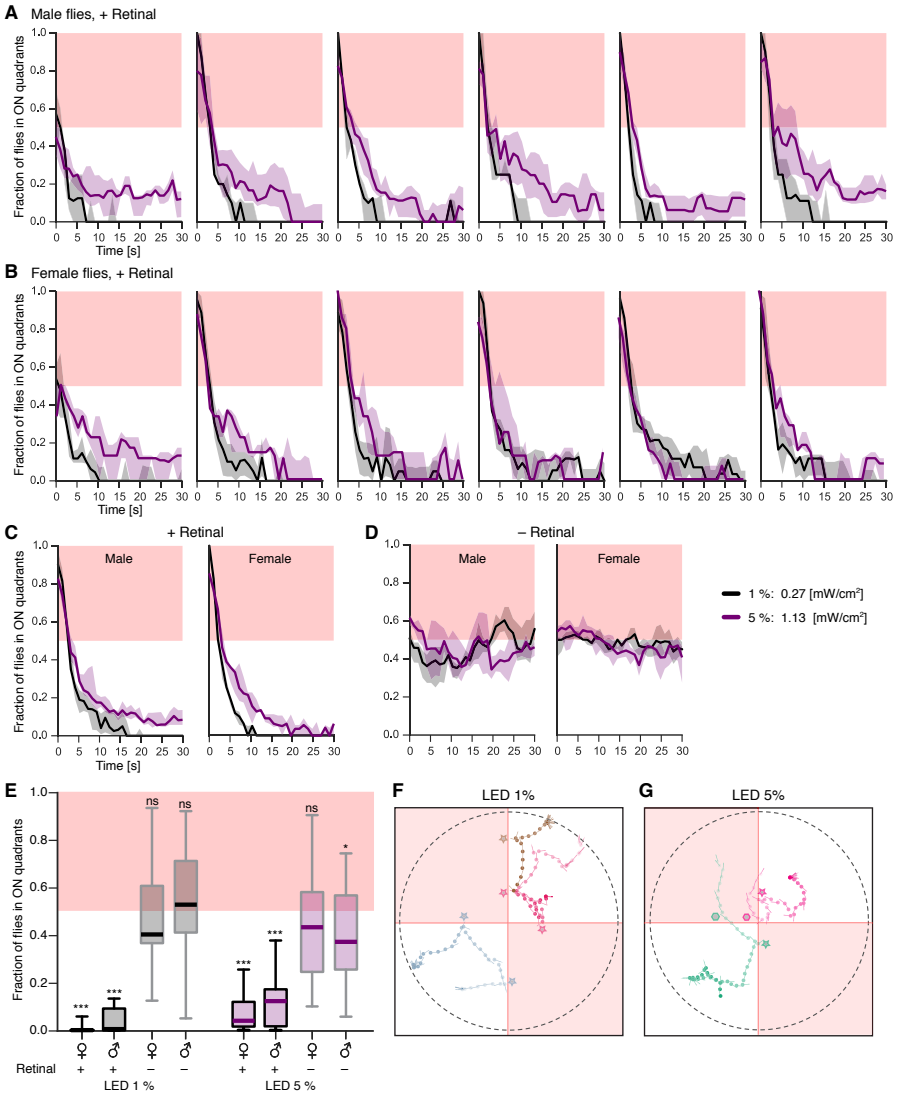

Figure 4.4: 'Virtual heat' aversion in freely walking flies with Hot cell-GAL4.
Preference test of free walking flies in the optogenetic quadrant assay. Data from flies expressing the red-shifted optogenetic activator CsChrimson in neurons labelled by the Hot cell (HC)-GAL4 line. **A, B:** Median avoidance responses over the time course of the 4 min long quadrant protocol. Each subplot shows the fraction of detected flies that reside in the red illuminated quadrants over the 30 s of one stimulation block. The 6 subplots per row depict the 6 sub-trials of quadrant stimulation over one trial. Each line within one subplot shows the median and IQR of 5-6 repeats with different sets of flies. Per repeat 12-20 flies were tested. Two stimulation light intensity levels were tested: 1 % (black, 0.27 mW/cm^2 in illuminated quadrants) and 5 % (violet, 1.13 mW/cm^2 in illuminated quadrants). **A:** Data from male, wing-clipped HC-GAL4 > CsChrimson flies reared on retinal-supplemented food. The sample size for both groups is n = 6. **B:** Data from female, wing-clipped HC-GAL4 > CsChrimson flies reared on retinal-supplemented food. The sample size for both groups is n=5. **C:** Response for male and female wing-clipped HC-GAL4 > CsChrimson flies reared on retinal-supplemented food averaged over the 6 sub-trials (median of sub trials). **D:** Same as C for flies reared on standard Würzburg food, i.e. without additional retinal supply. Female flies: n=6 (1 %) and n=6 (5 %) repeats. Male flies: n=4 (1 %) and n=4 (5 %) repeats. **E:** Boxplot of the mean response during the last 10 s of optogenetic stimulation. Using two-sided t-tests, we

tested whether the sample mean was different from 0.5. The t-test for LED 1 % and 5 % gave us a p<0.0001 for both male (n=36, each) and female (n=30, each) +Retinal flies. In the -Retinal control group, we got p=0.4600 in male and p=0.2634 in female flies for the 1 % LED level and for the 5 % level p=0.0266 in male and p=0.0667 in female flies (male: n=28, each; female: n=36, each). Significance codes: 0 ≤ '***' < 0.001 ≤ '**' < 0.01 ≤ '*' < 0.05 ≤ 'ns'. **F, G:** Example traces of male flies (+ Retinal group) during the last 10 s of optogenetic stimulation. **F:** Three flies at 1 % intensity level (repeat 3). **G:** Two flies at 5% intensity level. The dashed grey line indicates the arena border and the illuminated quadrants are marked with red-shaded boxes. Examples for turns upon encounter with the border to the ON quadrant are marked with a star. In G two examples for failure to turn upon encounter with the border at high walking speed are marked with a hexagon.

Visual landmark cues do not improve 'virtual heat' avoidance in 2D virtual reality

Next, we set out to transfer the 'virtual heat' avoidance paradigm from free walking to VR. At the border between quadrants in the free walking quadrant assay we had observed directed turns away from the 'virtual heat', suggesting that flies were able to detect the gradual increase in light intensity along the border zone. This observation led us to design circular 'virtual heat' zones in VR, which consisted of a radially symmetric gradient of increasing light intensity. We chose a linear gradient from 0 mW/cm^2 (0 % LED current) to 0.31 mW/cm^2 (15 % LED current) covering the range of intensities that had produced to the strongest avoidance in the free walking arena (***Figure 4.2 E***).

Since we had not found any indication for sex-specific differences in 'virtual heat' avoidance behaviour, we only tested male flies in the VR. Previous experiments in our VR system have shown that male flies walk more consistently on the ball and that their landmark interaction behaviour changed less over time than that of female flies (chapter 3) — an important aspect when comparing landmark interaction across trials.

To test whether flies are able to exploit visual cues to avoid 'virtual heat', we paired spatially restricted 'virtual heat' zones with visual landmarks. Each fly was exposed to four trials, two 'Landmark alone' trials separated by a 'Landmark with optogenetic stimulation' trial and an 'Optogenetic stimulation alone' trial (***Figure 4.2 D***). By comparing avoidance of 'virtual heat' zones in the 'Landmark with optogenetic stimulation' trial and in the 'Optogenetic stimulation alone' trial, we could assess to which degree virtual heat avoidance was improved in the presence of visual landmarks that could serve as guidance cues. 'Landmark alone' trials served as a control that allowed us to judge whether flies were sufficiently well tethered and positioned on the ball to be able to interact with the visual stimulus. Additionally, the set of three trials consisting of a 'Landmark alone', a 'Landmark with optogenetic stimulation' and a

second 'Landmark alone' trial (in this order) allowed us to probe whether experiencing 'virtual heat' paired with the visual landmark changed how flies interacted with the landmarks, i.e. whether there was an operant conditioning effect. We will first compare 'virtual heat' avoidance in VR in the presence and absence of visual cues before analysing in more detail how flies interacted with the landmarks.

Much like freely walking flies, tethered walking flies in VR were also able to precisely avoid areas with 'virtual heat' stimulation (***Figure 4.5 A***). Clear avoidance of 'virtual heat' zones was observed in single trials and when pooling data across flies (***Figure 4.5 A, B***). The precision of the 'virtual heat' avoidance was somewhat surprising, because in the VR paradigm the 'virtual heat' stimulus is generated by exposing the whole fly to red stimulation light of a fixed intensity rather than providing graded stimulation across the body of the fly. Thus, in contrast to real thermal gradients or the virtual thermal gradient in the free walking assay, flies in the VR did not receive any directional spatial information about the gradient. To perform directed avoidance turns, flies would have needed to integrate the change in 'virtual heat' over time and integrate this information with their own movement.

To quantitatively compare 'virtual heat' avoidance in trials with visible and invisible landmarks, we computed a normalised radial residency measure for the two trials (***Figure 4.5 C***). The normalised radial residency quantifies how much time flies spent at a given radial distance from the closest landmark. Since the 'virtual heat' zones were radially symmetric with respect to the centrally located landmark, and stimulus intensity increased linearly with decreasing distance from the closest landmark, this visualisation also informs us about how much flies resided in areas with a certain level of 'virtual heat' stimulation. 'Virtual heat' avoidance in trials with and without visual cues was remarkably similar. In both situations, the radial residency decreased starting at a landmark distance of about 45 mm, corresponding to light intensity levels larger than 1 %, and flies rarely came closer to the landmark than 30 mm, where the stimulation light intensity increased above 6 %, corresponding to 0.07 mW/cm^2. Thus, in this paradigm we found no evidence for landmark-assisted avoidance behaviour. To confirm that flies did indeed avoided the 'virtual heat' stimulus and not simply the red stimulation light, we also tested HC-GAL4 > CsChrimson flies that were reared on standard food without additional retinal. These flies did not avoid the stimulation light, not even at high intensities close to the landmarks (***Figure 4.5 D***). The small difference in the radial residency between the two trials of the non-retinal fed group could be attributed to the presence of the visual landmark in one but not the other trial.

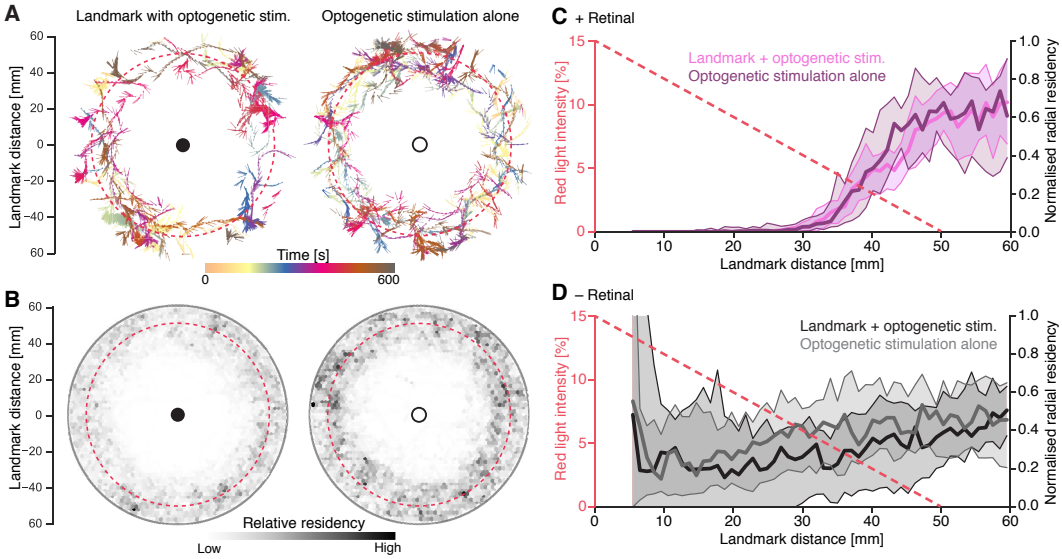

Figure 4.5: 'Virtual heat' avoidance in a 2D virtual reality.
Data from male HC-Gal4 > CsChrimson flies. **A:** Example traces of a male 7d old retinal-fed fly during trials with optogenetic stimulation: 'Landmark with optogenetic stimulation' and 'Optogenetic stimulation alone'. Only collapsed walking traces are shown. Each walking trace shows the fly's position with a dot and a short line indicating the fly's heading. The colour of the trace represents the trial time progressing from 0 s to 600 s. Black and empty circles mark the positions of visible and invisible landmarks, respectively. The dashed salmon line marks the outer boundary of the reinforcement zone (r_Z=50 mm). **B:** 2D residency histograms computed over the collapsed traces of n=20 retinal-fed flies for the two trials with optogenetic stimulation. The count is normalised within each histogram and colour-coded in grey scale (white indicates low count, black high count). Only time points during which flies were moving faster than 2 mm/s were taken into account. The position of landmarks and the reinforcement zones are visualised as in A. **C, D:** Comparison of the normalised radial residency in trials with optogenetic stimulation ('Landmark with optogenetic stimulation' and 'Optogenetic stimulation alone'). The radial residency is computed as the count of time points within a given radial distance range (relative to the landmark position) normalised by the area of that radial distance range. Only time points when the fly was moving faster than 2 mm/s were taken into account. Data from flies raised on food with retinal (**C**) and on standard Würzburg food (**D**). The dashed salmon-coloured line indicates the red stimulation light intensity (in % LED input current) at a given radial distance. Note that even though the optogenetic stimulus light intensity level is visualised as a continuous linear function of the landmark distance, the resolution of the intensity control was limited to steps of 1 %.

In the absence of any optogenetic stimulation, individual HC-GAL4 > CsChrimson flies exploring a virtual plane showed strong attraction to the dark landmarks ('Landmark alone' trials in ***Figure 4.6 A***). After a successful approach, flies tended to spend extended periods of time close to the object, sliding along the virtual surface. This behaviour was consistent across flies and resulted in a greatly increased residency close to the landmark (< 10 mm from the landmark centre)

compared to everywhere else in the virtual plane ('Landmark alone' trials in ***Figure 4.6 B***). The naive preference for residing close to the landmark was unchanged by the experience of 'virtual heat' paired with it (***Figure 4.6 B, C***). Thus, we did not find any evidence for conditioned landmark aversion in this paradigm.

As an alternative measure for the preference, we analysed the number of landmark visits each fly made over the course of a trial. A visit was defined as an approach to a landmark within a 20 mm radius. In retinal-fed flies the mean cumulative number of visits increased rapidly during the first half of the trial, before it plateaued in the second half (***Figure 4.6 E***). This might reflect a transition in the behaviour of retinal-fed flies from exploration and repeated approach of landmarks to extended stay close to a landmark (consider also the trajectory colour in ***Figure 4.6 A***). In contrast, the cumulative number of visits increased linearly with trial time in the non-retinal group (***Figure 4.6 F***). A comparison of the cumulative number of visits in the 'Landmark alone' trials before and after paired 'virtual heat' stimulation showed only a small decrease in visit frequency (***Figure 4.6 G***). This decrease was common to both retinal-fed and non-retinal-fed flies, indicating that this was not an effect of operant conditioning.

When we compared the radial residency in retinal-fed and non-retinal fed flies, we noticed that the strong preference for residing close to landmarks was less pronounced in the non-retinal group (***Figure 4.6 C, D***). The analysis of visits confirmed that the strong preference for landmarks was primarily the product of flies staying very close to the object after a successful approach rather than their frequent approaches (***Figure 4.6 G***). The strong preference for dark landmarks in retinal-fed flies compared to flies of the same genotype without functional CsChrimson made us wonder whether the varying brightness of the visual stimulus alone was sufficient to simulate varying levels of 'virtual heat'. In other words, whether the preference for dark objects was really a preference for a virtual cool spot. Experiments with varying stimulation light levels and tests with brightness-inverted virtual worlds substantiated the suspicion that the visual stimulus alone was able to activate HC (data not shown). Unintentional activation of HC by the visual stimulus would make it difficult to use HC activation as an aversive signal in an operant conditioning paradigm. In future experiments we will attempt to circumvent this issue by using a weaker opsin such as ChrimsonR (Klapoetke et al., 2014) and expressing it at lower levels.

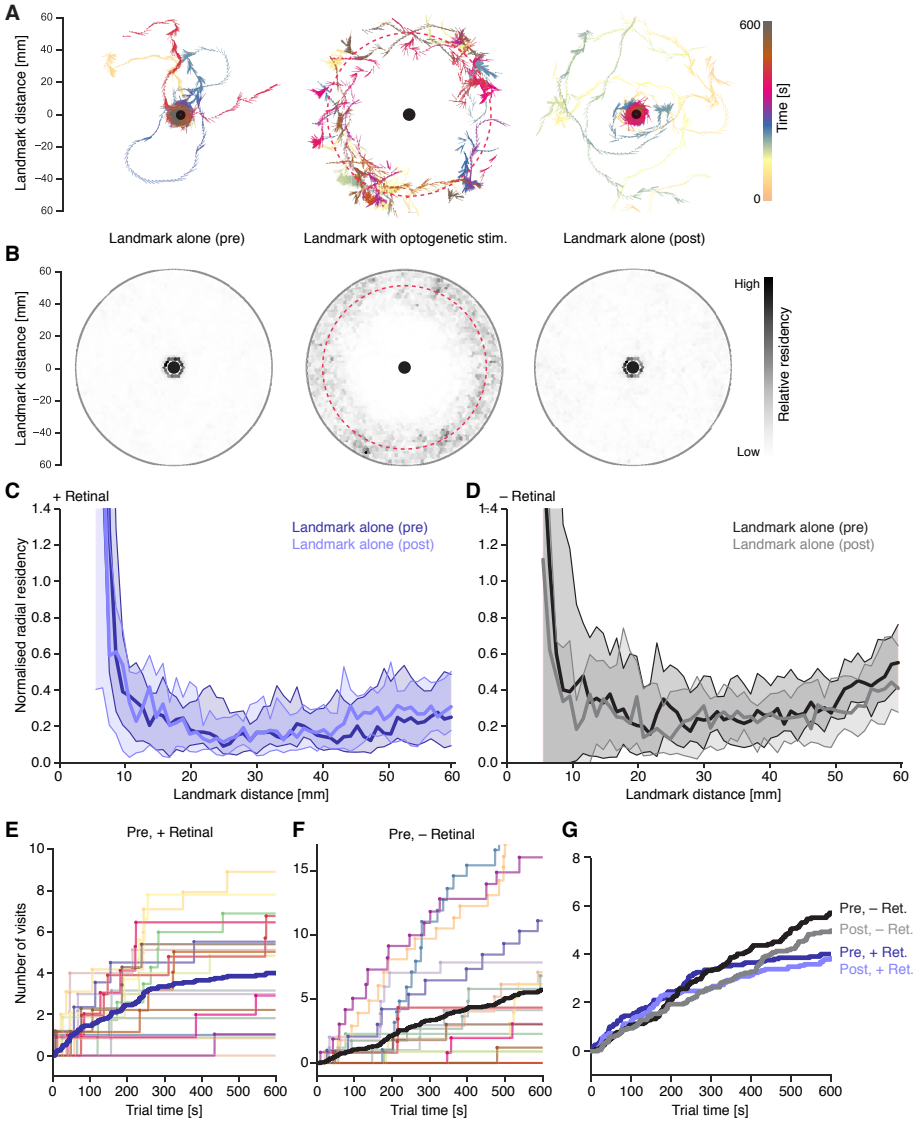

Figure 4.6: Evidence for unintentional activation of HC by the visual stimulus.
A: Example traces of a male 7d old retinal-fed fly during the three trials with visible landmarks: 'Landmark alone' (pre), 'Landmark with optogenetic stimulation' and 'Landmark alone' (post). Collapsed walking traces, indications of the landmark position and the optogenetic stimulation are visualised as in Figure 4.5 A. **B:** 2D residency histograms computed over the collapsed traces of n=20 retinal-fed flies for the three trials. The visualisation is analogous to Figure 4.5 B. **C, D:** Comparison of the radial residency in 'Landmark alone' trials before and after paired presentation of the landmark with 'virtual heat' in flies raised on food with retinal (**C**) and on standard food (**D**). The radial residency was computed as described in Figure 4.5. **E-G:** Cumulated number of visits to the landmark as a function of the trial time. A visit is defined as the fly approaching the landmark to within 20 mm radius. **E:** Number of visits of n=20 retinal-fed flies (thin coloured traces) and the mean number of visits (thick line) during the first 'Landmark alone' trial. **F:** Analogous visualisation to E for n=20 flies reared on standard food. Note that the y-axis has a different scale in E and F. **G:** Comparison of the average number of visits in the 'Landmark alone' trials in flies reared on food with retinal (blue traces, n=20) and on standard food (black and grey traces, n=20). All data shown in this figure comes from male HC-Gal4 > CsChrimson flies.

4.3.3. Avoidance of ascending aversive stimuli

Unintentional delivery of virtual aversive stimuli due to optogenetic activation of neurons by the visual stimulus seemed less likely with the second line we chose to investigate further after our pilot screen: SS01159. The split-GAL4 line SS01159, which induces an ascending aversive stimulus, only labelled central ascending neurons in the brain and VNC (***Figure 4.3 E***) and we therefore suspected that, compared to experiments with HC-GAL4, relatively higher light intensity levels would be necessary to elicit a behavioural response.

Avoidance of ascending aversive stimuli in freely walking flies

We began again by testing avoidance behaviour of SS01159 > CsChrimson flies in our optogenetic quadrant arena, using the same protocol as in experiments with HC-GAL4 > CsChrimson flies. We tested three levels of red light intensity corresponding to 1 %, 5 % and 10 % LED driver current. The corresponding light intensities in the illuminated quadrants were 0.27 mW/cm^2 (1 % level), 1.13 mW/cm^2 (5 % level) and 2.25 mW/cm^2 (10 % level).

At 5 % and 10 % light intensity level both male and female SS01159 > CsChrimson flies reliably avoided the illuminated quadrants and showed no adaptation over the course of the 4 min protocol (***Figure 4.7 A, B***). While at the 1 % level female flies seemed to show weak avoidance responses, we only found robust avoidance at higher light intensities in male flies (1.13 mW/cm^2 and higher, ***Figure 4.7 C, E***). Avoidance did not improve when the light was increased from 5 % to 10 %. SS01159 > CsChrimson flies reared on standard food without supplemented retinal, i.e. flies expressing reduced levels of functional CsChrimson or none at all, did not show avoidance responses to any of the tested light levels (***Figure 4.7 D, E***). This confirmed that the retinal-fed flies were indeed avoiding the optogenetically induced ascending aversive stimulus rather than the red light itself. Even at high stimulation intensity levels a minority of flies remained in the illuminated quadrants and as a result the avoidance response was less pronounced compared to the 'virtual heat' induced avoidance. One possibility is that SS01159 > CsChrimson flies were less successful at detecting the border between quadrants and initiating directed turns away from the illuminated quadrants. Indeed, visual inspection of individual trajectories suggested that flies were avoiding the illuminated quadrants with a combination of directed turns at the quadrant border, but also by increasing their walking speed after entering illuminated quadrants (***Figure 4.7 F***). Additionally some flies jumped when residing in the illuminated quadrant, consistent with SS01159-labelled neurons signalling an aversive, potentially nociceptive stimulus.

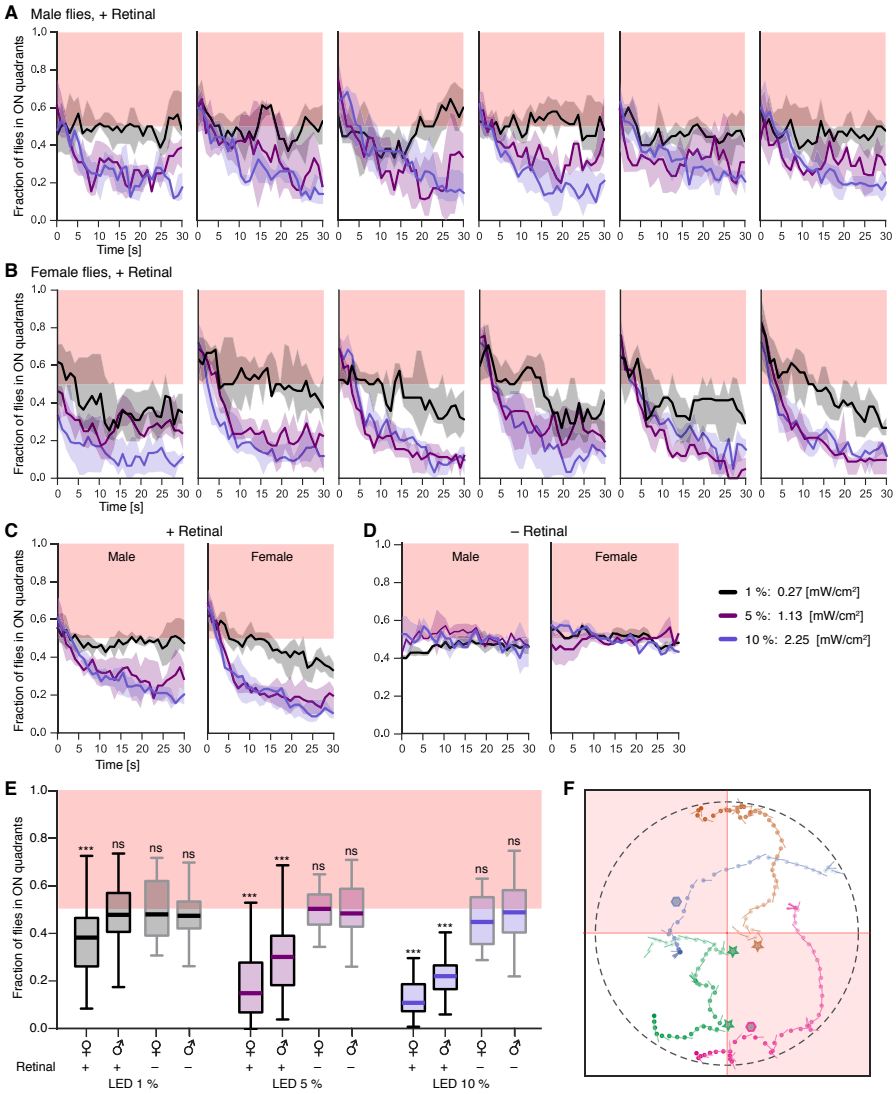

Figure 4.7: Avoidance of an ascending aversive stimulus generated through optogenetic activation of SS01159.

Preference test of freely walking flies in the optogenetic quadrant assay. Data from male and female flies expressing CsChrimson in ascending neurons labelled by the SS01159 split-GAL4 line. **A, B:** Median avoidance response over the time course of the 4 min long light stimulation protocol. Each line within one subplot shows the median and IQR of 6 repeats with different sets of flies (12-20 flies per repeat). Three levels of red light intensity were tested: 1 % (black, 0.27 mW/cm^2 in illuminated quadrants), 5 % (violet, 1.13 mW/cm^2 in illuminated quadrants) and 10 % (aubergine, 2.25 mW/cm^2 in illuminated quadrants). See legend of Figure 4.4 for a detailed explanation of the plot layout. **A:** Data from male, wing-clipped SS01159 > CsChrimson flies reared on retinal-supplemented food. The sample size for all three groups is n=6. **B:** Data from female, wing-clipped SS01159 > CsChrimson flies reared on retinal-supplemented food. The sample size for all three groups is n=6. **C:** Response for male and female wing-clipped SS01159 > CsChrimson flies reared on retinal-supplemented food averaged over the 6 sub-trials (median of sub-trials). **D:** Same as C for flies reared on standard Würzburg food, i.e. without additional retinal supply. The sample sizes for the male flies are n=4 repeats for 1 % and 5 % and n=5 repeats for 10 %. For female flies the sample sizes are n=2 repeats (1 %), n=4 repeats (5 %) and n=3 repeats (10%). **E:** Boxplot of the mean

response during the last 10 s of optogenetic stimulation. We tested whether the sample mean was different from 0.5 using two-sided t-tests. None of the groups reared on standard food showed significant avoidance to any of the tested stimulation light levels (female flies: p=0.8092 (1 %, n=12), p=0.7098 (5 %, n=24), p=0.0782 (10 %, n=18); male flies: p=0.1917 (1 %, n=24), p=0.8265 (5 %, n=24), p=0.4034 (10 %, n=30)). For female retinal-fed flies the t-test gave us a p<0.001 for 1% and p<0.0001 for both LED 5 % and 10 % (n=36, each). For male retinal-fed flies we got no significant shift from 0.5 with the 1% stimulation level, but significant shifts at 5 % and 10 % (both p<0.0001 and n=36). Significance codes: 0 ≤ '***' < 0.001 ≤ '**' < 0.01 ≤ '*' < 0.05 ≤ 'ns'. **F:** Example traces of 4 male, retinal-fed flies during the last 10 s of optogenetic stimulation at 10 % intensity level. The dashed grey line indicates the arena border and the red illuminated quadrants are marked with red-shaded boxes. Three examples for turns upon encounter with the border the illuminated quadrant are marked with stars. Two examples for acceleration after entering the illuminated quadrant are marked with hexagons.

The observation that SS01159 > CsChrimson flies show robust avoidance only at light intensity levels of 1.13 mW/cm^2 and higher whereas HC-GAL4 > CsChrimson flies showed robust avoidance already at 0.27 mW/cm^2 suggests that the low light intensities used in experiments with HC-GAL4 in VR were insufficient to activate the population of central neurons in the HC-GAL4 expression pattern. Furthermore, it is unlikely that the visual stimulus in the VR experiments would be sufficient to induce ascending aversive stimuli.

Landmark-assisted avoidance of ascending aversive stimuli in virtual reality

As with 'virtual heat' avoidance, we were wondering whether flies were able to use visual landmarks to improve the efficacy of their avoidance response. We therefore measured avoidance of ascending aversive stimuli in the presence and absence of visual cues in our 2D virtual reality in male SS01159 > CsChrimson flies. We used circular optogenetic stimulation zones placed around landmarks similar to the previously described 'virtual heat' zones, but we adjusted the radial size and maximum stimulation intensity based on our findings in freely walking flies.

In a first experiment in VR, we tested avoidance of virtual aversive zones with a 40 mm radius and a stimulation light intensity increasing from 0.00 mW/cm^2 at the edge to 0.58 mW/cm^2 in the centre (50 % LED input current in VR). The maximum intensity of 0.58 mW/cm^2 lies between the reliably effective stimulation intensity of 5 % (1.13 mW/cm^2) and the insufficient stimulation intensity of 1 % (0.27 mW/cm^2) measured in freely walking flies. Individual flies clearly avoided the ascending aversive areas both in presence and absence of visual cues. (***Figure 4.8 A, B***). As previously observed with 'virtual heat' this behaviour was highly consistent across the sample of 20 measured flies (***Figure 4.8 C, D***). In contrast to 'virtual heat', however,

flies seemed to avoid ascending aversive stimuli at lower stimulation intensities when landmark cues were present compared to when they were absent (***Figure 4.8 A-D***). The effect of visual landmarks on avoidance of the ascending aversive stimulus was particularly noticeable when we compared the radial residency across the two trials with optogenetic stimulation (***Figure 4.8 F***). In the absence of visual landmarks flies reliably avoided ascending aversive stimulation at intensities of about 0.14 mW/cm^2 (12 % LED current). In contrast, in trials with landmark cues the radial residency began to decrease well outside of the stimulation zone.

To probe whether the avoidance response depended on the stimulation intensity or relative change thereof, we tested two other stimulation profiles with varying gradients of steepness. The zone described above corresponded to an intermediate stimulation gradient with a 1.25 %/mm increase ('Medium', ***Figure 4.8 F***). We also tested a steep gradient with 2 %/mm increase in intensity ('Steep', ***Figure 4.8 E***), and a shallow gradient with 0.75 %/mm increase ('Shallow', ***Figure 4.8 G***). The steepness of the gradient was adjusted by changing the size and the maximum intensity of the zone; hence the range of values that the flies were exposed to differed between conditions too.

Under all three conditions flies spent less time in the optogenetic stimulation zone when it was paired with a visual landmark (***Figure 4.8 E-G***). However, the strength of the effect of the visual landmark depended on the spatial intensity profile of the optogenetic stimulus. When ascending aversive stimulation increased steeply as a function of landmark distance, the avoidance response was only weakly modulated by the presence of visual cues (***Figure 4.8 E***). Providing a visual guidance cue had the biggest effect when we used an intermediate gradient steepness (***Figure 4.8 F***): in the presence of the visual cue, flies avoided even the low-intensity edge of the optogenetic stimulation zone, whereas in the absence of landmark cues flies only avoided the higher intensity central areas of the zone. Under the latter condition, flies spent more time along the edge of the stimulation zone, possibly due to increased turning (***Figure 4.8 B***). The avoidance of the 'Shallow' gradient zone was less pronounced, possibly due to overall lower stimulation intensity levels, but we found similar trends in the radial residency as in the 'Medium' gradient condition (***Figure 4.8 G***). We also measured the responses of flies of the same genotype that were reared on standard food without additional retinal in the 'Medium' gradient (***Figure 4.8 H***). Standard Würzburg food contains small amounts of retinal. Thus, also flies reared on standard Würzburg food had limited access to retinal and may have been able to express functional CsChrimson at very low levels. Accordingly, they showed weak avoidance of the optogenetic stimulation zone, although the avoidance was much weaker compared to the

corresponding group of retinal-fed flies, confirming that the observed avoidance responses cannot be fully explained by direct responses to the red light. Interestingly, we only saw an avoidance response in non-retinal-fed flies when the ascending aversive stimulation was paired with a visible landmark cue. A possible explanation is that visual landmarks aid the avoidance response if the spatial avoidance task is relatively difficult, for example, when the stimulus is weak or the gradual increase in stimulus intensity is small.

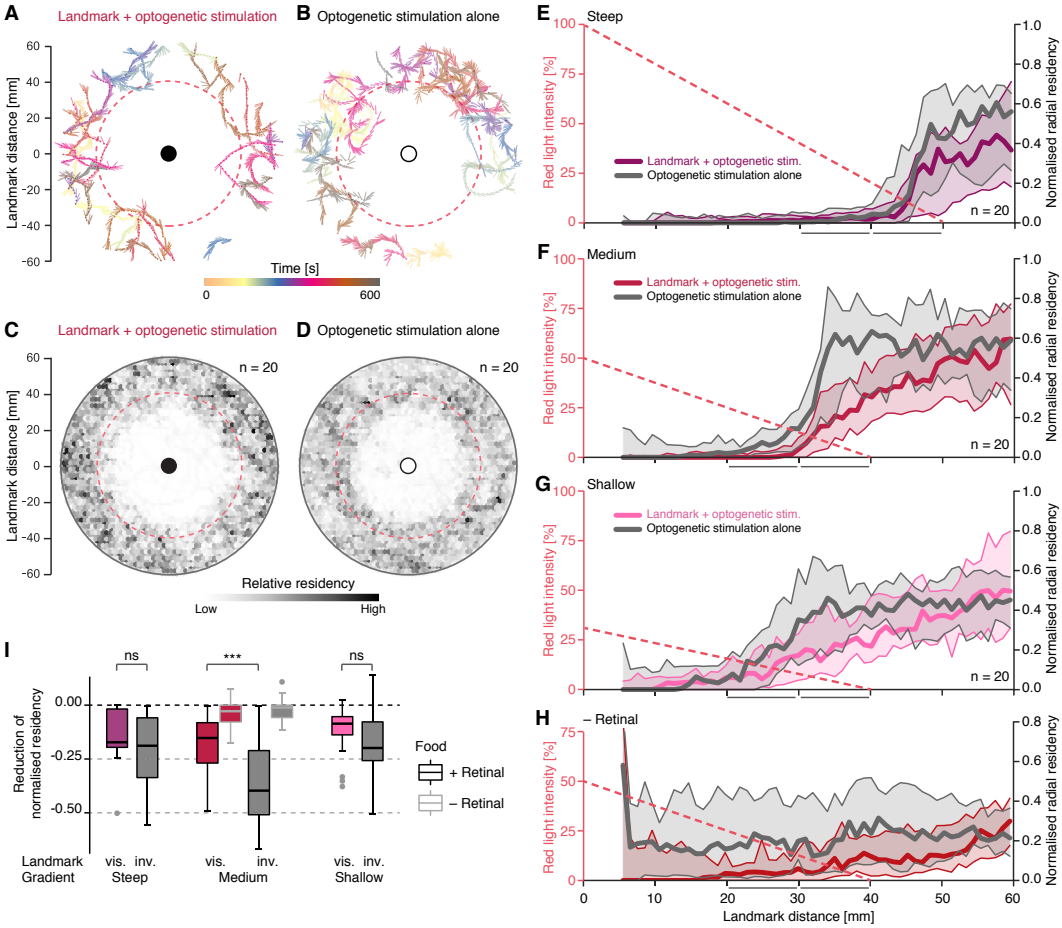

Figure 4.8: Landmark-assisted avoidance of ascending aversive stimuli in virtual reality. **A, B:** Example trace of a male 9d old fly during a 600 s long trial in a virtual world with spatially restricted ascending aversive stimulation paired with visible (**A**, 'Landmark with optogenetic stimulation') and invisible (**B**, 'Optogenetic stimulation alone') landmarks. The fly's trajectory, the landmark position and the optogenetic stimulation are visualised as in Figure 4.5 A. **C, D:** 2D residency histograms computed over the collapsed traces of n=20 retinal-fed flies for the two trials with optogenetic stimulation. Visualisation analogous to Figure 4.5 B. **E-G:** Comparison of the normalised radial residency in trials with optogenetic stimulation. Visualisation analogous to Figure 4.5 C, D. Avoidance behaviour of three types of optogenetic stimulation zones differing in size and steepness of the intensity gradient: 'Steep' (**E**), 'Medium' (**F**) and 'Shallow' (**G**). In addition, flies reared on standard food without additional retinal (-Retinal) were tested on a 'Medium' gradient (**H**). **I:** Boxplot of the reduction in normalised radial residency

over the outermost 20 mm ring of the stimulation zone. It is computed per fly as the difference between the median normalised radial residency inside the outermost 10 mm ring (lower stimulation intensities) of the stimulation zone compared to the second outermost 10 mm ring (higher stimulation intensities). This corresponds to the landmark distance 40-50 mm and 30-40 mm in E and 30-40 mm and 20-30 mm in F, G and H indicated by grey bars on the x-axis. No reduction means that flies spent equal amounts of time in the low and higher intensity regions. Negative values indicate that flies spent more time at the low compared to the higher intensity region. An ANOVA of the measured relative change in residency showed that there was a significant effect of both, the optogenetic stimulation zone profile ($F(2,114)=6.936$, $p=0.0014$) and the presence of a visible landmark ($F(1,114)=13.569$, $p=0.0004$). We did not find a significant interaction between the two factors ($F(2,114)=1.472$, $p=0.2338$). We also tested directly whether the 'Landmark with optogenetic stimulation' and the 'Optogenetic stimulation alone' trials were different under the three stimulus profile conditions using paired Wilcoxon singed rank tests. Steep gradient: $V=47$, $p=0.0979$. Medium gradient: $V=16$, $p=0.0003$. Shallow gradient: $V=66$, $p=0.2514$. The sample size for all four groups ('Steep', 'Medium', 'Shallow' and 'Medium, no retinal') was n=20. All data in this figure stems from male SS01159 > CsChrimson flies.

We quantified the difference in avoidance in the four conditions by computing the average reduction in normalised radial residency across the outermost 20 mm of the stimulation zone (***Figure 4.8 I***). The average reduction was computed as the difference between the average residency inside the outermost 10 mm ring (lower stimulation intensities) compared to the second outermost 10 mm ring (higher stimulation intensities). Non-retinal-fed flies (-Retinal group, boxes with grey edges, ***Figure 4.8 I***) showed no reduction indicating that those flies spend approximately equal amounts of time in the low and higher intensity range of the 'Medium' gradient. All retinal-fed flies spent less time at the higher intensity zones (negative values of black-lined boxes of + Retinal groups, ***Figure 4.8 I***). In a direct comparison of the 'Landmark with optogenetic stimulation' and the 'Optogenetic stimulation' trial we found a significant difference only in the 'Medium' shallow gradient ($p<0.001$, ***Figure 4.8 I***). Yet, an ANOVA revealed that the reduction in radial residency was generally larger in the absence of visual landmarks ($p < 0.001$, ***Figure 4.8 I***), most likely because the presence of a visual cue made flies avoid the zone at even lower stimulation or stopped them from even entering it.

Landmark-assisted avoidance is mediated by changes in the turning behaviour

To get a better understanding of how flies responded to the ascending aversive stimulus we compared walking behaviour inside and outside the stimulation zone in trials with and without the visual landmark cue (***Figure 4.9***). While the translational walking velocity was neither strongly affected by the ascending aversive stimulation nor by the presence of visible landmarks (***Figure 4.9 A***), the turning behaviour was affected by both factors. Flies walked with significantly larger rotational velocity inside compared to outside of the optogenetic stimulation

zones (p<0.0001, ***Figure 4.9 B***) and the rotational velocity was consistently larger in trials without landmarks (p<0.05, ***Figure 4.9 B***). We also quantified the number of turns, defined as peaks in the rotational velocity signal larger than twice the standard deviation. Likely due to the reduced residency inside the optogenetic stimulation zone, flies made significantly more turns outside compared to inside the zones (p<0.001, ***Figure 4.9 C***). In addition, the turn frequency was affected by the presence of landmark cues, with significantly fewer turns in trials with landmarks (p<0.001, ***Figure 4.9 C***).

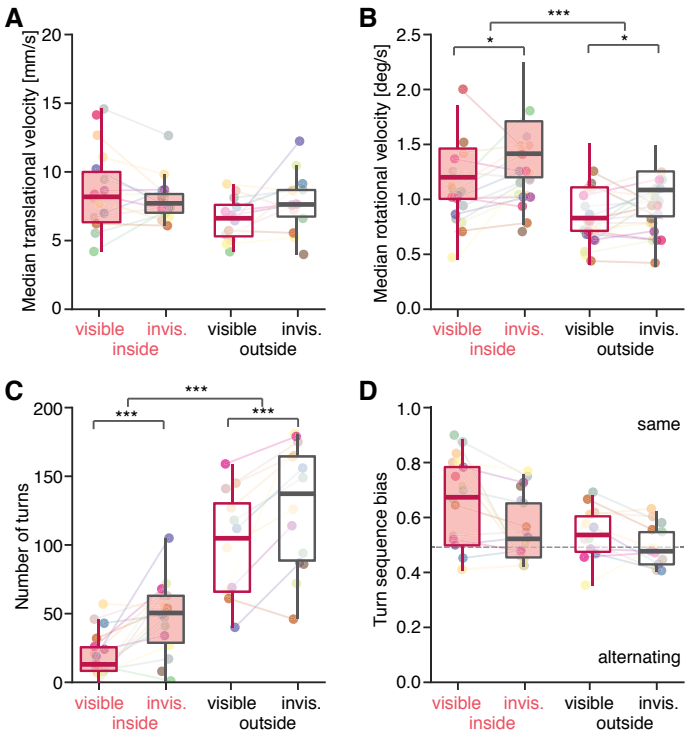

Figure 4.9: **The presence of a visual landmark affects turning behaviour during avoidance of ascending aversive stimuli.**
A comparison of the walking behaviour inside and outside of the optogenetic stimulation zone in the presence and absence of visual cues. For each walking parameter the corresponding value was computed per fly (shown as dots, corresponding values are connected by a line). Boxplots indicating the median and the interquartile range are overlaid. For each of the walking parameter we also performed an ANOVA with the presence of landmark cues (visible vs. invisible) and the location (inside vs. outside) as well as the fly identity as explanatory variables. Significant effects are indicated in the figure. **A:** Median translational velocity. In the ANOVA only the fly identity had a significant effect ($F(18,40)=5.615$, $p=2.86e-06$). **B:** Median absolute rotational velocity while the fly was moving with translational velocity > 2mm/s. The ANOVA indicated a significant effect of the location ($F(1,54)=41.592$ $p=3.22e-08$) and the visibility of the landmark ($F(1,54)=5.911$, $p=0.0184$) as well as of the fly identity ($F(19,54)=4.029$ $p=2.86e-05$). **C:** Total number of turns detected as events with rotational velocity > 2*standard deviation. The ANOVA identified a significant effect of location ($F(1,40)=131.785$, $p=3.12e-14$) and visibility of the landmark ($F(1,40)=14.358$, $p=0.0005$) and again a weak effect of the fly identity ($F(18,40)=2.023$, $p=0.0319$). **D:**

Turn sequence bias computed as the ratio of two subsequent turns in the same direction over the total number of turns - 1. The ANOVA detected only a significant effect of fly identity ($F(18,39)=1.951$ $p=0.0403$). All data shown in this figure came from male SS01159 > CsChrimson flies.

We next asked whether, in the presence of visual landmark cues, flies performed fewer turns to avoid the ascending aversive stimulus because individual turns were more effective. One simple strategy to avoid the optogenetic stimulation zone would be to keep turning in the same direction until the stimulus intensity decreases. To test whether flies used this strategy, we computed the turn sequence bias as the number of times a fly made two subsequent turns in the same direction divided by the total number of turns minus one. A turn bias index above 0.5 indicates a preference for turns in the same direction and values below 0.5 a preference for alternating turn direction. Although we did not find any significant effects, there seemed to be a trend with larger turn biases inside the optogenetic stimulation zone and in the presence of a visual landmark (***Figure 4.9 D***). Further analysis of the turn behaviour may reveal whether flies use the visual landmark to make more directed turns away from the increasing intensity of the ascending aversive stimulus.

Potential evidence for visual aversive conditioning with ascending aversive stimulation

After the fly had experienced the paired presentation of the landmark with ascending aversive stimulation we occasionally found a strong reduction of residency close to the landmark in the absence of virtual aversive stimulation (compare 'Landmark alone' (pre) and 'Landmark alone' (post) trials in ***Figure 4.10 A, D***). The effect appeared to be less pronounced in trials with flies reared on food without additional retinal (***Figure 4.10 B***). This looked promising and we therefore investigated this data set more closely in search of evidence for aversive conditioning.

Examination of individual traces revealed large variability in walking behaviour over the course of the three trials with visible landmarks. Representative traces from three flies are shown in ***Figure 4.10 C***. The walking speed, and correspondingly the amount to which flies explored the virtual world, varied not only between flies but also between trials. This raised the question of whether the reduced residency close to the landmarks after paired presentation with ascending aversive stimulation could simply be explained by a general reduction in walking speed rather than by active, conditioned avoidance behaviour. Fly 1 in ***Figure 4.10 C***, for example, frequently visited the object in the first trial, made repeated contacts with the optogenetic stimulation zone in the second trial and then barely walked in the third trial. It is possible that the lack of landmark approaches in the third trial was a secondary effect of the reduction in walking speed. Furthermore, it is unclear whether this reduction in walking speed is a specific response to the

paired presentation of the aversive stimulation with the landmark or an unspecific response to experiencing the ascending aversive stimulus. Other flies showed what looked like active avoidance of the landmark in the third trial (Fly 2 in ***Figure 4.10 C***) and still other flies did not visit the landmark much in the first trial (Fly 3 ***Figure 4.10 C***) or did not make much contact with the optogenetic stimulation zone in the second trial. The variability in the innate walking behaviour led to different experiences over the course of the three trials and, unsurprisingly, large variance in the landmark tracking behaviour in the 'post' trial, which makes it difficult to draw conclusions from the present data set.

To check whether the reduction in residency was specific to conditions where we expected flies to learn to avoid the landmarks we compared the residency close to the landmark in five experimental groups (relative residency within a 20 mm radius around landmarks, ***Figure 4.10 E***): four groups of retinal-fed flies exposed to virtual environments with varying optogenetic stimulation zones and one control group of flies reared on standard food. An ANOVA showed that across groups, flies on average spent more time close to the landmark in the first 'Landmark alone' trial compared to the second one ($p<0.05$, ***Figure 4.10 E***). However, the variation between two data sets from retinal-fed flies measured under the same experimental conditions two months apart ('Medium, set 1' and 'Medium, set 2') was comparable to the variance between groups of flies measured under differing experimental conditions. Correspondingly, the ANOVA did not detect a significant effect of the stimulation conditions on the relative residency close to the landmark (***Figure 4.10 E***). We also could not find any differences between groups when we looked at the pattern of visits to the landmarks in the first and second 'Landmark alone' trials (***Figure 4.10 F, G***). In accordance with the reduced residency close to the landmark, flies generally also made fewer visits to the landmark in the second trial. Even though the residency close to landmarks was reduced in all experimental groups, we cannot exclude the hypothesis that experiencing the paired ascending aversive stimulation causes the relative avoidance of landmarks in the post 'Landmark alone' trial in all experimental groups. That is, because we did see a reduced level of residency inside the optogenetic stimulation zone in the presence of visible landmarks in our only control group — flies reared on standard food ('Landmark with optogenetic stimulation' trial in ***Figure 4.10 E***) — suggesting that these flies too received at least mild levels of ascending aversive stimulation. To more rigorously test whether the reduction in residency close to the landmark in the second 'Landmark alone' trial is an unspecific effect of the paradigm rather than a signature of aversive conditioning we will need to perform control experiments where flies receive spatially uncorrelated ascending aversive stimulation.

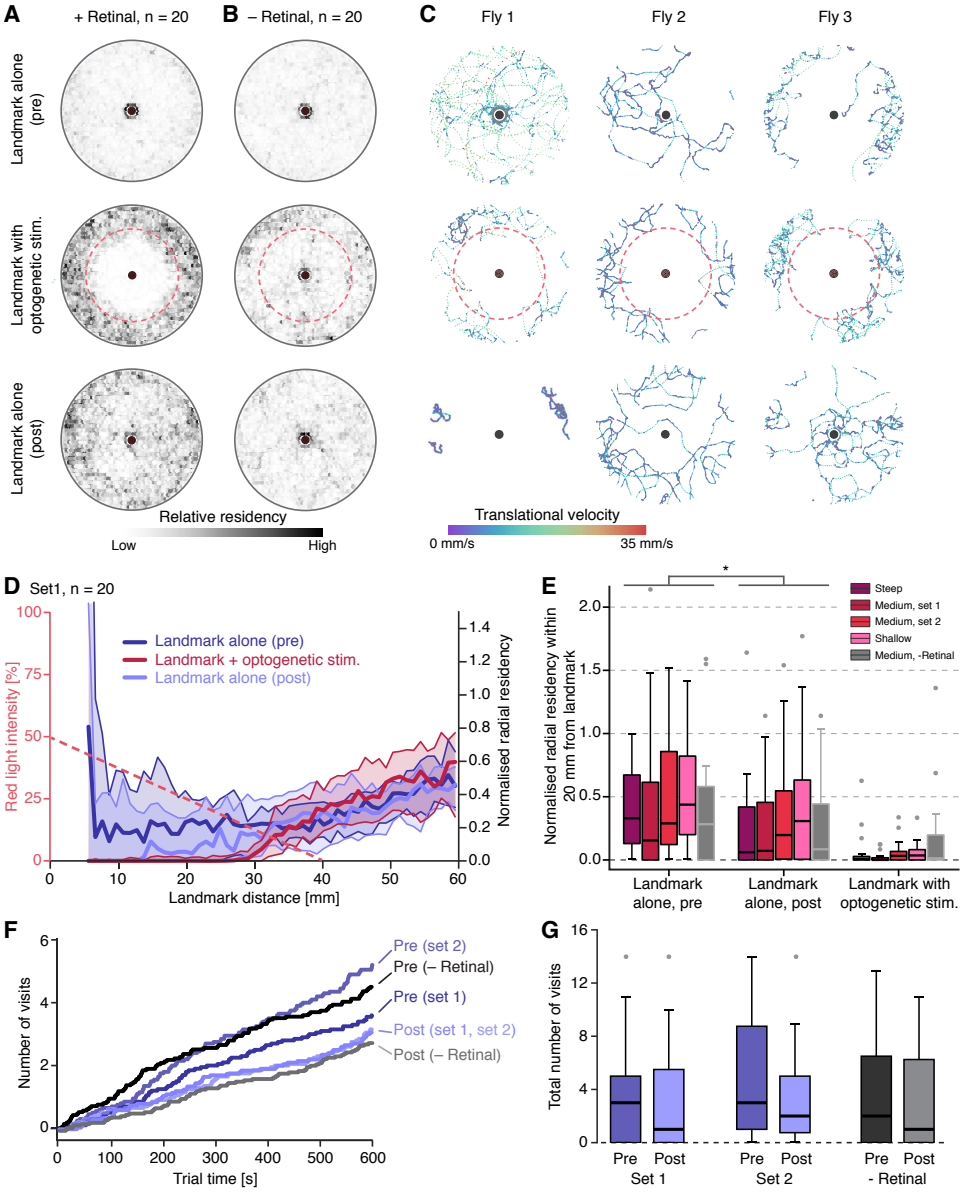

Figure 4.10: Reduction of landmark visit frequency after experience of paired ascending aversive stimulation.

A, B: 2D residency histograms computed over the collapsed traces of flies for the three trials with visible landmarks: 'Landmark alone' (pre), 'Landmark with optogenetic stimulation' and 'Landmark alone' (post). Visualisation is analogous to Figure 4.5 B. **A:** Retinal-fed flies, n=20. **B:** Control flies reared on standard food, n=20. **C:** Example traces from three flies from the same data set as shown in A (set 1) for the three trials with visible landmarks. The reinforcement zone and the landmark position are indicated as in Figure 4.5 A. The fly trajectories are colour-coded according to the translational velocity. **D:** Comparison of the radial residency in trials with visible landmark in flies raised on food with retinal. The radial residency was computed as described in Figure 4.5. Same data set from n=20 flies as shown in A (set 1). **E:** Comparison of the normalised radial residency within a 20 mm radius around the landmark in 5 data sets (n=20 each). Data from the three trials with visible landmarks are shown. The data sets are measurements in the steep stimulation gradient ('Steep'), two data sets with

retinal-fed flies collected in the medium steep gradient condition separated by two months ('Medium, set 1' and 'Medium, set 2'), measurements in the shallow gradient ('Shallow') and a data set from flies reared on standard food in the medium gradient ('Medium, -Retinal'). We performed an ANOVA of the normalised radial residency within a 20 mm radius around the landmarks on the two 'Landmark alone' trials using the trial (pre vs. post), the food, the experimental group ('Steep', 'Medium' set 1, 'Medium' set 2, 'Shallow', 'Medium, -Retinal') and the individual animals as explanatory variables. Only the trial ($F(1,152)=5.492$, $p<0.05$) and the animal identity ($F(38,152)=1.768$, $p<0.01$) had significant effects on the variance. **F:** Comparison of the cumulated number of visits to the landmark as a function of the trial time. A visit is defined as the fly approaching the landmark to within 20 mm radius. Pre and post 'Landmark alone' trials from set 1 and set 2 as well as from the -Retinal control group are shown. The sample sizes for all groups and trials are n=20. **G:** Boxplots of the total number of visits in pre and post 'Landmark alone' trials from set 1 and set 2 as well as from the -Retinal control group (corresponding to data shown in F). All data shown in this figure came from male SS01159 > CsChrimson flies.

4.4. Discussion

Here we present a new assay for studying visual guidance in a virtual environment in head-fixed walking Drosophila. With experiments in freely and tethered walking flies, we demonstrated that flies robustly avoid areas where they receive virtual aversive stimuli generated by optogenetic activation of small, genetically defined neuron populations. Specifically, we demonstrated avoidance behaviour in response to 'virtual heat' generated by activating HC-neurons and ascending aversive stimuli generated by optogenetically activating a small set of ascending neurons labelled by the split-GAL4 line SS00159. We then showed that under some conditions tethered walking flies in VR more effectively avoided areas with ascending aversive stimulation in the presence of visual landmark cues. We also found that SS00159 > CsChrimson flies visited landmarks less after experiencing paired ascending aversive stimulation around the landmarks. Since this effect was independent of the stimulation intensity, this could be an unspecific change in locomotion rather than a learned shift in landmark preference based on associating the landmark with the aversive stimulus.

We will first discuss in more detail advantages and challenges of using optogenetic stimulation as a substitute for real stimuli. Then we will discuss our main findings, effective avoidance of virtual aversive stimuli and evidence for landmark-assisted avoidance, before exploring possible future directions toward conditioning landmark preferences in VR.

Activating neurons using optogenetic tools

Optogenetic stimulation allows selective and temporally precise activation of neurons and relatively easy to use, which has made optogenetic tools popular in systems neuroscience in recent years (Fenno et al., 2011). Here we used CsChrimson, a red-shifted variant of channelrhodopsin (Klapoetke et al., 2014). CsChrimson and related channels are light-gated cation channels. Upon absorption of red light the CsChrimson channels open and the neuron expressing these channels is depolarised (Fenno et al., 2011). Two common complications with using the blue-light activated opsin channelrhodopsin in behavioural studies in flies are (a) that the animal can see and potentially responds to the stimulation light, leading to behavioural artefacts and (b) that blue light does not effectively penetrate through the cuticle, which means that high light intensities are necessary to generate behavioural effects (Klapoetke et al., 2014). The red-shifted absorption profile of CsChrimson has the advantage that one can use red light, to which fly eyes are relatively insensitive and which is more effective than blue light in penetrating the cuticle. This makes CsChrimson a convenient choice for behavioural experiments in intact flies.

A major challenge when using optogenetic stimulation compared to, for example, direct electrical stimulation lies in relating stimulation light intensities to actual neural activation. Given a certain stimulation light intensity the induced depolarisation of the neuron expressing the opsin heavily depends on the cell's membrane properties (Lin, 2011). The efficacy of the light-induced depolarisation depends on the membrane capacity and the reversal potential of cations that can enter the cell through the light-gated channel. Also the expression level of the opsin influences how light intensity links to activity of the genetically targeted cell. For example, the strength of the promotor under which CsChrimson is expressed in a given cell type affects how much protein is produced, which limits the maximal cation influx upon light-induced opening of CsChrimson channels. Thus, different cell types are likely to require different levels of light-induced depolarisation to induce spiking.

An additional complication is that the relationship between stimulation light intensity and neuronal activity — especially spike rate — is not necessarily linear. For example, it has been shown that stimulating neurons expressing channelrhodopsin-2 (ChR2) with high light intensity and for extended time periods can lead to a so-called depolarisation block (Herman et al., 2014). A depolarisation block can be induced by a large cation influx and results in the cell's failure to produce action potentials. Thus a depolarisation block can render optogenetically activated neurons functionally silenced. This is particularly problematic when optogenetic

activation us used in purely behavioural studies like ours when neuronal activity cannot be monitored during the optogenetic activation experiment.

Using optogenetic tools to generate virtual sensory stimuli

In fruit flies we can exploit relatively detailed knowledge of sensory systems and genetic access to sensory neurons to generate virtual stimuli by optogenetically activating genetically defined neurons (Aso et al., 2014b; Claridge-Chang et al., 2009). A number studies have used optogenetic activation of sensory neurons to generate highly controlled 'virtual sensory' stimuli: Bell and Wilson (2016) used 'virtual olfactory' stimuli in a study of the fly olfactory system, Lin et al. (2013) induced avoidance in adult flies by activating neurons involved in sensing CO_2 and Klein et al. (2015) characterised thermotaxis behaviour using optogenetic activation of thermosensory neurons in *Drosophila* larvae.

Using optogenetically generated virtual stimuli has several advantages with regard to experimental design. One can target a genetically defined subset of neurons, which can help tracing out circuits involved in a specific navigational task. Additionally, optogenetic activation allows delivery of strongly aversive stimuli without damaging the animal to the same degree as for example real high heat would. Similarly, we may be able to deliver appetitive stimuli related to sugar ingestion without satiating the fly and thereby altering its motivational state. The latter could potentially be very useful for designing appetitive visual conditioning paradigms. Moreover, by using virtual rather than real sensory stimuli the experimenter can flexibly pair different sensory modalities with our visual VR without having to make any modification in the hardware and software. Thus, our assay provides a time-efficient method for testing how various sensory signals are integrated with visual information and whether any of these stimuli can act as reinforcement in a visual conditioning paradigm. The same approach has been used to identify neural correlates of reward and punishment signals in the context of fly olfactory conditioning (Aso and Rubin, 2016; Aso et al., 2014b).

A difficulty with optogenetic activation experiments in general is the design of a suitable activation protocol for a given neuronal cell type and research question. If the firing pattern of the targeted neuronal cell type to its natural stimulus is known, one can calibrate light intensities for optogenetic activation by testing different light stimulation protocols and simultaneously monitoring the neurons firing rate using electrophysiological methods (Bell and Wilson, 2016). However, often the natural activity patterns of the neurons to be activated are unknown or may be hard to measure and electrophysiological recordings are challenging,

especially in small fly neurons. Therefore a second approach is to calibrate the activation protocol using a behavioural readout, as we did in this study. We calibrated the stimulation light intensity as well as the temporal protocol the avoidance of areas where flies received optogenetic stimulation as our behavioural readout. This approach, of course, is no substitute for post-hoc characterisation of the activity patterns of the respective neurons in response to 'natural' stimuli. In the future we would like to test, for example, whether neurons labelled by the SS01145 split-GAL4 line indeed respond to nociceptive stimuli such as high heat or electric shock. A second limitation of using virtual stimuli is that stimuli generated by optogenetically activating small sets of genetically defined sensory neurons may never occur in isolation. That is, environmental stimuli can often activate a range of sensory neurons and only together the corresponding neural signals form a realistic sensory percept. High levels of environmental heat, for example, should simultaneously be sensed by various thermosensors distributed across the body and may additionally recruit nociceptors (Barbagallo and Garrity, 2015). It is possible that some virtual stimuli do not have the potency to elicit behaviours that are associated with the natural activation of the respective sensory neurons and they may not generate potent reinforcement signals.

Potential crosstalk between the visual stimulus and optogenetic stimulation

Some of our results suggested that in experiments with 'virtual heat' stimulation the visual stimulus light was interfering with the optogenetic stimulation resulting in unintentional activation of heat sensing neurons. Such crosstalk between the visual stimulus and the optogenetically induced virtual aversive stimulus drastically limits the conclusiveness of behavioural experiments. In our experiments the evidence for crosstalk came from comparing behaviour of flies expressing high levels of CsChrimson (+ retinal group) with those not or barely expressing CsChrimson (- Retinal group) in the 'Landmark only' trials with no intended 'virtual heat' stimulation. If the visual stimulus was not able to activate the CsChrimson expressing HC neurons, we would expect to see no difference between the two experimental groups. However, we found that flies expressing high levels of functional CsChrimson showed a stronger attraction to the landmarks compared to flies of the same genotype reared on food without additional retinal. A second line of evidence for crosstalk came from behavioural experiments in virtual worlds with inverted contrast polarity. Here retinal-fed HC > CsChrimson flies avoided the bright landmarks, consistent with activation of HC by the bright visual stimulus close to virtual landmarks.

Generally, the following factors contribute to generating crosstalk between the visual display and the optogenetic stimulation. Firstly, using a visual stimulus with a wavelength within the absorption spectrum of the genetically expressed opsin. CsChrimson has a broad absorption spectrum that extends well into the wavelength spectrum of our visual stimulus (400-500 nm), and thus it is plausible that light from the visual display was able to activate CsChrimson expressing neurons (Klapoetke et al., 2014). Secondly, crosstalk was facilitated by the high light sensitivity of CsChrimson, i.e. that it only requires low light levels to be activated (Klapoetke et al., 2014). Finally, unintentional activation of peripheral neurons by the blue visual stimulus is much more likely than activation of central neurons, because tissue scatters blue light more than red light and thus higher intensities of blue light are required to activate centrally located neurons (Klapoetke et al., 2014).

To avoid unintentional activation of peripheral neurons by the visual stimulus in future experiments one may try expressing a less sensitive opsin such as ChrimsonR (Klapoetke et al., 2014) at lower levels. Further, if possible, one should try to use a visual stimulus of a wavelength that is unlikely to activate the opsin used for optogenetic activation of neurons. Simple behavioural tests, such as the trials with inverted contrast polarity mentioned above, can help to identify if crosstalk is happening.

Implications of landmark-assisted avoidance

We investigated the effect of visual landmark guidance cues on avoidance of two types of virtual aversive stimuli in VR. Under some conditions SS00159 > CsChrimson flies were able to more effectively avoid the ascending aversive stimuli when visual landmark cues were present, a behaviour we refer to as landmark-assisted avoidance. The effect of visual landmarks on avoidance was more pronounced in shallow compared to steep gradients. One interpretation is that, if avoidance is easy, non-visual cues are sufficient to drive effective avoidance manoeuvres. Avoidance may be easier when the border of the reinforcement zone is clearly defined such as in the free walking quadrant assay and in steep gradients in VR. Furthermore, the difficulty of generating directed avoidance manoeuvres might vary with the sensory modality, which might be one reason why we did not see clear evidence for landmark-assisted avoidance of ‘virtual heat’. However, for reasons detailed above the experiments with ‘virtual heat’ are hard to interpret. We can therefore not rule out that under certain conditions flies to use visual landmarks to avoid heat stimuli. It is possible that we would find evidence of landmark-assisted avoidance of ‘virtual heat’ in our paradigm if crosstalk with the visual stimulus was eliminated and the ‘virtual heat’ stimulation intensity lowered further.

Our finding of landmark-assisted avoidance in SS00159 > CsChrimson flies suggest that visual and ascending aversive stimuli are integrated. A finer analysis of the steering manoeuvres that contribute to avoidance of ascending aversive stimuli across the different experimental conditions may help us gain a better understanding of the contribution of the visual stimulus. One important open question concerns whether avoidance responses are directed in the presence of landmarks while being undirected without visual cues. We may be able to quantify this by analysing whether flies systematically turn toward lower ascending aversive stimulus intensities after saccades and whether the size of the saccade is adjusted according to relative heading to the ascending aversive stimulus gradient (van Breugel and Dickinson, 2012). In trials with landmarks, turns toward lower virtual aversive stimulation coincide with turns away from the landmark and it therefore may be easier for the fly to generate a directed avoidance response based on the visual cue rather than on temporal integration of the virtual aversive stimulus alone. The use of multisensory integration for better avoidance performance is reminiscent of reports about improved auditory or olfactory tracking performance in crickets and flies in the presence of visual cues (Duistermars and Frye, 2008; von Helversen and Wendler, 2000).

Flies may be able to generate directed avoidance responses to a virtual aversive stimulus alone, for example by integrating information across sensors along its body. Directed escape manoeuvres from mechanosensory and visual stimuli have been characterised in a range of insects (Card and Dickinson, 2008; Ramdya et al., 2014; Santer et al., 2005). In our VR paradigm, however, we did not provide instantaneous directional information about the spatial geometry of the virtual aversive stimulation zones. We were therefore surprised by the remarkably effective avoidance of 'virtual heat' also in the absence of visual landmark cues. It is possible that there was an unintentional asymmetry in the delivery of the optogenetic stimulation light. In case of the 'virtual heat' stimulation, for example, one antenna could have received slightly higher light intensities, which could have resulted in increased turn rates inside the 'virtual heat' zones and consequently effective avoidance of these zones. An other, more exciting possibility would be that flies are able to temporally integrate heat stimuli. Further analysis of the data presented here may shed light on the nature of the observed avoidance responses. We can then ask questions about the neural processing underlying the computations that need to be carried out to support the generation of directed avoidance manoeuvres — either based on temporal or multisensory integration.

What is known about convergence of visual information with temperature and nociceptive signals on the circuit level?

In insects a conserved neuropil located in the centre of the brain, the central complex (CX) receives sensory input from a range of modalities (Pfeiffer and Homberg, 2014) and has been implicated in higher order motor control (Pfeiffer and Homberg, 2014; Strauss, 2002; Strauss and Heisenberg, 1993). In particular, the observation that the CX receives visual feature information (Seelig and Jayaraman, 2013) and is necessary for short-term landmark orientation memory in flies (Neuser et al., 2008), suggests that this brain region may be involved in generating steering manoeuvres during landmark-assisted avoidance. It has yet not been explicitly shown that the CX also receives information about temperature or pain stimuli, but several visual conditioning paradigms that use heat as reinforcement signal require neural processing in the CX (Liu et al., 2006; Ofstad et al., 2011; Wang et al., 2008). Thus, the CX may be a good candidate region to look for convergence of visual information and temperature or nociceptive stimuli and it may be involved in generating directed avoidance manoeuvres.

Toward visual conditioning of landmark preferences

Landmark-guided navigation, which often involves selective approach of a certain visual landmark, has been extensively studied on a behavioural level (Collett and Collett, 2002; Collett and Graham, 2004), yet we still know little about the underlying neural processing. In fruit flies a variety of genetic and physiological tools are available to dissect neural circuits and the computations they perform, but no complex naïve landmark-guided navigation behaviours — comparable to those observed in foraging ants and bees (Bisch-Knaden and Wehner, 2003; Collett et al., 2002) — have been characterised. Rather, flies exhibit a number of simple landmark-interaction behaviours such as landmark fixation and tracking in walking and flight (Robie et al., 2010; van Breugel and Dickinson, 2012). Incidentally, the fact that flies have two distinct modes of movement may help to separate abstract and closely motor-related correlates of course control. The ability to train flies to perform specific tasks that require the use of visual landmarks as guidance cues would open up new paths for studying the neural basis for landmarks-guided goal-directed navigation.

Here we presented a highly flexible new VR system for studying visually guided navigation in a bimodal 2D environment, which is compatible with neurophysiological recording techniques. We showed that the visual VR can be combined with optogenetically induced virtual stimuli. Our findings suggest that flies integrate landmark cues and ascending aversive stimuli, representing a first step toward a new visual conditioning paradigm for head-fixed flies. We

have a number of future steps in mind toward establishing a visual conditioning paradigm in our VR system. Rather than conditioning landmark approaches in an environment with a single type of landmark, a more sensitive readout for conditioned behaviour may be to shift preferences between two or more landmark shapes. Also, a control for non-conditioned changes in landmark interaction behaviour due to extended time spent in the VR or the mere experience of the reinforcement stimulus needs to be designed. One approach is the use of a 'yoked' control, where a control fly has control over its movements in the visual VR, but receives reinforcement stimuli according to the actions of a matched experimental fly (Brembs and Heisenberg, 2000). Finally, we may want to test alternative reinforcement stimuli. Given that landmark-guided navigation has been frequently observed in the context of foraging, it may be worthwhile to explore pairing of virtual appetitive stimuli with landmarks.

Chapter 5

General Discussion

5. General Discussion

5.1. An explanatory gap in understanding navigational behaviours

Broadly speaking, research from three fields, each with its own distinct approach, focus and perspective, has contributed to our current understanding of navigational behaviours: behavioural and physiological research on sensory processing and sensorimotor integration, field studies of animal navigation and largely physiological investigations of neural representations of space.

Research on early sensory processing in a variety of animals in laboratory environments has shed light on sensory control of relatively simple movement patterns. These experiments are often performed on restrained animals, making it possible to closely monitor the animal's behaviour, tightly control sensory stimulation, and simultaneously record neural activity. Comprehensive behavioural and physiological studies of visual processing in tethered flying and walking flies, for instance, have generated a basic understanding of the mechanisms and algorithms that control elementary steering manoeuvres during visually guided behaviour (flying: Blondeau and Heisenberg, 1982; Borst, 2014; Götz, 1964; Haag et al., 2010; Poggio and Reichardt, 1973; Schnell et al., 2014, walking: Buchner, 1976; Chiappe et al., 2010; Longden et al., 2014). Similarly, the mechanisms underlying acoustic guidance in female crickets following a conspecific male's calling song during phonotaxis have been investigated in detail in tethered walking animals (Hedwig and Poulet, 2004; Kostarakos and Hedwig, 2012; Schildberger and Hörner, 1988). Traditionally, studies in this line of research have investigated navigational behaviours on a small spatial and temporal scale with simple sensory stimuli. Behavioural and neural responses to simplified and tightly controlled stimuli are easier to analyse, but such stimuli may not be rich enough to elicit complex navigational behaviours. The focus of many of these studies therefore tends to be on the sensory processing and the stimulus-response relationships that give rise to elementary modules of navigation such as course stabilisation and positive taxis.

At the other extreme are behavioural studies of animal navigation in the field. Here the animal moves freely in its natural environment and its ethological navigational behaviour can be studied. Field studies reveal the rich repertoire of navigational behaviours and strategies across phyla (Beugnon and Campan, 1989; Lipp et al., 2004; Müller and Wehner, 1988; Pfeffer and

Wittlinger, 2016; Tsoar et al., 2011) and help to form hypotheses about the role of elementary modules of navigation, which are studied in the lab in an ethological context. Unfortunately probing neural activity in the field is a challenge; consequently, the investigation of control mechanisms underlying navigation in natural habitats has been largely limited to purely behavioural studies (Wittlinger et al., 2007). Furthermore, some species such as ants and bees, which have been extensively studied in the field due to their remarkable behavioural repertoire, do not lend themselves to genetic manipulations due to their complex reproductive behaviour (Schulte et al., 2014).

A third line of research has been instrumental in providing an understanding of the nature of abstract, internal representations of space (Moser et al., 2008; Taube, 2007). Neural recordings in large, freely moving vertebrates have revealed a range of cell types, which encode various aspects of an animal's relationship to its physical space — for example place, grid and head direction cells in mammals. Imaging studies in tethered walking flies have demonstrated that also insects possess an abstract neural representation of their heading direction (Seelig and Jayaraman, 2015). Internal representations of space are thought to be necessary for solving complex navigational tasks such as route planning and navigation in novel terrain (Trullier et al., 1997). However, little is known about how the neural implementations of these internal representations are generated and even less about how they are used during navigation.

Each of the above approaches has produced insights regarding different aspects of navigational behaviours, but linking the findings made in different species and vastly different experimental conditions can be challenging (Götz, 1980; Reichardt and Poggio, 1976). We only have a limited mechanistic understanding of how elementary behavioural modules are coordinated to execute complex navigational strategies and how internal spatial representations are generated and used during navigation in natural conditions. Thus, there is a considerable gap in our understanding of the neural basis of navigation (Geva-Sagiv et al., 2015); closing this gap will require actively bridging the different approaches outlined above.

Electrophysiological and imaging studies in freely moving rodents navigating large and complex laboratory environments appear to be promising way forward to understanding the neural control of behavioural strategies. However, progress in gaining a mechanistic understanding of circuit function has been slow due to the size and complexity of the rodent brain. Studying moderately complex navigational behaviours in head-fixed insects navigating in virtual reality (VR) represents a practical compromise that could yield critical pieces of knowledge for bridging

the gap in our understanding of navigational. Simple navigational tasks, inspired by what an insect might need to accomplish in the wild, can be recreated for head-fixed animals in VR. In contrast to field studies, the VR environment, and the rules according to which the animal can interact with it, can be flexibly tailored to a specific research question (Minderer et al., 2016; Schuster et al., 2002). The complexity of the sensory environment can be adjusted depending on the studied behaviour, and behavioural paradigms for head-fixed animals can be combined with a range of neurophysiological recording techniques.

Here I will restrict myself to the discussion of how navigational behaviours may be studied under tightly controlled laboratory conditions in head-fixed preparations in crickets and flies. In the next section of this discussion I will describe how the two paradigms that I developed can help bridge the gap between behavioural studies in freely moving animals — in the field or in the laboratory — and tethered animals. I then discuss how my work may be continued in studies aimed to not only bridge behavioural studies in freely and tethered walking animals, but also link navigation behaviour to internal neural representations of space.

5.2. Virtual reality paradigms offer a balance between richness of behaviour and stimulus control

On the surface it may seem as if the full complexity of natural environments is required for an animal to display the true richness of its behavioural repertoire. Yet, we know from studies of sensory processing that central representations of natural stimuli are highly filtered and reduced to behaviourally relevant features(Borst and Helmstaedter, 2015; Hubel and Wiesel, 1959; Seelig and Jayaraman, 2013). Thus, some highly reduced sensory stimuli can elicit complex behavioural responses, presumably because these reduced stimuli include the relevant feature (ten Cate, 2009). This suggests that some naturalistic behaviours can be reliably evoked in the lab by presenting the animal with the relevant sensory environment and ways to interact with this environment.

Behavioural paradigms in VR can be designed to find the minimal sensory environment that is required to support a certain behaviour, or to study how increasingly complex environments give rise to a richer behavioural repertoire. The study of behavioural integration of mechanosensory antennal stimuli and phonotaxis presented in chapter 2 of this thesis is an

example for the first application of VR, whereas the study of landmark interaction of walking flies in two-dimensional (2D) environments presented in chapter 3 is an example of the latter.

5.2.1. Mechanosensory antennal stimulation can explain discrepancy between field and laboratory studies

Direct comparison of cricket phonotaxis in the field and in the laboratory has revealed striking behavioural differences between the two conditions. Under ideal sound-tracking conditions in the laboratory, female field crickets show fine tuning to various song parameters (Gerhardt and Huber, 2002; Pollack, 2000) and are able to resolve sound direction with remarkable spatial resolution (Schöneich and Hedwig, 2010). However, female crickets choosing between two calling song models in the field are less sensitive to small song pattern differences and take indirect routes to the selected target (Hirtenlehner and Römer, 2014). Similar observations were made for phonotaxis in male bush crickets following a female call, either in dense vegetation in the field or on a treadmill in the laboratory (von Helversen et al., 2001).
Two explanations for the observed discrepancies have been suggested. Firstly, the acoustic signal gets distorted in the field as it is reflected and blocked by vegetation, providing the cricket with a much noisier signal compared to laboratory conditions (Kostarakos and Römer, 2010). Secondly, the cricket, following a conspecific calling song in a natural environment, has to navigate through dense vegetation, where it must navigate past obstacles (Hirtenlehner and Römer, 2014; von Helversen et al., 2001). A walking cricket would likely detect obstacles in its path with its long antennae (Horseman et al., 1997; Okada and Akamine, 2012).
This motivated me to test more systematically — in the laboratory with tethered crickets walking on a treadmill — how female field crickets would respond to mechanosensory antennal stimulation during phonotaxis.

I simulated an object in the cricket's path by bringing a metal mesh into antennal reach and the cricket actively generated the mechanosensory stimulus by exploring the object with its antennae. In this situation the cricket still received a clean acoustic guidance signal, which in the absence of mechanosensory stimulation elicited robust phonotactic steering toward the sound source. I then compared responses to mechanosensory antennal stimulation in spontaneously walking crickets and crickets engaged in phonotaxis. Under both conditions the crickets slowed down and oriented themselves toward the presented object. Most striking was the suppression of phonotaxis by antennal stimulation even over long periods of time. Thus,

responses to antennal stimulation have high priority and are only mildly, if at all, modulated during phonotaxis.

Orientation toward the presented object and exploration with one and sometimes both antennae are reminiscent of early stages in the behavioural sequence triggered in freely moving crickets and cockroaches when they encounter a novel object (Okada and Akamine, 2012; Okada and Toh, 2004). One interpretation of the persistent orientation toward an unreachable object in my experiments therefore is that it represents one stage of a longer behavioural sequence, which stalls because the animal's movements do not influence its sensory experience in my paradigm. Thus, in the existing paradigm we cannot study how exploratory behaviour unfolds over time, but we can investigate how phonotactic steering is suppressed during antennal stimulation, which may well occur in the initial phase of obstacle negotiation of freely moving crickets.

5.2.2. The dimensionality of the visual environment shapes landmark fixation in walking flies

Characterisation of landmark interaction in naive tethered files has been largely restricted to experiments in one-dimensional (1D) environments, where the fly can only control the angular position of a landmark within its field of view (FOV). In this situation both flying and walking flies frequently show so-called fixation behaviour as they keep the landmark, typically a vertical stripe, at a fixed position within their field of view (Bahl et al., 2013; Götz, 1980; Reichardt and Poggio, 1976). Motivated by observations made in open-loop stimulation experiments with tethered flying and walking flies, a mechanism for this behaviour has been proposed (Bahl et al., 2013; Reichardt and Poggio, 1976): Fixation is achieved by directed turns toward the detected position of the landmark together with an asymmetry in the fly's compensatory response to rotational motion stimuli generated by its own movements.

In contrast to the simple case of stripe fixation in 1D, interactions with landmarks in a 2D plane in my VR experiments generated a richer set of visual features. In addition to position and angular motion cues, flies also experienced optic flow from the ground plane and looming stimuli as they approached landmarks. Looming stimuli have been primarily studied as a trigger of escape (Card and Dickinson, 2008; Santer et al., 2005; von Reyn et al., 2014) and collision avoidance responses (Chan and Gabbiani, 2013; Gabbiani et al., 1999; Srinivasan et al., 1993; van Breugel and Dickinson, 2012). One might expect that avoidance to self-induced looming

stimuli would be suppressed, possibly by an efference copy-like mechanism as proposed for suppression of optomotor responses during saccades (Kim et al., 2015). However, to my knowledge this has not been closely investigated. Translational optic flow is used by bees and ants to estimate travel speed and distance (Esch et al., 2001; Pfeffer and Wittlinger, 2016; Si et al., 2003). In flies, optic flow appears to play a role in flight control (Fry et al., 2009; Theobald et al., 2010), but less is known about responses to these stimuli during walking. Thus, walking in 2D environments involves coping with a range of different visual motion stimuli. Moreover, these different stimuli likely interact as the fly manoeuvres in the environment. In tethered flying flies, fixation behaviour has been shown to interact with responses to optic flow: Avoidance of the focus of expansion of a constant optic flow stimulus is suppressed in favour of stripe fixation, when a stripe is presented on top of the focus of expansion (Reiser and Dickinson, 2010a). In addition, the animal may perform certain movements to actively sample its 2D environment, for example for distance estimation (Esch et al., 2001; Pick and Strauss, 2005; Schuster et al., 2002). In light of this it is perhaps not surprising that I did not find clear correlations between the same fly's fixation behaviour in a 1D and 2D environment.

One of the most striking differences between landmark interaction in 1D and 2D is that fixation of a landmark in the frontal field of view leads to approach in a 2D environment. In this sense, the persistent stripe fixation of tethered walking or flying (Götz, 1987) flies could be seen as a stalled behavioural sequence aimed at approaching the landmark, similar to the persistent approach of the obstacle in the crickets path described in the chapter 2 of this thesis. Repeated fixation for long time periods can also be observed in wing-clipped freely walking flies in an arena with unreachable objects in the so-called 'Buridan's paradigm' (Bülthoff et al., 1982; Götz, 1980). However, if landmarks can be reached, flies spent little time approaching and exploring those objects, but rather climb and rest on top of them (Robie et al., 2010).
My experiments with tethered walking flies in my purely visual 2D VR environment, where landmarks were approachable (from all directions) but not climbable, form an intermediate situation. The high degree of similarity of landmark interaction behaviour in free and tethered walking flies — when tested under similar environmental conditions — shows that many elements of landmark interaction behaviour in freely walking flies are captured in this purely visual tethered walking paradigm.

5.2.3. Generation of behavioural sequences by a series of sensory triggers

During navigation, an animal's interactions with its environment produces characteristic temporal patterns of sensory stimulation, for example when it approaches an object (van Breugel and Dickinson, 2012). This opens up an elegant mechanism to generate behavioural sequences by sequential activation of sensory triggers that are dependent on the execution of a specific navigational manoeuvre. This mechanism seems to underlie visual control of several components of the landing sequence in *Drosophila* (van Breugel and Dickinson, 2012; van Breugel et al., 2015), and behavioural sequences during object exploration in crickets and cockroaches (Okada and Akamine, 2012; Okada and Toh, 2004) or during courtship in flies (Agrawal et al., 2014) may be generated in a similar way. A series of sensory triggers can also guide navigation on a larger spatiotemporal scale during route following (Trullier et al., 1997). This navigational strategy allows goal-directed movement along fixed routes by associating navigational decisions with sensory cues, such as visual landmarks, along the route (Collett and Collett, 2002; Geva-Sagiv et al., 2015).

If sensory feedback is removed in an experimental paradigm, behavioural sequences may stall. This has been illustrated in this thesis in the context of obstacle negotiation during phonotaxis in tethered walking crickets. Conversely, by adding degrees of freedom to the interaction of the animal with its environment to simple experimental paradigms one can potentially elicit behavioural sequences that resemble more naturalistic behaviours. The differences in landmark interaction behaviour in 1D and 2D environments demonstrate this point. Stalling sequences resulting in unnatural behaviour are probably common to laboratory studies using tethered preparations as the experimenter rarely simulates all the sensory feedback that the animal would generate if it were freely moving. Nonetheless these paradigms can be very useful as long as observations made in tethered preparations are only linked to behaviour in freely moving animals with appropriate caution.

5.3. Sources of variability in navigation behaviour

5.3.1. Behavioural variability of landmark-guided navigation

I began my work on visually guided navigation in tethered walking fruit flies by studying exploratory behaviour in naïve walking flies in simple environments with sparsely distributed visual landmarks. Based on previous work I had expected to find landmark fixation behaviour manifesting itself in a clear preference for keeping the landmark in the FOV (Bahl et al., 2013; Horn and Wehner, 1975; Reiser and Dickinson, 2010b). However, behavioural studies of landmark interaction in both free and tethered walking flies presented in this thesis showed high levels of variability, and to my surprise I only saw an obvious preference for landmark fixation in the frontal FOV in a subset of trials.

My experiments, in accordance with published findings, suggest that several properties of the visual environment can influence landmark fixation behaviour. For example, when all other experimental conditions are kept constant, fixation behaviour degrades with decreasing background brightness (Poggio and Reichardt, 1973). This is important to keep in mind, as purely behavioural studies typically use much brighter visual stimuli (30-8000 cd/m^2, Colomb et al., 2012; Poggio and Reichardt, 1973; Reiser and Dickinson, 2008) than what would be chosen in conjunction with imaging experiments (0.85 cd/m^2, Reiser and Dickinson, 2008; Seelig et al., 2010). Also the elevation of the object within the field of view and presence of other visual patterns in the background can affect fixation behaviour (Bahl et al., 2013; Fox et al., 2014; Poggio and Reichardt, 1973). In addition to the added spatial dimension, both of the above features of the visual environment differ between my experiments of stripe fixation in 1D and landmark tracking in 2D, which could explain the low correlation of fixation behaviour between the two conditions.

I also found that landmark and stripe fixation behaviour systematically varied between flies of different wild type genotypes and sexes. This is reminiscent of genetic and sex-specific variability of phonotactic preference and locomotor activity (Ayroles et al., 2015; Kain et al., 2012; Martin et al., 1999). A fly's stress and starvation level may also influence its fixation performance, though this has not been systematically tested as far as I know. With regard to experimental design, this highlights limitations of comparisons across experimental conditions and genotypes. I found, for example, that once I carefully matched lighting conditions in landmark interaction experiments with tethered walking and free walking flies of the same genotype and sex, their behaviour was remarkably consistent.

5.3.2. Behavioural state modulation as a source of behavioural variability and a mechanism for structuring guidance cues

Differences in metabolic or motivational state between animals were likely a source of variability in landmark interaction behaviour in the 2D VR environment. For simplicity I will refer to the metabolic and motivational state of an animal as its behavioural state. An animal's behavioural state can modulate sensory responses and thereby affect navigation behaviour such as landmark interaction.

A behavioural state variable that is relatively easy to control experimentally is an animal's satiety level. Starved flies show different food (Dus et al., 2013) and odour preferences (Bräcker et al., 2013; Ko et al., 2015) and altered locomotor activity (Meunier et al., 2007). One mechanism that can lead to altered behavioural responses is a state-dependent modulation of early sensory processing. Neuromodulation-based mechanisms underlying adjustments of early sensory processing according to metabolic (Longden and Krapp, 2009; Root et al., 2011) and behavioural state (Chiappe et al., 2010; Maimon et al., 2010; Suver et al., 2012; Tuthill et al., 2014) have been described in flies. At least some of the adjustments of sensory processing depending on the fly's satiety level may allow an animal to meet its current metabolic needs: A hungry fly has higher locomotor activity (Meunier et al., 2007) and is more attracted to food-related odours (Ko et al., 2015), which increase the probability that it will find food. By actively controlling the fly's satiety state as an experimental variable in paradigms for navigation behaviour the 2D VR could enable a thorough investigation of the link between altered sensory processing and changes in how the animal samples its environment.

A second role for behavioural state modulation in navigation could be structuring the recall of memories to ensure that certain navigational behaviours are only executed when needed. Only a hungry animal needs to prioritise finding food and only a thirsty animal needs to seek out water. In flies the generation and recall of olfactory memories, which can guide hungry flies to food, are gated by the animal's behavioural state (Burke et al., 2012; Huetteroth et al., 2015; Lin et al., 2014). Interestingly, behavioural state modulation of naïve and learned olfactory behaviours appears to be closely linked through joint neuromodulatory networks (Cohn et al., 2015). Also, context-dependent recall of guidance memories in foraging ants and bees is likely linked to behavioural state modulation: Finding or collecting food could act as a state switch, which initiates the return to the hive or nest (Wehner et al., 2006). Many animals find their way to food or nest by means of landmark-guided navigation (Collett and Collett, 2002; Collett and Graham, 2004). However, mechanisms linking behavioural state to landmark-guided navigation

are still unknown. When following a learned route to the nest, an animal needs to integrate the current sensory environment and motivational state, representing its *global* goal to return to the nest, to recall navigational guidance memories, which can act as *local* goals (Trullier et al., 1997). Thus, neural representations of the global goal could drive the execution of goal-directed navigation without necessarily encoding directions toward this goal. Local goals, in contrast, represent guidance cues and should be tightly connected to sensory information and sensorimotor integration processes. Controlling an animal's motivational state might be an effective way to set local goals, which opens up new avenues for studying the neural mechanisms underlying selection, pursuit and representation of local goals.

5.1. Final conclusions and future directions

Insects may only have simple internal spatial representations and only few species may navigate based on cognitive maps similar to those proposed for vertebrates. Nonetheless, insects face — and solve — computational challenges common to all navigating animals and their small brains render them an attractive model for studying the complex, distributed computations that the nervous system carries out during navigation. A prerequisite for studying the neural basis of selection and execution of navigational strategies is the development of suitable behavioural paradigms for tethered, head-fixed animals.

In this thesis I have presented two new paradigms for studying navigation in tethered walking insects. Both paradigms build on previously developed spherical treadmill systems for tethered walking crickets (Hedwig and Poulet, 2004) and flies (Seelig et al., 2010). My goal was to extend these existing systems to translate some characteristics of natural behaviours in crickets and flies, which had previously only been studied in freely moving animals, to tethered preparations.

Future directions extending the work on integration of responses to antennal stimulation with phonotaxis in the cricket

Motivated by observations regarding cricket phonotaxis in the field, I developed a paradigm for studying behavioural integration of obstacle negotiation with acoustic guidance in tethered walking crickets. In future experiments, it would be instructive to provide the cricket with partial control over the position of the object. One could, for example, move the object within

antennal detection distance and then couple its relative angular position to the cricket's steering manoeuvres. It is possible that under such conditions phonotactic stimulation would alter the cricket's interaction with the object, in contrast to the observations I made in the simpler paradigm presented in this thesis. In addition, the nature of the bimodal integration of antennal mechanosensory stimuli and the acoustic stimulus could be investigated further by systematically testing combinations of the antennal stimulus and different calling song patterns, which vary in attractiveness to the female cricket. Since this behavioural paradigm works with tethered walking crickets, it may also be combined with electrophysiological methods to investigate neural mechanisms underlying the integration of antennal mechanosensory and acoustic stimuli during phonotaxis. Finally, it may be helpful to investigate how freely walking crickets tracking a male's calling song during phonotaxis respond to encounters with a mesh like the one I used in my experiments here. Comparisons between matching free and tethered walking data sets, like the ones I presented in chapter 4 on landmark interaction in walking flies, can be helpful in highlighting which aspects of a behaviour are likely due to artefacts from the experimental preparation.

Training flies to use landmarks in a defined navigational task in virtual reality

In chapters 3 I presented a new flexible system for studying visually guided navigation in tethered walking fruit flies in 2D virtual environments. I then showed in chapter 4 how this setup can be used for studying visual guidance cues during directed avoidance of virtual aversive stimuli. I showed that the presence of landmarks improves avoidance of virtual aversive stimuli where the fly receives only limited directional direction from the aversive stimulus itself. This suggests two things: first, that information from the aversive stimulus is integrated with the visual environment and second, that flies can use visual landmark cues to guide their steering manoeuvres. This provides a proof of concept that landmark-guided navigation can be studied in the 2D VR for tethered walking flies presented in this thesis.

As a next step I am planning to establish a paradigm for conditioning naïve landmark preferences, building on my findings presented in chapter 3 and 4 of this thesis. Rather than trying to change a fly's landmark interaction behaviour in the presence of a single landmark, I would like attempt changing its relative preference when it is presented with two different landmark types. To do this, I would first let flies explore virtual worlds with two types of landmarks and establish the fly's naïve landmark preference, quantified for example as the difference in residency at the two landmarks or the difference in visits. After this 'pre' trial I would attempt to train flies by pairing one of the two landmarks with a virtually aversive

stimulus akin to those used in the landmark-assisted avoidance paradigm presented in chapter 4. Finally, I would test the fly's landmark preferences again under the same conditions as in the first trial. If flies had learned to associate the 'punished' landmark with the presence of the virtual aversive stimulus, I would expect that in the 'post' the relative preference for this compared to the second, neutral landmark was reduced compared to the 'pre' trial. As aversive stimulus one could use for example the ascending aversive, but it may also be worthwhile to test 'virtual heat' after eliminating crosstalk with the visual stimulus as discussed in chapter 4.

The VR system I developed could be used to design behavioural paradigms inspired by visually guided foraging described in ants and bees (Collett and Collett, 2002). It would be interesting to test, for example, whether hungry flies could be trained in an environment in which certain landmark shapes are associated with the delivery of food-related stimuli. By using optogenetically delivered virtual food-related stimuli, it may be possible to reward flies with an illusionary food intake instead of actually feeding the fly (Miyamoto et al., 2012). This has the advantage that flies do not get satiated and remain motivated to search for food.

Combining a visually guided navigation paradigm with in vivo calcium imaging

A promising behavioural paradigm for conditioning landmark preferences could be to transferred to the two-photon imaging rig (Seelig et al., 2010) to monitor neural activity in flies performing a relatively defined navigational task. This would allow me to address a wide range of currently open questions, for example, whether and how the fly's internal compass is used during goal-directed navigation, which mechanisms underlie the association of valence with visual landmarks, and how behavioural state-dependent recall of memories is achieved, to name just a few. In the long term this line of research could yield insights into the neural mechanisms underlying landmark-based guidance strategies in a given navigational problem, i.e. navigating to a safe spot in an aversive environment or navigating to a known food source.

Chapter 6

References

6. References

Abraham, N. M., Spors, H., Carleton, A., Margrie, T. W., Kuner, T. and Schaefer, A. T. (2004). Maintaining accuracy at the expense of speed: Stimulus similarity defines odor discrimination time in mice. *Neuron* **44**, 865–876.

Acharya, L., Aghajan, Z. M., Vuong, C., Moore, J. J. and Mehta, M. R. (2016). Causal Influence of Visual Cues on Hippocampal Directional Selectivity. *Cell* **164**, 197–207.

Adamo, S. and Hoy, R. R. (1994). Mating behaviour of the field cricket *Gryllus bimaculatus* and its dependence on social and environmental cues. *Anim. Behav.* 857–868.

Aghajan, Z. M., Acharya, L., Moore, J. J., Cushman, J. D., Vuong, C. and Mehta, M. R. (2015). Impaired spatial selectivity and intact phase precession in two-dimensional virtual reality. *Nat Neurosci* **18**, 121–128.

Agrawal, S., Safarik, S. and Dickinson, M. H. (2014). The relative roles of vision and chemosensation in mate recognition of *Drosophila melanogaster. J. Exp. Biol.* **217**, 2796–805.

Aronov, D. and Tank, D. W. (2014). Engagement of Neural Circuits Underlying 2D Spatial Navigation in a Rodent Virtual Reality System. *Neuron* **84**, 442–456.

Aso, Y. and Rubin, G. M. (2016). Dopaminergic neurons write and update memories with cell-type-specific rules. *eLife* **5**, e16135.

Aso, Y., Hattori, D., Yu, Y., Johnston, R. M., Iyer, N. a, Ngo, T.-T., Dionne, H., Abbott, L., Axel, R., Tanimoto, H., et al. (2014a). The neuronal architecture of the mushroom body provides a logic for associative learning. *eLife* **3**, 1–47.

Aso, Y., Sitaraman, D., Ichinose, T., Kaun, K. R., Vogt, K., Belliart-Guérin, G., Plaçais, P.-Y., Robie, A. a., Yamagata, N., Schnaitmann, C., et al. (2014b). Mushroom body output neurons encode valence and guide memory-based action selection in *Drosophila*. *eLife* **3**, e04580.

Avarguès-Weber, A. and Giurfa, M. (2013). Conceptual learning by miniature brains. *Proc. R. Scociety B* **280**, 20131907.

Ayroles, J. F., Buchanan, S. M., O'Leary, C., Skutt-Kakaria, K., Grenier, J. K., Clark, A. G., Hartl, D. L. and de Bivort, B. L. (2015). Behavioral idiosyncrasy reveals genetic control of phenotypic variability. *Proc. Natl. Acad. Sci.* **112**, 6706–6711.

Baddeley, B., Graham, P., Husbands, P. and Philippides, A. (2012). A model of ant route navigation driven by scene familiarity. *PLoS Comput. Biol.* **8**, e1002336.

Bahl, A., Ammer, G., Schilling, T. and Borst, A. (2013). Object tracking in motion-blind flies. *Nat. Neurosci.* **16**, 730–738.

Balakrishnan and Pollack (1997). The role of antennal sensory cues in female responses to courting males in the cricket *Teleogryllus oceanicus*. *J. Exp. Biol.* **200**, 511–522.

Barbagallo, B. and Garrity, P. A. (2015). Temperature sensation in *Drosophila*. *Curr. Opin. Neurobiol.* **34**, 8–13.

Bath, D. E., Stowers, J. R., Hormann, D., Poehlmann, A., Dickson, B. J. and Straw, A. D. (2014). FlyMAD: rapid thermogenetic control of neuronal activity in freely walking *Drosophila*. *Nat Meth* **11**, 756–762.

Bech, M., Homberg, U. and Pfeiffer, K. (2014). Receptive Fields of Locust Brain Neurons Are Matched to Polarization Patterns of the Sky. *Curr. Biol.* **24**, 2124–2129.

Bell, J. S. and Wilson, R. I. (2016). Behavior Reveals Selective Summation and Max Pooling among Olfactory Processing Channels. *Neuron* **91**, 425–438.

Bender, J. A., Pollack, A. J. and Ritzmann, R. E. (2016). Neural activity in the central complex of the insect brain Is linked to locomotor changes. *Curr. Biol.* **20**, 921–926.

Bennett, A. T. D. (1996). Do animals have cognitive maps? *J. Exp. Biol.* **199**, 219–224.

Beugnon, G. and Campan, R. (1989). Homing in the field cricket, *Gryllus campestris*. *J. Insect Behav.* **2**, 187–198.

Bisch-Knaden, S. and Wehner, R. (2003). Local vectors in desert ants: context-dependent landmark learning during outbound and homebound runs. *J. Comp. Physiol. A. Neuroethol. Sens. Neural. Behav. Physiol.* **189**, 181–187.

Blondeau, J. and Heisenberg, M. (1982). The three-dimensional optomotor torque system of *Drosophila melanogaster*. *J. Comp. Physiol.* **145**, 321–329.

Bockhorst, T. and Homberg, U. (2015). Compass Cells in the Brain of an Insect Are Sensitive to Novel Events in the Visual World. *PLoS One* **10**, e0144501.

Bockhorst, T. and Homberg, U. (2017). Interaction of compass sensing and object-motion detection in the locust central complex. *J. Neurophysiol.*

Böhm, H., Schildberger, K. and Huber, F. (1991). Visual and Acoustic Course Control in the Cricket *Gryllus bimaculatus*. *J. Exp. Biol.* **159**, 235–248.

Borst, A. (2014). Fly visual course control: behaviour, algorithms and circuits. *Nat. Rev. Neurosci.* **15**, 590–599.

Borst, A. and Helmstaedter, M. (2015). Common circuit design in fly and mammalian motion vision. *Nat. Neurosci.* **18**, 1067–1076.

Bräcker, L. B., Siju, K. P., Arela, N., So, Y., Hang, M., Hein, I., Vasconcelos, M. L. and Grunwald Kadow, I. C. (2013). Essential role of the mushroom body in context-dependent CO_2 avoidance in *Drosophila*. *Curr. Biol.* **23**, 1228–1234.

Braitenberg, V. (1986). Vehicles: Experiments in Synthetic Psychology. *Proc. SAMPE Annu. Conf.* 152.

Branson, K., Robie, A. A., Bender, J., Perona, P. and Dickinson, M. H. (2009). High-throughput ethomics in large groups of *Drosophila*. *Nat. Methods* **6**, 451–457.

Bregy, P., Sommer, S. and Wehner, R. (2008). Nest-mark orientation versus vector navigation in desert ants. *J. Exp. Biol.* **211**, 1868–1873.

Brembs, B. and Heisenberg, M. (2000). The Operant and the Classical in Conditioned Orientation of *Drosophila melanogaster* at the Flight Simulator. *Learn. Mem.* **7**, 104–115.

Buchanan, S. M., Kain, J. S. and de Bivort, B. L. (2015). Neuronal control of locomotor handedness in *Drosophila*. *Proc. Natl. Acad. Sci.* **112**, 6700–6705.

Buchler, E. R. and Childs, S. B. (1981). Orientation to distant sounds by foraging big brown bats (*Eptesicus fuscus*). *Anim. Behav.* **29**, 428–432.

Buchner, E. (1976). Elementary movement detectors in an insect visual system. *Biol. Cybern.* **24**, 85–101.

Buehlmann, C., Graham, P., Hansson, B. S. and Knaden, M. (2014). Desert ants locate food by combining high sensitivity to food odors with extensive crosswind runs. *Curr. Biol.* **24**, 960–964.

Bülthoff, H., Götz, K. G. and Herre, M. (1982). Recurrent Inversion of Visual Orientation in the Walking Fly, *Drosophila melanogaster*. *J. Comp. Physiol.* **148**, 471–481.

Burke, C. J., Huetteroth, W., Owald, D., Perisse, E., Krashes, M. J., Das, G., Gohl, D., Silies, M., Certel, S. and Waddell, S. (2012). Layered reward signalling through octopamine and dopamine in *Drosophila*. *Nature* **492**, 433–437.

Cade, W. (1975). Acoustically Orienting Parasitoids: Fly Phonotaxis to Cricket Song. *Science* **190**, 1312–1313.

Capaldi, E. A. and Dyer, F. C. (1999). The role of orientation flights on homing performance in honeybees. *J. Exp. Biol.* **202**, 1655–1666.

Carcaud, J., Roussel, E., Giurfa, M. and Sandoz, J.-C. (2009). Odour aversion after olfactory conditioning of the sting extension reflex in honeybees. *J. Exp. Biol.* **212**, 620–626.

Card, G. (2012). Escape behaviors in insects. *Curr. Opin. Neurobiol.* **22**, 180–186.

Card, G. and Dickinson, M. H. (2008). Visually Mediated Motor Planning in the Escape Response of *Drosophila*. *Curr. Biol.* **18**, 1300–1307.

Cardona, A., Saalfeld, S., Preibisch, S., Schmid, B., Cheng, A., Pulokas, J., Tomancak, P. and Hartenstein, V. (2010). An Integrated Micro- and Macroarchitectural Analysis of the *Drosophila* Brain by Computer-Assisted Serial Section Electron Microscopy. *PLoS Biol.* **8**, e1000502.

Cartwright, B. A. and Collett, T. S. (1987). Landmark maps for honeybees. *Biol. Cybern.* **57**, 85–93.

Cassenaer, S. and Laurent, G. (2012). Conditional modulation of spike-timing-dependent plasticity for olfactory learning. *Nature* **482**, 47–52.

Chan, R. W. M. and Gabbiani, F. (2013). Collision-avoidance behaviors of minimally restrained flying locusts to looming stimuli. *J. Exp. Biol.* **216**, 641–55.

Chapman, J. W., Reynolds, D. R. and Wilson, K. (2015). Long-range seasonal migration in insects: Mechanisms, evolutionary drivers and ecological consequences. *Ecol. Lett.* **18**, 287–302.

Chiappe, M. E., Seelig, J. D., Reiser, M. B. and Jayaraman, V. (2010). Walking modulates speed sensitivity in *Drosophila* motion vision. *Curr. Biol.* **20**, 1470–1475.

Chittka, L. and Kunze, J. (1995). The Significance of Landmarks for Path Integration in Homing Honeybee Foragers. *Naturwissenschaften* **82**, 137–140.

Chittka, L., Rossiter, S. J., Skorupski, P. and Fernando, C. (2012). What is comparable in comparative cognition? *Philos. Trans. R. Soc. B Biol. Sci.* **367**, 2677–2685.

Claridge-Chang, A., Roorda, R. D., Vrontou, E., Sjulson, L., Li, H., Hirsh, J. and Miesenböck, G. (2009). Writing Memories with Light-Addressable Reinforcement Circuitry. *Cell* **139**, 405–415.

Cohn, R., Morantte, I. and Ruta, V. (2015). Coordinated and Compartmentalized Neuromodulation Shapes Sensory Processing in *Drosophila*. *Cell* **163**, 1742–1755.

Collett, M. (2012). How navigational guidance systems are combined in a desert ant. *Curr. Biol.* **22**, 927–932.

Collett, T. S. and Collett, M. (2000). Path integration in insects. *Curr. Opin. Neurobiol.* **10**, 757–762.

Collett, T. S. and Collett, M. (2002). Memory use in insect visual navigation. *Nat. Rev. Neurosci.* **3**, 542–552.

Collett, T. S. and Graham, P. (2004). Animal Navigation: Path Integration, Visual Landmarks and Cognitive Maps. *Curr. Biol.* **14**, R475–R477.

Collett, T. S. and Land, M. F. (1975). Visual control of flight behaviour in the hoverfly *Syritta pipiens* L. *J. Comp. Physiol. A* **99**, 1–66.

Collett, M., Harland, D. and Collett, T. S. (2002). The use of landmarks and panoramic context in the performance of local vectors by navigating honeybees. *J. Exp. Biol.* **205**, 807–814.

Colomb, J., Reiter, L., Blaszkiewicz, J., Wessnitzer, J. and Brembs, B. (2012). Open Source Tracking and Analysis of Adult *Drosophila* Locomotion in Buridan's Paradigm with and without Visual Targets. *PLoS One* **7**, e42247.

Comer, C. and Baba, Y. (2011). Active touch in orthopteroid insects: behaviours, multisensory substrates and evolution. *Philos. Trans. R. Soc. B Biol. Sci.* **366**, 3006–3015.

Comer, C. M., Mara, E., Murphy, K. A., Getman, M. and Mungy, M. C. (1994). Multisensory control of escape in the cockroach *Periplaneta americana*. II. Patterns of touch-evoked behavior. *J. Comp. Physiol. A* **174**, 13–26.

Dombeck, D. A., Harvey, C. D., Tian, L., Looger, L. L. and Tank, D. W. (2010). Functional imaging of hippocampal place cells at cellular resolution during virtual navigation. *Nat. Neurosci.* **13**, 1433–1440.

Duer, A., Paffhausen, B. H. and Menzel, R. (2015). High order neural correlates of social behavior in the honeybee brain. *J. Neurosci. Methods* **254**, 1–9.

Duhamel, Colby, C. L. and Goldberg, M. E. (1992). The updating of the representation of visual space in parietal cortex by intended eye movements. *Science* **255**, 90–92.

Duistermars, B. J. and Frye, M. A. (2008). Crossmodal visual input for odor tracking during fly flight. *Curr. Biol.* **18**, 270–275.

Dus, M., Ai, M. and Suh, G. S. B. (2013). Taste-independent nutrient selection is mediated by a brain-specific Na+ /solute co-transporter in *Drosophila*. *Nat. Neurosci.* **16**, 526–528.

Eibl, E. and Huber, F. (1979). Central projections of tibial sensory fibers within the three thoracic ganglia of crickets (*Gryllus campestris* L., *Gryllus bimaculatus* DeGeer). *Zoomorphologie* **92**, 1–17.

el Jundi, B., Warrant, E. J., Byrne, M. J., Khaldy, L., Baird, E., Smolka, J. and Dacke, M. (2015). Neural coding underlying the cue preference for celestial orientation. *Proc. Natl. Acad. Sci.* **112**, 11395–11400.

Esch, H., Huber, F. and Wohlers, D. W. (1980). Primary auditory neurons in crickets: Physiology and central projections. *J. Comp. Physiol. A* **137**, 27–38.

Esch, H. E., Zhang, S., Srinivasan, M. V and Tautz, J. (2001). Honeybee dances communicate distances measured by optic flow. *Nature* **411**, 581–583.

Etienne, A. S. and Jeffery, K. J. (2004). Path integration in mammals. *Hippocampus* **14**, 180–192.

Etienne, A. S., Maurer, R., Berlie, J. and Reverdin, B. (1998). Navigation through vector addition. *Nature* **396**, 161–164.

Fenno, L., Yizhar, O. and Deisseroth, K. (2011). The development and application of optogenetics. *Annu. Rev. Neurosci.* **34**, 389–412.

Fetsch, C. R., Pouget, A., DeAngelis, G. C. and Angelaki, D. E. (2012). Neural correlates of reliability-based cue weighting during multisensory integration. *Nat Neurosci* **15**, 146–154.

Foucaud, J., Burns, J. G. and Mery, F. (2010). Use of spatial information and search strategies in a water maze analog in *Drosophila melanogaster*. *PLoS.One.* **5**, e15231.

Fox, J. L., Aptekar, J. W., Zolotova, N. M., Shoemaker, P. A. and Frye, M. A. (2014). Figure-ground discrimination behavior in *Drosophila*. I. Spatial organization of wing-steering responses. *J. Exp. Biol.* **217**, 558–69.

Franz, M. O. and Mallot, H. A. (2000). Biomimetic robot navigation. *Rob. Auton. Syst.* **30**, 133–153.

Fry, S. N., Sayaman, R. and Dickinson, M. H. (2003). The aerodynamics of free-flight maneuvers in *Drosophila*. *Science* **300**, 495–498.

Fry, S. N., Sayaman, R. and Dickinson, M. H. (2005). The aerodynamics of hovering flight in Drosophila. *J. Exp. Biol* **208**, 2303–2318.

Fry, S. N., Rohrseitz, N., Straw, A. D. and Dickinson, M. H. (2009). Visual control of flight speed in *Drosophila melanogaster*. *J. Exp. Biol.* **212**, 1120–1130.

Frye, M. A. and Dickinson, M. H. (2004). Motor output reflects the linear superposition of visual and olfactory inputs in *Drosophila*. *J. Exp. Biol.* **207**, 123–131.

Gabbiani, F., Krapp, H. G. and Laurent, G. (1999). Computation of object approach by a wide-field, motion-sensitive neuron. *J. Neurosci.* **19**, 1122–41.

Galili, D. S., Dylla, K. V., Lüdke, A., Friedrich, A. B., Yamagata, N., Wong, J. Y. H., Ho, C. H., Szyszka, P. and Tanimoto, H. (2014). Converging Circuits Mediate Temperature and Shock Aversive Olfactory Conditioning in *Drosophila*. *Curr. Biol.* **24**, 1712–1722.

Gallio, M., Ofstad, T. A., Macpherson, L. J., Wang, J. W. and Zuker, C. S. (2011). The Coding of Temperature in the *Drosophila* Brain. *Cell* **144**, 614–624.

Gallistel, C. R. (1990). *The organization of learning*. Cambridge, Mass: MIT Press.

Gebhardt, M. and Honegger, H. W. (2001). Physiological characterisation of antennal mechanosensory descending interneurons in an insect (*Gryllus bimaculatus*, *Gryllus campestris*) brain. *J. Exp. Biol.* **204**, 2265–2275.

Gerhardt, H. C. and Huber, F. (2002). *Acoustic communication in insects and anurans: common problems and diverse solutions*. University of Chicago Press.

Geva-Sagiv, M., Las, L., Yovel, Y. and Ulanovsky, N. (2015). Spatial cognition in bats and rats: from sensory acquisition to multiscale maps and navigation. *Nat. Rev. Neurosci.* **16**, 94–108.

Giurfa, M., Zhang, S., Jenett, A., Menzel, R. and Srinivasan, M. V (2001). The concepts of "sameness" and "difference" in an insect. *Nature* **410**, 930–933.

Goodridge, J. P. and Taube, J. S. (1995). Preferential use of the landmark navigational system by head direction cells in rats. *Behav. Neurosci.* **109**, 49–61.

Götz, K. G. (1964). Optomotorische Untersuchung des visuellen systems einiger Augenmutanten der Fruchtfliege *Drosophila*. *Kybernetik* **2**, 77–92.

Götz, K. G. (1975). The Optomotor Equilibrium of the *Drosophila* Navigation System. *J. Comp. Physiol.* **99**, 187–210.

Götz, K. G. (1980). Visual Guidance In *Drosophila*. In *Development and Neurobiology of Drosophila* (ed. Siddiqi, O.), p. New York 1980: Springer Science+Business Media.

Götz, K. G. (1987). Course-control, metabolism and wing interference during ultralong tethered flight in *Drosophila melanogaster*. *J. Exp. Biol.* **128**, 35–46.

Götz, K. G. (1994). Exploratory strategies in Drosophila. In *Neural Basis of Behavioral Adaptations* (ed. Schildberger, K.) and Elsner, N.), pp. 47–58. Stuttgart, Germany: Fischer.

Graham, P. and Cheng, K. (2009). Ants use the panoramic skyline as a visual cue during navigation. *Curr. Biol.* **19**, R935–R937.

Grant, R. A., Mitchinson, B., Fox, C. W. and Prescott, T. J. (2009). Active touch sensing in the rat: anticipatory and regulatory control of whisker movements during surface exploration. *J. Neurophysiol.* **101**, 862–874.

Gray, J. R., Pawlowski, V. and Willis, M. A. (2002). A method for recording behavior and multineuronal CNS activity from tethered insects flying in virtual space. *J. Neurosci. Methods* **120**, 211–223.

Grover, D., Katsuki, T. and Greenspan, R. J. (2016). Flyception: imaging brain activity in freely walking fruit flies. *Nat Meth* **13**, 569–572.

Guerra, P. A. and Reppert, S. M. (2015). Sensory basis of lepidopteran migration: Focus on the monarch butterfly. *Curr. Opin. Neurobiol.* **34**, 20–28.

Haag, J., Wertz, A. and Borst, A. (2010). Central gating of fly optomotor response. *Proc. Natl. Acad. Sci. U. S. A.* **107**, 20104–9.

Hamada, F. N., Rosenzweig, M., Kang, K., Pulver, S. R., Ghezzi, A., Jegla, T. J. and Garrity, P. a (2008). An internal thermal sensor controlling temperature preference in *Drosophila*. *Nature* **454**, 217–220.

Harley, C. M., English, B. A. and Ritzmann, R. E. (2009). Characterization of obstacle negotiation behaviors in the cockroach, *Blaberus discoidalis*. *J. Exp. Biol.* **212**, 1463–1476.

Harvey, C. D., Coen, P. and Tank, D. W. (2012). Choice-specific sequences in parietal cortex during a virtual-navigation decision task. *Nature* **484**, 62–68.

Hedwig, B. (2000). Control of cricket stridulation by a command neuron: efficacy depends on the behavioral state. *J. Neurophysiol.* **83**, 712–722.

Hedwig, B. (2006). Pulses, patterns and paths: neurobiology of acoustic behaviour in crickets. *J. Comp. Physiol. A* **192**, 677–89.

Hedwig, B. and Poulet, J. F. A. (2004). Complex auditory behaviour emerges from simple reactive steering. *Nature* **430**, 781–785.

Hedwig, B. and Poulet, J. F. A. (2005). Mechanisms underlying phonotactic steering in the cricket *Gryllus bimaculatus* revealed with a fast trackball system. *J. Exp. Biol.* **208**, 915–927.

Heinze, S. and Homberg, U. (2007). Maplike representation of celestial E-vector orientations in the brain of an insect. *Science* **315**, 995–997.

Heisenberg, M. and Wolf, R. (1979). On the fine structure of yaw torque in visual flight orientation of *Drosophila melanogaster*. *J. Comp. Physiol. A* **130**, 113–130.

Helmchen, F., Fee, M. S., Tank, D. W. and Denk, W. (2001). A Miniature Head-Mounted Two-Photon Microscope: High-Resolution Brain Imaging in Freely Moving Animals. *Neuron* **31**, 903–912.

Herman, A. M., Huang, L., Murphey, D. K., Garcia, I. and Arenkiel, B. R. (2014). Cell type-specific and time-dependent light exposure contribute to silencing in neurons expressing Channelrhodopsin-2. *eLife* **3**, e01481.

Hige, T., Aso, Y., Rubin, G. M. and Turner, G. C. (2015a). Plasticity-driven individualization of olfactory coding in mushroom body output neurons. *Nature* **526**, 258–262.

Hige, T., Aso, Y., Modi, M. N., Rubin, G. M. and Turner, G. C. (2015b). Heterosynaptic plasticity underlies aversive olfactory learning in *Drosophila*. *Neuron* **88**, 985–998.

Hinterwirth, A. J. and Daniel, T. L. (2010). Antennae in the hawkmoth *Manduca sexta* (Lepidoptera, Sphingidae) mediate abdominal flexion in response to mechanical stimuli. *J. Comp. Physiol. A* **196**, 947–956.

Hirtenlehner, S. and Römer, H. (2014). Selective phonotaxis of female crickets under natural outdoor conditions. *J. Comp. Physiol. A* **200**, 239–250.

Hirtenlehner, S., Römer, H. and Schmidt, A. K. D. (2014). Out of phase: Relevance of the medial septum for directional hearing and phonotaxis in the natural habitat of field crickets. *J. Comp. Physiol. A* **200**, 139–148.

Hölscher, C., Schnee, a, Dahmen, H., Setia, L. and Mallot, H. a (2005). Rats are able to navigate in virtual environments. *J. Exp. Biol.* **208**, 561–569.

Hori, E., Nishio, Y., Kazui, K., Umeno, K., Tabuchi, E., Sasaki, K., Endo, S., Ono, T. and Nishijo, H. (2005). Place-related neural responses in the monkey hippocampal formation in a virtual space. *Hippocampus* **15**, 991–996.

Horn, E. and Wehner, R. (1975). The Mechanism of Visual Pattern Fixation in the Walking Fly, *Drosophila melanogaster*. *J. Comp. Physiol.* **101**,.

Horseman, B. G., Gebhardt, M. J. and Honegger, H. W. (1997). Involvement of the suboesophageal and thoracic ganglia in the control of antennal movements in crickets. *J. Comp. Physiol. A* **181**, 195–204.

Hubel, D. H. and Wiesel, T. N. (1959). Receptive fields of single neurones in the cat's striate cortex. *J. Physiol.* **148**, 574–591.

Huetteroth, W., Perisse, E., Lin, S., Klappenbach, M., Burke, C. and Waddell, S. (2015). Sweet Taste and Nutrient Value Subdivide Rewarding Dopaminergic Neurons in *Drosophila*. *Curr. Biol.* **25**, 751–758.

Huston, S. J. and Jayaraman, V. (2011). Studying sensorimotor integration in insects. *Curr. Opin. Neurobiol.* **21**, 527–534.

Isono, K., Tanimura, T., Oda, Y. and Tsukahara, Y. (1988). Dependency on light and vitamin A derivatives of the biogenesis of 3-hydroxyretinal and visual pigment in the compound eyes of *Drosophila melanogaster*. *J. Gen. Physiol.* **92**, 587–600.

Jacob, P. F. and Hedwig, B. (2015). The impact of cercal air currents on singing motor pattern generation in the cricket (*Gryllus bimaculatus* DeGeer). *J. Neurophysiol.* jn.00669.2015.

Judd, S. P. D. and Collett, T. S. (1998). Multiple stored views and landmark guidance in ants. *Nature* **392**, 710–714.

Kain, J. S., Stokes, C. and de Bivort, B. L. (2012). Phototactic personality in fruit flies and its suppression by serotonin and white. *Proc. Natl. Acad. Sci. U. S. A.* **109**, 19834–9.

Kennedy, J. S. (1940). The Visual Responses of Flying Mosquitoes. *Proc. Zool. Soc. London* **A109**, 221–242.

Kim, A. J., Fitzgerald, J. K. and Maimon, G. (2015). Cellular evidence for efference copy in *Drosophila* visuomotor processing. *Nat. Neurosci.* **18**, 1247–1255.

Kimmerle, B., Eickermann, J. and Egelhaaf, M. (2000). Object fixation by the blowfly during tethered flight in a simulated three-dimensional environment. *J. Exp. Biol.* **203**, 1723–1732.

Klapoetke, N. C., Murata, Y., Kim, S. S., Pulver, S. R., Birdsey-Benson, A., Cho, Y. K., Morimoto, T. K., Chuong, A. S., Carpenter, E. J., Tian, Z., et al. (2014). Independent optical excitation of distinct neural populations. *Nat. Methods* **11**, 338–346.

Klein, M., Afonso, B., Vonner, A. J., Hernandez-Nunez, L., Berck, M., Tabone, C. J., Kane, E. A., Pieribone, V. A., Nitabach, M. N., Cardona, A., et al. (2015). Sensory determinants of behavioral dynamics in *Drosophila* thermotaxis. *Proc. Natl. Acad. Sci.* **112**, E220–E229.

Knierim, J. J. and Zhang, K. (2012). Attractor dynamics of spatially correlated neural activity in the limbic system. *Annu. Rev. Neurosci.* **35**, 267–285.

Ko, K. I., Root, C. M., Lindsay, S. A., Zaninovich, O. A., Shepherd, A. K., Wasserman, S. A., Kim, S. M. and Wang, J. W. (2015). Starvation promotes concerted modulation of appetitive olfactory behavior via parallel neuromodulatory circuits. *eLife* **4**,.

Kostarakos, K. and Hedwig, B. (2012). Calling Song Recognition in Female Crickets: Temporal Tuning of Identified Brain Neurons Matches Behavior. *J. Neurosci.* **32**, 9601–9612.

Kostarakos, K. and Römer, H. (2010). Sound transmission and directional hearing in field crickets: Neurophysiological studies outdoors. *J. Comp. Physiol. A Neuroethol. Sensory, Neural, Behav. Physiol.* **196**, 669–681.

Krasne, F. B. and Lee, S. C. (1988). Response-dedicated trigger neurons as control points for behavioral actions: selective inhibition of lateral giant command neurons during feeding in crayfish. *J. Neurosci.* **8**, 3703–3712.

Kühn, A. (1919). Die Orientierung der Tiere im Raum.

Labhart, T. and Meyer, E. P. (2002). Neural mechanisms in insect navigation: Polarization compass and odometer. *Curr. Opin. Neurobiol.* **12**, 707–714.

Labhart, T., Hodel, B. and Valenzuela, I. (1984). The physiology of the cricket's compound eye with particular reference to the anatomically specialized dorsal rim area. *J. Comp. Physiol. A* **155**, 289–296.

Labhart, T., Petzold, J. and Helbling, H. (2001). Spatial integration in polarization-sensitive interneurones of crickets: a survey of evidence, mechanisms and benefits. *J. Exp. Biol.* **204**, 2423–30.

Land, M. F. (1997). Visual Acuity in Insects. *Annu. Rev. Entomol.* **42**, 147–177.

Legge, E. L. G., Wystrach, A., Spetch, M. L. and Cheng, K. (2014). Combining sky and earth: desert ants (*Melophorus bagoti*) show weighted integration of celestial and terrestrial cues. *J. Exp. Biol.* **217**, 4159–4166.

Lemon, W. C., Pulver, S. R., Höckendorf, B., McDole, K., Branson, K., Freeman, J. and Keller, P. J. (2015). Whole-central nervous system functional imaging in larval *Drosophila*. *Nat. Commun.* **6**, 7924.

Lin, J. Y. (2011). A user's guide to channelrhodopsin variants: features, limitations and future developments. *Exp. Physiol.* **96**, 19–25.

Lin, H.-H., Chu, L.-A., Fu, T.-F., Dickson, B. J. and Chiang, A.-S. (2013). Parallel Neural Pathways Mediate CO_2 Avoidance Responses in *Drosophila*. *Science* **340**, 1338 LP-1341.

Lin, S., Owald, D., Chandra, V., Talbot, C., Huetteroth, W. and Waddell, S. (2014). Neural correlates of water reward in thirsty *Drosophila*. *Nat. Neurosci.* **17**, 1536–1542.

Lipp, H. P., Vyssotski, A. L., Wolfer, D. P., Renaudineau, S., Savini, M., Tröster, G. and Dell'Omo, G. (2004). Pigeon homing along highways and exits. *Curr. Biol.* **14**, 1239–1249.

Liu, L., Wolf, R., Ernst, R. and Heisenberg, M. (1999). Context generalization in *Drosophila* visual learning requires the mushroom bodies. *Nature* **400**, 753–756.

Liu, G., Seiler, H., Wen, A., Zars, T., Ito, K., Wolf, R., Heisenberg, M. and Liu, L. (2006). Distinct memory traces for two visual features in the *Drosophila* brain. *Nature* **439**, 551–556.

Longden, K. D. and Krapp, H. G. (2009). State-dependent performance of optic-flow processing interneurons. *J. Neurophysiol.* **102**, 3606–3618.

Longden, K. D., Muzzu, T., Cook, D. J., Schultz, S. R. and Krapp, H. G. (2014). Nutritional state modulates the neural processing of visual motion. *Curr. Biol.* **24**, 890–895.

Lott, G. K., Rosen, M. J. and Hoy, R. R. (2007). An inexpensive sub-millisecond system for walking measurements of small animals based on optical computer mouse technology. *J. Neurosci. Methods* **161**, 55–61.

Maimon, G., Straw, A. D. and Dickinson, M. H. (2008). A simple vision-based algorithm for decision making in flying *Drosophila*. *Curr. Biol.* **18**, 464–70.

Maimon, G., Straw, A. D. and Dickinson, M. H. (2010). Active flight increases the gain of visual motion processing in *Drosophila*. *Nat. Neurosci.* **13**, 393–399.

Mappes, M. and Homberg, U. (2004a). Behavioral analysis of polarization vision in tethered flying locusts. *J. Comp. Physiol. A Neuroethol. Sensory, Neural, Behav. Physiol.* **190**, 61–68.

Mappes, M. and Homberg, U. (2004b). Behavioral analysis of polarization vision in tethered flying locusts. *J. Comp. Physiol. A* **190**, 61–8.

Markow, T. A. (1979). Phototactic behavior of *Drosophila* species at different temperatures. *Am. Nat.* **114**, 884–892.

Martin, J.-R. (2004). A portrait of locomotor behaviour in *Drosophila* determined by a video-tracking paradigm. *Behav. Processes* **67**, 207–219.

Martin, J.-R., Ernst, R. and Heisenberg, M. (1999). Temporal pattern of locomotor activity in Drosophila melanogaster. *J. Comp. Physiol. A Sensory, Neural, Behav. Physiol.* **184**, 73–84.

Martin, J. P., Guo, P., Mu, L., Harley, C. M. and Ritzmann, R. E. (2015). Central-complex control of movement in the freely walking cockroach. *Curr. Biol.* **25**, 2795–2803.

Mason, A. C., Oshinsky, M. L. and Hoy, R. R. (2001). Hyperacute directional hearing in a microscale auditory system. *Nature* **410**, 686–690.

McNaughton, B. L., Battaglia, F. P., Jensen, O., Moser, E. I. and Moser, M.-B. (2006). Path integration and the neural basis of the "cognitive map." *Nat. Rev. Neurosci.* **7**, 663–678.

Menzel, R., Greggers, U., Smith, A., Berger, S., Brandt, R., Brunke, S., Bundrock, G., Hülse, S., Plümpe, T., Schaupp, F., et al. (2005). Honey bees navigate according to a map-like spatial memory. *Proc. Natl. Acad. Sci. U. S. A.* **102**, 3040–3045.

Meunier, N., Belgacem, Y. H. and Martin, J.-R. (2007). Regulation of feeding behaviour and locomotor activity by takeout in *Drosophila*. *J. Exp. Biol.* **210**, 1424–1434.

Minderer, M., Harvey, C. D., Donato, F. and Moser, E. I. (2016). Neuroscience: Virtual reality explored. *Nature* **533**, 324–325.

Mischiati, M., Lin, H.-T., Herold, P., Imler, E., Olberg, R. and Leonardo, A. (2014). Internal models direct dragonfly interception steering. *Nature* **517**, 333–338.

Miyamoto, T., Slone, J., Song, X. and Amrein, H. (2012). A Fructose Receptor Functions as a Nutrient Sensor in the *Drosophila* Brain. *Cell* **151**, 1113–1125.

Morris, R. G. M. (1981). Spatial localization does not require the presence of local cues. *Learn. Motiv.* **12**, 239–260.

Moser, E. I., Kropff, E. and Moser, M.-B. (2008). Place cells, grid cells, and the brain's spatial representation system. *Annu. Rev. Neurosci.* **31**, 69–89.

Moser, E. I., Roudi, Y., Witter, M. P., Kentros, C., Bonhoeffer, T. and Moser, M.-B. (2014). Grid cells and cortical representation. *Nat. Rev. Neurosci.* **15**, 466–481.

Müller, M. and Wehner, R. (1988). Path integration in desert ants, *Cataglyphis fortis*. *Proc. Natl. Acad. Sci.* **85**, 5287–5290.

Murphey, R. K. and Zaretsky, M. D. (1972). Orientation to calling song by female crickets, *Scapsipedus marginatus* (Gryllidae). *J. Exp. Biol.* **56**, 335–352.

Narendra, A. (2007). Homing strategies of the Australian desert ant *Melophorus bagoti* II. Interaction of the path integrator with visual cue information. *J. Exp. Biol.* **210**, 1804–1812.

Neuser, K., Triphan, T., Mronz, M., Poeck, B. and Strauss, R. (2008). Analysis of a spatial orientation memory in *Drosophila*. *Nature* **453**, 1244–1247.

Ni, L., Bronk, P., Chang, E. C., Lowell, A. M., Flam, J. O., Panzano, V. C., Theobald, D. L., Griffith, L. C. and Garrity, P. a (2013). A gustatory receptor paralogue controls rapid warmth avoidance in *Drosophila*. *Nature* **500**, 580–584.

Nishiyama, K., Okada, J. and Toh, Y. (2007). Antennal and locomotor responses to attractive and aversive odors in the searching cockroach. *J. Comp. Physiol. A* **193**, 963–971.

O'Keefe, J. and Dostrovsky, J. (1971). The hippocampus as a spatial map. Preliminary evidence from unit activity in the freely-moving rat. *Brain Res.* **34**, 171–175.

Ofstad, T. A., Zuker, C. S. and Reiser, M. B. (2011). Visual place learning in *Drosophila* melanogaster. *Nature* **474**, 204–207.

Okada, J. (2004). Spatio-temporal patterns of antennal movements in the searching cockroach. *J. Exp. Biol.* **207**, 3693–3706.

Okada, J. and Akamine, S. (2012). Behavioral response to antennal tactile stimulation in the field cricket *Gryllus bimaculatus*. *J. Comp. Physiol. A* **198**, 557–565.

Okada, J. and Toh, Y. (2004). Antennal system in cockroaches: a biological model of active tactile sensing. *Int. Congr. Ser.* **1269**, 57–60.

Okada, J. and Toh, Y. (2006). Active tactile sensing for localization of objects by the cockroach antenna. *J. Comp. Physiol. A* **192**, 715–726.

Owald, D., Felsenberg, J., Talbot, C. B., Das, G., Perisse, E., Huetteroth, W. and Waddell, S. (2015). Activity of defined mushroom body output neurons underlies learned olfactory behavior in *Drosophila*. *Neuron* **86**, 417–427.

Paulk, A. C., Stacey, J. A., Pearson, T. W. J., Taylor, G. J., Moore, R. J. D., Srinivasan, M. V. and van Swinderen, B. (2014). Selective attention in the honeybee optic lobes precedes behavioral choices. *Proc. Natl. Acad. Sci.* **111**, 5006–5011.

Payne, M., Hedwig, B. and Webb, B. (2010). Multimodal Predictive Control in Crickets. In *From Animals to Animats 11; Volume 6226 of the series Lecture Notes in Computer Science*, pp. 167–177.

Perez-Orive, J., Mazor, O., Turner, G. C., Cassenaer, S., Wilson, R. I. and Laurent, G. (2002). Oscillations and sparsening of odor representations in the mushroom body. *Science* **297**, 359–365.

Pfeffer, S. E. and Wittlinger, M. (2016). Optic flow odometry operates independently of stride integration in carried ants. *Science* **353**, 1155 LP-1157.

Pfeiffer, K. and Homberg, U. (2014). Organization and Functional Roles of the Central Complex in the Insect Brain. *Annu. Rev. Entomol.* **59**, 165–184.

Pfeiffer, B. D., Ngo, T. T. B., Hibbard, K. L., Murphy, C., Jenett, A., Truman, J. W. and Rubin, G. M. (2010). Refinement of tools for targeted gene expression in *Drosophila*. *Genetics* **186**, 735–755.

Philipsborn, A. von and Labhart, T. (1990). A behavioural study of polarization vision in the fly, *Musca domestica*. *J. Comp. Physiol. A* **167**, 737–743.

Pick, S. and Strauss, R. (2005). Goal-driven behavioral adaptations in gap-climbing *Drosophila*. *Curr. Biol.* **15**, 1473–8.

Poggio, T. and Reichardt, W. (1973). A theory of the pattern induced flight orientation of the fly *Musca domestica*. *Kybernetik* **12**, 185–203.

Pollack, G. (2000). Who, what, where? Recognition and localization of acoustic signals by insects. *Curr. Opin. Neurobiol.* **10**, 763–767.

Poulet, J. F. A. and Hedwig, B. (2005). Auditory orientation in crickets: Pattern recognition controls reactive steering. *Proc. Natl. Acad. Sci.* **102**, 15665–15669.

Prescott, T. J. (1994). *Explorations in reinforcement and model-based learning*. PhD Thesis: University of Sheffield, U.K.

Prescott, T. J., Diamond, M. E. and Wing, A. M. (2011). Active touch sensing. *Philos. Trans. R. Soc. B Biol. Sci.* **366**, 2989–2995.

Ramdya, P., Lichocki, P., Cruchet, S., Frisch, L., Tse, W., Floreano, D. and Benton, R. (2014). Mechanosensory interactions drive collective behaviour in *Drosophila*. *Nature* **519**, 233–236.

Ravassard, P., Kees, A., Willers, B., Ho, D., Aharoni, D., Cushman, J., Aghajan, Z. M. and Mehta, M. R. (2013). Multisensory Control of Hippocampal Spatiotemporal Selectivity. *Science* **340**, 1342–1346.

Regen, J. (1913). Über die Anlockung des Weibchens von *Gryllus campestris L*. durch telephonisch übertragene Stridulationslaute des Männchens. *Pfluegers Arch. ges. Physiol.* 193–200.

Reichardt, W. and Poggio, T. (1976). Visual control of orientation behaviour in the fly: Part I. A quantitative analysis. *Q. Rev. Biophys.* **9**, 311.

Reiser, M. B. and Dickinson, M. H. (2008). A modular display system for insect behavioral neuroscience. *J. Neurosci. Methods* **167**, 127–139.

Reiser, M. B. and Dickinson, M. H. (2010). *Drosophila* fly straight by fixating objects in the face of expanding optic flow. *J. Exp. Biol.* **213**, 1771–81.

Ritzmann, R. E., Harley, C. M., Daltorio, K. A., Tietz, B. R., Pollack, A. J., Bender, J. A., Guo, P., Horomanski, A. L., Kathman, N. D., Nieuwoudt, C., et al. (2012). Deciding Which Way to Go: How Do Insects Alter Movements to Negotiate Barriers? *Front. Neurosci.* **6**, 1–16.

Robie, A. A., Straw, A. D. and Dickinson, M. H. (2010). Object preference by walking fruit flies, *Drosophila melanogaster*, is mediated by vision and graviperception. *J. Exp. Biol.* **213**, 2494–2506.

Rodríguez-Muñoz, R., Bretman, A., Slate, J., Walling, C. A. and Tregenza, T. (2010). Natural and sexual selection in a wild insect population. *Science* **328**, 1269–1272.

Root, C. M., Ko, K. I., Jafari, A. and Wang, J. W. (2011). Presynaptic facilitation by neuropeptide signaling mediates odor-driven food search. *Cell* **145**, 133–144.

Rosner, R. and Homberg, U. (2013). Widespread Sensitivity to Looming Stimuli and Small Moving Objects in the Central Complex of an Insect Brain. *J. Neurosci.* **33**, 8122 LP-8133.

Rospars, J. P. (1988). Structure and development of the insect antennodeutocerebral system. *Int. J. Insect Morphol. Embryol.* **17**, 243–294.

Sakaluk, S. K. and Belwood, J. J. (1984). Gecko phonotaxis to cricket calling song: A case of satellite predation. *Anim. Behav.* **32**, 659–662.

Sakura, M., Lambrinos, D. and Labhart, T. (2008). Polarized skylight navigation in insects: model and electrophysiology of e-vector coding by neurons in the central complex. *J. Neurophysiol.* **99**, 667–82.

Santer, R. D., Yamawaki, Y., Rind, F. C. and Simmons, P. J. (2005). Motor activity and trajectory control during escape jumping in the locust *Locusta migratoria*. *J. Comp. Physiol. A Neuroethol. Sensory, Neural, Behav. Physiol.* **191**, 965–975.

Schildberger, K. and Hörner, M. (1988). The function of auditory neurons in cricket phonotaxis. *J. Comp. Physiol. A* **163**, 621–631.

Schmitz, B., Scharstein, H. and Wendler, G. (1982). Phonotaxis in *Gryllus campestris* L. (Orthoptera, Gryllidae) - I. Mechanism of acoustic orientation in intact female crickets. *J. Comp. Physiol. A* **148**, 431–444.

Schnell, B., Weir, P. T., Roth, E., Fairhall, A. L. and Dickinson, M. H. (2014). Cellular mechanisms for integral feedback in visually guided behavior. *Proc. Natl. Acad. Sci.* **111**, 5700–5705.

Schöneich, S. and Hedwig, B. (2010). Hyperacute directional hearing and phonotactic steering in the cricket (*Gryllus bimaculatus* deGeer). *PLoS One* **5**,.

Schöneich, S., Schildberger, K. and Stevenson, P. A. (2011). Neuronal organization of a fast-mediating cephalothoracic pathway for antennal-tactile information in the cricket (*Gryllus bimaculatus* DeGeer). *J. Comp. Neurol.* **519**, 1677–1690.

Schöneich, S., Kostarakos, K. and Hedwig, B. (2015). An Auditory Feature Detection Circuit for Sound Pattern Recognition. *Sci. Adv.* **1**, 1–15.

Schulte, C., Theilenberg, E., Muller-Borg, M., Gempe, T. and Beye, M. (2014). Highly efficient integration and expression of piggyBac-derived cassettes in the honeybee (*Apis mellifera*). *Proc. Natl. Acad. Sci.* **111**, 9003–9008.

Schuster, S., Strauss, R. and Götz, K. G. (2002). Virtual-reality techniques resolve the visual cues used by fruit flies to evaluate object distances. *Curr. Biol.* **12**, 1591–1594.

Schütz, C. and Dürr, V. (2011). Active tactile exploration for adaptive locomotion in the stick insect. *Philos. Trans. R. Soc. B Biol. Sci.* **366**, 2996–3005.

Seeds, A. M., Ravbar, P., Chung, P., Hampel, S., Jr, F. M. M., Mensh, B. D. and Simpson, J. H. (2014). A suppression hierarchy among competing motor programs drives sequential grooming in *Drosophila*. *eLife* 1–23.

Seelig, J. D. and Jayaraman, V. (2013). Feature detection and orientation tuning in the *Drosophila* central complex. *Nature* **503**, 262–266.

Seelig, J. D. and Jayaraman, V. (2015). Neural dynamics for landmark orientation and angular path integration. *Nature* **521**, 186–191.

Seelig, J. D., Chiappe, M. E., Lott, G. K., Dutta, A., Osborne, J. E., Reiser, M. B. and Jayaraman, V. (2010). Two-photon calcium imaging from head-fixed *Drosophila* during optomotor walking behavior. *Nat. Methods* **7**, 535–540.

Shaffer, S. a, Tremblay, Y., Weimerskirch, H., Scott, D., Thompson, D. R., Sagar, P. M., Moller, H., Taylor, G. a, Foley, D. G., Block, B. a, et al. (2006). Migratory shearwaters integrate oceanic resources across the Pacific Ocean in an endless summer. *Proc. Natl. Acad. Sci. U. S. A.* **103**, 12799–12802.

Si, A., Srinivasan, M. V and Zhang, S. (2003). Honeybee navigation: properties of the visually driven "odometer". *J. Exp. Biol.* **206**, 1265–1273.

Simmons, L. W. (1988). Male size, mating potential and lifetime reproductive success in the field cricket, *Gryllus bimaculatus* (De Geer). *Anim. Behav.* **36**, 372–379.

Sobel, E. C. and Tank, D. W. (1994). In vivo Ca^{2+} dynamics in a cricket auditory neuron: an example of chemical computation. *Science* **263**, 823–6.

Srinivasan, M. V., Zhang, S. W. and Chandrashekara, K. (1993). Evidence for two distinct movement-detecting mechanisms in insect vision. *Naturwissenschaften* **80**, 38–41.

Staudacher, E. and Schildberger, K. (1999). A newly described neuropile in the deutocerebrum of the cricket: Antennal afferents and descending interneurons. *Zoology* **102**, 212–226.

Staudacher, E. M., Gebhardt, M. and Dürr, V. (2005). Antennal Movements and Mechanoreception: Neurobiology of Active Tactile Sensors. In *Advances In Insect Physiology*, pp. 49–205.

Stein, B. E. and Stanford, T. R. (2008). Multisensory integration: current issues from the perspective of the single neuron. *Nat. Rev. Neurosci.* **9**, 255–266.

Stierle, I. E., Getman, M. and Comer, C. M. (1994). Multsensory control of escape in the cockroach *Periplaneta americana*. I. Initial evidence from patterns of wind-evoked behavior. *J. Comp. Physiol. A* **174**, 1–11.

Stowers, J. R., Fuhrmann, A., Hofbauer, M., Streinzer, M., Schmid, A., Dickinson, M. H. and Straw, A. D. (2014). Reverse Engineering Animal Vision with Virtual Reality and Genetics. *Computer (Long. Beach. Calif).* **47**, 38–45.

Strauss, R. (2002). The central complex and the genetic dissection of locomotor behaviour. *Curr. Opin. Neurobiol.* **12**, 633–638.

Strauss, R. and Heisenberg, M. (1993). A Higher Control Center of Locomotor Behavior in the *Drosophila* Brain. *J. Neurosci.* **13**, 1852–1861.

Strauss, R., Schuster, S. and Götz, K. G. (1997). Processing of artificial visual feedback in the walking fruit fly *Drosophila melanogaster*. *J. Exp. Biol.* **1296**, 1281–1296.

Suver, M. P., Mamiya, A. and Dickinson, M. H. (2012). Octopamine Neurons Mediate Flight-Induced Modulation of Visual Processing in *Drosophila*. *Curr. Biol.* **22**, 2294–2302.

Takalo, J., Piironen, A., Honkanen, A., Lempeä, M., Aikio, M., Tuukkanen, T. and Vähäsöyrinki, M. (2012). A fast and flexible panoramic virtual reality system for behavioural and electrophysiological experiments. *Sci. Rep.* **2**, 1–9.

Takemura, S., Xu, C. S., Lu, Z., Rivlin, P. K., Parag, T., Olbris, D. J., Plaza, S., Zhao, T., Katz, W. T., Umayam, L., et al. (2015). Synaptic circuits and their variations within different columns in the visual system of *Drosophila*. *Proc. Natl. Acad. Sci.* **112**, 13711–13716.

Tammero, L. F. and Dickinson, M. H. (2002). The influence of visual landscape on the free flight behavior of the fruit fly *Drosophila melanogaster*. *J. Exp. Biol.* **205**, 327–343.

Tang, X., Platt, M. D., Lagnese, C. M., Leslie, J. R. and Hamada, F. N. (2013). Temperature Integration at the AC Thermosensory Neurons in *Drosophila*. *J. Neurosci.* **33**, 894–901.

Taube, J. S. (2007). The head direction signal: origins and sensory-motor integration. *Annu. Rev. Neurosci.* **30**, 181–207.

Taube, J. S., Muller, R. U. and Ranck, J. B. (1990a). Head-direction cells recorded from the postsubiculum in freely moving rats. I. Description and quantitative analysis. *J. Neurosci.* **10**, 420–435.

Taube, J. S., Muller, R. U. and Ranck, J. B. (1990b). Head-direction cells recorded from the postsubiculum in freely moving rats. II. Effects of environmental manipulations. *J. Neurosci.* **10**, 436–447.

ten Cate, C. (2009). Niko Tinbergen and the red patch on the herring gull's beak. *Anim. Behav.* **77**, 785–794.

Theobald, J. C., Ringach, D. L. and Frye, M. A. (2010). Dynamics of optomotor responses in *Drosophila* to perturbations in optic flow. *J. Exp. Biol.* **213**, 1366–75.

Thomas, S. J., Harrison, R. R., Leonardo, A. and Reynolds, M. S. (2012). A battery-free multichannel digital neural/EMG telemetry system for flying insects. *IEEE Trans. Biomed. Circuits Syst.* **6**, 424–436.

Tian, L., Hires, S. A., Mao, T., Huber, D., Chiappe, M. E., Chalasani, S. H., Petreanu, L., Akerboom, J., McKinney, S. A., Schreiter, E. R., et al. (2009). Imaging neural activity in worms, flies and mice with improved GCaMP calcium indicators. *Nat. Methods* **6**, 875–881.

Tolman, E. C. (1948). Cognitive maps in rats and men. *Psychol. Rev.* **55**, 189–208.

Tracey, W. D., Wilson, R. I., Laurent, G. and Benzer, S. (2003). painless, a *Drosophila* Gene Essential for Nociception. *Cell* **113**, 261–273.

Trullier, O., Wiener, S. I., Berthoz, A. and Meyer, J.-A. (1997). Biologically based artificial navigation systems: Review and prospects. *Prog. Neurobiol.* **51**, 483–544.

Tsoar, A., Nathan, R., Bartan, Y., Vyssotski, A., Dell, G. and Ulanovsky, N. (2011). Large-scale navigational map in a mammal. *Proc. Natl. Acad. Sci.* **108**, E718–E724.

Tuthill, J. C., Nern, A., Rubin, G. M. and Reiser, M. B. (2014). Wide-Field Feedback Neurons Dynamically Tune Early Visual Processing. *Neuron* **82**, 887–895.

van Breugel, F. and Dickinson, M. H. (2012). The visual control of landing and obstacle avoidance in the fruit fly *Drosophila melanogaster*. *J. Exp. Biol.* **215**, 1783–1798.

van Breugel, F., Riffell, J., Fairhall, A. and Dickinson, M. H. (2015). Mosquitoes Use Vision to Associate Odor Plumes with Thermal Targets. *Curr. Biol.* **25**, 2123–2129.

Van Wyk, J. W. and Ferguson, J. W. H. (1995). Communicatory constraints on field crickets *Gryllus bimaculatus* calling at low ambient temperatures. *J. Insect Physiol.* **41**, 837–841.

Varga, A. G. and Ritzmann, R. E. (2016). Cellular Basis of Head Direction and Contextual Cues in the Insect Brain. *Curr. Biol.* **26**, 1816–1828.

Visalberghi, E., Addessi, E., Truppa, V., Spagnoletti, N., Ottoni, E., Izar, P. and Fragaszy, D. (2009). Selection of Effective Stone Tools by Wild Bearded Capuchin Monkeys. *Curr. Biol.* **19**, 213–217.

von Frisch, K. (1967). The dance language and orientation of bees. *Heredity (Edinb).* **90**, 212.

von Helversen, D. and von Helversen, O. (1995). Acoustic pattern recognition and orientation in orthopteran insects: parallel or serial processing? *J. Comp. Physiol. A* **177**, 767–774.

von Helversen, D. and Wendler, G. (2000). Coupling of visual to auditory cues during phonotactic approach in the phaneropterine bushcricket *Poecilimon affinis*. *J. Comp. Physiol. A* **186**, 729–36.

von Helversen, D., Schul, J. and Kleindienst, H.-U. (2001). Male recognition mechanism for female responses implies a dilemma for their localisation in a phaneropterine bushcricket. *J. Comp. Physiol. A* **186**, 1153–1158.

von Holst, E. and Mittelstaedt, H. (1950). Das Reafferenzprinzip. *Naturwissenschaften* **37**, 464–476.

von Reyn, C. R., Breads, P., Peek, M. Y., Zheng, G. Z., Williamson, W. R., Yee, A. L., Leonardo, A. and Card, G. M. (2014). A spike-timing mechanism for action selection. *Nat Neurosci* **17**, 962–970.

Vu, E. T. and Krasne, F. B. (1992). Evidence for a computational distinction between proximal and distal neuronal inhibition. *Science* **255**, 1710–1712.

Vu, E. T., Lee, S. C. and Krasne, F. B. (1993). The mechanism of tonic inhibition of crayfish escape behavior: distal inhibition and its functional significance. *J. Neurosci.* **13**, 4379–4393.

Wang, Z., Pan, Y., Li, W., Jiang, H., Chatzimanolis, L., Chang, J., Gong, Z. and Liu, L. (2008). Visual pattern memory requires foraging function in the central complex of *Drosophila*. *Learn. Mem.* **15**, 133–142.

Wang, X., Wang, T., Ni, J. D., von Lintig, J. and Montell, C. (2012). The Drosophila Visual Cycle and De Novo Chromophore Synthesis Depends on rdhB. *J. Neurosci.* **32**, 3485–3491.

Webb, B. (2004). Neural mechanisms for prediction: do insects have forward models? *Trends Neurosci.* **27**, 278–282.

Webb, B. (2012). Cognition in insects. *Philos. Trans. R. Soc. B Biol. Sci.* **367**, 2715–2722.

Weber, T. and Thorson, J. (1989). Phonotactic behaviour of walking crickets. In *Cricket Behavior and Neurobiology* (ed. Huber, F., Moore, T., and Loher, W.), pp. 301–339. Ithaca, NY: Cornell University Press.

Wehner, R. (2003). Desert ant navigation: how miniature brains solve complex tasks. *J. Comp. Physiol. A Sensory, Neural, Behav. Physiol.* **189**, 579–588.

Wehner, R. and Srinivasan, M. V (1981). Searching Behaviour of Desert Ants, Genus *Cataglyphis* (Formicidae, Hymenoptera). *J. Comp. Physiol. A Sens. Neural Behav. Physiol.* **142**, 315–338.

Wehner, Michel and Antonsen (1996). Visual navigation in insects: coupling of egocentric and geocentric information. *J. Exp. Biol.* **199**, 129–140.

Wehner, R., Boyer, M., Loertscher, F., Sommer, S. and Menzi, U. (2006). Ant navigation: One-way routes rather than maps. *Curr. Biol.* **16**, 75–79.

Weimerskirch, H., Delord, K., Guitteaud, A., Phillips, R. A. and Pinet, P. (2015). Extreme variation in migration strategies between and within wandering albatross populations during their sabbatical year, and their fitness consequences. *Sci. Rep.* **5**, 8853.

Wilson, R. I. (2013). Early olfactory processing in *Drosophila*: mechanisms and principles. *Annu. Rev. Neurosci.* **36**, 217–41.

Witney, A. G. and Hedwig, B. (2011). Kinematics of phonotactic steering in the walking cricket *Gryllus bimaculatus* (de Geer). *J. Exp. Biol.* **214**, 69–79.

Wittlinger, M., Wehner, R. and Wolf, H. (2007). The desert ant odometer: a stride integrator that accounts for stride length and walking speed. *J. Exp. Biol.* **210**, 198–207.

Wolff, T., Iyer, N. A. and Rubin, G. M. (2015). Neuroarchitecture and neuroanatomy of the *Drosophila* central complex: A GAL4-based dissection of protocerebral bridge neurons and circuits. *J. Comp. Neurol.* **523**, 997–1037.

Wurtz, R. H. and Goldberg, M. E. (1971). Superior colliculus cell responses related to eye movements in awake monkeys. *Science* **171**, 82–4.

Wystrach, A., Schwarz, S., Baniel, A. and Cheng, K. (2013). Backtracking behaviour in lost ants: an additional strategy in their navigational toolkit. *Proc. Biol. Sci.* **280**, 20131677.

Yoder, R. M., Peck, J. R. and Taube, J. S. (2015). Visual Landmark Information Gains Control of the Head Direction Signal at the Lateral Mammillary Nuclei. *J. Neurosci.* **35**, 1354–1367.

Yoritsune, A. and Aonuma, H. (2012). The anatomical pathways for antennal sensory information in the central nervous system of the cricket, *Gryllus bimaculatus*. *Invertebr. Neurosci.* **12**, 103–117.

Zhang, S. W., Lehrer, M. and Srinivasan, M. V (1999). Honeybee memory: navigation by associative grouping and recall of visual stimuli. *Neurobiol. Learn. Mem.* **72**, 180–201.

Zorović, M. and Hedwig, B. (2011). Processing of species-specific auditory patterns in the cricket brain by ascending, local, and descending neurons during standing and walking. *J. Neurophysiol.* **105**, 2181–2194.

Zorović, M. and Hedwig, B. (2013). Descending brain neurons in the cricket *Gryllus bimaculatus* (de Geer): Auditory responses and impact on walking. *J. Comp. Physiol. A* **199**, 25–34.

Zugaro, M. B., Arleo, A., Berthoz, A. and Wiener, S. I. (2003). Rapid spatial reorientation and head direction cells. *J. Neurosci.* **23**, 3478–3482.